



---

**A neuropharmacological study of 5-HT<sub>4</sub> and 5-HT<sub>6</sub> receptors and  
their relevance to Alzheimer's disease**

---

**by Wedad Shubily Sarawi (BSc, MSc)**

**A thesis submitted to the University of Birmingham for the Degree of  
DOCTOR OF PHILOSOPHY**

Institute of Clinical Science  
School of Pharmacy  
College of Medical and Dental Sciences  
University of Birmingham

March 2019.

UNIVERSITY OF  
BIRMINGHAM

**University of Birmingham Research Archive**

**e-theses repository**

This unpublished thesis/dissertation is copyright of the author and/or third parties. The intellectual property rights of the author or third parties in respect of this work are as defined by The Copyright Designs and Patents Act 1988 or as modified by any successor legislation.

Any use made of information contained in this thesis/dissertation must be in accordance with that legislation and must be properly acknowledged. Further distribution or reproduction in any format is prohibited without the permission of the copyright holder.

## **Abstract**

Serotonin or 5-hydroxytryptamine (5-HT) is implicated in the control of many physiological processes including cognitive functions. Among its fourteen receptor subtypes, 5-HT<sub>4</sub> and 5-HT<sub>6</sub> receptors have gained the greatest research attention as promising therapeutic targets for Alzheimer's disease (AD) and its associated symptoms. Pharmacological modulation of these receptors showed beneficial outcomes in preclinical studies in terms of memory and cognition thus showing potential to improve disease symptoms. Evaluation of the expression of 5-HT receptors during disease progression is necessary as it can enhance understanding of the regulation of 5-HT neurotransmission and its relation to the cognitive decline of AD. Therefore, this study aimed to determine the expression, functionality and potential interaction of 5-HT<sub>4</sub> and 5-HT<sub>6</sub> receptors in two commonly used human cell lines, HEK293 and SH-SY5Y, to identify and specify the role of *N*-linked glycosylation of the 5-HT<sub>4</sub> receptor upon trafficking to the cell membrane, and to assess the expression of these receptors at different stages of AD.

At the protein level, both the HEK293 and SH-SY5Y cells natively express the 5-HT<sub>4</sub> receptors but at a very low level, and neither cell line expresses detectable levels of the 5-HT<sub>6</sub> receptor. The low expression of the 5-HT<sub>4</sub> receptors in these cells prevented the detection of any functional readout represented by extracellular signal-regulated kinase 1 and 2 (ERK<sub>1/2</sub>) phosphorylation. In contrast, overexpression of the 5-HT<sub>4</sub> and 5-HT<sub>6</sub> receptors individually in HEK293 cells showed transient ERK<sub>1/2</sub> phosphorylation in response to 5-HT, while concurrent overexpression of the receptors did not show any augmentation effects in pERK<sub>1/2</sub> level following 5-HT stimulation.

Moreover, the overexpressed 5-HT<sub>4</sub> receptor in HEK293 cells showed an approximate receptor weight that indicated the presence of *N*-glycosylation. Subsequently this was supported since the apparent receptor weight was reduced by growing cells in the presence of tunicamycin. Site directed mutagenesis confirmed that the asparagine at amino acid position 180 was *N*-glycosylated and that abrogation of the *N*-glycosylation consensus sequence at this position reduced the apparent molecular weight of the receptor and reduced trafficking leading to a decrease in expression in the cell membrane.

The immunoreactivities of the 5-HT<sub>4</sub> and 5-HT<sub>6</sub> receptors were assessed in post-mortem prefrontal cortex sections of AD patients at different stages of the disease. The 5-HT<sub>4</sub> receptor was found to be significantly down-regulated in limbic (early) and neocortical (advance) stages of AD relative to controls, whereas the 5-HT<sub>6</sub> receptor only displayed reduced levels of expression in the neocortical stage relative to the limbic stage of AD. Importantly the variations in the expression of these receptors significantly correlated with the cognitive status of AD patients as well as AD-related phospho-tau. These data suggest that the early pharmacological intervention to modulate these receptors alone, or as an adjunct to other AD treatments, might improve AD cognitive deficits and potentially slow disease progression.



## Acknowledgements

All praise and glory to Almighty Allah, who blessed and strengthened me to finish this work. I am deeply indebted to **King Saud University** and **the Ministry of Education in Saudi Arabia** for giving me this opportunity and for supporting me financially to pursue my studies. I wish to express my full gratitude and appreciation to my supervisors: **Professor Nicholas Barnes**, for his supervision, encouragement, and valuable suggestions over the years for allowing me to grow as an independent scientist; and **Dr. Zsuzsanna Nagy**, for her supervision, support and constructive counsel. I truly appreciate their immense knowledge and experience and I have gained a great deal from them. I am grateful to all patients participated in **OPTIMA** study and to the clinicians and scientists involved in the clinical data collection. Special thanks to **Dr. Gillian Grafton** and **Dr. Hatun Alomar**, for their valuable advice, productive discussions and emotional support during my difficult days. Thanks to **Dr. Jeremy Pike** for his advice and assistance in the IHC image analysis and quantification, to **Dr. Robert show** for his training of Confocal and Axioscan microscopes and to the lab colleagues for their cooperation and assistance, as well as all the friends I have met and known.

Undertaking this PhD journey has been a wonderful ‘but also difficult’ experience. Almost four years of hard work have honed my skills and intentions, not only as a scientist, but also at home, and I would not have reached this day and gained all this without my husband **Mohammed Akkam**, who has always supported me, ever since high school. My deep and sincere gratitude and appreciation for his love, understanding and sacrifices. I will never be able to express the extent of my sincere appreciation for my Mother, Sisters and Brothers, for their unconditional love, support and encouragement. Deep and warm thanks to my Father’s spirit, who was my source of strength and may Allah have mercy upon my parents, as they brought me up. Big thanks with love to my children **Layan, Faisal and Majed**, for making my life more joyful and every effort worthwhile and to them I dedicate this thesis.

## Table of Contents

<b>1. Introduction.....</b>	<b>1</b>
1.1. Alzheimer's disease .....	1
1.1.1. AD classification and risk factors .....	2
1.1.2. Pathological mechanisms involved in AD .....	4
1.1.3. AD therapies and clinical trials.....	21
1.2. Serotonin .....	24
1.2.1. Serotonin discovery .....	24
1.2.2. Serotonergic transmission .....	24
1.2.3. Serotonin action and localisation .....	27
1.2.4. Role of serotonin in cognitive functions.....	31
1.2.5. Role of serotonin in mood and emotions .....	32
1.2.6. Role of serotonin in neuronal plasticity and development .....	33
1.3. Serotonin transporter (SERT) .....	34
1.4. Serotonin receptors .....	35
1.4.1. 5-HT <sub>4</sub> receptor.....	38
1.4.2. 5-HT <sub>6</sub> receptor.....	47
1.5. Possible crosstalk between the 5-HT <sub>4</sub> and 5-HT <sub>6</sub> receptor-signalling pathways in the context of memory and cognition.....	53
1.6. The potential of a multi-target drug paradigm .....	54
1.7. Research hypotheses .....	55
1.8. Aims and objectives .....	55
<b>2. Methods .....</b>	<b>58</b>
2.1. Cell culture .....	58
2.1.1. Cell line maintenance.....	58
2.1.2. Cryopreservation and resuscitation of cells .....	59
2.2. Nucleic acid quantification and quality control .....	59
2.3. Polymerase chain reaction .....	60
2.3.1. RNA extraction .....	60
2.3.2. Complementary DNA (cDNA) synthesis .....	61
2.3.3. End-point (PCR).....	61
2.3.4. Real-time PCR.....	63
2.4. Plasmid cloning.....	66
2.4.1. Subcloning of 5-HT <sub>4</sub> and 5-HT <sub>6</sub> Receptor: .....	66
2.4.2. Gel extraction and DNA purification .....	67
2.4.3. Ethanol DNA precipitation .....	68

2.4.4. Vector dephosphorylation .....	68
2.4.5. Ligation .....	68
2.4.6. Preparation of chemically competent bacteria .....	69
2.4.7. Bacterial transformation.....	70
2.4.8. Plasmid purification.....	71
2.5. Site-directed mutagenesis (SDM) .....	73
2.5.1. 5-HT <sub>4</sub> receptor mutant constructs .....	74
2.6. DNA sequencing .....	77
2.7. Transfection .....	78
2.8. Western blotting.....	80
2.8.1. Cell stimulation .....	80
2.8.2. Cell lysate preparation. ....	81
2.8.3. Gel electrophoresis and membrane blotting.....	82
2.8.4. Blocking, probing and detection .....	84
2.8.5. Quantification of band intensity .....	85
2.9. Flow cytometry .....	86
2.10. Immunocytochemistry .....	87
2.11. Immunohistochemistry .....	89
2.11.1. Quantification of the IHC image .....	93
2.12. Single point radioligand binding assay .....	94
2.13. Statistical analysis .....	95
<b>3. Experimental developments and determinations for the endogenous expression of 5-HT<sub>4</sub> and 5-HT<sub>6</sub> receptors in SH-SY5Y and HEK293 cell lines</b> .....	<b>97</b>
3.1. The analysis of gene expression levels of 5-HT <sub>4</sub> and 5-HT <sub>6</sub> receptors in SH- SY5Y and HEK293 cell lines .....	97
3.2. The analysis of receptor proteins expression in SH-SY5Y and HEK293 cell lines.....	101
3.3. Plasmid constructs.....	104
3.4. Determination of 5-HT <sub>4</sub> and 5-HT <sub>6</sub> receptors gene expression post- transfection relative to their endogenous level in the HEK293 cells .....	110
3.5. The re-analysis of the protein expression of 5-HT <sub>4</sub> and 5-HT <sub>6</sub> receptors in both the SH-SY5Y and HEK293 cell lines using recombinant proteins as controls .....	112
3.6. Cellular localisation of exogenous and endogenous expressed 5-HT <sub>4</sub> and 5- HT <sub>6</sub> receptors .....	116

3.7. Functional characterisation of the endogenous 5-HT <sub>4</sub> receptor in HEK293 and SH-SY5Y cell lines via ERK <sub>1/2</sub> phosphorylation.....	123
3.8. Assessment of the radioligand binding affinity of the 5-HT <sub>4</sub> receptor in HEK293 cells .....	126
3.9. Summary .....	127
<b>4. Evaluation of the 5-HT<sub>4</sub> and 5-HT<sub>6</sub> receptors' interaction by measuring the pERK<sub>1/2</sub> level.....</b>	<b>129</b>
4.1. Optimisation of transfection ratio .....	129
4.2. Time-dependent effect of 5-HT-induced ERK <sub>1/2</sub> phosphorylation in transfected HEK293 cells .....	131
4.3. Dose-dependent effect of 5-HT-induced ERK <sub>1/2</sub> phosphorylation in transfected HEK293 cells .....	135
4.4. The 5-HT-mediated ERK <sub>1/2</sub> phosphorylation was specific to 5-HT <sub>4</sub> and 5-HT <sub>6</sub> receptors.....	139
4.5. Heterogeneity of the cell population of the co-transfected HEK293 cells.....	141
4.6. Attempts to generate stable cell lines expressing each of the 5-HT <sub>4</sub> receptor and 5-HT <sub>6</sub> receptors alone and in combination.....	143
4.7. Summary .....	143
<b>5. Determination of potential N-glycosylation sites in the 5-HT<sub>4</sub> receptor and their role in receptor trafficking .....</b>	<b>145</b>
5.1. Stable expression of the 5-HT <sub>4</sub> receptor in HEK293 cells.....	145
5.2. Radioligand binding assay of the 5-HT <sub>4</sub> receptor stable cell line .....	148
5.3. The effect of tunicamycin on the size of the Flag-5-HT <sub>4</sub> receptors.....	149
5.4. Generating single and double mutant constructs of N7 and N180 glycosylation sites of the 5-HT <sub>4</sub> receptor. ....	150
5.5. The differences in the glycosylation pattern of the wild type and mutant 5-HT <sub>4</sub> receptor following transient and stable protein expression .....	154
5.6. Stable integration of the 5-HT <sub>4</sub> receptor coding sequence in the cell genome .....	157
5.7. The role of N-linked glycosylation on 5-HT <sub>4</sub> receptor trafficking and cell surface expression.....	159
5.8. Summary .....	167
<b>6. Assessment of the 5-HT<sub>4</sub> and 5-HT<sub>6</sub> receptors and SERT expression in mild and advanced stages of AD relative to healthy age-matched controls. ....</b>	<b>169</b>
6.1. Receptors quantitative gene expression assay .....	169
6.1.1. 5-HT <sub>4</sub> receptor.....	169
6.1.2. 5-HT <sub>6</sub> receptor.....	171
6.2. Area selection for IHC quantification .....	173

6.3. Evaluation of the specificity of the 5-HT <sub>4</sub> and 5-HT <sub>6</sub> receptors antibodies by isotype control .....	175
6.4. Changes in the 5-HT <sub>4</sub> and 5-HT <sub>6</sub> receptor immunoreactivities with AD progression .....	177
6.4.1. 5-HT <sub>4</sub> receptor.....	177
6.4.2. 5-HT <sub>6</sub> receptor.....	184
6.5. Changes in SERT immunoreactivity in different AD stages.....	190
6.6. Effects of demographics and PMD on 5-HT <sub>4</sub> and 5-HT <sub>6</sub> receptors immunoreactivity .....	197
6.7. Elevated homocysteine level did not influence the protein expression of 5-HT <sub>4</sub> and 5-HT <sub>6</sub> receptors and SERT.....	198
6.8. Effect of ApoE genotype on the expression of serotonin receptors and transporter .....	200
6.9. Correlation between serotonin receptors and cognitive functions .....	202
6.10. Summary.....	204
<b>7. Discussion .....</b>	<b>206</b>
7.1. Expression profile of 5-HT <sub>4</sub> and 5-HT <sub>6</sub> receptors in SH-SY5Y and HEK293 cell lines .....	206
7.1.1. The transcript and protein expressions of the 5-HT receptors .....	206
7.1.2. Functionality and radioligand binding to the endogenous 5-HT <sub>4</sub> receptor .....	210
7.1.3. Future work.....	212
7.2. Evaluation of the 5-HT <sub>4</sub> and 5-HT <sub>6</sub> receptors interaction by measuring the pERK <sub>1/2</sub> level.....	214
7.2.1. Overexpressed 5-HT <sub>4</sub> and 5-HT <sub>6</sub> receptors are functional .....	216
7.2.2. Concomitant stimulation of overexpressed 5-HT <sub>4</sub> and 5-HT <sub>6</sub> receptors provides no evidence of functional synergy in ERK <sub>1/2</sub> phosphorylation .....	217
7.2.3. Future prospects to enhance this work .....	219
7.3. The presence and impact of <i>N</i> -linked glycosylation of the human 5-HT <sub>4</sub> receptor .....	220
7.3.1. <i>N</i> -glycosylation from protein synthesis to the final destination .....	221
7.3.2. The human 5-HT <sub>4</sub> receptor is <i>N</i> -glycosylated in HEK293 cells .....	223
7.3.3. The N180 of the 5-HT <sub>4</sub> receptor is the only site of glycosylation in HEK293 cells .....	224
7.3.4. N180 is important for 5-HT <sub>4</sub> membrane integration .....	228
7.3.5. Further studies on the role of <i>N</i> -glycosylation of the 5-HT <sub>4</sub> receptors; future prospects .....	229
7.4. Differential expression of 5-HT <sub>4</sub> and 5-HT <sub>6</sub> receptors in accordance with the pathological severity of AD.....	230
7.4.1. Changes in the expression of the 5-HT receptors in the frontal cortex of AD patients at different disease stages.....	231

7.4.2. Changes in SERT expression in the frontal cortex of AD patients at different disease stages .....	237
7.4.3. The influence of AD risk factors on the expression of serotonin proteins .....	238
7.4.4. Association between the expression of serotonin receptors in the prefrontal cortex and cognitive functions .....	240
7.4.5. Future directions .....	241
7.5. Limitations and critique .....	242
7.6. Conclusion .....	244
<b>8. References.....</b>	<b>247</b>
<b>9. Appendices.....</b>	<b>267</b>
9.1. Peer reviewed posters .....	267
9.2. Supplementary figures .....	268

## List of Figures

Figure 1. The pathological mechanisms and evolution of AD .....	7
Figure 2. Various anti-AD drugs are currently available in clinical trials and their therapeutic outcomes .....	23
Figure 3. The metabolic cycle and regulation of serotonin neurotransmission .....	26
Figure 4. Serotonergic neuronal origins and their projections in the rat brain .....	30
Figure 5. The protein sequence of the 5-HT <sub>4</sub> receptor and its isoforms .....	40
Figure 6. Schematic diagram of the interaction between the 5-HT <sub>4</sub> and 5-HT <sub>6</sub> receptors' signalling pathways .....	46
Figure 7. The protein sequence of the 5-HT <sub>6</sub> receptor .....	49
Figure 8. The immunohistochemistry quantification pipeline .....	94
Figure 9. Amplified PCR products corresponding to $\beta$ actin, 5-HT <sub>4</sub> and 5-HT <sub>6</sub> receptors .....	99
Figure 10. Pairwise alignments of the PCR products amplified from the SH-SY5Y cell line using the NCBI database .....	100
Figure 11. The endogenous expression of 5-HT <sub>4</sub> and 5-HT <sub>6</sub> receptors in the human hippocampus, SH-SY5Y cells and HEK293 cells .....	103
Figure 12. Schematic diagram illustrating the sub-cloning workflow of the 5-HT <sub>4</sub> receptor .....	106
Figure 13. Schematic diagram illustrating the sub-cloning workflow of the 5-HT <sub>6</sub> receptor .....	108
Figure 14. Schematic drawing showing the structure of the expression constructs for 5-HT <sub>4</sub> and 5-HT <sub>6</sub> receptors .....	109
Figure 15. The fold increase in expression of 5-HT <sub>4</sub> and 5-HT <sub>6</sub> receptor genes in the transfected cells relative to the untransfected HEK293 cells .....	111
Figure 16. Characterisation of the 5-HT <sub>4</sub> receptor expression in the HEK293 and SH-SY5Y cell lines .....	113
Figure 17. Characterisation of the 5-HT <sub>6</sub> receptor expression in both the HEK293 and SH-SY5Y cell lines .....	115
Figure 18. Immunofluorescence of the 5-HT <sub>4</sub> receptors and its cellular localisation .....	119
Figure 19. Immunofluorescence of the 5-HT <sub>6</sub> receptors and its cellular localisation .....	122
Figure 20. A representative blot revealing the time dependent and the dose dependent effects of 5-HT on pERK <sub>1/2</sub> in the HEK293 cell line .....	124
Figure 21. A representative blot illustrated the time-dependent and the dose-dependent effects of 5-HT on pERK <sub>1/2</sub> in the SH-SY5Y cell line .....	125
Figure 22. The lack of specific binding affinity of [ <sup>3</sup> H]-5-HT to the 5-HT <sub>4</sub> receptor in HEK293 cells .....	126
Figure 23. Titration of DNA: PEI transfection ratio of plasmids encoding 5-HT <sub>4</sub> and 5-HT <sub>6</sub> receptors .....	130
Figure 24. Time-dependent effect of 5-HT-mediated ERK <sub>1/2</sub> phosphorylation in transient transfected HEK293 cells .....	133

Figure 25. The immunoreactivity of monoclonal Flag and Myc antibodies in transfected HEK293 cells at different time point stimulation .....	134
Figure 26. Dose-dependent effect of 5-HT-mediated ERK <sub>1/2</sub> phosphorylation in transient transfected HEK293 cells .....	137
Figure 27. The immunoreactivity of monoclonal Flag and Myc antibodies of transfected HEK293 cells following treatment with different doses of 5-HT .....	138
Figure 28. The effect of 5-HT receptor antagonists on the ERK <sub>1/2</sub> phosphorylation .....	140
Figure 29. Immunofluorescent imaging showed the cell populations following transient transfection with constructs of the 5-HT <sub>4</sub> and 5-HT <sub>6</sub> receptor .....	142
Figure 30. Stable expression of the 5-HT <sub>4</sub> receptor in HEK293 cells .....	146
Figure 31. The potential glycosylation motifs in the 5-HT <sub>4</sub> receptors.....	147
Figure 32. Radioligand binding for the 5-HT <sub>4</sub> receptor stable cell line .....	148
Figure 33. Enzymatic inhibition of <i>N</i> -glycosylation of the 5-HT <sub>4</sub> receptor by tunicamycin .....	149
Figure 34. Blue-light image of agarose gel electrophoresis of the wild type and mutant 5-HT <sub>4</sub> receptor plasmids .....	151
Figure 35. The sequence chromatogram showing the wild type, N7Q and N180Q mutants of the 5-HT <sub>4</sub> receptor.....	153
Figure 36. The differences in 5-HT <sub>4</sub> receptor migration due to <i>N</i> -glycosylation .	156
Figure 37. Confirmation of the stable integration of the CDS of the wild-type and mutant 5-HT <sub>4</sub> receptor in cells chromosome.....	158
Figure 38. The impact of <i>N</i> -glycosylation on Flag-5-HT <sub>4</sub> receptor localisation ..	166
Figure 39. 5-HT <sub>4</sub> receptor gene expression in control, and limbic and neocortical stages of AD .....	170
Figure 40. 5-HT <sub>6</sub> receptor gene expression in control, and limbic and neocortical stages of AD .....	172
Figure 41. Neocortical layers of human brain stained with DAB and haematoxylin .....	174
Figure 42. Example of isotype control staining and colour segmentation .....	176
Figure 43. Illustration of signal decomposition from DAB and haematoxylin stained-images for 5-HT <sub>4</sub> receptors .....	182
Figure 44. Differences in 5-HT <sub>4</sub> receptor expression in the control, and limbic and neocortical stages of AD .....	183
Figure 45. Illustration of signal decomposition from DAB and haematoxylin stained-images for 5-HT <sub>6</sub> receptor .....	188
Figure 46. Differences in 5-HT <sub>6</sub> receptor expression in the control, and limbic and neocortical stages of AD .....	189
Figure 47. SERT immunoreactivity and its neuronal distributions in layer III of the cortex.....	191
Figure 48. Illustration of signal decomposition from DAB and haematoxylin stained-images for SERT .....	195
Figure 49. Changes in SERT immunoreactivity in the control, and limbic and neocortical stages of AD .....	196



Figure 50. Effect of homocysteine level on the expression of 5-HT <sub>4</sub> and 5-HT <sub>6</sub> receptors and SERT in different AD stages .....	199
Figure 51. Effect of ApoE genotype and disease evolution on the expression of 5-HT <sub>4</sub> and 5-HT <sub>6</sub> receptors and SERT in different AD stages .....	201
Figure 52. The mRNA expression profile of 5-HT and Ach receptors in HEK293 cells .....	207
Figure 53. Illustration of the interaction between the 5-HT <sub>4</sub> and 5-HT <sub>6</sub> receptors and their effect on ERK <sub>1/2</sub> activation .....	215

## List of Tables

Table 1. Summary of the type, mechanism and therapeutic uses of 5-HT receptors. ....	37
Table 2. The primer sequences and cycling conditions used in the PCR reactions. ....	62
Table 3. The compositions of TAE electrophoresis buffer and agarose gel. ....	63
Table 4. Demographics of AD cases and controls used in the qPCR experiments. ....	65
Table 5. Primers used in the quantitative gene expression assay. ....	66
Table 6. General double digestion protocol to release the insert from the vector. ....	67
Table 7. Ligation reaction protocol. ....	69
Table 8. The components of the buffer, broth and agar used in competent bacterial preparation and transformation. ....	71
Table 9. Site-directed mutagenesis protocol. ....	75
Table 10. Designed primers for SDM and the annealing temperature used. ....	76
Table 11. Primers commonly used in plasmid sequencing. ....	77
Table 12. Transfection mixture preparation protocol. ....	79
Table 13. The compositions of the buffers used in cell lysate preparation for Western blotting. ....	82
Table 14. The components of the hand cast gels and buffers used in Western blotting. ....	83
Table 15. Antibodies used in Western blotting and their dilutions. ....	85
Table 16. Primary and secondary antibodies and their dilutions. ....	87
Table 17. ICC antibodies used. ....	88
Table 18. Demographics of AD patients and age-matched controls. ....	91
Table 19. Antibodies used in IHC staining and their dilution. ....	92
Table 20. Buffers and solutions used in IHC and their compositions. ....	93
Table 21. Calculation of fold change in gene expression using the $2^{-\Delta\Delta C_t}$ method. ....	111
Table 22. Demographic variables of controls and AD patients. ....	197
Table 23. Regression analysis of the relationship between cognitive function, the level of serotonin proteins and AD-pathological proteins. ....	203

## List of Abbreviations

4-HN	4-Hydroxynonenal
5-HIAA	5-Hydroxyindolel acetic acid
5-HT	5-Hydroxytryptamine
5-HTP	5-hydroxytryptophan
5-HTT	5-HT transporter
5-HTTLPR	5-HT transporter-linked polymorphic region
8-HG	8-Hydroxyguanine
A $\beta$	Amyloid $\beta$
ABC	Avidin-biotin-peroxidase complex
AC	Adenylyl cyclase
ACh	Acetylcholine
AChE	Acetylcholinesterase
AChEIs	Acetylcholinesterase inhibitors
AD	Alzheimer's disease
ADL	Activities of daily living
AF	Alexa Fluor
AGEs	Advanced glycation end products
AICD	APP intracellular domain
AMPK	Adenosine monophosphate-activated protein kinase
ANOVA	Analysis of variance
APC	Allophycocyanin
ApoE	Apolipoprotein E
APP	Amyloid precursor protein
APS	Ammonium per sulphate
ATP	Adenosine triphosphate
BA09	Brodmann area 09
BACE1	$\beta$ -site APP cleaving enzyme 1
BBB	Blood brain barrier
BDNF	Brain derived neurotrophic factor
BLAST	Basic local alignment search tool
bp	Base pair
BPSD	Behavioural and psychological symptoms of dementia
BSA	Bovine serum albumin
CA	<i>Cornu ammonis</i>
CAA	Cerebral amyloid angiopathy
CAMCOG	Cambridge Cognition Examination
CaMKII	Ca <sup>2+</sup> /calmodulin-dependent kinase type II
cAMP	Cyclic adenosine monophosphate
CDKs	Cyclin dependant kinases
cDNA	Complementary deoxyribonucleic acid
CDS	Coding sequence
ChAT	Choline acetyltransferase
CNS	Central nervous system
CREB	cAMP-responsive element binding protein
CST	Cell Signalling Technology
Ct	Cycle threshold
DAB	Diaminobenzidine
DAG	Diacylglycerol
DAPI	Diamidino-2-phenylindole
DMEM	Dulbecco's modified eagle medium
DMSO	Dimethyl sulfoxide
DTT	Dithiothreitol
ECL	Extracellular loop
EDTA	Ethylenediaminetetraacetic acid
EIF4A2	Eukaryotic translation initiation factor 4A2
Epac	Exchange protein directly activated by cAMP

ER	Endoplasmic reticulum
ERK <sub>1/2</sub>	Extracellular signal-regulated kinase 1 and 2
FACS	Fluorescence-activated cell sorting
FAD	Familial Alzheimer's disease
FBS	Foetal bovine serum
FDA	Food and Drug Administration
FFPE	Formalin-fixed paraffin-embedded
F/S	Filter sterile
GABA	$\gamma$ -aminobutyric acid
GalNAc	N-acetyl galactosamine
GAPDH	Glyceraldehyde 3-phosphate dehydrogenase
GFAP	Glial fibrillary acidic protein
GlcNAc	N-acetylglucosamine
GIPs	GPCR-interacting proteins
GPCR	G-protein coupled receptor
GRKs	GPCR kinases
GS	Glutamine synthetase
GSK3	Glycogen synthase kinase 3
GTP	Guanosine triphosphate
HEK293	Human embryonic kidney 293 cell line
Hcy	Homocysteine
HHcy	Hyperhomocysteinaemia
H <sub>2</sub> O <sub>2</sub>	Hydrogen peroxide
HPRT1	Hypoxanthine phosphoribosyl-transferase 1
ICC	Immunocytochemistry
ICL	Intracellular loop
IDO	Indoleamine dioxygenase
IFN- $\gamma$	Interferon- $\gamma$
IgG	Immunoglobulin G
IHC	Immunohistochemistry
IL	Interleukin
IP3	Inositol triphosphate
IUPHAR	International Union of Basic and Clinical Pharmacology
Jab1	Jun activation domain-binding protein-1
JNK	Jun N-terminal kinase
kb	Kilobase
kDa	Kilodalton
LB	Luria broth
LGIC	Ligand-gated ion channel
LSD	Lysergic acid diethylamide
LTD	Long-term depression
LTP	Long-term potentiation
MAO	Monoamine oxidase
MAOIs	Monoamine oxidase inhibitors
MAPK	Mitogen activated protein kinase
MCI	Mild cognitive impairment
MMPs	Matrix metalloproteinases
MMSE	Mini-Mental State Examination
MRI	Magnetic resonance imaging
mRNA	Messenger ribonucleic acid
mTOR	Mammalian target of rapamycin
MW	Molecular weight
NCBI	National centre for biotechnology information
NEB	New England Biolab
NeuN	Neuronal nuclear antigen
NFTs	Neurofibrillary tangles
NHERF	Na <sup>+</sup> /H <sup>+</sup> exchanger regulatory factor
NMDA	N-methyl-D-aspartate
NSB	Non-specific binding

NTs	Neuropil threads
OD	Optical density
OPTIMA	Oxford Project to Investigate Memory and Ageing
PBS	Phosphate buffered saline
PCR	Polymerase chain reaction
PE	Phycoerythrin
PEI	Polyethyleneimine
pERK <sub>1/2</sub>	Phospho-ERK <sub>1/2</sub>
PET	Positron emission tomography
PKA	Protein kinase A
PLC	Phospholipase C
PMD	Post-mortem delay
PMSF	Phenyl-methyl-sulfonyl fluoride
PS	Presenilin
PTMs	Post-translational modifications
PVDF	Polyvinylidene difluoride
qPCR	Quantitative PCR
RIPA	Radioimmunoprecipitation assay buffer
RLB	Radioligand binding
RNA	Ribonucleic acid
ROI	Region of interest
ROS	Reactive oxygen species
RT	Room temperature
RT-PCR	Reverse transcription PCR
SAD	Sporadic Alzheimer's disease
sAPP $\beta$	Soluble amyloid precursor protein $\beta$
SD	Standard deviation
SDM	Site-directed mutagenesis
SDS	Sodium dodecylsulphate
SDS-PAGE	Sodium dodecylsulphate-polyacrylamide gel electrophoresis
SEM	Standard error of mean
SERT	Serotonin transporter
SFM	Serum-free medium
SH-SY5Y	Human neuroblastoma cell line
SNP	Single nucleotide polymorphism
SNX27	Sorting nexin 27
SOB	Super optimal broth
SPs	Senile plaques
SSRI	Selective serotonin reuptake inhibitor
TAE	Tris-acetate-EDTA buffer
TCA	Tricyclic antidepressant
T/E	Trypsin/EDTA
TEMED	Tetra-methyl-ethylene-diamine
TGF- $\beta$	Transforming growth factor- $\beta$
TM	Transmembrane
TMDs	Transmembrane domains
TNF- $\alpha$	Tumour necrosis factor- $\alpha$
TPH	Tryptophan hydroxylase
TREM2	Triggering receptor expressed on myeloid cells 2
UDP	Uridine diphosphate
USB	Urea sample buffer
VMAT	Vesicular monoamine transporter
WHO	World Health Organisation

# **Chapter 1. Introduction**

## **1. Introduction**

### **1.1. Alzheimer's disease**

Alzheimer's disease (AD) is the primary cause of dementia in the elderly contributing to approximately two-thirds of dementia-affected patients worldwide (WHO, 2017). In 2018, the estimation of AD cases in the US alone was 5.7 million. This number continues to increase as the world sees a global increase in the ageing population (Alzheimer's Association, 2018). AD causes disability and worsening in the patient's quality of life, which may also affect the family caregivers particularly if they become entirely dependent on others for their basic needs. It has a substantial socioeconomic burden which increases with ageing, disease severity, late diagnosis and the presence of comorbid conditions.

AD is characterised by progressive cognitive decline, memory loss and neuropsychiatric symptoms, referred to as the behavioural and psychological symptoms of dementia (BPSD). These include depression, anxiety, apathy, psychosis and agitation (Francis et al., 2010, Lanctôt et al., 2001). The preclinical changes in the brain and the pathology of the disease could take effect 15 to 20 years before symptoms appear (Bateman et al., 2012, Villemagne et al., 2013). During this silent phase and due to early and minor changes in the neurones, the brain can compensate to maintain the neuronal functions and enable individuals to live normally. Nevertheless, there comes a point when the brain can no longer compensate for those changes leading to memory lapses and mild cognitive decline (Alzheimer's Association, 2018). At the advanced stage of the disease and following a massive neuronal loss, the whole brain shrinks, and the ventricles expand. The atrophy becomes obvious particularly in regions involved in the regulation of higher

cognitive functions, such as the prefrontal cortex and hippocampus (Francis et al., 1999). The patients show severe cognitive decline and ultimately need assistance with activities of daily living (ADL) (Alzheimer's Association, 2018).

#### **1.1.1. AD classification and risk factors**

AD can be classified based on both disease onset and the genetic factors into early-onset familial Alzheimer's disease (FAD) and, the more commonly occurring, late-onset sporadic Alzheimer's disease (SAD). The inherited FAD occurs earlier than SAD (before the age of 65 years) and is caused by mutations in three genes positioned on chromosomes 14, 1, and 21 encoding for the presenilin 1 (PS-1), presenilin 2 (PS-2) and amyloid precursor protein (APP) respectively (Amemori et al., 2015, Orlacchio et al., 2002, Rodriguez et al., 2012). Till today, there is a lack of knowledge regarding the main cause of SAD. However, multiple factors might trigger the disease pathology in vulnerable individuals with ageing identified as a fundamental risk factor. Other environmental factors may also contribute such as unhealthy lifestyles, limited social life and low education. Comorbidities such as psychological diseases, cardiovascular diseases, diabetes and brain trauma can increase the likelihood of developing AD or other types of dementia (Alzheimer's Association, 2018)

The most important genetic risk factor for the late onset SAD is the apolipoprotein E (ApoE) genotype. ApoE is a lipoprotein which transports and metabolises the circulating cholesterol and triglycerides in the blood and lymphatic system (Amemori et al., 2015). The ApoE gene is located on chromosome 19 and has three polymorphic alleles ( $\epsilon 2$ ,  $\epsilon 3$  and  $\epsilon 4$ ) with protein isoforms that vary by a single amino acid in two positions 112 and 158. Both positions contain cysteine ( $\epsilon 2$ ), cysteine and

arginine ( $\epsilon 3$ ) or both arginine ( $\epsilon 4$ ) (Liu et al., 2013, Riedel et al., 2016). This variation leads to differences in ApoE's structure and function. Inheriting one copy of the ApoE4 allele ( $\epsilon 2/\epsilon 4$  and  $\epsilon 3/\epsilon 4$  heterozygous genotypes) increases the risk of developing AD by threefold, but it increases by 15 fold in those carriers of two copies of the ApoE4 allele ( $\epsilon 4/\epsilon 4$  homozygous genotype) (Amemori et al., 2015). Furthermore, the homozygous ApoE4 carriers display significantly higher accumulation of the amyloid  $\beta$  ( $A\beta$ ) plaque in their brains than the non-carriers (Rius-Perez et al., 2018). ApoE2 or ApoE3 proteins bind to the insoluble form of the  $A\beta$  plaque facilitating its clearance through the blood brain barrier (BBB) or by enzymatic degradation. However, ApoE4 has a lower binding affinity to  $A\beta$  and thus enhances  $A\beta$  aggregation (Dong et al., 2012).

Furthermore, whole genome sequencing studies of AD have identified another rare genetic risk factor for AD in the gene encoding for triggering receptor expressed on myeloid cells 2 (*TREM2*) (Guerreiro et al., 2013, Jonsson et al., 2013). A single nucleotide polymorphism (SNP) in the *TREM2* gene causes a substitution of arginine to histidine at position 47 (R47H). TREM2 is a cell surface receptor expressed in microglia and implicated in the inflammatory microglial response to AD pathology (Kametani and Hasegawa, 2018). It facilitates microgliosis and microglia phagocytic activity which sequesters the  $A\beta$  plaques and suppresses cytokines release (Wang et al., 2016).

Moreover, elevated blood homocysteine (Hcy) level is a modifiable risk factor of AD. Hcy is a sulphur containing amino acid synthesised in the methionine cycle (Zhuo et al., 2011). When the Hcy level is high, it converts to cysteine or remethylates to methionine by the aid of B vitamins as cofactors (Zhuo et al., 2011).

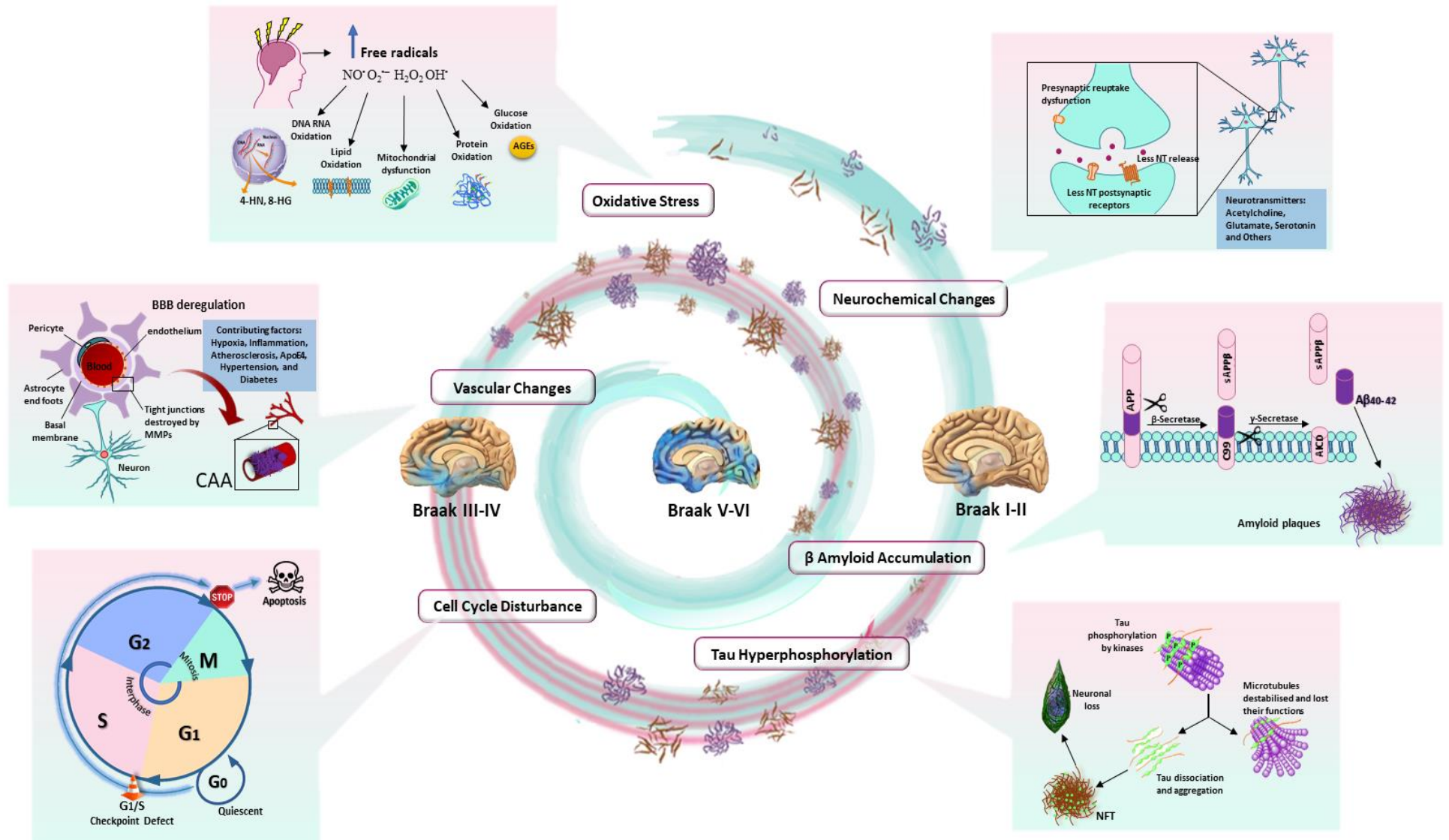


Low dietary intake of these vitamins in a transgenic mouse model of AD increases the Hcy level which is accompanied by an increase in brain amyloidosis (Zhuo and Pratico, 2010). Therefore, in the absence of a genetic cause, dietary enrichment of these cofactors could be useful in managing hyperhomocysteinaemia (HHcy) (Morris, 2003). The deleterious effects of HHcy in the brain are attributed to its induction of vascular endothelium dysfunction, ischaemia, cerebral angiopathy, neurotoxic effect of A $\beta$ , oxidative stress and tau phosphorylating kinases (Kim and Lee, 2014, Smith and Refsum, 2016). A longitudinal cohort study (Oulhaj et al., 2010) revealed a concentration-response association between baseline homocysteine levels in AD patients and their cognitive score as assessed by the Cambridge Cognition Examination (CAMCOG). Higher homocysteine levels were associated with faster cognitive decline predominantly after the age of 75 years (Oulhaj et al., 2010).

### **1.1.2. Pathological mechanisms involved in AD**

AD pathology consists of extraneuronal depositions of amyloid- $\beta$  (A $\beta$ ) and intraneuronal hyperphosphorylated tau lesions that form the neuritic elements of senile plaques (SPs) and neurofibrillary tangles (NFTs), respectively (Rodriguez et al., 2012). These pathological hallmarks are used to confirm the diagnosis of AD at post-mortem examination. Many mechanisms have been postulated to contribute to the pathogenesis of AD such as; neurochemical changes, vascular changes, oxidative stress and cell cycle disturbance. Despite the abundance of evidence that substantiate the implication of these mechanisms in disease pathology, their relative chronological orders in disease evolution remain ambiguous. Any of these mechanisms alone is insufficient to cause the disease, but rather the complex

interactions between them can trigger the development of pathology in vulnerable individuals. Summary of those mechanisms is shown in **Figure 1**.



## **Figure 1. The pathological mechanisms and evolution of AD**

*The oxidative stress generated increases the formation of free radicals resulting in oxidation of the cellular components and impairment of energy metabolism. ROS damage the neurones by oxidising cellular components including lipids, proteins, glucose and DNA, leading to their abnormal functions. Neurotransmitter systems such as the cholinergic, glutamatergic and serotonergic systems are affected in AD. Generally, the expression of some protein components of those systems is reduced particularly at a late stage of AD. Their functional components in the synapse are reduced as the neurones degenerate. The AD hallmarks; amyloid  $\beta$  and phospho-tau gradually accumulate outside and inside the neurones. In AD, the APP is cleaved by  $\beta$ - and  $\gamma$ -secretases which leads to amyloid plaques accumulation. The tau protein is hyperphosphorylated which lowers its binding affinity to microtubules, disturbing protein trafficking and signal propagation and ultimately leads to neuronal apoptosis. These pathological proteins accumulate and become distributed differentially in the brain, representing Braak stages I-VI. Mitogenic stimuli enforce the neurones to leave the quiescent phase and progress down a path of no return. This continues to the G<sub>2</sub> pre-mitotic phase, at which point the neurones will die. Dysfunction of the neurovascular unit of the brain barrier causes toxin accumulation in the brain and cerebral vessels. The junctional proteins in these units are degraded by MMPs, which increase in AD, thus leading to the alterations in BBB permeability. 4-HN: 4-Hydroxynonenal, 8-HG: 8-Hydroxyguanine, AGEs: Advanced glycation end products, A $\beta$ : Amyloid  $\beta$ , AICD: APP intracellular domain, BBB: Blood-brain barrier, CAA: Cerebral amyloid angiopathy, MMPs: Matrix metalloproteinases, NT: Neurotransmitter, sAPP $\beta$ : Soluble amyloid precursor protein  $\beta$ . This figure is constructed using the neuroscience toolkit purchased from motifolio.com. The swirl shape background is adapted from Ramos-Cejudo et al. (2018).*

#### *1.1.2.1. Amyloid $\beta$ ( $A\beta$ ) deposits*

The amyloid precursor protein (APP) is a transmembrane protein involved in the regulation of synaptic plasticity and neuronal interactions. APP undergoes two alternate proteolytic pathways; namely amyloidogenic and non-amyloidogenic proteolysis (Dong et al., 2012, LaFerla et al., 2007). In amyloidogenic proteolysis, APP is initially cleaved by  $\beta$ -secretase 1 (BACE1) to release a soluble fragment (sAPP $\beta$ ) leaving the C-terminal 99 amino acid fragment attached to the membrane. Subsequently,  $\gamma$ -secretase cleaves the membrane-bound C99 into several fragments from 38 to 43 residues (**Figure 1**) (Dong et al., 2012). The primary component of amyloid plaques is A $\beta_{40}$  and A $\beta_{42}$ . The former represents the majority of the plaque while the latter is less abundant but the more toxic variant that forms more aggregates in the plaque than A $\beta_{40}$  (Selkoe, 2001). The presence of A $\beta$  deposits hinders neuronal crosstalk, long-term potentiation (LTP) and synaptic plasticity while also stimulating the proliferation of surrounding astrocytes and its associated inflammatory response (astrogliosis) (Selkoe and Hardy, 2016).

On the other hand, the non-amyloidogenic proteolysis pathway is mediated through  $\alpha$ -secretase which precludes the formation of A $\beta$  because it cleaves the APP at amino acid position 83 and producing soluble APP (sAPP $\alpha$ ) and a membrane-bound C-terminal fragment (C83). This fragment is further cleaved by  $\gamma$ -secretase which generates soluble peptide (p3). The sAPP $\alpha$  exhibits neuroprotective effects through the increase in neuronal survival rates and inhibiting neurotoxicity and apoptosis (Dong et al., 2012, LaFerla et al., 2007). In the inherited form of AD, genetic mutations cause domination of the amyloidogenic proteolysis via  $\beta$ -secretase and  $\gamma$ -secretase and therefore increases in toxic amyloid production (Hardy and Selkoe,

2002). Whereas, the sporadic form of AD is associated with a reduction in A $\beta$  clearance, hence gradual A $\beta$  accumulation (Selkoe and Hardy, 2016).

Notably, Braak and Braak (1991) classified AD evolution according to A $\beta$  deposits into three stages ranked from A to C in accordance with the density of A $\beta$  deposits. Nevertheless, the A $\beta$  deposits are less significant regarding the differentiation of the stage of the disease than tau-related staging due to variability of amyloid distribution in individual patients, particularly in the early disease stages. The amyloid deposits are not limited to demented brains but are also present in normal brains and on occasion the level of the deposits in AD brains can be less than in normal brains, thereby indicating that the increasing amyloid burden is a phenomenon of normal ageing rather than being linked to AD severity (Li et al., 2008).

#### ***1.1.2.2. Hyperphosphorylated Tau***

Tau is a microtubule-associated protein predominantly expressed in the neurones (Gendron and Petrucelli, 2009). It stabilises the neuronal morphology by binding to microtubule ( $\beta$ -tubulin) and in doing so supporting neuronal outgrowth and maintaining the axonal elongation (Ballatore et al., 2007, Kitagishi et al., 2014). It also regulates neuronal signal transmission and transport along the axon (Gendron and Petrucelli, 2009). In AD, tau is hyperphosphorylated at several serine (S) and threonine (T) amino acid sites, and this lowers its binding affinity to microtubules, consequently destabilising the microtubules and disturbing protein transportation inside the neurones (Kitagishi et al., 2014). As a result, dysfunctional tau accumulates to form inclusions that physically disrupt the axonal trafficking and signal propagation ultimately leading to neuronal apoptosis (Ballatore et al., 2007, Garcia and Cleveland, 2001, Wischik et al., 2014). The tau lesions formed are either

located in the neuronal cell bodies and are known as neurofibrillary tangles (NFTs), or in the axons and dendrites where they are referred to as neuropil threads (NTs) (Kametani and Hasegawa, 2018).

Numerous kinases contribute to tau hyperphosphorylation, including glycogen synthase kinase 3 (GSK3), adenosine monophosphate-activated protein kinase (AMPK), cyclin-dependent kinase 2 and 5 (CDK2/5) and  $\text{Ca}^{2+}$ /calmodulin-dependent protein kinase II (CaMKII) (Kitagishi et al., 2014, Nagy, 2005, Tam and Pasternak, 2017). Contrastingly, down-regulation of the phosphatases is indirectly attributed to the accumulation of phosphorylated-tau, and so explains the presence of low expression and activity of phosphatase 2A in AD-affected brains (Voronkov et al., 2011).

Based on the transgenic AD mouse models, the cross-talk between the  $\text{A}\beta$  and tau is significant in which there is substantial evidence that  $\text{A}\beta$ , at least in part, exerts its neurotoxicity via tau phosphorylation and tangle formation through the Fyn kinase (Chabrier et al., 2014). Furthermore, reducing the tau expression showed beneficial effects in hAPP mice, which develop  $\text{A}\beta$ -plaques and synapse loss, by prevented the learning and memory deficits, synaptic transmission deficits and the spontaneous epileptiform activity (Roberson et al., 2011). The effect of overexpressed human wild-type tau on  $\text{A}\beta$  plaque was studied by crossing the APP/PS1 mice with rTg21221 mice. Accumulation of misfolded tau exacerbates the  $\text{A}\beta$  pathology as it increases in the plaque size and the neurite deformation (Jackson et al., 2016).

The relationship between the AD histopathologic lesions and the cognitive status was studied by Nelson and others (2007). This group found that higher accumulation of NFTs in post-mortem cortices of AD patients was associated with greater pre-

mortem cognitive deterioration. AD progresses gradually and cumulatively; however, the rate of progression may vary between the patients. In accordance with the distribution pattern of tau positive-lesions in the AD brain, Braak and Braak (1991) differentiated AD severity into 6 overlapping stages (I-VI). The transentorhinal stages, including stages I and II which are characterised by mild lesions mainly affecting the transentorhinal cortex, and few changes in the entorhinal layer Pre  $\alpha$ , as well as small areas of hippocampal *Cornu ammonis* (CA1) and of the anterodorsal nucleus of the thalamus. The neocortical regions remain mostly unaffected. The patients at this stage are usually asymptomatic. In limbic stages III and IV, the tau lesions increase, and ghost tangles appear throughout the entorhinal regions. Furthermore, the lesions extend to include limbic regions causing mild to moderate changes in the hippocampal multipolar CA4 neurones and pyramidal neurones of the subiculum. The neocortex remains devoid of these changes but may occasionally show mild NFT lesions in cortical layers III and V. Patients at the limbic stages have mild cognitive symptoms, for instance, short-term memory deficit. As the disease progresses to stages V and VI, the lesions of the previous entorhinal and limbic stages become more profound. Significant loss of entorhinal neurones is associated with large numbers of ghost tangles. Tau lesions extend to affect pyramidal neurones in the cortex; thus, the term neocortical stages used to refer to them. Most of the brain regions are affected in the late stages leading to severe cognitive impairment and long-term memory loss (**Figure 1**).



### ***1.1.2.3. Neurochemical changes***

#### **Cholinergic changes**

Acetylcholine (ACh) has many pivotal roles in the central nervous system (CNS) and the peripheral organs. ACh is synthesised by choline acetyltransferase (ChAT) in the presynaptic nerve terminal and stored to be released upon neuronal stimulation. ACh mediates its action through stimulation of two types of receptors; nicotinic and muscarinic receptors. The cholinergic neuronal cell bodies are localised in the nucleus basalis of Meynert which send their neuronal projections to various brain regions throughout the forebrain, midbrain and brain stem (Mesulam et al., 2004, Schliebs and Arendt, 2011).

It is well recognised that AD is accompanied with degeneration in the nucleus basalis cholinergic neurones, which causes loss in the cholinergic input to many parts of the cortex and hippocampus (Francis et al., 2010, Giacobini, 2003). AD-related neuropathology; SPs and NFTs, have been associated with the loss of the cholinergic neurones. The ACh synthesis is also reduced due to the reduction in choline uptake and the ChAT enzyme activity (Francis et al., 1999, Potter et al., 2011). The early pharmacological interventions for AD targeted acetylcholinesterase (AChE) which is responsible for deactivation of ACh. AChE inhibitor (AChEIs) increase the ACh levels in the synapse leading to improvement in the behavioural and psychological symptoms of AD (Kandimalla and Reddy, 2017). However, the activity of AChE is also reduced in parallel with the increase in AD severity (Giacobini, 2003). This might explain why AChEIs are more effective for mild and moderate AD but less effective for severe AD.

Results of a recent positron emission tomography (PET) study reported by Sabri et al. (2018) has revealed that the expression of the  $\alpha 4\beta 2$  nicotinic receptor was lower in mild AD compared to controls. This reduction was predominant within the cholinergic projections of the basal forebrain and hippocampal regions, and it is directly correlated with a decline in cognitive functions mainly episodic and working memory. A longitudinal cohort study revealed no change in the density of the muscarinic  $M_1$  receptor in the frontal and temporal cortex of postmortem AD while the receptor coupling to the G-protein was remarkably reduced in the frontal cortex only, and this reduction in the receptor coupling was associated with the degree of cognitive decline (Tsang et al., 2006).

Several *in vitro* studies demonstrated the toxic effect of  $\beta$  amyloid on the nicotinic receptor; for example, the use of  $A\beta$  peptides at nanomolar concentrations (0.1-100 nM) for 7 days can reduce the expression of the nicotinic receptor in the PC12 cell line (Guan et al., 2001). These peptides can also block the ACh mediated response on the neuronal  $\alpha 7$  nicotinic receptor in the primary neurones of the rat hippocampus (Liu et al., 2001). Various studies have confirmed the binding affinity of  $A\beta$  to the  $\alpha 7$  receptor and inhibition of the receptor-mediated calcium activation and acetylcholine release (Wang et al., 2000a, Wang et al., 2000b). Nicotine and nicotinic agonists currently show beneficial outcomes in terms of cognition and attention improvements in mild cognitive impairment (MCI) and AD patients as evaluated by Levin et al. (2006) and Newhouse et al. (2012). Nicotine analogues showed neuroprotective effects against  $A\beta_{1-42}$  and glutamate-induced neurotoxicity in rat cortical neurones (Gao et al., 2014).

## **Glutamatergic changes**

Glutamate is the main excitatory neurotransmitter of the cortical and hippocampal neurones (Francis, 2003). It is involved in the cognitive process and plays a role in synaptic plasticity. Glutamate is synthesised in nerve terminals from glutamine and aspartate, released upon neuronal depolarisation, and its action is tightly regulated by rapid reuptake to the presynaptic nerve terminal via the vesicular glutamate transporters, and by glutamine synthetase (GS) which converts glutamate to glutamine (Butterfield and Pocernich, 2003, Revett et al., 2013).

The loss of glutamatergic pyramidal neurones is a crucial feature of AD. Initial loss begins with the entorhinal and hippocampal CA1 regions and ends with the neocortex layers III and V (Francis et al., 2010, Revett et al., 2013). Likewise, both ionotropic and metabotropic glutamatergic receptor densities are reduced in AD. Radioligand binding of metabotropic receptors was assessed in AD cases, and the results indicated that the metabotropic receptor expression was decreased in early Braak stages I and II even before the involvement of the frontal cortex and that drastic reduction appeared at the neocortical stages (Albasanz et al., 2005). Moreover, the ionotropic N-methyl-D-aspartate receptor (NMDA) receptor binding sites were assessed by quantitative autoradiography, and the results showed that NMDA receptors were down-regulated in the hippocampal CA1 region in AD patients (Ulas et al., 1992). This reduction was not correlated with the deposition of the AD pathological proteins (Ulas et al., 1992).

Despite the reduction in glutamate receptors, the level of glutamate in the synapse is increased due to the defect in the regulatory feedback mechanism. Reduction in the expression and function of the reuptake transporter in the surrounding astrocytes

can lead to inadequate removal of the glutamate from the synapse, and this causes persistent activation of the remaining NMDA receptor and impairs their capability for long-term potentiation (LTP) causing cognitive dysfunctions (Anand et al., 2014, Francis et al., 2010, Segovia et al., 2001). Further increase in the glutamate level can become more pathological by elevating the intracellular  $\text{Ca}^{+2}$  levels over the buffering capacity of the cellular organelles; such as the endoplasmic reticulum (ER). This can lead to excitotoxicity and neuronal loss (Francis et al., 2010). Antagonising the NMDA receptor can reduce excitotoxicity whilst maintaining the normal activation of this receptor which is necessary for LTP (Benhamu et al., 2014).

### **Serotonergic changes**

In the AD brain, substantial loss of serotonergic neurones in raphe nuclei has been demonstrated by Chen et al. (2000). It is not clear yet whether this denervation is a cause contributing to disease development and progression or a consequence of overall neuronal loss in AD (Francis et al., 2010, Ramirez, 2013). The detrimental effects of amyloid pathology mostly affect serotonergic projections, which in turn leads to weakness in the neuronal connection and subsequent degeneration of the axons and cell bodies (Liu et al., 2008). The tau positive cell density is significantly increased in AD patients in correlation to the decrease in serotonergic neuronal density (Hendricksen et al., 2004). On the other hand, the level of 5-HT and its metabolite 5-HIAA (5-hydroxyindolacetic acid) were found to be significantly decreased in two cortical Brodmann areas (BA10 and BA20) (Garcia-Alloza et al., 2005).

The variations in 5-HT transporter (SERT, 5-HTT) or receptors might be correlated to cognitive and non-cognitive symptoms of the disease. For example, a lower SERT level was detected in the midbrain, striatum and thalamus particularly in depressed in comparison to non-depressed AD patients (Ouchi et al., 2009). It was also reduced in the mesial temporal cortex of AD patients (Marner et al., 2012) and in cortical and limbic regions in MCI cases which is a prodromal stage of AD (Smith et al., 2017). A clinical longitudinal study showed that patients with MCI have high risk of developing AD as their cognitive function rapidly declined, which suggested that these conditions were closely linked (Boyle et al., 2006).

Most of the serotonin receptors are reduced in the AD brains, and this reduction is correlated with the disease-associated symptoms and disease progression. The binding densities of 5-HT<sub>1A</sub> receptors in the hippocampus were reduced in AD patients, but the reduction was more profound in depressed patients as Lai et al. (2011) demonstrated in their study. Further, PET binding of 5-HT<sub>1A</sub> receptors showed a decrease in the receptor density in the raphe nuclei and hippocampus, and this was directly correlated with a decrease in the cognitive functions and glucose utilisation but inversely with neuropathological AD burdens (Kepe et al., 2006).

The 5-HT<sub>1B/1D</sub> receptors were also reduced in the frontal and temporal cortices obtained from AD patients and also correlated to the reduction in the Mini-Mental State Examination (MMSE) score (Garcia-Alloza et al., 2004). Lai et al. (2005) assessed the density of 5-HT<sub>2A</sub> receptors in these cortices using [<sup>3</sup>H]-ketanserin. They showed a marked loss of this receptor in both cortices particularly in severe cases, but the extent of receptor loss in the temporal cortex was directly correlated to the rate of cognitive decline. Moreover, a gene associations study found that the

5-HT<sub>2A</sub> receptor's gene exhibited SNP (102T/C) in AD patients who had psychosis, agitation or aggression (Assal et al., 2004). However, radioligand labelling of the 5-HT<sub>3</sub> receptors by [<sup>3</sup>H]-(S)-zacopride showed that there was no change in the density of 5-HT<sub>3</sub> receptor in the limbic region of AD patients (Barnes et al., 1990). An early work by Reynolds et al. (1995) studied the density and distribution of the 5-HT<sub>4</sub> receptor in several neurodegenerative diseases including AD using [<sup>3</sup>H]-GR 113808 binding. The results revealed there was a significant decrease in the 5-HT<sub>4</sub> receptor's density in the hippocampus of AD cases.

Clinical observations of serotonin modulating drugs suggest the possible relationship between the serotonergic changes and the neuropsychiatric aspects of AD and their importance for managing BPSD. Selective serotonin reuptake inhibitors (SSRIs), such as fluoxetine and citalopram, can manage the depression and slow down the progression of MCI to AD (Bartels et al., 2018). By using a transgenic PS1APP mouse model of AD, Cirrito and others found that the administration of SSRIs can reduce the brain A $\beta$  level in interstitial fluid by activating the extracellular regulated kinase 1 and 2 (ERK<sub>1/2</sub>) signalling cascade (Cirrito et al., 2011). The activation of ERK<sub>1/2</sub> can stimulate  $\alpha$  secretase activity *in vitro* (Kojro et al., 2006). Furthermore, retrospective evaluation of healthy elderly individuals who used SSRIs for five years was accompanied by a marked decrease in the cortical amyloid burden (Cirrito et al., 2011). A clinical study of Mowla et al. (2007) revealed that the concurrent use of fluoxetine and rivastigmine improved the cognition and ADL in AD patients. Atypical antipsychotics, like risperidone and olanzapine, are effective against agitation, aggression and psychosis accompanied AD. They have an affinity to antagonise 5-HT<sub>2</sub> and 5-HT<sub>6</sub> receptors besides the dopamine D<sub>2</sub> receptor (Ballard and Waite, 2006). Moreover, buspirone, a 5-HT<sub>1A</sub>

agonist, is also considered a non-sedating anxiolytic in AD patients (Cooper, 2003, Desai and Grossberg, 2003). Further details on the role of serotonin in the CNS will be discussed in detail later.

#### ***1.1.2.4. Vascular changes***

Dysfunction of the vascular system has been linked to AD pathology. Accumulation of the insoluble  $\beta$ -amyloid is aggravated by dysregulation of the blood brain barrier (BBB), capillary hypoperfusion and inflammation (Rius-Perez et al., 2018). The BBB has highly selective permeability which controlled by endothelial junctional proteins to prevent harmful substances in the blood from passing to the brain. It is also the site of excretion of neurotoxins from the brain to the blood circulation. These junctional proteins are degraded by matrix metalloproteinases (MMPs), which increase in AD, thus leading to the alterations in BBB permeability (Rius-Perez et al., 2018, Zenaro et al., 2017). Cerebral amyloid angiopathy (CAA) is a pathological condition that manifests when the clearance of  $A\beta$  is impaired due to dysfunction of the BBB leading to accumulation of  $A\beta$  on the wall of the cerebral blood vessels (Bell and Zlokovic, 2009). It usually accompanies the neuritic pathology of AD. An immunohistochemistry study by Attems et al. (2007) found that the incidence and severity of CAA are significantly increased with increasing AD pathology, particularly in the occipital lobe.

Many chronic diseases such as hypertension, atherosclerosis and diabetes cause cerebral hypoperfusion damaging the cerebral microvasculature especially if they are co-morbid with AD and may eventually lead to cerebral hypoxia. The hypoxia promotes  $A\beta$  production via up-regulation of  $\beta$ -secretase and increasing the oxidative stress of the neurones (Rius-Perez et al., 2018). In response to AD cerebral

hypoxia, vascular endothelial cells are activated and release many angiogenic factors that activate the surrounding astrocytes and microglia (Grammas, 2011). Despite the persistence of overwhelming angiogenic stimuli, angiogenesis is not likely to occur in the AD brain. This, in turn, prevents the physiological feedback inhibition of endothelium activation leading to irreversible endothelium dysfunction. The ultimate loss of the neurones can occur due to over-reactive microglia and astrocytes (Grammas, 2011). Additionally, alterations in metabolic functions of the vascular system in AD can stimulate the secretion of several inflammatory mediators such as; nitric oxide, thrombin, tumour necrosis factor- $\alpha$  (TNF- $\alpha$ ). It also increases the release of interleukins (IL-1 $\beta$ , IL-6 and IL-8), transforming growth factor- $\beta$  (TGF- $\beta$ ) and interferon- $\gamma$  (IFN- $\gamma$ ) (Grammas, 2011, Rius-Perez et al., 2018). These inflammatory mediators can stimulate the astrocytes to induce A $\beta$ / tau production which leads to further inflammation in the blood vessels (Zhao et al., 2011).

#### ***1.1.2.5. Oxidative stress***

Ageing increases the oxidative stress in vulnerable organs particularly the brain due to its high lipid content and high oxygen and glucose demands (Huang et al., 2016). Oxidative stress is a complex and damaging event in which the scavenging of free radicals, e.g. reactive oxygen species (ROS), by antioxidants is reduced due to impairment in cellular energy metabolism in mitochondria, transition metals such as iron or copper, calcium homeostasis, excitotoxicity or injury (Huang et al., 2016, Mattson, 2004). Antioxidants such as glutathione can detoxify the free radicals by donating electrons while antioxidant enzymes such as glutathione peroxidases prevent the oxidative damage by free radical hydrolysis (Feng and Wang, 2012).



Oxidative stress could emerge as a cause or consequence of the disease pathology (Perry et al., 2002). ROS damage the neurones by oxidising cellular components including lipids, proteins, glucose and DNA, leading to their abnormal functions (Huang et al., 2016). The oxidation products include; 4-hydroxynonenal (4-HN), isoprostanes, protein carbonyls, 8-hydroxyguanosine (8-HG) and advanced glycation end products (AGEs) (Gella and Durany, 2009). Generally, these products are considered markers for oxidative stress of AD as they colocalise with A $\beta$  deposits and NFTs (Cheignon et al., 2018, Gella and Durany, 2009). Oxidation of one cellular component can initiate endless oxidative events due to their complex interactions. For example, lipid peroxidation products could disrupt the phospholipid membrane and conjugate with many membrane proteins leading to alterations of their structures and physiological functions (Cheignon et al., 2018).

In neuroblastoma cell lines, membrane lipid peroxidation caused by A $\beta$  in the SH-SY5Y cells can induce cholinergic changes by reducing the expression of the nicotinic receptor (Qi et al., 2005). In addition, Tamagno et al. (2003) found the exposure of the SK-N-BE cells to A $\beta$  peptide stimulated the production of 4-HN and hydrogen peroxide (H<sub>2</sub>O<sub>2</sub>) which induced stress-activated protein kinases; c-Jun N-terminal kinase (JNK) and mitogen-activated protein kinase p38 (MAPK) thereby leading to apoptotic cell death.

#### ***1.1.2.6. Cell cycle dysregulation***

The cell cycle is a tightly regulated process of cell division consisting of several checkpoints to detect any DNA damage and arrest the cells until such damage is repaired (for a review see Frade and Ovejero-Benito, 2015). Dysregulation of the neuronal cell cycle is deemed as a further pathological mechanism that contributes to

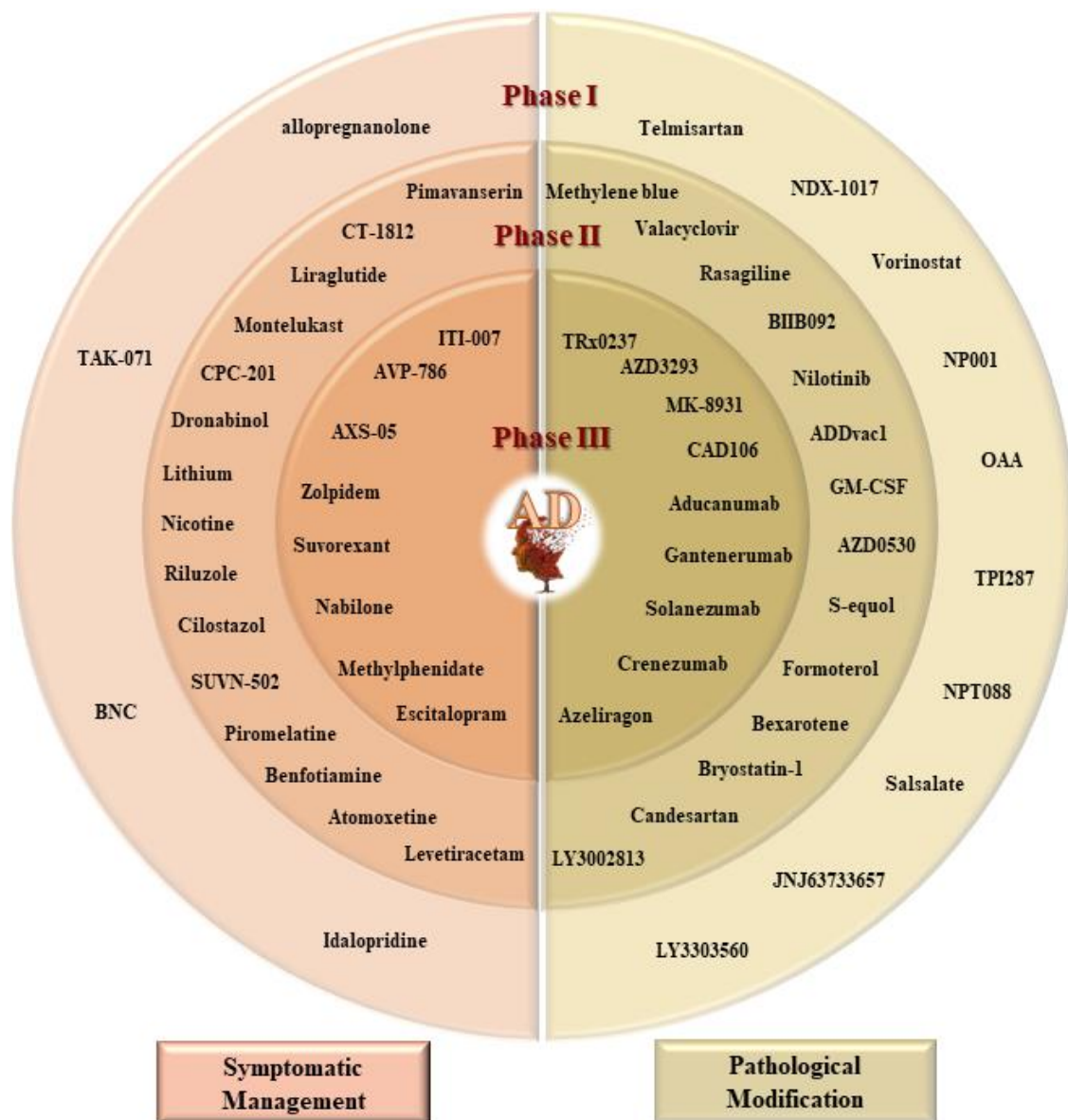
the development of AD. It is initiated on exposure of the neurones to mitogenic stimuli such as ageing, injury, hypoxia, elevation of Hcy level and synaptic loss. These mitogens can enforce the terminally differentiated neurones to re-enter the cell cycle (Lee et al., 2009a, Nagy, 2007). In AD, and due to a defect in the G<sub>1</sub>/S checkpoint, the neurones can elude this checkpoint and progress through interphase (**Figure 1**) (Nagy, 2007). Since the differentiated neurones at the G<sub>0</sub> phase are incapable of dividing, they activate the mitotic machinery and stimulate CDKs to predispose the cell to cell division (Moh et al., 2011, Nagy, 2007, Nagy et al., 1998). These kinases also contribute to the phosphorylation of the tau protein and thus NFTs accumulation (Moh et al., 2011).

Mitotic markers, for instance, Ki-67 nuclear protein, cyclins, CDKs, and CDK inhibitors are ectopically expressed in vulnerable neurones of AD brains (Nagy et al., 1998, Vincent et al., 1997). Neuronal DNA replication and the progression to S-phase were detected by Bonda et al. (2009) through evaluation of minichromosome maintenance complex component-2 which is a licensing component for DNA replication. Others reported the presence of binucleated neurones in the hippocampus of AD patients (Zhu et al., 2008). Ultimately, as a result of the inability of the neurones to complete the initiated cycle and their prolonged presence at G<sub>2</sub> phase (pre-mitosis), the neurones encounter apoptosis or develop AD-related pathology (Nagy et al., 1998).

### **1.1.3. AD therapies and clinical trials**

The clinically approved drugs for AD are involved in the modulation of the cholinergic and glutamatergic systems and include four AChEIs (tacrine, donepezil, rivastigmine, galantamine) and an NMDA receptor antagonist (memantine). Tacrine

is no longer available due to its hepatotoxicity (Godyn et al., 2016). Nevertheless, these drugs do not cure nor halt disease progression. Instead, they provide symptomatic management (Godyn et al., 2016). The history of AD drug developments is associated with many failures due to ineffectiveness or toxicity, even when many druggable targets are considered. The clinical trials for AD are still ongoing in the hope of identifying alternative therapies that can provide the patients with better therapeutic outcomes. **Figure 2** illustrates an update for various drugs under the clinical phases of investigation. There are two main therapeutic outcomes for AD; namely symptomatic management and disease modification. Symptomatic management is achieved by the previously approved drugs, although more drugs are still under investigation. The modification of AD by preventing or slowing its progression can be achieved by targeting the pathological mechanisms of the disease, immunotherapy or neuroprotection (Cummings et al., 2018). Notably, some of these drugs are already approved by the FDA for other therapeutic applications.



**Figure 2. Various anti-AD drugs are currently available in clinical trials and their therapeutic outcomes**

*The pathological modifications include disease-modifying therapies which can be classified according to their mechanisms or targets into anti-amyloid, anti-tau, anti-inflammatory, neuroprotective or immunotherapies, while the symptomatic management is neurotransmitter-based therapies which targeted Ach, glutamate, serotonin, GABA, norepinephrine, and dopamine to improve the behavioural and psychological symptoms associated with AD. Adapted from Cummings et al. (2018).*

## **1.2. Serotonin**

### **1.2.1. Serotonin discovery**

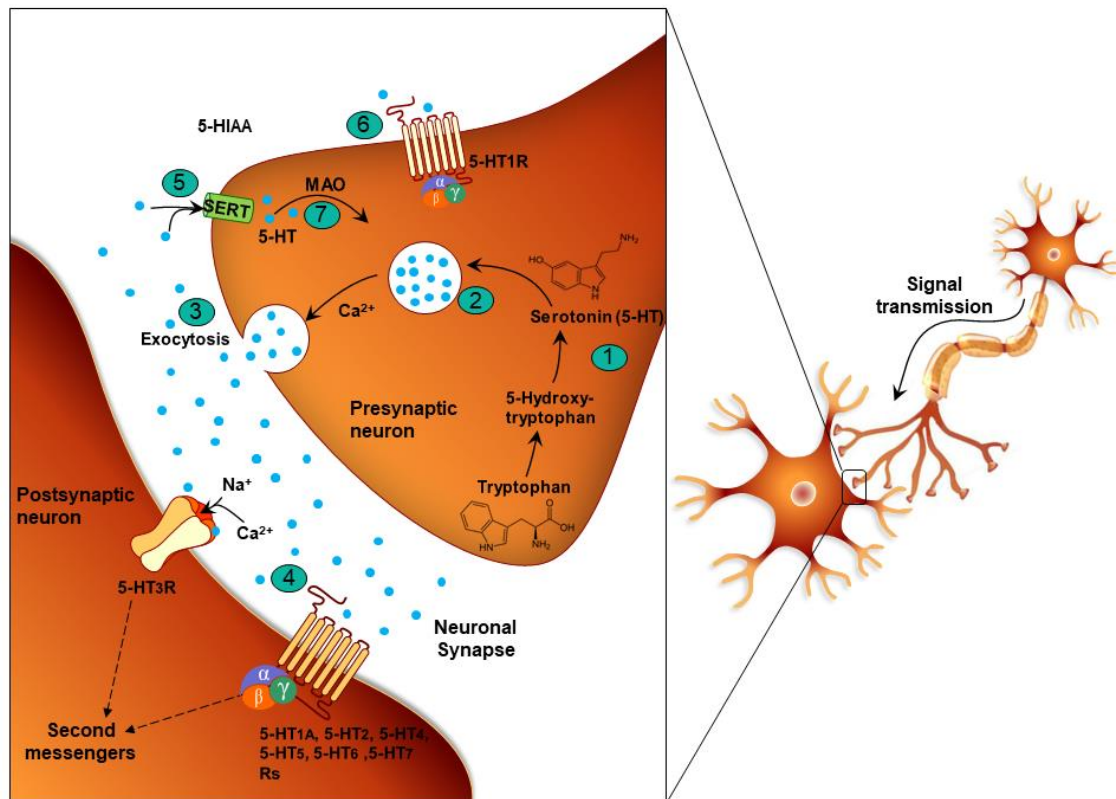
Serotonin (5-hydroxytryptamine, 5-HT) is an ancient monoamine. In the late 1930's, Vittorio Erspamer discovered the contractile function of an indole substance, extracted from gastric mucosa, on uterine smooth muscle naming it "enteramine" (Nichols and Nichols, 2008, Whitaker-Azmitia, 1999). This was until 1952 when he realised that enteramine indeed had the same entity to a pre-identified and isolated substance termed serotonin. Serotonin was named by Irvine Page and his co-researchers; Maurice Rapport and Arda Green. They isolated serotonin from the serum 'sero' as an unwanted vasoconstrictor or tonic substance 'tonin' after blood had clotted (Gothert, 2013, Whitaker-Azmitia, 1999). In 1952, Betty Twarog and Irvine Page identified the presence of serotonin in the mammalian brain. This finding was catapulted to a greater degree of importance when Dilworth Woolley discovered that the psychological actions of lysergic acid diethylamide (LSD) can modulated the action of serotonin in the brain. Subsequently, Woolley and Shaw (1954) proposed the role of serotonin in brain development and mental illnesses (Nichols and Nichols, 2008, Whitaker-Azmitia, 1999). This initiated the surge of endless research on serotonin and its actions in the body.

### **1.2.2. Serotonergic transmission**

5-HT, like many other neurotransmitters, is regulated by autoreceptors, enzymes and transporters. It is biochemically synthesised from the essential amino acid L-tryptophan via tryptophan hydroxylase (TPH). There are two isoforms of this enzyme; TPH-1 an enzyme that acts in the periphery, and TPH-2 which is mainly

expressed in the central serotonergic neurones (Walther et al., 2003). L-tryptophan is converted to 5-hydroxytryptophan (5-HTP) which subsequently decarboxylated to form 5-HT. Following its biosynthesis, serotonin is stored into vesicles and released upon neuronal stimulation leading to the propagation of an action potential through calcium influx and the eventual release of serotonin via exocytosis (Nichols and Nichols, 2008, Zhang et al., 2004). Serotonin stimulates pre-and post-synaptic receptors which initiate the downstream signalling cascades within the cells (**Figure 3**).

Tight regulation of 5-HT release is processed through 5-HT<sub>1</sub> autoreceptors which provide a system of negative feedback inhibition, thereby leading to a reduction in the release of serotonin (Mohammad-Zadeh et al., 2008). The action of serotonin is terminated by two main mechanisms; reuptake transporters and enzymatic degradation. The serotonin transporter (SERT) is the main regulator of the intensity and duration of the 5-HT signal (Zhou et al., 2007). It is expressed in serotonergic neurones and acts by the uptake of any released 5-HT, with Na<sup>+</sup> and Cl<sup>-</sup> into the presynaptic nerve terminal in an exchange with K<sup>+</sup> (Zhou et al., 2007). Once the 5-HT is transported into the neuron, it is either stored into vesicles by the vesicular monoamine transporter (VMAT) for recycling or metabolised by mitochondrial monoamine oxidase (MAO) and then by aldehyde dehydrogenase to the inactive metabolite; 5-HIAA which is used as an indicator for 5-HT turnover (Daubert and Condron, 2010, Tamir and Gershon, 1990).



**Figure 3. The metabolic cycle and regulation of serotonin neurotransmission**

*The metabolic cycle involves synthesis, storage and release of 5-HT (represented as small blue circles) into the synaptic cleft via exocytosis. Serotonin mediates its actions on presynaptic or post-synaptic receptors. Serotonin transmission is regulated by SERT which uptakes the released serotonin into the cytoplasm for recycling. Presynaptic 5-HT<sub>1</sub> receptors provide feedback inhibition for serotonin release. Cytoplasmic 5-HT is either stored into synaptic vesicles or enzymatically degraded. This figure is constructed using the neuroscience toolkit.*

### **1.2.3. Serotonin action and localisation**

Soon after serotonin discovery, many researchers identified the action and localisation of serotonin and its receptors. It possesses complex modulatory responses in many peripheral organs such as the gastrointestinal tract, platelets, cardiovascular system and most recently in bones (Ducy and Karsenty, 2010). In addition, it is a neuromodulator playing a role in the function of the CNS contributing to the increase or decrease of neuronal excitability based on the 5-HT receptors involved.

#### ***1.2.3.1. In the periphery***

Nearly, 95% of the total serotonin is synthesised and stored in enterochromaffin cells of the gut and, to a much lesser extent, in enteric neurones where it functions as a hormone and neurotransmitter respectively (Gershon, 2004). Many gastrointestinal functions including motility, reflexes, secretion, and neurotransmission are regulated by 5-HT via its receptors which act to differentially modulate these functions according to their types and localisations within the gut (Gershon and Tack, 2007). The abnormal regulation of the serotonin system is involved in the pathophysiology of gastrointestinal disorders, for instance, irritable bowel syndrome and chronic constipation (Manocha and Khan, 2012).

Platelets are the early site of serotonin extraction. Rather than synthesising it, platelets take up circulating serotonin by SERT. They then store it in dense granules to control its action and circumvent the free plasma serotonin from inducing harmful changes in blood pressure (Maurer-Spurej, 2005). The platelet-stored serotonin can maintain blood flow and regulate haemostasis. This stored serotonin is also released at the site of injury to promote platelets aggregation and vasoconstriction of blood



vessels (Brunton et al., 2011, Herr et al., 2017, Mohammad-Zadeh et al., 2008). Multiple factors control the action of 5-HT in the cardiovascular system; such as the size of the blood vessels, the stimulated receptors, the presence of injury and the sympathetic activity (Berger et al., 2009, Maurer-Spurej, 2005). The classical actions carried out are vasoconstriction and stimulation of heart contractions. However, 5-HT may also possess inhibitory effects via the release of endothelial nitric oxide or inhibiting sympathetic action on the heart and blood vessels (Brunton et al., 2011).

In addition, 5-HT and its receptors are expressed in various immune cells and regulate their functions. For example, an inflammatory response can trigger the release of serotonin from monocytes, macrophages and dendritic cells. Serotonin, in turn, will inhibit the production of TNF- $\alpha$  and the antigen-presenting capacity induced by IFN- $\gamma$ . It also increases the release of IL-1 $\beta$ , IL-6, IL-8 and causes T-cell activation, migration and proliferation in response to inflammation (reviewed in Herr et al., 2017).

Furthermore, 5-HT regulates bone remodelling by influencing the balance between osteoblast and osteoclast functions and proliferation. This role is based on the production source of serotonin in which gut-derived 5-HT can slow down bone growth, whereas brain-derived 5-HT decreases bone resorption and enhances bone formation (Ducy and Karsenty, 2010).

#### ***1.2.3.2. In the CNS***

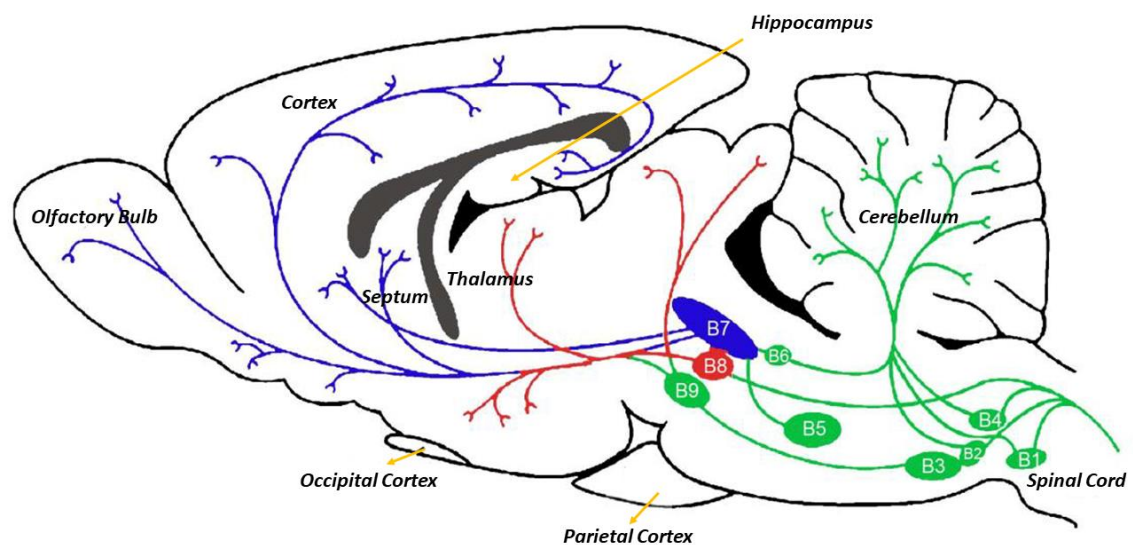
Serotonergic neurones originate from nine raphe nuclei, designated B1–B9, and located along the midline of the brainstem (Hensler, 2006, Lesch and Waider, 2012). These nuclei are clustered into two groups according to their localisations and neural

projections. The first caudal group, consists of B1, B2, B3 and B4 nuclei, confined in the caudal pons forming descending projections to the medulla oblongata, cerebellum and spinal cord (Lesch and Waider, 2012). The second rostral group, localised in the mesencephalon and rostral pons and subclassified into principal dorsal raphe nuclei B6 and B7, which represent most of the serotonergic origins, and the median raphe nuclei B5, B8 and B9. The dorsal nuclei send their ascending projections to most of the brain structures including the forebrain, basal ganglia, thalamus and limbic areas (Bear et al., 2007, Hornung, 2003, Lesch and Waider, 2012).

The rostral raphe nuclei have distinct axonal morphology in which the axons originating from the dorsal raphe nuclei (D fibres) are very fine, diffused, and demonstrate regularly spaced varicosities. While those originating from the median raphe nuclei (M fibres) have thick and non-varicose axons but short and clustered branches which have irregularly spaced varicosities (Hensler, 2006, Noristani et al., 2010, Tork, 1990). The serotonergic origins and projections in the brain are depicted in **Figure 4**.

This wide distribution of the serotonergic neurones in the brain is attributed to the roles of serotonin in neuropsychological, developmental and behavioural processes, such as cognition functions, mood, neuronal growth, the sleep-wake cycle and appetite. Correspondingly, the disturbance of the serotonergic system is implicated in the pathogenesis of many diseases such as schizophrenia, anxiety, dementia, depression, obsessive-compulsive disorders, migraine, obesity, insomnia and eating disorders (for reviews see Barnes and Neumaier, 2011, Barnes and Sharp, 1999, Svob Strac et al., 2016). With respect to diverse physiological actions of serotonin

in the CNS, the following will emphasise the physiological functions that are affected by AD, i.e. cognitive functions, mood and emotions, and neuronal plasticity and development.



**Figure 4. Serotonergic neuronal origins and their projections in the rat brain**

*The neuronal cell bodies are clustered in the raphe nuclei located in the brainstem. They send extensively branching axons to most of the brain regions. The caudal serotonergic system consists of B1-B4 forms the descending pathways that innervating the spinal cord. The rostral ascending serotonergic system consists of B5-B9 and innervates the diencephalon, basal ganglia, limbic system and cortex. Modified from Noristani (2012).*

#### **1.2.4. Role of serotonin in cognitive functions**

Higher cognitive functions include a spectrum of complex mental processes; memory, learning, attention, perception, decision-making, as well as emotional behaviour (Puig and Gener, 2015, Svob Strac et al., 2016). The modulatory action of serotonin in cognitive functions is mediated by its receptors and transporters which are expressed in the prefrontal cortex and hippocampus—the cognitive controlling regions of the brain (Berumen et al., 2012, Celada et al., 2013).

Preclinical and clinical studies have shown that the changes in 5-HT level or activity can influence cognitive performance. Chronic depletion of dietary tryptophan, a precursor for serotonin synthesis, caused a significant reduction in 5-HT and 5-HIAA in the rat hippocampus, frontal cortex and striatum (Jenkins et al., 2010). Such rats exhibited object-recognition memory defects which were reversed by prior administration of risperidone (Jenkins et al., 2010). In humans, acute tryptophan depletion significantly affected episodic memory and more specifically diminished the consolidation of verbal information on visual learning. Semantic memory, however, remained for the most part unaffected in healthy individuals (Mendelsohn et al., 2009).

The level of 5-HT is mainly regulated by SERT. Smith et al., (2017) found a reduction in the binding of SERT in MCI patients, particularly in the cortical and limbic areas. This reduction was associated with lower performance in auditory-verbal and visual-spatial memory tests in those patients in comparison to controls. Furthermore, the serotonin's cognitive actions are mediated directly on the serotonergic system and indirectly by modulating other cognitive associated neurochemical systems including; cholinergic, glutamatergic, dopaminergic and

GABAergic systems (King et al., 2008, Lesch and Waider, 2012, Seyedabadi et al., 2014). For instance, stimulation of the Gi-coupled 5-HT<sub>1A</sub> receptor located in the glutamatergic pyramidal neurones and GABAergic interneurones, produces hyperpolarisation and neuronal inhibition, whereas inhibition of the 5-HT<sub>1A</sub> receptor can reverse drug-induced cognitive impairments by increasing Ach and glutamate levels and preventing glutamatergic hyperpolarisation (Celada et al., 2013, King et al., 2008). Moreover, the chemical-induced lesion of 5-HT or Ach systems individually caused minor behavioural alterations in the rat while dual lesions induced severe deficit in learning and memory (Jeltsch-David et al., 2008, Lehmann et al., 2002, Lehmann et al., 2000).

#### **1.2.5. Role of serotonin in mood and emotions**

Mood disorders such as major depressive disorder, are caused by an imbalance in the neurotransmitters and neurotrophic factors in the brain. It is well known that low levels of 5-HT and other monoamines, noradrenaline in particular, have been implicated in the pathogenesis of these disorders as proposed very early on in the monoamine theory by Schildkraut (1965). Reduction in the levels of total plasma tryptophan had been found in clinically depressed patients (Cowen et al., 1989). This might be attributed to the depression associated-immunological disturbance and oxidative stress which induce indoleamine dioxygenase (IDO) and tryptophan dioxygenase (TDO). These enzymes can deviate tryptophan from the 5-HT synthesis pathway to the deleterious kynurenine synthesis pathway (Maes et al., 2011).

Antidepressants, namely monoamine oxidase inhibitors (MAOIs), tricyclic antidepressants (TCAs) and serotonin selective reuptake inhibitors (SSRIs) increase the synaptic level of 5-HT within hours. Contrastingly, symptomatic relief in

depressed patients requires several weeks of continuous use to reach the full therapeutic outcomes (Gray et al., 2013). This therapeutic delay occurs due to the feedback inhibition of the 5-HT neuronal firing and 5-HT release, which is caused by somatodendritic 5-HT<sub>1A</sub> and nerve terminals 5-HT<sub>1B</sub> autoreceptors as a response to the initial increase in 5-HT following acute treatment. However, chronic treatment for at least two weeks stimulates adaptive desensitisation of the autoreceptors, restores the serotonergic neuronal firing and evokes neural plasticity changes thought to result in mood improvement (Gray et al., 2013, Sharp and Cowen, 2011). In addition, increased 5-HT mediates neurophysiological changes in the processing of emotional information through shifting the patients from negative affective bias to positive bias and aiding them to re-learn the positive emotions which can ultimately lead to prolonged mood improvement (Harmer and Cowen, 2013, Sharp and Cowen, 2011).

#### **1.2.6. Role of serotonin in neuronal plasticity and development**

During brain development, 5-HT regulates many neuronal growth processes which are critical for normal brain functions. They include neurite outgrowth, dendrites spreading and connection, axonal direction, neurogenesis, as well as neural division, migration, survival and differentiation (Daubert and Condron, 2010, Gaspar et al., 2003). Very little is known about the role of serotonin in prenatal brain developmental stages during which the expression pattern of serotonin proteins is highly plastic and sensitive. Early exposure to genetic or environmental factors could cause long-term expression changes persisting into adulthood (Velasquez et al., 2013). Therefore, dysfunction of 5-HT transmission can influence the neuronal structures and functions causing a broad spectrum of neurodevelopmental disorders

such as autism and attention deficit hyperactivity disorder (ADHD), psychiatric disease such as schizophrenia, and neurodegenerative disorders such as AD (Lesch and Waider, 2012). In the adult brain, 5-HT has a role in regulating synaptic plasticity by strengthening the synaptic signal transmission (Derkach et al., 2007, Lesch and Waider, 2012). In addition, 5-HT modulates cell adhesion molecules that are localised in the synapse, essential for the stability of the synaptic structure and specify the connectivity between the neurones (Lesch and Waider, 2012).

The downstream signalling cascade raised from stimulation of post-synaptic Gs-coupled-5-HT receptors can phosphorylate protein kinase A (PKA) and extracellular signal-regulated kinases (ERKs). These enzymes activate the cAMP response element binding protein (CREB) which enhances the gene transcription of brain-derived neurotrophic factor (BDNF). The cycle is pursued as synthesised BDNF activates its TrkB receptor in serotonergic neurones and promotes their survival, plasticity and function (Martinowich and Lu, 2008, Mattson et al., 2004).

### **1.3. Serotonin transporter (SERT)**

The serotonin transporter (SERT or 5-HTT) is a  $\text{Na}^+/\text{Cl}^-$ -dependent transporter which controls the 5-HT level in the plasma and synapse and is also the principal site of action of the antidepressant SSRIs. It is encoded by the *SLC6A4* gene which belongs to a gene family of neurotransmitter transporters (Bröer., 2018, D'Souza and Craig, 2010). The SERT proteins are located in the plasma membrane and contain 12 transmembrane spanning segments with both amino- and carboxylic-termini present intracellularly. These have the potential sites of glycosylation which may regulate the transporter trafficking and stability (Ni and Watts, 2006).

SERT was initially cloned from rat brain and functionally expressed in non-neuronal cells (Blakely et al., 1991). Soon after that, the human homologue SERT was identified in human placental trophoblastic cells (Ramamoorthy et al., 1993). Within the brain, SERT is localised in the cell bodies of the raphe nuclei and in the serotonergic neuronal projections which extend to the cortex, amygdala and hippocampus (Hrdina et al., 1990). Immunoreactivity to SERT could reflect the brain regions that receive serotonergic innervations (Barnes and Neumaier, 2011). It is used as a phenotypic marker for serotonergic neurones since its expression is not influenced by the metabolic changes in the 5-HT level (Nielsen et al., 2006). The SERT coding gene (*SLC6A4*) has several polymorphic loci in the promoter regions known as the serotonin-transporter-linked polymorphic region (5-HTTLPR). This generates two allele phenotypes; short and long alleles (Lesch et al., 1996). Carrying the short allelic form of *SLC6A4* is associated with a high risk of depression (Pezawas et al., 2005) and AD (Hu et al., 2000).

#### **1.4. Serotonin receptors**

Despite the early discovery of serotonin, research into serotonin is continuously growing due to the abundance of its receptors and their distinct actions and distributions throughout the body. Serotonin produced its actions via fourteen receptor subtypes that are classified into seven distinct receptor families (5-HT<sub>1-7</sub>). This classification is based on sequence data, signal transduction mechanisms and pharmacological profile. Six of these receptors belong to the largest family of G-protein-coupled receptors (GPCRs), the rhodopsin-like family (Class A). They share a typical structure, comprised of seven linked transmembrane-spanning domains. 5-HT<sub>3</sub>, however, is a ligand-gated ion channel (LGIC, ionotropic receptor). Several of



these receptor families are further divided into subclasses according to the International Union of Basic and Clinical Pharmacology (IUPHAR) Database as follows: the 5-HT<sub>1</sub> receptors include the 5-HT<sub>1A</sub>, 5-HT<sub>1B</sub>, 5-HT<sub>1D</sub>, 5-HT<sub>1E</sub> and 5-HT<sub>1F</sub> receptor subclasses. The 5-HT<sub>2</sub> receptor class has 5-HT<sub>2A</sub>, 5-HT<sub>2B</sub>, and 5-HT<sub>2C</sub> receptors. The 5-HT<sub>5</sub> receptors include two subclasses namely the 5-HT<sub>5A</sub> and 5-HT<sub>5B</sub> receptors. In addition, 5-HT receptor genes like many other GPCRs are subjected to mRNA alternative splicing such as 5-HT<sub>2A</sub>, 5-HT<sub>2B</sub>, 5-HT<sub>2C</sub>, 5-HT<sub>3</sub>, 5-HT<sub>4</sub>, 5-HT<sub>5A</sub>, 5-HT<sub>6</sub> and 5-HT<sub>7</sub> receptors, thus creating more receptor isoforms which could be functional or non-functional (Bockaert et al., 2006). The post-transcriptional diversity of these receptors sequence is also increased by RNA editing as in the case of the second cytoplasmic loop of the 5-HT<sub>2C</sub> receptor or due to the presence of SNPs which can sometimes change the structure, the function and the expression of the translated proteins, thereby linking disease risks (Bockaert et al., 2006, Roth, 2006).

Most of the 5-HT receptors have been implicated in the pathogenesis of CNS disorders, in particular depression and anxiety (**Table 1**). Studies show that most of the 5-HT receptors including 5-HT<sub>1A</sub>, 5-HT<sub>3</sub>, 5-HT<sub>4</sub>, 5-HT<sub>6</sub> and 5-HT<sub>7</sub> receptors are linked to the cognitive and neuropsychiatric symptoms associated with AD (King et al., 2008, Rodriguez et al., 2012, Terry et al., 2008). This thesis focuses on both the 5-HT<sub>4</sub> and 5-HT<sub>6</sub> receptors, thus the following will specifically address these receptors in more detail.

**Table 1. Summary of the type, mechanism and therapeutic uses of 5-HT receptors.**

Receptor	Type	Second messenger/ effector	Potential effect	Therapeutic Target
<b>5-HT<sub>1</sub> R</b>	GPCR (G <sub>ai</sub> -coupled)	Decrease cAMP by inhibiting AC	Inhibitory	Migraine, anxiety, depression, aggression, cognition and drug addiction
<b>5-HT<sub>2</sub> R</b>	GPCR (G <sub>αq/11</sub> -coupled)	Increase IP3/DAG/Ca <sup>+2</sup> by activating PLC	Excitatory	Schizophrenia, eating disorders, sleep disorder, depression, and anxiety.
<b>5-HT<sub>3</sub> R</b>	LGIC (Na <sup>+</sup> /K <sup>+</sup> /Ca <sup>+2</sup> conductance)	Depolarisation of plasma membrane	Excitatory	Emesis, anxiety, cognition, analgesia and drug addiction
<b>5-HT<sub>4</sub> R</b>	GPCR (G <sub>αs</sub> -coupled)	Increase cAMP by activating AC	Excitatory	Cognition and anxiety
<b>5-HT<sub>5</sub> R</b>	GPCR (G <sub>αi</sub> -coupled)	Decrease cAMP by inhibiting AC	Inhibitory	Not known
<b>5-HT<sub>6</sub> R</b>	GPCR (G <sub>αs</sub> -coupled)	Increase cAMP by activating AC	Excitatory	Schizophrenia, cognition, depression, anxiety, epilepsy and obesity
<b>5-HT<sub>7</sub> R</b>	GPCR (G <sub>αs</sub> -coupled)	Increase cAMP by activating AC	Excitatory	Schizophrenia, cognition, depression, epilepsy and sleep disorder.

*(Adapted from Barnes and Neumaier, 2011, Bockaert et al., 2006, Pytliak et al., 2011).*

### 1.4.1. 5-HT<sub>4</sub> receptor

#### 1.4.1.1. Receptor cloning and genetics

The 5-HT<sub>4</sub> receptor gene was initially cloned from rat brain in two forms that were varied in length; a short 5-HT<sub>4S</sub> and long 5-HT<sub>4L</sub> (Gerald et al., 1995). Soon after that other forms were cloned. The 5-HT<sub>4</sub> receptor gene (*HTR4*) is complex. It has multiple introns and exons which are alternatively spliced to produce at least 11 receptor isoforms (Bockaert et al., 2006, Coupar et al., 2007, Rebholz et al., 2018). As shown in **Figure 5**, the 5-HT<sub>4</sub> receptor isoforms are mainly varied in their C-terminal domain downstream of the leucine 358 (L358) residue. This is with the exception of the 5-HT<sub>4h</sub> isoform, which differs by 14 amino acids in the second extracellular loop (ECL2) of the receptor but has a similar C-terminal sequence to the 5-HT<sub>4b</sub> variant (Andrade et al., 2016, Rebholz et al., 2018). Although these isoforms have a similar ligand binding domain, they are diverse in terms of anatomical distribution, ligand affinity, signal transduction pathways and desensitisation rates (Medhurst et al., 2001, Roth, 2006).

#### 1.4.1.2. Protein structure and distribution

The 5-HT<sub>4</sub> receptor is a GPCR possessing seven transmembrane (TM)  $\alpha$ -helical domains linked by three intracellular loops and three extracellular loops (McCorvy and Roth, 2015). The ECL2 of the 5-HT<sub>4</sub> receptor is longer than the other 5-HT receptors. The N-terminus is relatively short and directed towards the extracellular surface, while the C-terminal length varies with different isoforms and is directed towards the cytoplasm. Two cysteine residues in the TM2 domain and the ECL3 are linked by a disulphide bridge (McCorvy and Roth, 2015). In addition, the 5-HT<sub>4</sub>

receptor is subjected to different post-translational modifications (PTMs) such as glycosylation at asparagine residues, phosphorylation at serine, threonine and tyrosine residues by several kinases, and palmitoylation of cysteine residues resulting in the tethering of the carboxyl terminus to the plasma membrane (Salom et al., 2012).

The 5-HT<sub>4</sub> receptor is abundantly distributed peripherally in the gastrointestinal tract and heart as well as centrally in the brain. In the brain, the 5-HT<sub>4</sub> receptors are expressed in the basal ganglia structures such as striatum, nucleus accumbens, globus pallidus, substantia nigra as well as amygdala, hypothalamus, hippocampus and cortex (Andrade et al., 2016, Bockaert et al., 2006). The 5-HT<sub>4</sub> receptors are mainly located post-synaptically however it can be found in the presynaptic nerve terminals of cholinergic, glutamatergic, GABAergic and serotonergic neurones as the release of the neurotransmitters is regulated by the action of the 5-HT<sub>4</sub> agonists through blocking of the K<sup>+</sup> channel which leads to the influx of Ca<sup>+2</sup> into the neuron (Ahmad and Nirogi, 2011, Bockaert et al., 2006).



#### ***1.4.1.3. Receptor signalling and desensitisation***

The signalling pathways evoked after the activation of the 5-HT<sub>4</sub> receptor can result from the receptor /G-protein coupling (G protein-dependent pathway) or by activation of other intracellular proteins (G protein-independent pathway) (Bockaert et al., 2008). In neurones, and at physiological conditions, stimulation of this receptor can activate adenylyl cyclase (AC) which leads to an increase in the level of cyclic adenosine monophosphate (cAMP). This second messenger has a well-recognised role in memory formation and consolidation. It also regulates the neuronal plasticity and functions by activating other intracellular effectors, such as protein kinase A (PKA) (Chen et al., 2012, Vitolo et al., 2002) and exchange protein directly activated by cAMP (Epac) (Grandoch et al., 2010, Maillet et al., 2003). Activation of PKA leads to phosphorylation of many substrates including the transcription factor CREB (Ahmad and Nirogi, 2011, Chen et al., 2012). This factor, in turn, promotes the transcription of various procognitive genes like BDNF and the expression of such gene is essential for LTP (Ahmad and Nirogi, 2011, Diniz and Teixeira, 2011, Suzuki et al., 2011, Teich et al., 2015). Other PKA-mediated effects following 5-HT<sub>4</sub> receptor activation are blocking of K<sup>+</sup> channels, enhancing the release of Ach in the hippocampus and frontal cortex, activating of Ca<sup>2+</sup> channels in the atria and stimulating of the cardiac muscle (Roth, 2006).

Furthermore, the diversity of the 5-HT<sub>4</sub> receptor signalling is also increased as the cAMP-mediated activation of the exchange factor Epac which controls many ERK-dependent processes such as cell proliferation and survival, gene transcription and Ca<sup>2+</sup> homeostasis (Gelinas et al., 2008, Grandoch et al., 2010). Epac enhances the synaptic strength and maintenance in mouse hippocampal slices, and this effect

requires ERK phosphorylation and the synthesis of new protein at the synapse (Gelinas et al., 2008). Epac is involved in the activation of small GTPases Rap1 and Rac (Maillet et al., 2003, Robert et al., 2005). These GTPases activate  $\alpha$ -secretases in the neurones and subsequently generate sAPP $\alpha$  which confers neuroprotective effects (Lezoualc'h, 2007).

Furthermore, 5-HT<sub>4</sub> receptor stimulation leads to G-protein-independent activation of the non-canonical pathway and transient phosphorylation of ERK<sub>1/2</sub> at threonine 202 and tyrosine 204 in primary neurones and HEK293 transfected cells. This activation depends on the activation of Src; a non-receptor tyrosine kinase (Barthet et al., 2007). In neurones, the activation of ERK and its signalling pathways is involved in neuroplasticity: neurite and dendritic outgrowth and synaptogenesis (Peng et al., 2010). Therefore, the 5-HT<sub>4</sub> receptor has the capacity to activate these pathways which lead to improvements in recognition memory, spatial learning and cognition.

The desensitisation of the 5-HT<sub>4</sub> receptor occurs when the active receptor is distinctively phosphorylated by GPCR kinase (GRKs) at its C-terminus. This can interfere with the G-protein coupling process and thus the activation of second messenger cascades (homologous desensitisation) (Mnie-Filali and Piñeyro, 2012). The rate of desensitisation of 5-HT<sub>4</sub> receptors depends on the expression level of GRK. The colliculi neurones, which tend to have high GRK expression, showed rapid desensitisation of these receptors following agonist activation but not in HEK293 cells or COS-7 cells which have low levels of GRK expression (Barthet et al., 2005). The desensitised receptor is sequestered from the cell surface when the  $\beta$ -arrestin binds to the phosphorylated receptor which recruits clathrin-coated

vesicles to initiate receptor internalisation. Next, the internalised receptor can either be recycled once again to the cell membrane by dephosphorylation or degraded by lysosomes (receptor down-regulation) (Mnie-Filali and Piñeyro, 2012).

#### ***1.4.1.4. Role of the 5-HT<sub>4</sub> receptor in AD***

Considerable research interest is directed towards understanding the role of the 5-HT<sub>4</sub> receptor in neuroprotection, LTP and cognition. Some *in vitro* and *in vivo* evidence indicates that activation of this receptor by an agonist produces protective effects in the context of AD and its pathological proteins. For example, the use of prucalopride in CHO cells transfected with the 5-HT<sub>4</sub> receptor and human APP enhances the cellular sAPP $\alpha$  release through cAMP but not PKA (Lezoualc'h and Robert, 2003). Therefore, the 5-HT<sub>4</sub> receptor-mediated release of APP $\alpha$  may involve the second cAMP effector, Epac in which the overexpression of Epac in such cells increases the sAPP $\alpha$  release through the activation of small GTPases signalling as in **Figure 6** (Maillet et al., 2003, Robert et al., 2005). Treating the primary cortical neurones derived from Tg2576 mice with RS-67333 which is a partial agonist for the 5-HT<sub>4</sub> receptor can interfere with A $\beta$  formation and minimises the neuronal death through the control of APP metabolic processing (Cho and Hu, 2007). Moreover, Cochet et al. (2013) suggested that this control resulted from the physical interaction between this receptor and  $\alpha$ -secretase which could be up-regulated through agonist stimulation. The involvement of cAMP in 5-HT<sub>4</sub> receptor-directed activity of  $\alpha$ -secretase, however, was refuted by Pimenova et al. (2014) who instead used the SH-SY5Y human neuroblastoma cells and related the activity of  $\alpha$ -secretase to the action of Src tyrosine kinase.



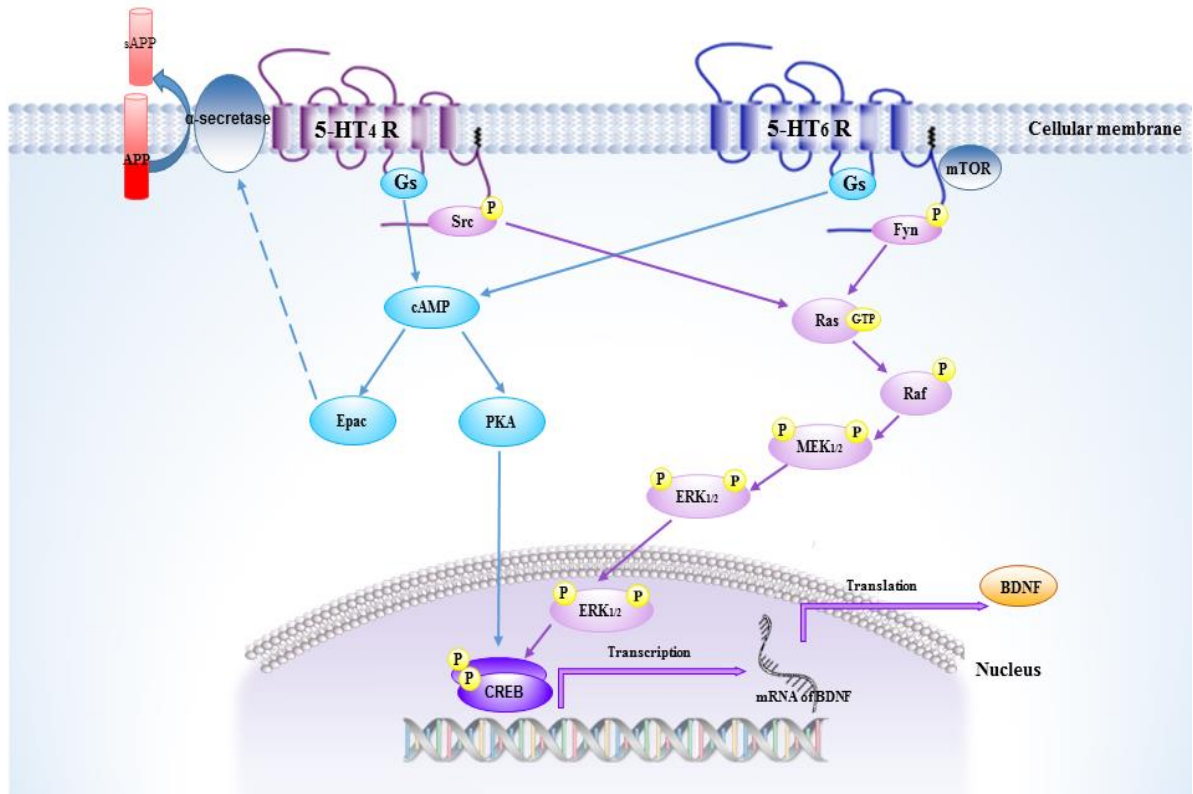
Furthermore, Giannoni and colleagues (2013) used an AD model in the form of 5XFAD transgenic mice generated by Oakley et al. (2006)—to study the effect of RS-67333 and its administration at chronic levels on the prodromal and late stages of the disease. They found the reduction of the amyloid accumulation was more significant with earlier intervention. In addition, the decrease in levels of A $\beta$  was associated with a reduction in the neuroinflammatory responses; in particular of astrogliosis and microgliosis which usually surround the A $\beta$  deposits.

Moreover, 5-HT<sub>4</sub> receptor activation induces the expression of several proteins in the hippocampus which is essential for neuronal plasticity and cognitive functions such as BDNF, PKA, and CREB (Pascual-Brazo et al., 2012). These proteins are usually dysregulated in AD. Compelling evidence reported the AD-associated decrease in the BDNF expression in serum and brain (Holsinger et al., 2000, Laske et al., 2007, Lee et al., 2009b). In addition, A $\beta$  can inhibit the phosphorylation of CREB in rat hippocampal neurones via disturbing the dissociation of the catalytic PKA subunit (Vitolo et al., 2002). Moreover, increasing the neuronal  $\beta$ -secretase expression can physically interact with AC which contributed to lower the signal transduction through cAMP/PKA/CREB pathway (Chen et al., 2012).

Furthermore, Chapin et al. (2002) recorded the neuronal electrophysiology in the CA1 area of the hippocampus after the 5-HT addition, and found that the 5-HT provoked depolarisation and diminished the afterhyperpolarisation (AHP) selectively through 5-HT<sub>4</sub> receptor activation. Moreover, Restivo et al. (2008) studied the impact of SL65.0155, a 5-HT<sub>4</sub> partial agonist, on the neuronal outgrowth in mouse hippocampus. They found that SL65.0155 potentiates the training-induced dendritic plasticity as well as advances the olfactory discrimination response in mice

(Restivo et al., 2008). From a pre-clinical memory model, enhancements of the object recognition by young rats and the linear maze performance by aged rats were observed following use of SL65.0155 which also synergise the rivastigmine action (Moser et al., 2002). The activation of 5-HT<sub>4</sub> receptors improves memory acquisition and consolidation in other types of learning task (King et al., 2008).

In spite of the apparent progress that has been made in preclinical research on the role of 5-HT<sub>4</sub> receptor agonists in AD, and to the best of our knowledge only one clinical trial has been initiated to test a 5-HT<sub>4</sub> partial agonist PRX-03140 for AD. This is potentially related to the abundance of the 5-HT<sub>4</sub> receptor in the gut and cardiac muscles which may interfere with the intended therapeutic purpose for AD.



**Figure 6. Schematic diagram of the interaction between the 5-HT<sub>4</sub> and 5-HT<sub>6</sub> receptors' signalling pathways**

*The activation of the Gs-coupled 5-HT receptors enhances the BDNF transcription as a result of CREB activation. Another signalling pathway that promotes the BDNF synthesis involves activation of ERK<sub>1/2</sub> through the association of non-receptor tyrosine kinases (e.g. Fyn and Src) with the receptor C-terminus. Based on that, the ERK<sub>1/2</sub> activation and CREB-evoked BDNF expression emerge as converging targets in the 5-HT<sub>4</sub> and 5-HT<sub>6</sub> signalling pathways. This figure is constructed using the neuroscience toolkit.*

## 1.4.2. 5-HT<sub>6</sub> receptor

### 1.4.2.1. Receptor cloning and genetics

The 5-HT<sub>6</sub> receptor has been cloned from a rat striatum cDNA library by two independent research groups (Monsma et al., 1993, Ruat et al., 1993). Monsma et al. suggested the involvement of this receptor in neuropsychological disorders due to its distinct affinity for tricyclic psychotropic drugs and its brain localisation. In the same year, Ruat et al. cloned this receptor through the use of the histamine H<sub>2</sub> receptor sequence which shared partial sequence homology with the 5-HT<sub>6</sub> receptor. Three years later, Kohen and colleagues (1996) cloned the human 5-HT<sub>6</sub> receptor. Sequencing of this receptor showed that it consisted of two introns located in the third intracellular and third extracellular loops of the corresponding protein (**Figure 7**), but that these intronic variants appeared non-functional (Monsma et al., 1993, Olsen et al., 1999, Ramirez, 2013). A single silent mutation was identified at bp 267C/T corresponding to tyrosine at position 89 producing the *Rsa* I polymorphism and potentially associated with late-onset AD in Chinese (Kan et al., 2004, Tsai et al., 1999). This association, however, was not replicated in other ethnic AD populations (Alvarez-Alvarez et al., 2003, Orlacchio et al., 2002, Thome et al., 2001). The sequence homology of 5-HT<sub>6</sub> receptor between rat and human showed that 85% and 89% similarities of the DNA and amino acid sequences respectively (Kohen et al., 1996). Furthermore, the DNA sequence of the mouse 5-HT<sub>6</sub> receptor was 94% and 84% identical to rat and human respectively, and the corresponded peptide sequence had 97% and 89% sequence similarities with rat and human receptors (Kohen et al., 2001). Therefore, the rat and mouse 5-HT<sub>6</sub> receptor

sequences differ from its human homologue which may elicit species differences in the receptor pharmacology.

#### ***1.4.2.2. Protein structure and distribution***

The seven transmembrane structure of the 5-HT<sub>6</sub> receptor is characterised by a shorter ECL2 and longer C-terminus relative to the 5-HT<sub>4</sub> receptor (**Figure 7**). The protein sequence has several potential sites for post-translational modifications; a few putative sites for *N*-glycosylation in asparagine residues and multiple phosphorylation sites in the third intracellular loop (ICL3) and the C-terminus (Barnes and Sharp, 1999, Kohen et al., 1996).

5-HT<sub>6</sub> receptors are predominantly expressed in the CNS, with higher receptor densities found in striatum structures; including the olfactory tubercle, caudate nucleus and nucleus accumbens. Moderate expression is found in the entorhinal cortex and hippocampus, and the least expression in the substantia nigra, amygdala and hypothalamus (Ferrero et al., 2016). A radioligand binding assay demonstrated higher binding affinity of [<sup>125</sup>I]-SB-258585 for the human striatum than the hippocampus and prefrontal cortex (Marazziti et al., 2012). Generally, expression of 5-HT<sub>6</sub> receptors within these regions reflects their involvement in learning and cognitive processes. This, therefore, explains their implication in neurocognitive diseases. With regard to neuronal localisation, it has been suggested that the 5-HT<sub>6</sub> receptors are expressed post-synaptically on serotonergic neurones (Gerard et al., 1996), and heterologously expressed in cholinergic glutamatergic and GABAergic neurones (King et al., 2008).



#### ***1.4.2.3. Receptor signal transduction***

It is well recognised that the stimulated 5-HT<sub>6</sub> receptor is coupled to Gα<sub>s</sub> protein, which activates the cAMP signalling. Apart from this, this receptor also activates other cellular pathways; namely ERK<sub>1/2</sub>, Jun activation and the mammalian target of rapamycin (mTOR) pathways (Karila et al., 2015, Meffre et al., 2012) as shown in **Figure 6**. The identification of these pathways is corroborated by the development of selective ligands and the use of the proteomic approaches. Researchers have determined that the C-terminus of the 5-HT<sub>6</sub> receptor physically interacts with Fyn-tyrosine kinase (Yun et al., 2007). Fyn belongs to the tyrosine kinases of the Src family (Millan et al., 2008). The significance of this interaction is bidirectional in which Fyn increases the 5-HT<sub>6</sub> receptor expression on the cell membrane and the stimulation of this receptor by 5-HT enhances Fyn phosphorylation (Yun et al., 2007) which subsequently activates the ERK<sub>1/2</sub> via Ras/Raf/MEK<sub>1/2</sub> signalling cascade (Codony et al., 2010, Millan et al., 2008). However, in transgenic APP mice, the increase of Fyn expression can reduce the pERK<sub>1/2</sub> immunoreactivity in the granule cells of dentate gyrus and produce spatial memory defect (Chin et al., 2005). In the Jun activation pathway, Yun et al. (2010) also determined that the C-terminus of the 5-HT<sub>6</sub> receptor physically interacts with the Jun activation domain-binding protein-1 (Jab1). This protein is an activator for c-Jun transcription factor which regulates the cell cycle. Yun et al. suggested that this interaction might be required for 5-HT<sub>6</sub> receptor expression and function.

The third cellular pathway that the 5-HT<sub>6</sub> receptor is coupled to is mTOR-mediated signalling. The ubiquitously expressed mTOR kinase has been implicated in the control of many cellular processes such as protein synthesis, synaptic remodelling

and neuronal development, proliferation and survival and several metabolic pathways (Hoeffler and Klann, 2010, Oddo, 2012, Yates et al., 2013). Activation of 5-HT<sub>6</sub> receptors was capable of recruiting and activating mTOR in the mouse prefrontal cortex and striatum. This kinase also activates other downstream signalling proteins (Meffre et al., 2012). Dysregulation of mTOR-signalling has been linked to some neuropsychiatric diseases including AD as the use of rapamycin, an mTOR antagonist, can inhibit the A $\beta$ <sub>42</sub> accumulation and improve the spatial memory in transgenic AD mice (Spilman et al., 2010). This dysregulation of mTOR and its downstream proteins is peripherally detected in lymphocytes of mild AD patients and can be used to predict the AD risk (Yates et al., 2013).

#### ***1.4.2.4. Role of the 5-HT<sub>6</sub> receptor in AD***

Numerous cellular and behavioural data supported the role of the 5-HT<sub>6</sub> receptor in cognitive functions. This receptor is considered a promising therapeutic target for AD and other type of dementia as it is largely distributed in the CNS and thus has minimal systemic side-effects. Down-regulation of the 5-HT<sub>6</sub> receptor in rats by injecting antisense oligonucleotides caused characteristic behaviours of stretching, yawning and chewing; that resembled those observed following cholinergic receptor activation (Bourson et al., 1995). In addition, pharmacological inhibition of the cholinergic receptor by muscarinic antagonists attenuated such behaviours, indicating that the 5-HT<sub>6</sub> receptor modulated Ach transmission (Bentley et al., 1999, Woolley et al., 2001). A post-mortem study of Garcia-Alloza et al. (2004) showed a marked loss of the 5-HT<sub>6</sub> receptor's density in the frontal and temporal cortex of post-mortem AD patients when assessed by [<sup>125</sup>I]-SB-258585 binding. This loss in



the receptor density might be a compensatory response to restore Ach transmission (Ramirez, 2013).

Several studies have shown that both activation and inhibition of the 5-HT<sub>6</sub> receptors by agonist and antagonist respectively showed similar pro-cognitive effects in preclinical animal models of learning and memory (Borsini et al., 2011, Fone, 2008, Woods et al., 2012). Furthermore, both 5-HT<sub>6</sub> receptor ligands had similar neuroprotective effects on the PC-12 cells against A $\beta$ -induced neurotoxicity (Bokare et al., 2017). The reason behind this ambiguous effect is not fully understood, however, it may be attributed to the differences in animal ages and the types of memory tasks as well as the selectivity and the signalling of the 5-HT<sub>6</sub> receptor ligands (Borsini et al., 2011, Fone, 2008, Woods et al., 2012). Moreover, the 5-HT<sub>6</sub> receptor has direct and indirect neurochemical regulatory mechanisms which depend on the cellular localisation of this receptor in distinct neuronal phenotypes (Woods et al., 2012).

In a novel object discrimination task, the 5-HT<sub>6</sub> receptor agonists, E-6801 and EMD 386088, had cognitive enhancement properties when used alone or as an adjunct to the 5-HT<sub>6</sub> receptor antagonist SB-271046 (Kendall et al., 2011). Likewise, post-training administration of these compounds significantly reversed the memory impairment produced after scopolamine or MK-801 injection in conditioned fear response of rats (Woods et al., 2012). Nonetheless, a larger array of behavioural studies investigated the 5-HT<sub>6</sub> receptor antagonists more than the agonists for this receptor. These studies have been used the 5-HT<sub>6</sub> antagonists to reverse the drug-induced or age-dependent memory deficits. For instances, Foley and others (2004) used rat passive avoidance response to assess the effect of 5-HT<sub>6</sub> receptor antagonist

SB-271046. They found the administration of SB-271046 in rats significantly antagonised the amnesia produced after scopolamine injection. They further showed the repeated administration of SB-271046 in aged-memory impaired rats produced a significant enhancement in spatial memory in Morris water maze (Foley et al., 2004). Likewise, the selective 5-HT<sub>6</sub> antagonist SB-399885 inhibited the drug- and age-related memory impairments through increasing Ach release in the rat prefrontal cortex (Hirst et al., 2006), whereas SB-271046 elevated glutamate levels in the rat frontal cortex and hippocampus (Dawson et al., 2001). These findings appear to indicate that these antagonists enhance both cholinergic and glutamatergic transmission through the disinhibition of GABAergic neurones (Codony et al., 2011, King et al., 2004, Ramirez, 2013).

Indeed, some clinical trials investigated the effect of 5-HT<sub>6</sub> receptor antagonists for symptomatic management of mild to moderate AD. The results of the two most predominant multi-centre phase-II trials revealed that SB-742457 failed to show any beneficial outcomes in cognitive function as a monotherapy but when augmented by donepezil, it showed more improvements in cognition and ADL in AD patients (Maher-Edwards et al., 2015). Based on the negative outcomes of the 5-HT<sub>6</sub> antagonist monotherapy, the clinical trial investigations may be directed towards the use of 5-HT<sub>6</sub> receptor agonists or possibly inverse agonists for AD symptoms.

### **1.5. Possible crosstalk between the 5-HT<sub>4</sub> and 5-HT<sub>6</sub> receptor-signalling pathways in the context of memory and cognition**

From the literature review it was clear that the classical G protein pathway which positively coupled to AC leading to cAMP formation was common to 5-HT<sub>4</sub> and 5-HT<sub>6</sub> receptors and that through this, effectors found intracellularly (e.g. Epac and

PKA) are activated. These receptors also converge by utilising non-receptor tyrosine kinases (i.e. Src and Fyn) to control the ERK<sub>1/2</sub> pathway. However, the pharmacological impact of the 5-HT<sub>4</sub> receptor on memory and cognition is much clearer than that of the 5-HT<sub>6</sub> receptor because both simulation and inhibition of the 5-HT<sub>6</sub> receptor have procognitive effects in preclinical studies. The 5-HT<sub>4</sub> receptor has been investigated more often than the 5-HT<sub>6</sub> receptor on the APP metabolic pathway. As the 5-HT<sub>4</sub> and 5-HT<sub>6</sub> receptors are colocalised in the glutamatergic pyramidal neurones (King et al., 2008), their functions are possibly linked. In addition, pharmacological modulation of both receptors can regulate the release of acetylcholine and glutamate. Further proteins contributing to the interaction of these receptors in the memory regulating processes are highlighted in **Figure 6**.

#### **1.6. The potential of a multi-target drug paradigm**

After more than a decade of AD discovery, memantine and AChEIs are the only therapies for AD regardless of the apparent advances in understanding the mechanisms implicated in this disease. These drugs are approved clinically to manage the behavioural and psychological symptoms but do not prevent the disease evolution. These drugs have rarely used as a monotherapy, instead they are usually combined with antipsychotics, antidepressants and anxiolytics to achieve better clinical outcomes. AD research necessitates a multi-target drug paradigm which possibly changes the future of AD clinical trials. The Lecoutey et al. (2014) group has addressed this approach as they synthesised a compound called donecopride which exhibited pro-cognitive properties in animals by activating the 5-HT<sub>4</sub> receptor while inhibiting the AChE enzyme. Furthermore, another research group designed

compounds which exhibited anti-amnesic effects in mice through dual activation and inhibition of the 5-HT<sub>4</sub> and 5-HT<sub>6</sub> receptors respectively (Yahiaoui et al., 2016).

### **1.7. Research hypotheses**

It has been suggested that pharmacological targeting the 5-HT<sub>4</sub> and 5-HT<sub>6</sub> receptors simultaneously can show beneficial effects, in terms of cognition and memory. Changes in the expression of these receptors during AD progression are yet to be assessed. From this standpoint, hypotheses are formed that combining the activation of 5-HT<sub>4</sub> receptors and 5-HT<sub>6</sub> receptors may show synergistic or additive effects on the pERK<sub>1/2</sub> expression which is critical for neuroplasticity. The presence and significance of *N*-glycosylation motifs in 5-HT<sub>4</sub> receptors is essential for its cell surface expression as well as interaction with extracellular 5-HT. Moreover, the AD neurochemical changes and neuronal loss can cause a reduction in the expression of serotonin proteins in human prefrontal cortex early in the course of the disease.

### **1.8. Aims and objectives**

This research aimed to:

1. Determine the endogenous expression of 5-HT<sub>4</sub> and 5-HT<sub>6</sub> receptors in HEK293 and SH-SY5Y cell lines—the two most commonly used cell lines for studying the signalling mechanisms of serotonin receptors in the context of AD.
  - Generate receptor constructs for the 5-HT<sub>4</sub> and 5-HT<sub>6</sub> receptors and used them for transfecting the HEK293 cells to be used as positive controls during the protein expression assay.

2. Study the effect of stimulation of the overexpressed 5-HT<sub>4</sub> and the 5-HT<sub>6</sub> receptors either singly or simultaneously on the activation of ERK<sub>1/2</sub>, a kinase with a vital role in cell proliferation, survival and apoptosis.
  - Optimise the transfection ratio of DNA:PEI to select the optimum ratio of cell transfectability with high tolerability.
  - Measure the changes in the pERK<sub>1/2</sub> expression level in response to activation of the transiently expressed 5-HT<sub>4</sub> or 5-HT<sub>6</sub> receptors by 5-HT and compare the pERK<sub>1/2</sub> level to double transfected cells.
3. Investigate the impact of *N*-glycosylation of 5-HT<sub>4</sub> receptor trafficking and localisation.
  - Generate mutant constructs for putative N7 and N180 asparagine residues.
  - Stabilise the wild type and mutant 5-HT<sub>4</sub> receptors in HEK293 cells and determine the differences in the receptor sizes and cell surface expression.
4. Assess the expression of 5-HT<sub>4</sub> and 5-HT<sub>6</sub> receptors in the human prefrontal cortex in different AD stages.
  - Quantify the transcript and protein expressions of 5-HT<sub>4</sub> and 5-HT<sub>6</sub> receptors in control, limbic and neocortical stage of AD.
  - Determine the influence of AD categorical variables such as ApoE genotype and homocysteine level on the expression of serotonin receptor and transporter.
  - Assess the correlation between the level of serotonin proteins and cognitive functions of the AD cases and controls.

## **Chapter 2. Methods**

## **2. Methods**

### **2.1. Cell culture**

All cell culture methods were conducted by applying aseptic techniques to prevent any contamination risks and by using a biosafety cabinet, sterile culture vessels, serological pipettes, filter sterilised buffers and autoclaved tips, coverslips and forceps.

#### **2.1.1. Cell line maintenance**

Human embryonic kidney 293 (HEK293) cells were maintained in Dulbecco's Modified Eagles Medium (DMEM, Sigma-Aldrich, D6429), supplemented with 10% foetal bovine serum (FBS, Sigma-Aldrich) and 1% antibiotics (penicillin and streptomycin, Sigma-Aldrich). The cells were allowed to grow in a humidified incubator at 37°C with 5% CO<sub>2</sub>. When the cell line reached 90% confluency, the medium was decanted, and the cells were washed twice with pre-warmed filter sterile phosphate buffered saline (F/S PBS, Sigma-Aldrich). The cells were harvested by adding 0.5 ml of trypsin/EDTA (T/E, Sigma-Aldrich) for every 10 cm<sup>2</sup> of the culture vessel. The vessel was then incubated for 2 min at 37°C. When the cells detached, the pre-warmed complete medium was added to inactivate the trypsin reaction. Then, the cell suspension was split into different ratios as required.

The SH-SY5Y neuroblastoma cell line was grown in Dulbecco's modified Eagle medium/F-12 nutrient mixture (DMEM/F-12, Gibco, 11039021), supplemented with 10% FBS and 1% antibiotics. The harvesting of these cells differed from the HEK293 cells because these cells were grown as floating and adherent cells. The floating cells were recovered from the medium by centrifugation at 400 g for 5 min

while the adherent cells were harvested by trypsin. Both cell types were then combined with complete medium and subsequently seeded at the recommended density.

### **2.1.2. Cryopreservation and resuscitation of cells**

Cryopreservation was used to maintain backup reserves of cell lines, and to limit them at lower passage numbers, usually below 25, thus minimising the phenotypic and genotypic alterations of the cells that associated with over passaging. Typically, around  $1 \times 10^7$  cells were harvested from the T75 flask and frozen in 1 ml of the cryomedium which contained 10% dimethyl sulfoxide (DMSO) in FBS. When the flask reached 90% confluency, the culture medium was decanted, and the cells were washed with PBS and trypsinised. The cells were collected in complete medium, spun down and resuspended with cryomedium at a concentration of  $1 \times 10^7$  viable cells/ml and transferred into pre-labelled cryovials. The vials were immediately transferred into a Mr. Frosty and then kept at  $-80^\circ\text{C}$  for a minimum overnight period prior to being stored in liquid nitrogen. To recover the cells after freezing, the vial was thawed at  $37^\circ\text{C}$ , the vial content was slowly diluted with 10 ml of pre-warmed complete medium in a centrifuge tube. The tube was spun at 400 g for 5 min followed by cell resuspension in complete medium, cultured in a T75 flask and allowed to grow in the incubator.

### **2.2. Nucleic acid quantification and quality control**

The concentration of nucleic acids; RNA, DNA or plasmid, was measured by loading 2  $\mu\text{l}$  of the purified samples on the NanoDrop 2000 spectrophotometer (Thermo Fisher Scientific). The nucleic acids have a maximal absorbance at 260 nm ( $A_{260}$ ). The absorbance ratios  $A_{260/280}$  and  $A_{260/230}$  were used to estimate sample purity.



Ideally, the  $A_{260/280}$  ratio should range from 1.8 to 2. Recording of a lower ratio can be attributed to protein contamination which absorbs light at 280 nm. While the  $A_{260/A230}$  ratio should lie between 2-2.2 and a lower reading would indicate salt or solvent contamination as such contaminants absorb light at 280 nm. If the absorbance ratios were within the required range then, the samples were deemed pure and suitable for downstream applications (Matlock, 2015).

### **2.3. Polymerase chain reaction**

Polymerase chain reaction, or PCR, is a biochemical technique utilised in many applications such as gene expression assays, cloning, mutation and sequencing. It initially involves the extraction of nucleic acid—in this case RNA—and ends with thermal cycling for DNA amplification,

#### **2.3.1. RNA extraction**

In accordance with the RNeasy Mini Kit (Qiagen, Cat No. 74104) instruction manual, the cells were harvested and counted by a haemocytometer. Based on cell count data, an appropriate volume of RLT lysis buffer containing 1%  $\beta$ -mercaptoethanol, was added to the cells and homogenised by passing the cell lysate through a narrow-gauge needle fitted to a syringe. One volume of 70% ethanol was mixed with the homogenate and loaded to the spin column at the maximum capacity of 700  $\mu$ l. Next, the columns were spun for 15 sec at  $\geq 8000$  g. This was followed by washing of the silica membrane with 350  $\mu$ l of RW1 buffer. The DNase I digestion step was performed in the spin column to eliminate the genomic DNA by adding a mixture of 10  $\mu$ l DNase I and 70  $\mu$ l of RDD buffer per column followed by incubation for 15 min at room temperature (RT). The columns were washed again with 350  $\mu$ l of RW1 buffer, followed by 500  $\mu$ l of RPE buffer (twice) and centrifuged

at 14,000 g for one min. The total RNA was eluted with 50 µl of nuclease-free water in fresh collection tubes by centrifugation. The RNA concentration was measured by the NanoDrop.

### **2.3.2. Complementary DNA (cDNA) synthesis**

The first strand cDNA was synthesised from the RNA template by reverse transcription. Typically, in an RNase free tube, the reaction was set up by adding the following; 2 µg of the extracted RNA, 1 µl of oligo (dT)<sub>12-18</sub> primers (Life Technologies Corp.), 1 µl of 10 mM deoxynucleotide triphosphate (dNTP) (Invitrogen) and nuclease-free water up to 12 µl. The mixture was heated to 65°C for 5 min and then chilled on ice. Next, 4 µl of 5X First Strand buffer (Invitrogen), 2 µl of 0.1 M dithiothreitol (DTT) (Invitrogen), 1 µl of RNaseout (Thermofisher Life Technologies) and finally 1 µl of Superscriptase II (Invitrogen) were added and mixed by pipetting. The tube was subsequently placed in the thermal cycler which was set to 42°C for 50 min, inactivation at 70°C for 15 min and then held at 4°C.

### **2.3.3. End-point (PCR)**

Following determination of the cDNA concentration, end-point PCR was carried out by mixing 200 ng of each primer (Sigma-Aldrich), 400 ng of cDNA, 45 µl of Platinum Blue PCR SuperMix (Invitrogen) in PCR tubes and nuclease-free water up to 50 µl to complete the reaction volume. Positive and negative controls had been prepared in parallel with the test samples. The PCR cycling parameters for each gene were set as shown in **Table 2**. The amplified DNA samples were loaded into agarose gel stained with SYBR Safe DNA Gel Stain (Invitrogen) and allowed to run for 30 min at 120 V in Tris-acetate-EDTA buffer (TAE) (see **Table 3**). The gel was imaged

with the Gene Genius Bioimaging System (Syngene). The amplified DNA products were purified from other reaction components by the GenElute PCR Clean-Up Kit (Sigma-Aldrich) prior to sequencing.

**Table 2. The primer sequences and cycling conditions used in the PCR reactions.**

Gene	Primer pair sequence (Forward/Reverse)	Cycling parameters
<b>β-actin</b>	5'-CACCGCAAATGCTTCTAGGC-3' 5'-GTCCTCGGCCACATTGTGAA-3'	- Initial denaturation at 94°C for 1 min. - Thirty-five cycles of denaturation 94°C for 20 sec, annealing 62°C for 30 sec and extension 72°C for 1 min. - Final extension at 72°C for 10 min.
<b>5-HT<sub>4</sub> receptor</b> <i>(PCR product flanks the N7)</i>	5'-TGGATTACAAGGATGACGACG-3' 5'-TTGAACCAGCTCAATGGCAC-3'	- Initial denaturation at 94°C for 1 min. - Forty cycles of 94°C for 20 sec, 58°C for 30 sec and 72°C for 1 min. - Final extension at 72°C for 10 min.
<b>5-HT<sub>4</sub> receptor</b> <i>(PCR product flanks the N180)</i>	5'-CCCTATAATGCAAGGCTGGA-3' 5'-ATGCGATGAGTGCTATGCTG-3'	- Initial denaturation at 94°C for 1 min. - Forty cycles of 94°C for 20 sec, 58°C for 30 sec and 72°C for 1 min. - Final extension at 72°C for 10 min.
<b>5-HT<sub>6</sub> receptor</b>	5'-CCGCCGGCCATGCTGAACG-3' 5'-GCCCCGACGCCACAAGGACAAAAG-3'	- Initial denaturation at 94°C for 1 min. - Forty cycles of 94°C for 20 sec, 62°C for 30 sec and 72°C for 1 min. - Final extension at 72°C for 10 min.

The primers used in this work were designed by the primer designing tool in NCBI online tools. Several factors were considered during the primer design; the length of the primer (range between 18-30 nucleotides), the G/C content (to be between 40% to 60%) and primer pairs should not have complementary regions. In addition, the melting temperature of both primers should be close to each other. To ensure the target specificity of the primers, Primer-BLAST tool was used.

**Table 3.**The compositions of TAE electrophoresis buffer and agarose gel.

Buffer/gel	Compositions	Concertation/volume used
TAE (50X) buffer	Tris base Acetic acid Disodium EDTA dH <sub>2</sub> O	2 M 57.1 ml 50 mM Up to 1 L, this stock was diluted to 1X before use
1% Agarose Gel	TAE buffer (1X) Agarose SYBR Safe Stain	40 ml 0.4 g 4 µl
3.5% Agarose Gel	TAE buffer (1X) Agarose SYBR Safe Stain	40 ml 1.4 g 4 µl

#### **2.3.4. Real-time PCR**

Real-time PCR—or quantitative PCR (qPCR)—was conducted to determine the differences in gene expression levels of 5-HT<sub>4</sub> and 5-HT<sub>6</sub> receptors in the frontal lobe of the cerebral cortices of AD patients by comparing the results to age-matched controls. The human cDNA was obtained from the Oxford Project to Investigate Memory and Ageing (OPTIMA) (ethical approval no: 07/Q2707/98). The study cases were allocated into three groups; control (entorhinal stage, E), early stage of AD (limbic stage, L) and late stage of AD (neocortical stage, N), based on the Braak staging, as in **Table 4**. Human Tissue Act 2004 was considered in all the procedures involved using human tissues or samples. Notably, the human samples were processed and quantified by an investigator blind to the clinical details. Unblinding of the study AD patients and controls was achieved only following completion of gene quantification.

Due to the limited amount of precious human DNA samples, the standard curves for the target and the house-keeping gene were generated using a ten-fold dilution

series, from 50 ng to 0.0005 ng, of cDNA obtained from the HEK293 cell line transfected with 5-HT<sub>4</sub> and 5-HT<sub>6</sub> receptor plasmids. The gene expression assay was conducted using a TaqMan® primer/probe set (**Table 5**), and the TaqMan® Gene Expression Master Mix obtained from Thermo Fisher Scientific. All the primers were intron-spanning to exclude genomic DNA amplification. Each PCR reaction contained; 10 µl of the master mix, 1 µl of the primer, 4 µl of nuclease-free water and 5 µl of the DNA template. The mixture was made up to a 20 µl final volume per well. The 96 well PCR plate was sealed, spun briefly and placed in an ABI 7500 real-time PCR thermal cycler. The cycling conditions include: hold 50°C for 2 min, denaturation at 95°C for 10 min, 40 cycles of 95°C for 15 sec followed by annealing and extension at 60°C for 1 min. Upon DNA amplification, the TaqMan probe reporter physically separated from the quencher by hydrolysis and the fluorescence increased proportionally as the amplicon quantity increased. The absolute quantities of the genes of interest were calculated by interpolation of the Ct value for each sample from the standard curve followed by normalisation to the quantities of the house-keeping gene. In addition, fold change in gene expression pre- and post-transfection of the HEK293 cell line was calculated by the Livak method (2<sup>-ΔΔCt</sup> method) from three replicates (Livak and Schmittgen, 2001). The first difference was calculated by subtracting the Ct values of the reference gene from the target gene for both transfected and untransfected HEK293 cells (ΔCt). This was followed by a calculation of the difference in the expression between the transfected and untransfected HEK293 cells (ΔΔCt) as summarised by the equation:

$$\Delta\Delta C_t = (C_{t, HTR4/6} - C_{t, EIF4A2})_{\text{Transfected cells}} - (C_{t, HTR4/6} - C_{t, EIF4A2})_{\text{Untransfected cells}}$$

The amplification efficiency percentage was calculated from the following

$$\text{equation: } (E\%) = (10^{-1/\text{slope}} - 1) \times 100.$$

**Table 4. Demographics of AD cases and controls used in the qPCR experiments.**

*(E) entorhinal stage, (L) limbic stage, and (N) neocortical stage of AD.*

Sample ID	Gender	Age	ApoE genotype	Post-mortem delay (PMD, hr)	Disease severity	Diagnosis
RI02 0050	F	93	E2E3	72	E	Not AD
RI02 0048	M	89	E3E3	72	E	Not AD
RI03 0024	M	77	E2E3	24	E	Not AD
RI02 0025	F	88	E3E3	48	E	Not AD
RI99 1147	F	93	E2E3	60	E	Not AD
RI99 1077	M	91	E3E3	25	E	Not AD
RI04 0110	M		E3E3	96	E	Not AD
RI00 1050	F	81	E3E3	48	E	Not AD
RI04 0199	M	87	E2E3	72	E	Not AD
RI00 1187	M	78	E2E3	63	E	Not AD
RI02 0038	F		E3E4	96	L	AD
RI01 0173	F		E2E4	72	L	AD
RI99 1003	M	100	E3E3	48	L	AD
RI97 1202	F	89	E2E3	24	L	AD
RI99 1160	M	77	E3E3	24	L	AD
RI92 1020	F	84	E3E3	12	L	AD
RI94 1315	F	83	E3E4	20	L	AD
RI02 0102	M	83	E3E3	96	L	AD
RI94 1034	M	89	E3E3	16	L	AD
RI95 1003	M		E3E4		L	AD
RI03 0077	M	88	E3E3	24	N	AD
RI02 0046	F		E3E4		N	AD
RI97 1013	F	77	E3E4	36	N	AD
RI92 1142	F	81	E3E3	72	N	AD
RI91 1250	F	74	E4E4	30	N	AD
RI04 0021	F	94	E3E3	72	N	AD
RI99 1002	M	70	E3E4	79	N	AD
RI94 1216	M	89	E3E4	59	N	AD
RI98 1004	F	82	E2E3		N	AD
RI91 1327	F	58	E3E3	60	N	AD

**Table 5. Primers used in the quantitative gene expression assay.**

<b>Gene</b>	<b>Reporter dye</b>	<b>Assay ID</b>	<b>Cat. No. Thermo Fisher Scientific</b>
5-HT <sub>4</sub> receptor ( <i>HTR4</i> )	FAM	Hs00410577_m1	4331182
5-HT <sub>6</sub> receptor ( <i>HTR6</i> )	FAM	Hs00168381_m1	4331182
Eukaryotic translation initiation factor 4A2 ( <i>EIF4A2</i> )	VIC	Hs00756996_g1	4331182

## **2.4. Plasmid cloning**

### **2.4.1. Subcloning of 5-HT<sub>4</sub> and 5-HT<sub>6</sub> Receptor:**

In molecular biology, subcloning is a method used to transfer a target DNA fragment (gene) from one vector to another with the aim of adding a desired feature to the target. Virtual sub-cloning was simulated by Serial Cloner 2.6 software prior to conducting the lab procedure to select the appropriate restriction sites and avoid improper fragment ligation.

#### ***Restriction digest:***

The untagged human 5-HT<sub>4</sub> receptor insert (in house) was sub-cloned from pCDNA3.1 into the pCMV6-Entry C-terminal Myc-DDK tagged vector (Origene). The untagged human 5-HT<sub>6</sub> receptor insert in VersaClone (R&D Systems) was sub-cloned into the pCMV6-AN-His-Myc N-terminal tagged vector, or into the pCMV6 entry C-terminal tagged vector (Origene). Both the donor and recipient plasmids were digested by Hind III and Xho I restriction enzymes (NEB). The restriction procedure was summarised in **Table 6**. These enzymes create non-compatible overhangs in the DNA and thus facilitate directional subcloning of the insert thereby reducing the possibility of re-ligation of the recipient plasmid.

**Table 6. General double digestion protocol to release the insert from the vector.**

DNA	1 µg
10x CutSmart buffer <sub>(NEB)</sub>	5 µl
Restriction endonucleases <sub>(NEB)</sub>	1 µl of each enzyme (20 units)
Nuclease-free water	Up to 50 µl
Incubated at 37°C for an hour, enzymatic inactivation at 80°C for 20 min and then hold at 4°C	

#### **2.4.2. Gel extraction and DNA purification**

Following digestion and based on the DNA size differences, the bands for the genes of both 5-HT<sub>4</sub> and 5-HT<sub>6</sub> receptors (insert) were separated from their vectors by 1% agarose gel electrophoresis. The DNA fragments of interest were carefully excised from the gel, weighed and extracted using the GeneElute gel extraction kit (Sigma-Aldrich, Cat No. NA1111). According to the kit instructions, three gel volumes of the solubilisation solution were added to one volume of the gel. The mixture was maintained at 55°C for 10 min to solubilise the gel. The DNA was then precipitated with equal gel volumes of 100% isopropanol. The mixtures were loaded into pre-prepared binding columns and centrifuged at 14,000 g for 1 min. Contaminants were eliminated by washing the column with 700 µl of wash solution and centrifuged at 14,000 g for 1 min. The column bound DNA was eluted in 25-50 µl of nuclease-free water by centrifugation. The concentration of DNA was measured by the NanoDrop. If the A<sub>260/230</sub> ratio was low, an additional ethanol DNA precipitation step was performed to improve the purity.



### 2.4.3. Ethanol DNA precipitation

Excess salt in the DNA solution was removed by mixing 1/10 volume of sodium acetate (3M, pH 5.2), glyco-blue (2 µl) and two volumes of cold ethanol (100%) to the DNA on ice where it was kept for 30 min. Later, the mixture was centrifuged at  $\geq 12,000$  g for 20 min at 4°C. The supernatant was carefully decanted, and the pellet was washed with two volumes of cold ethanol (70%) and centrifuged again for 10 min. After removing the supernatant, the DNA was allowed to dry for a few minutes prior to resuspension in the desired quantity of nuclease-free water.

### 2.4.4. Vector dephosphorylation

The pre-digested recipient vector was dephosphorylated by Antarctic Phosphatase (NEB) in the presence of the Antarctic phosphatase buffer (10x) (NEB) and placed in the thermal cycler at 37 °C for 30 min. Dephosphorylation can minimise any possibility of vector re-ligation.

### 2.4.5. Ligation

The purified inserts were ligated with their corresponding recipient vectors by the aid of T4 DNA Ligase which links between the 3'-hydroxyl groups and 5'-phosphate group of the DNA in the presence of  $Mg^{2+}$ , ATP and DTT from the ligation buffer. The ligation components and the reaction conditions are summarised in **Table 7**. The amount of the insert required for the reaction was calculated using the following equation:

$$\text{Insert amount (ng)} = \frac{\text{vector amount (ng)} \times \text{size of the insert (kb)}}{\text{size of the vector (kb)}} \times \text{molar ratio} \frac{\text{insert}}{\text{vector}}$$

**Table 7. Ligation reaction protocol.**

10X T4 ligase buffer (Promega)	1 $\mu$ l
T4 ligase (Promega, 1–3u/ $\mu$ l)	0.5 $\mu$ l
Vector DNA	100 ng
Insert DNA	Calculated from the equation using pre-optimised 5:1 molar ratio
nuclease-free water	Up to 10 $\mu$ l
Incubated at RT for 3 hr or at 4°C overnight.	

#### **2.4.6. Preparation of chemically competent bacteria**

All works involving bacterial culturing were carried out aseptically. Chemically competent *E. coli* were prepared by pre-treating them with divalent cations such as calcium chloride, thereby enhancing the bacterial membrane permeability to uptake the plasmid DNA in a process termed ‘transformation’. Inoue transformation buffer was used for this purpose (**Table 8**) (Inoue et al., 1990).

The appropriate bacterial strain stock was diluted with super optimal broth (SOB+) in a 1 to 1000 ratio. Different volumes; 25  $\mu$ l, 50  $\mu$ l and 100  $\mu$ l were spread on to SOB+ agar plates and incubated overnight at 37°C. One colony was inoculated in 5 ml of SOB medium without antibiotic and allowed to grow overnight at 20°C with agitation. Next day, the growing bacteria was added to 200 ml of SOB medium in a pre-autoclaved conical flask. The bacteria were grown at 20°C with frequent monitoring of the optical density at 600 nm (OD<sub>600</sub>) to ensure that the culture growth was still in the exponential (log) phase using the Eppendorf BioPhotometer Plus. When the OD<sub>600</sub> of the culture reached 0.6, the flask was placed on ice for 10 min, and then the bacterial suspension was pelleted at 2,400 g for 15 min at 4°C using the

Beckman J2-MC centrifuge. The bacteria were gently resuspended with 320 ml of ice-cold, filter sterilised Inoue buffer, and the centrifugation was repeated. Again, the pellet was gently resuspended in a mixture of 80 ml of ice-cold Inoue buffer and 6 ml of DMSO prior to quick aliquoting of the bacterial suspension in Eppendorf tubes. These were subsequently flash frozen in liquid nitrogen and stored at -80°C for up to 6 months. The transformation efficiency was calculated by transforming the bacteria with a known amount of plasmid.

#### **2.4.7. Bacterial transformation**

Transformation is a process that uses competent bacteria to amplify the plasmid for further applications. An aliquot of highly efficient 5-alpha (NEB) or the in-house made  $\alpha$  select *E. coli* competent bacteria was taken from -80°C storage and allowed to thaw on ice. As soon as thawing was complete, 100 ng of the DNA plasmid was mixed with the bacteria and placed on ice for 30 min. This was followed by heat shocking the mixture at 42°C for 30 sec then placement back on ice. Then, 950  $\mu$ l of SOC outgrowth medium (NEB) was added to recover the bacteria after heat shock, and the bacteria were then incubated at 37°C for 1 hr with continuous shaking. Small volumes of the transformation mixture were spread onto LB agar plates containing either 100  $\mu$ g/ml of ampicillin or 50  $\mu$ g/ml of kanamycin according to the antibiotic resistance gene in the plasmid. The plates were inverted and incubated overnight at 37°C. Typically, and due to the presence of the antibiotic, only the bacteria harbouring the plasmid are expected to form colonies. The following day, few colonies were individually picked, dispersed in 5 ml LB broth media with antibiotic and incubated at 37°C overnight with agitation. A portion of the bacterial suspension was mixed with 50% sterile glycerol to make stocks which were stored at -80°C for

later use. The remaining suspension was used for plasmid purification from the hosting bacteria.

**Table 8. The components of the buffer, broth and agar used in competent bacterial preparation and transformation.**

Inoue buffer	MnCl <sub>2</sub> ·4H <sub>2</sub> O CaCl <sub>2</sub> ·4H <sub>2</sub> O KCl Piperazinediethanesulfonic acid (PIPES, pH 6.7) dH <sub>2</sub> O	55 mM 15 mM 250 mM 10 mM Up to 1 L filter
SOB+ broth pH 7.0	Tryptone Yeast extract NaCl KCl MgCl <sub>2</sub> MgSO <sub>4</sub> dH <sub>2</sub> O	20 g 5 g 10 mM 2.5 mM 10 mM 10 mM Up to 1 L filter
SOB+ agar	SOB+ broth Agar	100 ml 1.2 g
LB broth	Tryptone Yeast extract NaCl dH <sub>2</sub> O	10 g 5 g 10 g Up to 1 L
LB agar	LB broth Agar	1 L 12 g

#### 2.4.8. Plasmid purification

The plasmid purification obtained from the harbouring bacteria was conducted using the alkaline-SDS lysis method which was firstly developed by Bimboim and Doly (1979). The lysis solution used contains SDS, which disrupts the bacterial membrane and denatures most of the cellular proteins. It also contains sodium hydroxide which denatures the genomic and plasmid DNA by breaking the hydrogen bonds making them single-stranded DNA. Neutralising the alkaline pH can selectively renature the small plasmid DNA to its double-stranded soluble form. However, the large genomic

DNA, as well as other lysed proteins on treatment, will precipitate as insoluble clots which easily fall out of the solution by centrifugation. Two plasmid purification scales were used; small-scale purification (miniprep) to initially screen for a positive bacterial clone by analysing the sequence of the purified plasmids and then a large-scale purification (maxiprep) used to purify high plasmid yield which is sufficient for downstream applications such as transfection.

After the transformation step, the GenElute™ Plasmid Miniprep Kit (Sigma-Aldrich, Cat No. PLN70) was used to purify up to 5 ml of the overnight culture. According to the kit instructions, the bacteria were harvested via centrifugation at 15,000 g for 1 min. The pellet was completely resuspended with 200 µl of prechilled resuspension buffer. Then, 200 µl of the lysis solution was added, mixed by gentle inversion and incubated for less than 5 min. The lysis reaction was terminated by adding 350 µl of the neutralisation solution. Insoluble precipitates were separated from the solution by centrifugation at 15,000 g for 10 min. The clear lysate solution was then transferred into a silica column and centrifuged again for 1 min. Contaminants were removed by adding 750 µl of washing solution followed by spinning and discarding of the flow through. Next, the plasmid DNA was eluted in 100 µl of nuclease-free water, and the concentration was determined by the NanoDrop. The isolated plasmids were sequenced to select the positive clone.

For large scale purification, 200 ml LB medium was inoculated with a positive clone in the presence of the antibiotic and grown overnight at 37°C. According to the Plasmid Maxi kit (Qiagen, Cat No. 12163) instructions, the bacteria were transferred to the centrifuge bottle and spun at 6000 g for 15 min at 4°C. The pellet was resuspended in 10 ml of P1 buffer then lysed by adding 10 ml of buffer P2 which

changed the colour of the solution to blue due to the presence of Lyseblue reagent. The solution was mixed until the blue colour was evenly distributed (optimum lysing) and incubated for no more than 5 min. Pre-chilled neutralising P3 buffer (10 ml) was added and mixed until the blue indicator disappeared, and the mixture was then kept on ice for 20 min. Next, the insoluble precipitate was separated by centrifugation at 17,000 g for 30 min at 4°C. The supernatant was transferred to a pre-prepared column and allowed to flow through by gravity. To remove the contaminants, the column was washed twice with 30 ml of buffer QC. The plasmid was eluted from the column using 15 ml of QF buffer and then mixed with 10.5 ml of isopropanol aiding the precipitation of the plasmid after centrifugation at 17,000 g for 30 min at 4°C. The supernatant was decanted carefully, and the pelleted plasmid was washed with 5 ml of 70% ethanol which was then removed by centrifugation. The plasmid was dissolved in 1 ml of nuclease-free water. To assess the plasmid quantity and purity, the concentration was determined by the NanoDrop and the absorbance ratios measured had to be within the acceptable range to allow the use of samples in future applications. Furthermore, 2 µl of the plasmid were loaded in 1% agarose gel to determine if the purified plasmid was intact and mainly in a supercoiled form which is required for successful transfection.

## **2.5. Site-directed mutagenesis (SDM)**

SDM is a technique used to introduce targeted DNA mutations; insertions, substitutions or deletions, to plasmid DNA. This is achieved by using custom designed oligonucleotides that incorporate the desired mutation in their sequence or flank the sequence to be deleted. The Q5 Site-Directed Mutagenesis Kit (NEB, Cat No. E0554S) was used. The three steps SDM protocol is summarised in **Table 9**. All

oligonucleotides used in this work were designed by the NEBaseChanger tool to anneal back-to-back and obtained from Sigma-Aldrich.

### **2.5.1. 5-HT<sub>4</sub> receptor mutant constructs**

The human 5-HT<sub>4</sub> receptor in pCMV3-Flag vector plasmid was purchased from Sino Biological (Cat No. HG10753-NF) and was used as a template for SDM. The potential sites were detected by NetNglyc 1.0 online server of Center for Biological Sequence Analysis. This server has a prediction accuracy as high as 76%. The 5-HT<sub>4</sub> receptor mutant constructs were generated based on disrupting the potential *N*-glycosylation sites by replacing asparagine residues at position 7 (AAT) and 180 (AAC) with glutamine (CAA). Single mutant constructs (N7Q and N180Q) were generated separately then, the double mutant construct (N7/180Q) was generated using the single mutant (N7Q) as a template for SDM to add the second mutation site. The mutagenic oligonucleotides are listed in **Table 10**.

**Table 9. Site-directed mutagenesis protocol.**

<b>1- Exponential amplification</b>	
Q5 High-Fidelity 2X Master Mix	12.5 µl
10 µM of each primer	1.25 µl for each primer
1-25 ng of template DNA plasmid	1 µl
Nuclease-free water	9 µl
<p>The cycling conditions started with denaturation at 98°C for 20 sec, then 25 cycles of 95°C for 10 sec, annealing for 20 sec and extension at 72°C for 30 sec/kb, then final extension at 72°C for 2 min. The primer annealing temperature was optimised for each mutant.</p>	
<b>2- Kinase, Ligase and DpnI (KLD) Treatment</b>	
PCR Product	1 µl
2X KLD Reaction Buffer	5 µl
10X KLD Enzyme Mix	1 µl
Nuclease-free water	3 µl
<p>The mixture was incubated for 1 hr at RT</p>	
<b>3- Transformation</b>	
<p>After KLD treatment the mixture was transformed into competent bacteria as previously described in <b>Section 2.4.7</b>.</p>	



**Table 10. Designed primers for SDM and the annealing temperature used.**

<b>Insert/ Vector</b>	<b>Mutation</b>	<b>Primer pair sequence (Forward/Reverse)</b>	<b>Annealing temperature</b>
Human 5-HT <sub>4</sub> receptor in pCMV6 Entry	<b>Deletion</b> of a stop codon between the tag and the receptor C-terminus (open frame)	5'- CTCGAGCAGAAACTCATCTCAG -3' 5'- AGTGTCACTGGGCTGAGC -3'	63°C
Human 5-HT <sub>6</sub> receptor in pCMV6 Entry	<b>Insertion</b> of Myc tag in the receptors N-terminus.	5'- AGCGAAGAAGATCTGGAGCCGGGCCCCAACCGCC-3' 5'- AATCAGTTTCTGTTCTGGGACCATGGTGGCGGC -3'	72°C
Human 5-HT <sub>4</sub> receptor in pCMV3- Flag vector	<b>Substitution</b> of N7 asparagine residue with glutamine	5'-ACTTGATGCTCAAGTGAGTTCTGAGGAGGG-3' 5'-TTGTCGCTACCGCCTCCA-3'	63°C
Human 5-HT <sub>4</sub> receptor in pCMV3- Flag vector	<b>Substitution</b> of N180 asparagine residue with glutamine	5'-CCAGAACTCTCAATCTACGTACTG-3' 5'-TTGAACTTCCTCTTTTCTATC-3'	54°C

## **2.6. DNA sequencing**

The DNA plasmids (200-500 ng) or purified PCR products (3-10 ng) were mixed with 3.2 pmol of primer and nuclease-free water up to 10 µl. The standard primers used in plasmid sequencing are listed in **Table 11**. The PCR products were mostly sequenced using primers used for PCR amplification. The sequencing was performed on the 3730 DNA analyser (Applied Biosystems) which is run as a service provided by the functional genomics, proteomics and metabolomics facility in the School of Bioscience, University of Birmingham. The data were retrieved as Chroma Lite 2.1. files which were then exported to Serial Cloner 2.6. NCBI's basic local alignment search tool (BLAST) was utilised to confirm if the nucleotide and peptide sequences were correct.

**Table 11. Primers commonly used in plasmid sequencing.**

<b>Primer name</b>	<b>Primer sequence</b>
VP1.5 forward	5'-GGACTTTCCAAAATGTCG-3'
XL39 reverse	5'-ATTAGGACAAGGCTGGTGGG-3'
CMV forward	5'-CGCAAATGGGCGGTAGGCGTG-3'
T7 forward	5'-TAATACGACTCACTATAGGG-3'
BGH reverse	5'-TAGAAGGCACAGTCGAGG-3'
M13 forward	5'-TGTA AACGACGGCCAGT-3'
M13 reverse	5'-CAGGAAACAGCTATGAC-3'

## **2.7. Transfection**

Transfection is a method used to introduce plasmid DNA into mammalian cells through various physical or chemical approaches. In this study, chemical-based transfection was used by mixing the plasmid DNA with either of Polyethyleneimine (PEI, Polysciences, Cat. No. 23966), Lipofectamine 2000 or Lipofectamine 3000 (Thermo Fisher Scientific) in serum-free medium (SFM). The mixing was performed in specific ratios. The transfection mixture preparation and amounts are abridged in **Table 12** for 10 cm<sup>2</sup>. The transfection mixture amount was scaled according to the surface area of the cultural vessels. These cationic liposomes or polymers form a complex with the DNA at certain dilution ratios and neutralise its negative charge, thus permitting the DNA penetration through the cell membrane. When the cells attained 70-90% confluency, the medium was removed, and the transfection mixture was added dropwise on the cells and incubated for at least 4 hr at 37°C. Next, the transfection mixture was diluted by adding complete medium and then incubated for 24 to 96 hr to transiently express the transfected protein.

To generate a stable cell line, 24 hr post-transfection, the cells were trypsinised and cultured at very low density in the presence of selection antibiotics; geneticin (G418, 600 µg/ml, Gibco) or hygromycin B (120 µg/ml, Thermo Fisher Scientific). The G418 containing medium was changed every 2–3 days while the hygromycin-containing medium was changed every 5-6 days. Usually, the cells that do not uptake the plasmid die after a few days of selection. The stable clones became visible 3 weeks after transfection. The clones were individually picked using cloning discs (Sigma-Aldrich) and then expanded for an additional two weeks in a maintenance dose of selection antibiotic (half the selection dose) to prevent the loss of the

overexpressed protein. The purity of each clone was assessed using flow cytometry and Western blotting. If the clones showed positive results, then they were expanded with a portion being frozen for future use.

**Table 12. Transfection mixture preparation protocol.**

<b>Reagent and ratio (weight/volume)</b>	<b>Mixture preparation protocol For one well of 6 well plate (10 cm<sup>2</sup>).</b>
DNA/ PEI 1:2, 1:3 and 1:4	<ul style="list-style-type: none"> <li>- In one tube, 2 µg of the plasmid DNA was diluted in 250 µl of SFM and vortexed for 10 sec.</li> <li>- Then, 4 µl, 6 µl or 8 µl of PEI was added and mixed by pipetting.</li> <li>- The mixture was incubated for 25 to 30 min at RT then added to the cells.</li> </ul>
DNA/ Lipofectamine 2000 1:2 and 1:3	<ul style="list-style-type: none"> <li>- In the first tube, 125 µl of SFM and 2.5 µg of DNA were mixed by pipetting and incubated for 5 min</li> <li>- In the second tube, 5 µl or 7.5 µl of lipofectamine 2000 was diluted in 125 µl of SFM and vortexed for 3 sec.</li> <li>- Then, the contents of both tubes were combined, mixed by pipetting, incubated for 20 min at RT and then added to the cells.</li> </ul>
DNA/ Lipofectamine 3000 1:2	<ul style="list-style-type: none"> <li>- In the first tube, 125 µl of SFM, 2.5 µg of DNA and 5 µl of P3000 reagent were mixed by pipetting and incubated for 5 min.</li> <li>- In the second tube, 5 µL of lipofectamine 3000 was diluted in 125 µl of SFM and vortexed for 3 sec.</li> <li>- Then, the content of the second tube was transferred to the first tube, mixed by pipetting, incubated for 10 min at RT and then added to the cells.</li> </ul>

## **2.8. Western blotting**

Western blotting is used to determine the protein expression in a cell or tissue lysate through antigen and antibody interactions. It is also used as a semi-quantitative approach to detect the changes in protein expression by measuring the signal intensity relative to loading control.

### **2.8.1. Cell stimulation**

#### ***Functionality assay (ERK<sub>1/2</sub> activation)***

Drugs used in this experiment were dissolved in SFM. The cells were seeded onto a poly-D-lysine pre-coated 6-well plates to minimise the cell detachment during starvation and stimulation. After overnight serum starvation, the cells were challenged with the required dose of 5-HT and left in contact with the cells for specific time points. The stimulation was terminated by flicking the plate to remove the stimulation medium followed by two washes with ice-cold PBS. In the case of antagonists, the cells were incubated with the antagonist for 30 min before being challenged with 5-HT.

#### ***Tunicamycin deglycosylation***

To inhibit *N*-linked glycosylation, the HEK293 cells stably expressing the wild-type or mutant 5-HT<sub>4</sub> receptor were grown for 48 hr in the presence of tunicamycin which was added to complete medium at a final concentration of 1 µg/ml. In case of transient transfection, tunicamycin was added to the complete medium 4 hr after transfection and again kept for 48 hr.

### **2.8.2. Cell lysate preparation.**

The cells were scraped off from the flask in ice-cold PBS and collected by centrifugation at 400 g for 5 min. The pelleted cells were suspended in 25 mM Tris-HCl buffer (pH 7.4) and sonicated while being kept on ice. Bradford protein assay was employed to determine the protein concentrations to ensure the samples were equally loaded. The lysis was performed by the addition of a radio-immunoprecipitation assay (RIPA) buffer which pre-mixed with protease and phosphatase inhibitors. This lysate was mixed with 2X urea sample buffer (USB) containing 10% 2-mercaptoethanol in a 1:1 ratio (**Table 13**). Regarding the cells that were grown in the 6-well plates, the cells were lysed in the plate by adding 100 µl of freshly prepared complete lysis buffer per well. The plates were placed on ice for 5 min. The lysed cells were collected in 1.5 ml tubes, sonicated briefly and spun down at 4°C for 10 min.

**Table 13. The compositions of the buffers used in cell lysate preparation for Western blotting.**

Buffer	Component	Concentration
<b>1X RIPA lysis buffer</b>	Tris-HCl (pH 7.5)	20 mM
	NaCl	150 mM
	Na <sub>2</sub> EDTA	1 mM
	EGTA	1 mM
	NP-40	1%
	Sodium deoxycholate	1%
	Sodium pyrophosphate	2.5 mM
	β-glycerophosphate	1 mM
	Na <sub>3</sub> VO <sub>4</sub>	1 mM
	leupeptin.	1 µg/ml
<b>2X USB</b>	Tris HCl pH 6.8	125 mM
	SDS	4%
	Urea	9 M
	Glycerol	20%
	Bromophenol blue	0.01%
	β-mercaptoethanol	10%, added before use

### 2.8.3. Gel electrophoresis and membrane blotting

Sodium dodecyl sulphate-polyacrylamide gel electrophoresis (SDS-PAGE) was employed to determine protein expression and size. Initially, 10% or 12% acrylamide hand-cast gels (**Table 14**) were freshly made for each experiment. Pre-stained Protein Ladder (Thermo Fisher Scientific) or Precision Plus Protein Standard (Bio-Rad) was loaded alongside 20 to 30 µg of protein lysate. The gel electrophoresis chamber was filled with the running buffer, and the samples were run at 35 mA per gel. The gel was gently teased from the glass plates and soaked along with the blotting papers in transfer buffer for 10 min. Polyvinylidene difluoride (PVDF) membranes were cut to a size of 6.5 x 8.5 cm and soaked in absolute methanol followed by transfer buffer for 10 min. The transfer sandwich was

assembled on Hoefer SemiPhor semi-dry blotter. The proteins were then transferred at 1.10 mA/cm<sup>2</sup> for 1 hr.

**Table 14. The components of the hand cast gels and buffers used in Western blotting.**

<b>Gel/ Buffer</b>	<b>Component</b>	
<b>Resolving gel (10%)</b>	dH <sub>2</sub> O	2,045 µl
	Tris, pH 8.8	1,250 µl
	10% SDS	50 µl
	30% Acrylamide	1,625 µl
	10% APS	25 µl
	TEMED	5 µl
<b>Resolving gel (12%)</b>	dH <sub>2</sub> O	1,720 µl
	Tris, pH 8.8	1,250 µl
	10% SDS	50 µl
	30% Acrylamide	1,950 µl
	10% APS	25 µl
	TEMED	5 µl
<b>Stacking gel (4%)</b>	dH <sub>2</sub> O	1,500 µl
	Tris, pH 6.8	625 µl
	10% SDS	25 µl
	30% Acrylamide	335 µl
	10% APS	12.5 µl
	TEMED	2.5 µl
<b>Running buffer (10X)</b>	Tris pH 8.3	250 mM
	Glycine	1.92 M
	SDS	1%
	DH <sub>2</sub> O	Up to 2 L
<b>Transfer buffer</b>	Tris pH 8.3	25 mM
	Glycine	150 mM
	SDS	0.1%
	Methanol	20%
	dH <sub>2</sub> O	Up to 2.5 L
<b>Washing buffer (10X)</b>	Tris pH 7.5	100 mM
	NaCl	1 M
	Tween 20	1%
	dH <sub>2</sub> O	Up to 2.5 L



#### **2.8.4. Blocking, probing and detection**

Blocking of the free binding site in the PVDF membranes was essential to minimise the nonspecific probing of the antibodies, and this was achieved by placing the membranes in 10% non-fat milk in washing buffer for two hr at RT. Next, the membrane was incubated overnight at 4°C with primary antibody diluted in 5% blocking buffer. The following day, the membranes were then washed four times with washing buffer for 5 min each and incubated for two hr at RT with a secondary antibody diluted in the blocking buffer. This was followed by a further washing step as previously described. The membranes were developed using the EZ-ECL chemiluminescent detection kit (Biological Industries) for 5 min and then visualised on the ChemiDoc MP imaging system (Bio-Rad). **Table 15** lists the antibodies used.

**Table 15. Antibodies used in Western blotting and their dilutions.**

Primary antibody	Secondary antibody
Rabbit anti-5-HT <sub>4</sub> receptor (1:1000, Abcam, ab60359), used by Hodge et al. (2013).	Goat anti-rabbit IgG (1:3000, CST, 7074)
Rabbit anti-5-HT <sub>4</sub> receptor (1:500, Abcam, ab113004).	Goat anti-rabbit IgG (1:3000, CST, 7074)
Rabbit anti-5-HT <sub>6</sub> receptor (1:1000, Abcam, ab207400).	Goat anti-rabbit IgG (1:3000, CST, 7074)
Rabbit anti-Hypoxanthine phosphoribosyl-transferase 1 (HPRT1) (1:3000, Abcam, ab10479), used by Fernández-Mosquera et al. (2017).	Goat anti-rabbit IgG (1:3000, CST, 7074)
Mouse anti-Myc tag (1:1000, CST, 2276), used by Beranek et al. (2018).	Horse anti-mouse IgG (1:3000, CST, 7076)
Rabbit anti-Flag (DDK) tag (1:1000, CST, 14793), used by Chen et al. (2017).	Goat anti-rabbit IgG (1:3000, CST, 7074)
Rabbit anti-pERK <sub>1/2</sub> (1:1000, CST, 9101), used by Baschieri et al. (2018).	Goat anti-rabbit IgG (1:3000, CST, 7074)
Rabbit anti-total ERK <sub>1/2</sub> (1:1000, CST, 4695), used by Businaro et al. (2018).	Goat anti-rabbit IgG (1:3000, CST, 7074)

### 2.8.5. Quantification of band intensity

The quantification of band intensity was determined by Image Lab 5.2.1 software (Bio-Rad). The immunoreactive signal for the protein of interest was normalised to the loading control protein signal in each lane, for example, pERK<sub>1/2</sub> was normalised to the total ERK<sub>1/2</sub> for each sample. The changes resulted from cell stimulation were then calculated as percentages or fold of change relative to the basal level.

## **2.9. Flow cytometry**

Flow cytometry is laser-based technology that is used to characterise cell properties, such as protein expression and phenotyping, while the cells are passing in a flowing stream of fluid. It was utilised to optimise the transfection ratio and screen for stable clones. Negative controls, no primary control and untransfected cells were stained in each experiment. Initially, the cells were washed with PBS and harvested using 10 mM EDTA without trypsin which was added to the cells and incubated for 20 min at 4°C. When the cells detached, complete medium was used to suspend the cells which were subsequently collected by centrifugation. The cell pellet was resuspended in PBS, and the total cell count was determined. The cells were seeded at a density of  $2 \times 10^5$  cell/ well in a 96 well round bottom plate. For cell surface staining, primary antibodies diluted in a fluorescence-activated cell sorting (FACS) buffer (2% FBS in PBS) were added to the cells and incubated for 30 min at 4°C. This was followed by two washes with FACS buffer. The fluorophore-conjugated secondary antibody was diluted in the FACS buffer and added to the cells which were kept in the dark for 20 min at RT. Following this step, the cells were washed as previously described and transferred in 300 µl of FACS buffer into polypropylene tubes. The CyAn ADP flow cytometer (Beckman Coulter) was used for measuring the fluorescence, and the results were analysed with Kaluza software (Beckman Coulter) by comparing the median fluorescence intensity (MFI) of the test cells to the appropriate controls. The antibodies used are listed in **Table 16**.

**Table 16. Primary and secondary antibodies and their dilutions.**

Primary antibody	Secondary antibody
Mouse anti-Myc tag (1:250, CST, 2276)	Goat anti-mouse IgG phycoerythrin (PE) (1:200, Abcam, Ab97024)
Rabbit anti-Flag (DDK) tag (1:500, CST, 14793)	Goat anti-rabbit IgG allophycocyanin (APC) (1:1000, Thermo Fisher Scientific, A10931)

### **2.10. Immunocytochemistry**

Immunocytochemistry (ICC) is used for protein expression and localisation within the cell via antigen-antibody interaction while maintaining the cellular composition. All the staining and washing steps were performed at RT unless otherwise mentioned. Typically, a day before immunostaining, sterile glass coverslips were placed on a 24 well plate coated with poly-D-lysine to enhance cell adherence to the glass. The cells were then seeded at a density of  $5 \times 10^4$  cells/ well. The next day, the culture medium was removed, and the cells were washed three times with PBS for 5 min each. To fix the cells, formaldehyde 2% solution in PBS was added, kept in the dark for 20 min and subsequently washed as previously described. For extracellular epitopes (N-terminus of the membrane-bound proteins), the permeabilisation step was omitted, and the cells were incubated with the blocking buffer (10% FBS in PBS) for 1 hr. The primary antibody was mixed with the blocking buffer in the recommended dilution as in **Table 17** and added to the cells and incubated overnight at 4°C. Later, the cells were washed four times with PBS for 5 min each and incubated with secondary fluorescent antibody for 2 hr in the dark. After that, the cells were washed four times with PBS for 5 min. If the protein

epitope is located intracellularly, the cell membrane should be permeabilised with a detergent such as 0.3% Triton X-100 in PBS for 1 hr to facilitate antibody penetration. For protein localisation experiments, surface and intracellular proteins were discriminated by using two different secondary fluorescent antibodies that conjugated with red and green fluorophore with and without the addition of the detergent, respectively. Consequently, this allowed the detection of protein localisation within the cell compartments. The coverslips were gently inverted on the slide that had a drop of Vectashield mounting medium (Vector Laboratories) with DAPI to counterstain the nucleus. The coverslips were sealed with nail polish and visualised under the Zeiss 780 LSM confocal microscope.

**Table 17. ICC antibodies used.**

Primary antibody	Secondary antibody
Rabbit anti-5-HT <sub>4</sub> receptor (1:1000, Abcam, ab60359)	AF 568 Goat anti-rabbit (1:1000, Thermo Fisher Scientific A11011)
Rabbit anti-5-HT <sub>6</sub> receptor (1:1000, Abcam, ab207400)	AF 568 Goat anti-rabbit (1:1000, Thermo Fisher Scientific A11011)
Mouse anti-Myc tag (1:1000, CST, 2276)	AF 488 Goat anti-mouse (1:1000, Thermo Fisher Scientific A21131)
Rabbit anti-Flag (DDK) tag (1:1000, CST, 14793)	AF 488 Goat anti-rabbit (1:1000, Thermo Fisher Scientific A11034)
Mouse anti-Flag (DDK) tag (1:1000, CST, 8146)	AF 488 Goat anti-mouse (1:1000, Thermo Fisher Scientific A21131) Or, AF 568 Goat anti-mouse (1:1000, Thermo Fisher Scientific A11031)

### **2.11. Immunohistochemistry**

Immunohistochemistry (IHC) is used for characterising the expression and localisation of proteins via an antibody binding in a tissue section while preserving the native structure of the tissue. Formalin-fixed paraffin-embedded (FFPE) brain sections were provided by the Thomas Willis brain bank under the ethical approval no: 07/Q2707/98. Clinical data for the patients were collected as part of the OPTIMA study. The samples provided originated from post-mortem AD patients and elderly individuals who were age-matched for the study as controls (**Table 18**). The samples were resected from Brodmann area 09 (BA09) of the frontal cortex.

All the staining and washing steps were performed at RT unless otherwise mentioned. Prior to staining, the slides were dewaxed using xylene and then gradually rehydrated through their incubation in a series of sequential washes; 100% ethanol, 95% ethanol, 70% ethanol to dH<sub>2</sub>O for 10 min each. Antigen retrieval was performed by heating the slides in a microwave oven in a boiled 10 mM citrate buffer (pH 6.0) for 7 min. This was followed by cooling of the slides by placing them under running tap water. The heat induced antigen retrieval exposes antigenic binding sites and breaks the protein cross-links that form during the fixation process. After that, the slides were placed in hydrogen peroxide (H<sub>2</sub>O<sub>2</sub>) to quench the endogenous peroxidase for 30 min as this can minimise the non-specific staining in the detection step. The slides were washed with dH<sub>2</sub>O followed by three washes in PBS and incubated in permeabilising buffer for 1 hr. The slides had been placed over cover plates, and the assemblies were secured and processed in a Sequenza rack (Thermo Fisher Scientific). The sections were covered with the blocking buffer and incubated for 1 hr. Subsequently, the slides were covered with the primary antibody or isotype

control at the required dilution and incubated overnight at 4°C (see **Table 19**). The concentrations of the antibodies used, and the blocking buffers were optimised to IHC. The following day, the slides were washed extensively with permeabilising buffer three times for 10 min each and incubated with the secondary biotin-conjugated antibody for two hr. Next, the slides were extensively washed as previously described and incubated with an avidin-biotin-peroxidase complex (ABC, Vector Laboratories) for 30 min. This complex amplified the detection signal due to the high affinity between avidin and biotin. Diaminobenzidine (DAB, Vector) was added to the slides which were kept in the dark until a brown precipitate formed. DAB is a chromogenic substrate to biotinylated peroxidase enzyme that allows the indirect visualisation and localisation of the target protein using a light microscope. Following this, the slides were washed with permeabilised buffer and dH<sub>2</sub>O. To counterstain the nucleus, the slides were immersed in haematoxylin for 30 sec, differentiated with two quick dips in (0.3%) acid alcohol and then immersed for 30 sec in Scott's tap water. In between these steps, a tap water wash was performed to remove the excess solution from the previous step. Finally, the slides were gradually dehydrated, mounted using DePeX and then scanned with the ZEISS Axio Scan automated microscope. Notably, all sections were scanned at constant light intensity. The buffers used in IHC are listed in **Table 20**.

**Table 18. Demographics of AD patients and age-matched controls.***(E) entorhinal stage, (L) limbic stage, and (N) neocortical stage of AD.*

Sample ID	Gender	Age at death	ApoE genotype	Post-mortem delay (PMD, hr)	Disease severity	Diagnosis
RI00 1187	M	78	E2E3	63	E	Not AD
RI00 1050	F	81	E3E3	48	E	Not AD
RI98 1148	M	70	E2E3	46	E	Not AD
RI03 0128	M	87	E2E3	24	E	Not AD
RI97 1288	F	88	E4E4	120	E	Not AD
RI95 1385	M	70	E3E4	62	E	Not AD
RI03 0211	M	85	E3E4	24	E	Not AD
RI02 0025	F	88	E3E3	48	E	Not AD
RI02 0054	M	87	E3E3	48	E	Not AD
RI03 0096	F	90	E3E3	72	E	Not AD
RI99 1003	M	100	E3E3	48	L	AD
RI96 1058	M	70	E3E4	88	L	AD
RI96 1102	M	72	E2E3	41	L	AD
RI99 1121	M	83	E3E3	38	L	AD
RI99 1160	M	77	E3E3	24	L	AD
RI03 0012	F	73	E3E3	48	L	AD
RI95 1214	F	82	E3E3	22	L	AD
RI96 1287	F	85	E2E4	83	L	AD
RI95 1334	F		E4E4	72	L	AD
RI02 0171	M	81	E3E3	48	L	AD
RI01 0173	F		E2E4	72	L	AD
RI03 0173	M	89	E2E3	96	L	AD
RI03 0183	F	83	E3E3	48	L	AD
C 2567	M	85	E3E3	36	L	AD
RI97 1001	F	81	E3E4	66	N	AD
RI99 1002	M	70	E3E4	79	N	AD
RI98 1004	F	82	E2E3		N	AD
RI96 1018	F	73	E3E3	36	N	AD
RI95 1068	F	77	E4E4	12	N	AD
RI96 1086	M	66	E4E4	30	N	AD
RI96 1089	M	71	E3E3	28	N	AD
RI00 1094	M	84	E4E4	30	N	AD
RI00 1125	M	71	E4E4	49	N	AD
RI98 1154	F	68	E3E4	106	N	AD
RI00 1191	M	62	E3E4	97	N	AD
RI95 1232	F	69	E3E4	83	N	AD
RI95 1302	M	77	E3E4	68	N	AD
RI02 0168	M	79	E3E4	96	N	AD
RI04 0021	F	94	E3E3	72	N	AD
RI03 0027	F	80	E3E4	72	N	AD
RI02 0036	F	70	E3E4	96	N	AD



Sample ID	Gender	Age at death	ApoE genotype	Post-mortem delay (PMD, hr)	Disease severity	Diagnosis
RI03 0036	M	98	E4E4	48	N	AD
RI02 0046	F		E3E4		N	AD
RI03 0046	M	70	E3E3	48	N	AD
RI03 0077	M	88	E3E3	24	N	AD
RI01 0093	F	63	E2E3	48	N	AD
RI99 1058	F	59	E2E3	15	N	AD
C 3970	F	87	E3E3	39	N	AD
C 4295	M	85	E3E3	36	N	AD

**Table 19. Antibodies used in IHC staining and their dilution.**

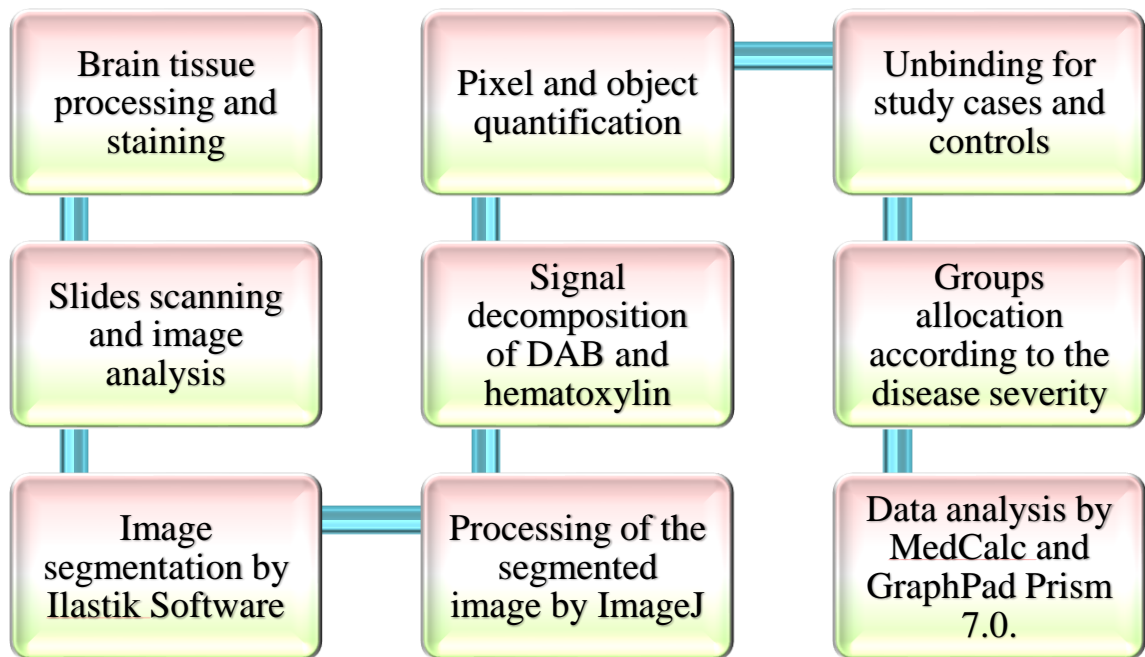
Primary antibody/ isotype	Secondary antibody
Rabbit anti-5-HT <sub>4</sub> receptor (1:500, Abcam, ab60359)	Biotinylated goat anti-rabbit IgG (1:1000, Vector laboratories, BA-1000)
Rabbit anti-5-HT <sub>6</sub> receptor (1:500, Abcam, ab207400)	Biotinylated goat anti-rabbit IgG (1:1000, Vector laboratories, BA-1000)
Rabbit polyclonal IgG, isotype control (1:500, Abcam, ab27478)	Biotinylated goat anti-rabbit IgG (1:1000, Vector laboratories, BA-1000)
Mouse anti-SERT (1:2000, MAb Technologies, ST51-1)	Biotinylated horse anti-mouse IgG (1:1000, Vector laboratories, BA-2000)

**Table 20. Buffers and solutions used in IHC and their compositions.**

<b>Buffers and solutions</b>	<b>Compositions</b>
<b>Permeabilising buffer</b>	0.3% Triton x100 in PBS
<b>Blocking buffer</b>	10% FBS in the permeabilising buffer
<b>Peroxidase quenching solution</b>	0.3% H <sub>2</sub> O <sub>2</sub> in dH <sub>2</sub> O
<b>ABCelite solution</b>	One drop of each reagents A and B in 2.5 ml of PBS
<b>DAB (peroxidase substrate)</b>	One drop of buffer solution, 2 drops of DAB and one drop of H <sub>2</sub> O <sub>2</sub> in 2.5 ml of dH <sub>2</sub> O.

#### **2.11.1. Quantification of the IHC image**

For quantification of the immunoreactivity, the number of positive cells and pixels in cortical layer III of the frontal lobe were segmented sequentially using Ilastik software. As this software had been trained on several representative images, it can be automatically applied to segment a large number of images in a unified way (Sommer et al., 2011). The segmented images were stacked in patches and processed by ImageJ software using pre-recorded macros. The total DAB positive area in  $\mu\text{m}^2$  was calculated after setting the image scale by using the image scale bar. Then, the segmented three-colour image was split into three channels. The DAB positive area in the red channel was analysed and calculated. Nuclei were used to calculate the number of cells per field to be used for normalisation since the cell number will certainly differ in each region of interest (ROI). All the staining and quantification steps were conducted and completed blindly (**Figure 8**).



**Figure 8. The immunohistochemistry quantification pipeline**

### **2.12. Single point radioligand binding assay**

The radioligand binding (RLB) assay is used to study the pharmacology of receptor-ligand interactions. Typically, cell homogenates are incubated with a radioligand until they reach equilibrium in the absence or presence of a competing drug which represents the total and non-specific binding (NSB), respectively (Davenport, 2012). The cells expressing the target proteins were scraped in ice-cold PBS and briefly homogenised in ice-cold 50 mM Tris-HCl (pH 7.4). The membrane proteins were fractionated from other cellular compositions by centrifugation twice at 48,000 g for 15 min and then resuspended in tris buffer. Protein concentrations were measured by the Bradford protein assay. Next, the proteins were diluted to the required concentrations in 2X TME buffer (1x TME contained 50 mM Tris-HCl (pH 7.4), 10 mM MgSO<sub>4</sub> and 0.5 mM EDTA (Kohen et al., 1996).

The assay was conducted in triplicate in a 500 µl total volume containing; 50 µl of tris or cold drug, 200 µl of radioligand [<sup>3</sup>H]-5-HT (specific activity 76 Ci/mmol, PerkinElmer) and 250 µl of the cell membrane protein fraction. The mixture was allowed to reach equilibrium for 1 hr at RT. Next, the equilibrium was terminated by 3 rapid filtrations with ice-cold tris over Whatman GF/B filters that had been pre-soaked in 0.3% PEI. Filter samples were placed into tubes with 4 ml scintillation fluid (Optiphase HiSafe 3; Perkin Elmer) and kept in the dark for at least 4 hr before being counted in Packard Tri-carb 1500 liquid scintillation counter.

### **2.13. Statistical analysis**

The statistical analysis was performed using GraphPad Prism 7 or Medcalc 17.7.2. software. The normality of the data was tested by the Shapiro-Wilk test to determine a suitable statistical analysis test. The differences between the means were determined by one-way analysis of variance (ANOVA). Two-way ANOVA was used to analyse the interactions between Hcy levels and the ApoE genotype on the expression of the 5-HT receptor or transporter. The association between the statistical variables was assessed by Spearman's correlation. Multiple regression analysis was used to determine the factors that significantly influenced the cognitive functions. The P-value was considered statistically significant if it was  $\leq 0.05$ .

**Chapter 3. Experimental developments  
and determinations for the endogenous  
expression of 5-HT<sub>4</sub> and 5-HT<sub>6</sub> receptors in  
SH-SY5Y and HEK293 cell lines**

### **3. Experimental developments and determinations for the endogenous expression of 5-HT<sub>4</sub> and 5-HT<sub>6</sub> receptors in SH-SY5Y and HEK293 cell lines**

#### **3.1. The analysis of gene expression levels of 5-HT<sub>4</sub> and 5-HT<sub>6</sub> receptors in SH-SY5Y and HEK293 cell lines**

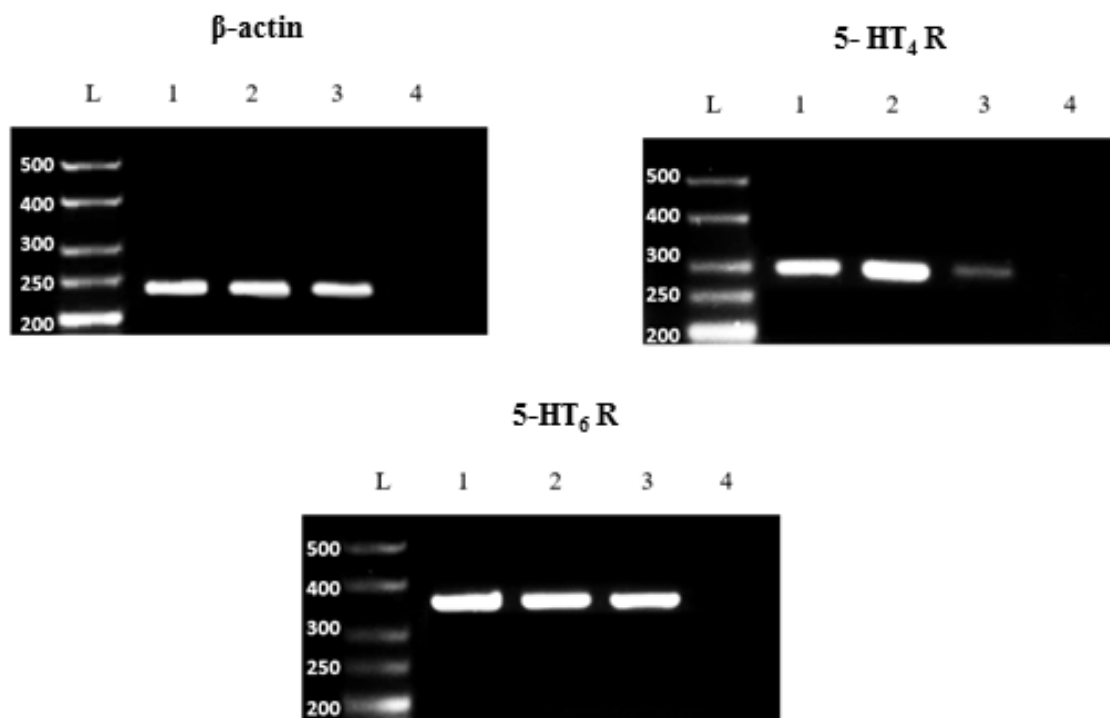
The aim of this analysis was to identify a cell line that natively expressed both 5-HT<sub>4</sub> and 5-HT<sub>6</sub> receptors to be used as a model for investigating the interaction of these receptors and their associated proteins in the context of AD. These receptors are known to be expressed in primary neurones. However, the maintenance of such cells was associated with difficulties since the cells cannot be propagated after cell culture. The reasons behind the selection of SH-SY5Y and HEK293 cell lines are their characteristics; the HEK293 cells are widely used as heterologously expressing system for GPCRs to study their signalling and interaction (Huang et al., 2005), while the SH-SY5Y cells have been utilised in AD research because of its neuronal origin and its expression of the AD's pathological proteins such as tau (Constantinescu et al., 2007). In addition, these cell lines were available as a cryopreserved stock in Barnes's lab.

The gene expression level of the two receptors was analysed using reverse transcriptase-polymerase chain reaction (RT-PCR). For the positive control, a cDNA sample was obtained from the autopsy of a post-mortem hippocampus of subject, not diagnosed with neuropsychiatric diseases. The hippocampus natively expresses 5-HT<sub>4</sub> and 5-HT<sub>6</sub> receptors at both the transcript and protein levels (Berumen et al., 2012). Negative controls containing the same reagents, but without the cDNA, were

amplified along with the tested samples to preclude any false positive results due to PCR contamination. The  $\beta$ -actin gene was utilised as an internal control to assure optimum workflow was performed from the RNA extraction step to the amplification step. This was included to eliminate the possibility of false negative results due to technical workflow defect. Moreover, amplification of the  $\beta$ -actin gene from the tested samples can provide a quantitative estimation of the DNA quantity. The agarose gel showed that the human hippocampus (positive control), SH-SY5Y cells and HEK293 cells natively expressed the transcripts of these target receptors. Moreover, the amplified PCR products for each targeted receptor appeared as distinct bands at expected sizes: 234 bp for  $\beta$ -actin; 288 bp for the 5-HT<sub>4</sub> receptor; and 342 bp for the 5-HT<sub>6</sub> receptor as shown in **Figure 9**.

Contrastingly, the negative controls did not show any amplified products, thus indicating the PCR was free from contaminants. The purified PCR products amplified from the SH-SY5Y cell line were sequenced. The results confirmed that the gel bands corresponded to the transcripts of the 5-HT<sub>4</sub> and 5-HT<sub>6</sub> receptors. Furthermore, NCBI's Nucleotide BLAST online tool was used to confirm 100% homology (**Figure 10**). The 5-HT<sub>4</sub> receptor amplified product showed homology to many receptor isoforms since the primers used targeted a universal region in all 5-HT<sub>4</sub> receptor isoforms and which was located away from their variant C-terminus.

Although this endpoint PCR is not a quantitative method, the results showed an unequivocal difference in the levels of gene expression of the 5-HT<sub>4</sub> receptor, relative to the stable  $\beta$ -actin level, in which HEK293 cells had the lowest transcript expression level in comparison to the SH-SY5Y cells and the human hippocampus while the 5-HT<sub>6</sub> receptor did not show any difference between the samples.



**Figure 9. Amplified PCR products corresponding to  $\beta$  actin, 5-HT<sub>4</sub> and 5-HT<sub>6</sub> receptors**

*Agarose gel electrophoresis illustrated the presence of receptor mRNA in the human hippocampus, SH-SY5Y cells and HEK293 cells (lanes 1, 2, and 3 respectively). Lanes 4 in each gel represented the negative control. Similar results were obtained from 3 independent repeats.*



a)

Homo sapiens 5-hydroxytryptamine receptor 4 (HTR4), transcript variant a, mRNA

Sequence ID: [NM\\_001040169.2](#) Length: 1364 Number of Matches: 1Range 1: 512 to 799 [GenBank](#) [Graphics](#)

▼ Next Match ▲ Previous Match

Score	Expect	Identities	Gaps	Strand
532 bits(288)	2e-147	288/288(100%)	0/288(0%)	Plus/Plus
Query 1	CCCTATAATGCAAGGCTGGAATAACATTGGCATAATTGATTTGATAGAAAAGAGGAAGTT			60
Sbjct 512	CCCTATAATGCAAGGCTGGAATAACATTGGCATAATTGATTTGATAGAAAAGAGGAAGTT			571
Query 61	CAACCAGAACTCTAACTCTACGTACTGTGCTTCATGGTCAACAAGCCCTACGCCATCAC			120
Sbjct 572	CAACCAGAACTCTAACTCTACGTACTGTGCTTCATGGTCAACAAGCCCTACGCCATCAC			631
Query 121	CTGCTCTGTGGTGGCCTTCTACATCCCATTCTCCTCATGGTGTGCGCTATTACCGCAT			180
Sbjct 632	CTGCTCTGTGGTGGCCTTCTACATCCCATTCTCCTCATGGTGTGCGCTATTACCGCAT			691
Query 181	CTATGTCACAGCTAAGGAGCATGCCATCAGATCCAGATGTACAACGGGCAGGAGCCTC			240
Sbjct 692	CTATGTCACAGCTAAGGAGCATGCCATCAGATCCAGATGTACAACGGGCAGGAGCCTC			751
Query 241	CTCCGAGAGCAGGCCTCAGTCGGCAGACCAGCATAGCACTCATCGCAT			288
Sbjct 752	CTCCGAGAGCAGGCCTCAGTCGGCAGACCAGCATAGCACTCATCGCAT			799

b)

Homo sapiens 5-hydroxytryptamine receptor 6 (HTR6), mRNA

Sequence ID: [NM\\_000871.2](#) Length: 3427 Number of Matches: 1Range 1: 708 to 1049 [GenBank](#) [Graphics](#)

▼ Next Match ▲ Previous Match

Score	Expect	Identities	Gaps	Strand
632 bits(342)	2e-177	342/342(100%)	0/342(0%)	Plus/Plus
Query 1	CCGCCGGCCATGCTGAACGCGCTGTACGGGCGCTGGGTGCTGGCGCGCGGCTCTGCCTG			60
Sbjct 708	CCGCCGGCCATGCTGAACGCGCTGTACGGGCGCTGGGTGCTGGCGCGCGGCTCTGCCTG			767
Query 61	CTCTGGACCGCCTTCGACGTGATGCTGCAGCGCCTCCATCCTCAACCTCTGCCTCATC			120
Sbjct 768	CTCTGGACCGCCTTCGACGTGATGCTGCAGCGCCTCCATCCTCAACCTCTGCCTCATC			827
Query 121	AGCCTGGACCGCTACCTGCTCATCCTCTCGCCGCTGCGCTACAAGCTGCGCATGACGCC			180
Sbjct 828	AGCCTGGACCGCTACCTGCTCATCCTCTCGCCGCTGCGCTACAAGCTGCGCATGACGCC			887
Query 181	CTGCGTGCCCTGGCCCTAGTCCTGGGCGCCTGGAGCCTCGCCGCTCTCGCCTCCTTCCTG			240
Sbjct 888	CTGCGTGCCCTGGCCCTAGTCCTGGGCGCCTGGAGCCTCGCCGCTCTCGCCTCCTTCCTG			947
Query 241	CCCCTGCTGCTGGGCTGGCACGAGCTGGGCCACGCACGGCCACCCGTCCTTGCCAGTGC			300
Sbjct 948	CCCCTGCTGCTGGGCTGGCACGAGCTGGGCCACGCACGGCCACCCGTCCTTGCCAGTGC			1007
Query 301	CGCCTGCTGGCCAGCCTGCCTTTTGTCTTGTGGCGTCGGGC			342
Sbjct 1008	CGCCTGCTGGCCAGCCTGCCTTTTGTCTTGTGGCGTCGGGC			1049

**Figure 10. Pairwise alignments of the PCR products amplified from the SH-SY5Y cell line using the NCBI database**

**a)** Showing the aligned region of the 5-HT<sub>4</sub> receptor transcript spanning nucleotide positions 512 to 799 of the 5-HT<sub>4(a)</sub> isoform of the coding sequence (CDS) of the receptor. Other 5-HT<sub>4</sub> receptor isoforms; 5-HT<sub>4(c)</sub>, 5-HT<sub>4(d)</sub>, 5-HT<sub>4(g)</sub> and 5-HT<sub>4(i)</sub> have similar alignments and positions. The long isoform, 5-HT<sub>4(b)</sub>, aligned between nucleotide positions 978 to 1265. **b)** Showing the aligned region of the 5-HT<sub>6</sub> receptor transcript spanning nucleotide positions 708 to 1049 of the CDS of the receptor. The term “query” refers to the inserted nucleotide sequence of the purified products of the 5-HT<sub>4</sub> and 5-HT<sub>6</sub> receptor while the “subject, sbjct for short” refers to the NCBI nucleotide database.

### **3.2. The analysis of receptor proteins expression in SH-SY5Y and HEK293 cell lines**

To complement the gene expression analysis of 5-HT<sub>4</sub> and 5-HT<sub>6</sub> receptors, Western blotting was conducted to evaluate the protein expression of these receptors in protein lysates of SH-SY5Y and HEK293 cell lines. Human hippocampus protein lysate was used as a positive control and was run alongside the tested samples.

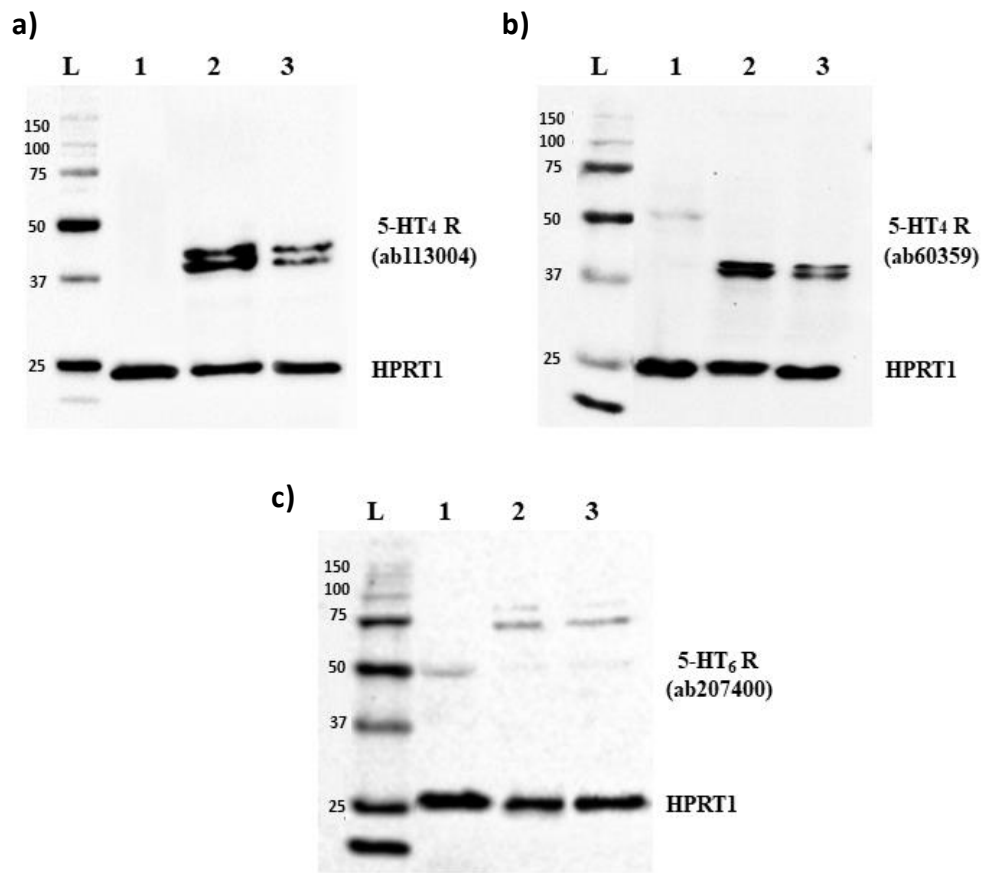
Regarding the 5-HT<sub>4</sub> receptor, two polyclonal 5-HT<sub>4</sub> receptor antibodies were utilised, and their immunoreactivities were compared, first by using anti-5-HT<sub>4</sub> antibody (ab113004), followed by the second anti-5-HT<sub>4</sub> antibody (ab60359). The former antibody was raised against the first 30 amino acids of the N-terminus of the 5-HT<sub>4</sub> receptor, a region that is identical in all receptor isoforms. Although this antibody failed to detect any band in the positive control lane as in **Figure 11a**, it did reveal two adjacent bands in the lysates of SH-SY5Y and HEK293 cell lines approximately at 41 and 43 kDa. Notably, 44 kDa was the expected molecular size of this receptor.

The second anti-5-HT<sub>4</sub> antibody (ab60359) is designed to detect the peptides spanning the first and second transmembrane domains (TMDs). The immunoreactivity revealed a faint band at 50 kDa in the positive control which was higher than expected, and a diffuse band or double band at approximately 41-42 kDa in both cell lines (**Figures 11b**). The signal intensity was stronger in the SH-SY5Y cells with both antibodies compared to the HEK293 cells.

Regarding the 5-HT<sub>6</sub> receptor, the antibody used recognised the C-terminus of the receptor and was tested by the manufacturer for IHC staining only. **Figure 11c** showed a faint band at approximately 50 kDa in the hippocampus lysate while the

predicted molecular weight for the 5-HT<sub>6</sub> receptors was 47 kDa. The tested cell lines showed non-specific bands (~70 and 80 kDa). Therefore, it seemed that neither the SH-SY5Y cells nor the HEK293 cells were shown to express the 5-HT<sub>6</sub> receptor. For further verification of the antibody's specificity and due to the low signal intensity of these GPCRs in the hippocampus, recombinant proteins were used instead as a positive control, by constructing DNA plasmids corresponding to these receptors and subsequently transfecting them into the HEK293 cells.

All blots confirmed the immunoreactivity of HPRT1, detected at 25 kDa, with minor differences in the signal intensity between the hippocampus tissue lysate in lane 1 and the HEK293 and SH-SY5Y cell line lysates in lanes 2 and 3, respectively. HPRT1 was chosen as a loading control because of its ubiquitous expression, consistent level and strong signal. In addition, the low protein size of HPRT1 made it easily distinguishable from other immunoreactive signals of the 5-HT receptors which have a protein size greater than 40 kDa.



**Figure 11. The endogenous expression of 5-HT<sub>4</sub> and 5-HT<sub>6</sub> receptors in the human hippocampus, SH-SY5Y cells and HEK293 cells**

Two different antibodies against the 5-HT<sub>4</sub> receptor were used in blots **a** and **b**, and one antibody was used against the 5-HT<sub>6</sub> receptor in blot **c**. The post-mortem human hippocampus lysate was used as a positive control (lane 1) besides the SH-SY5Y cell line (lane 2) and HEK293 cell line (lane 3). The experiment was repeated at least three times, and similar bands were detected in each repeat. HPRT1 was used as a loading control, L: ladder indicated protein size in kDa.

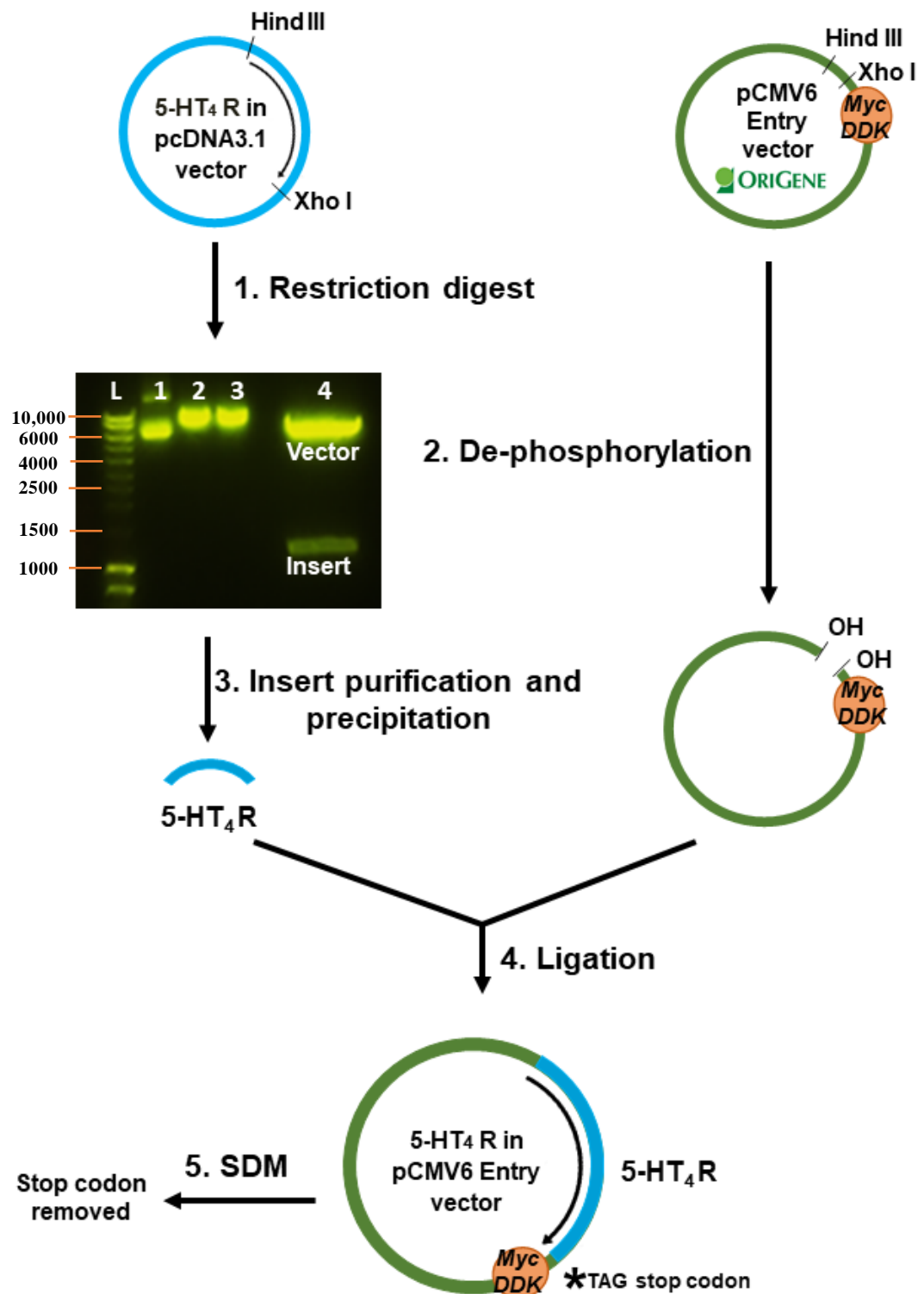
### **3.3. Plasmid constructs**

Multiple plasmid constructs for the 5-HT<sub>4</sub> and 5-HT<sub>6</sub> receptors were produced and transfected into the HEK293 cells to obtain: a) positive controls for the protein expression assay, b) preliminary evaluation of the two receptors interaction using transient transfection, and c) stable cell lines expressing either the 5-HT<sub>4</sub> receptors, 5-HT<sub>6</sub> receptors or both following antibiotic selection. The plasmid constructs for the 5-HT<sub>4</sub> receptor was precisely encoded for isoform a, but it will be denoted as the 5-HT<sub>4</sub> receptor for the remainder of this work. As described in the **Methods**, the coding sequence of the human 5-HT<sub>4</sub> and 5-HT<sub>6</sub> receptors were released from their parent vectors using restriction enzymes and subsequently ligated into the mammalian expression vectors (**Figures 12 and 13**). The restriction enzymes created non-compatible “overhang” ends in the DNA fragments, thereby facilitating directional sub-cloning of the inserts and reducing the possibility of re-ligation of the recipient vector.

In this study, specific changes in the plasmid DNA sequence were generated via SDM to facilitate the screening and detection of the expressed protein by inserting reporter tags, keeping the receptor coding sequence and the tag into an open reading frame by deleting a stop codon between them or substituting the asparagine residue with glutamine. Successful ligation and mutation were confirmed by sequencing.

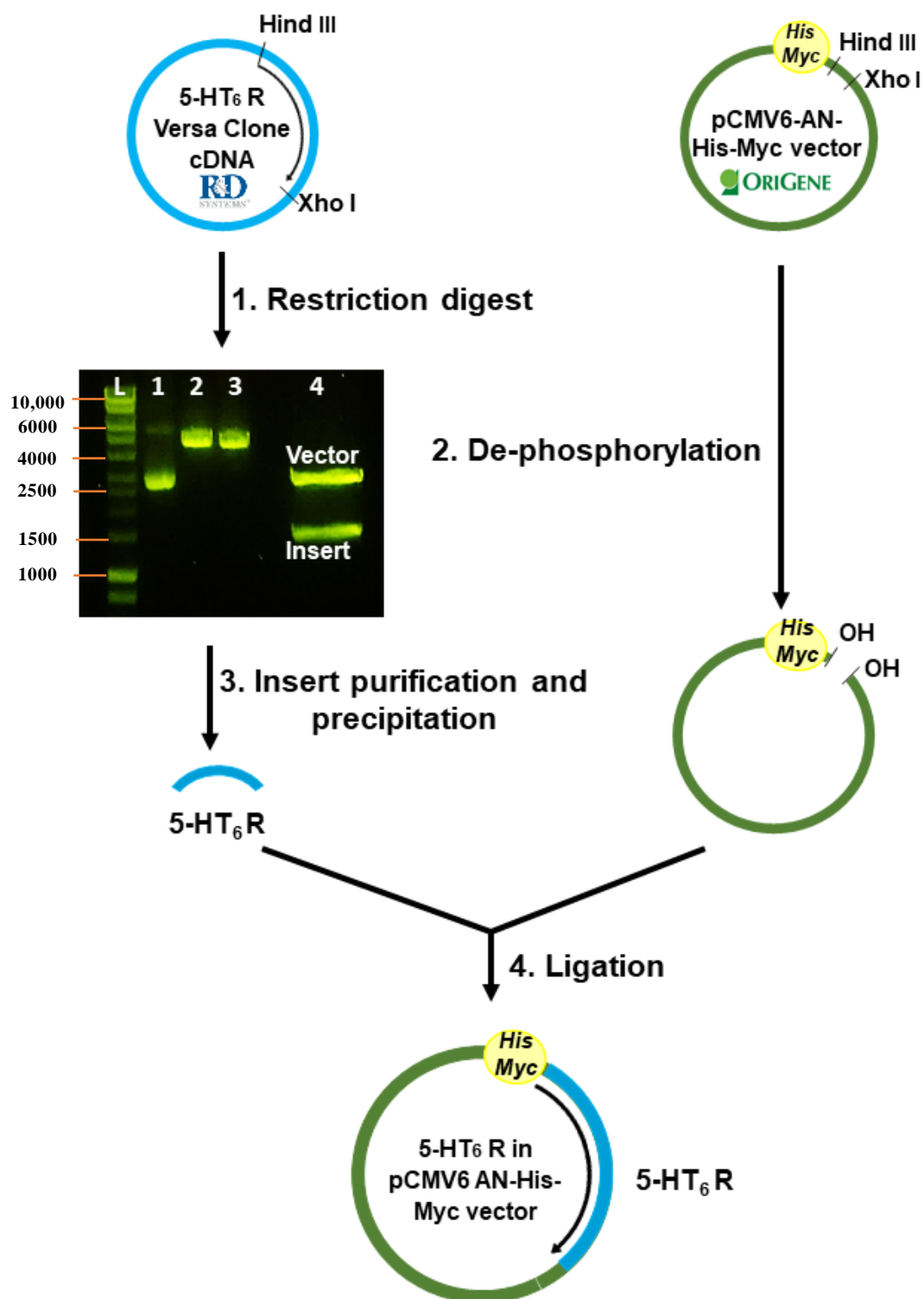
The plasmids that were initially cloned for both the 5-HT<sub>4</sub> and 5-HT<sub>6</sub> receptors had the same neomycin resistance marker (**Figure 14a**), and this was not an issue with transient protein expression. However, when stable co-expression of both receptors in the same cell line was considered, different resistance markers were required to increase the chance of selecting double positive cells, thereby generating a clonal

cell line expressing both desired receptors. Therefore, the full length of the human 5-HT<sub>4</sub> plasmid, isoform a (Catalogue no. HG10753-NF) was obtained from Sino biological which had an N-terminal Flag reporter and hygromycin resistance marker as depicted in **Figure 14b**.



**Figure 12. Schematic diagram illustrating the sub-cloning workflow of the 5-HT<sub>4</sub> receptor**

*The 5-HT<sub>4</sub> receptor insert was released from its parent vector (pcDNA3.1) via restriction enzymes; specifically, Hind III and Xho I. The insert was purified in the agarose gel and visualised under blue light. In the gel, lane 1 showed the uncut plasmid (mainly supercoiled), lanes 2 and 3 showed the linearised single digested plasmid with either Hind III or Xho I respectively and lane 4 represented the double digested plasmid with both enzymes. Two wells were used in lane 4 to purify more of the insert (the lower band) which was subsequently precipitated and ligated into the de-phosphorylated pCMV6 Entry vector tagged with Myc-DDK in the C-terminal end. The stop codon between the insert and the tag was removed by SDM.*





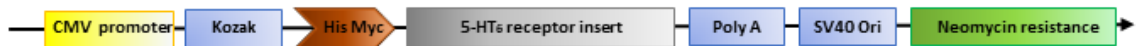
**Figure 13. Schematic diagram illustrating the sub-cloning workflow of the 5-HT<sub>6</sub> receptor**

*The 5-HT<sub>6</sub> receptor coding sequence was released from the shuttle plasmid using the Hind III and Xho I restriction enzymes and subsequently purified from the agarose gel. Lane 1 showed the uncut supercoiled plasmid, lanes 2 and 3 showed the single cut plasmid with either Hind III or Xho I, respectively, and lane 4 represented the double digested plasmid. The lower band was purified and subsequently ligated into the destination vector (pCMV6-AN-His-Myc tagged vector). Thus, the immunodetection of the target receptor was facilitated by His or Myc epitope following protein expression.*

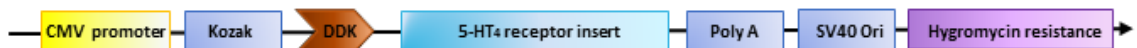
**a) Human 5-HT<sub>4</sub> receptor insert in the pCMV6-Entry C-Myc-Flag vector**



**Human 5-HT<sub>6</sub> receptor insert in pCMV6-AN-His-Myc vector**



**b) Human 5-HT<sub>4</sub> receptor insert in the pCMV3- Flag vector**

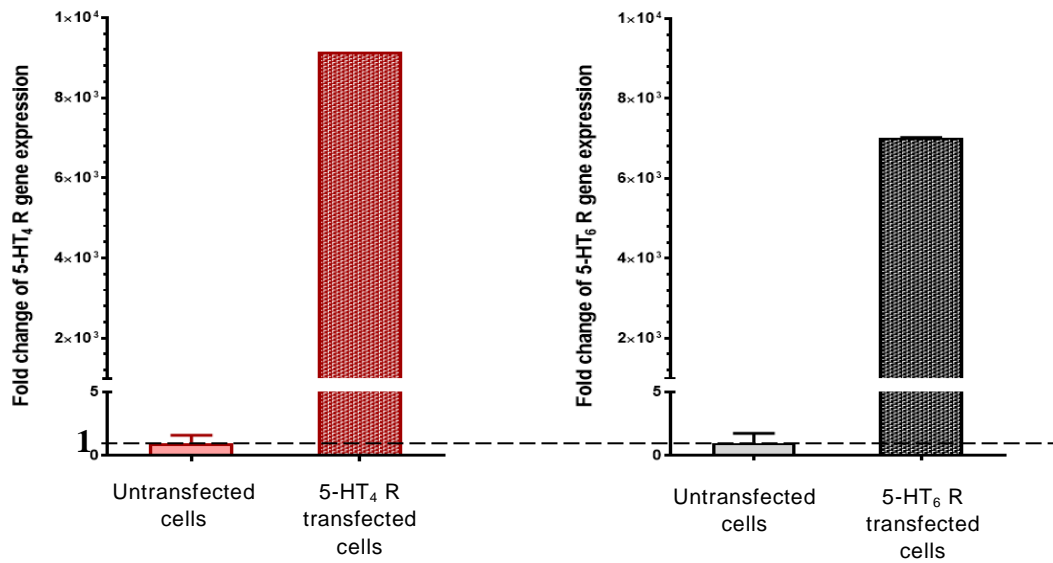


**Figure 14. Schematic drawing showing the structure of the expression constructs for 5-HT<sub>4</sub> and 5-HT<sub>6</sub> receptors**

*a) Represents the in-house constructs generated by sub-cloning and containing a neomycin resistance gene and Myc and Flag (DDK) tags for 5-HT<sub>4</sub> receptor insert and His and Myc tags for 5-HT<sub>6</sub> receptor insert. b) represents the Sino biological construct for the 5-HT<sub>4</sub> receptor which contains a hygromycin resistance gene and Flag tag in the receptor N-terminus. The expression of the insert was driven by the CMV promoter. Kozak consensus enhanced protein translation in the cell line. The SV40 origin of replication (SV40 Ori) depicts the initiation site for DNA synthesis. Poly A: the polyadenylation signal at the end of the mRNA transcript.*

### **3.4. Determination of 5-HT<sub>4</sub> and 5-HT<sub>6</sub> receptors gene expression post-transfection relative to their endogenous level in the HEK293 cells**

The 5-HT<sub>4</sub> and 5-HT<sub>6</sub> receptor constructs generated in **Section 3.3** were transiently transfected into the HEK293 cells separately. Forty-eight hours post-transfection, cells were harvested for RNA extraction which was followed by cDNA synthesis. The qPCR results showed there was an overexpression of 5-HT<sub>4</sub> and 5-HT<sub>6</sub> receptor genes by ~9000-fold and ~7000-fold, respectively relative to their endogenous expression in the untransfected HEK293 cells as illustrated in **Figure 15**. The Ct values and the fold change in the expression of the genes following transfection were calculated by applying the comparative  $2^{-\Delta\Delta C_t}$  method as listed in **Table 21**. The percentages of the amplification efficiency for the target and reference genes were calculated from the slopes of the standard curves of each amplified gene. The *EIF4A2* gene was amplified in parallel with the genes of interest and used for normalisation of the results (reference gene). In the 5-HT<sub>4</sub> receptor transfected HEK293 cells, the amplification efficiencies of the 5-HT<sub>4</sub> receptor and *EIF4A2* genes were 98.5% and 105.6% respectively, and in the 5-HT<sub>6</sub> receptor transfected HEK293 cells, the efficiencies were 100.9% for the 5-HT<sub>6</sub> receptor gene and 100.4% for the *EIF4A2* gene. These percentages were within the acceptable range ( $100 \pm 10\%$ ) indicating that the cDNA samples are free from PCR inhibitors (Applied Biosystems, 2008).



**Figure 15. The fold increase in expression of 5-HT<sub>4</sub> and 5-HT<sub>6</sub> receptor genes in the transfected cells relative to the untransfected HEK293 cells**

*After transfection, the 5-HT<sub>4</sub> and 5-HT<sub>6</sub> receptor genes expression increases by ~9000-fold and ~7000-fold, respectively over their basal levels which is very close to one ( $2^0 = 1$ ). The data represent mean  $\pm$  SD of three technical replicates.*

**Table 21. Calculation of fold change in gene expression using the  $2^{-\Delta\Delta Ct}$  method.**

Cells	Average Ct 5-HT <sub>4</sub> R	Average Ct EIF4A2	$\Delta Ct$ (5-HT <sub>4</sub> R – EIF4A2)	$\Delta\Delta Ct$ ( $\Delta Ct$ transfected – $\Delta Ct$ Untransfected)	Fold change relative to untransfected cells ( $2^{-\Delta\Delta Ct}$ )
Untransfected cells	36.252 $\pm$ 0.717	26.371 $\pm$ 0.045	9.881 $\pm$ 0.719	0.000 $\pm$ 0.719	1.000 $\pm$ 0.608
5-HT <sub>4</sub> R transfected cells	23.256 $\pm$ 0.069	26.535 $\pm$ 0.054	-3.279 $\pm$ 0.088	-13.160 $\pm$ 0.088	9155.885 $\pm$ 0.941
Cells	Average Ct 5-HT <sub>6</sub> R	Average Ct EIF4A2	$\Delta Ct$ (5-HT <sub>6</sub> R – EIF4A2)	$\Delta\Delta Ct$ ( $\Delta Ct$ transfected – $\Delta Ct$ Untransfected)	Fold change relative to untransfected cells ( $2^{-\Delta\Delta Ct}$ )
Untransfected cells	36.556 $\pm$ 0.403	26.503 $\pm$ 0.142	10.053 $\pm$ 0.427	0.000 $\pm$ 0.427	1.000 $\pm$ 0.744

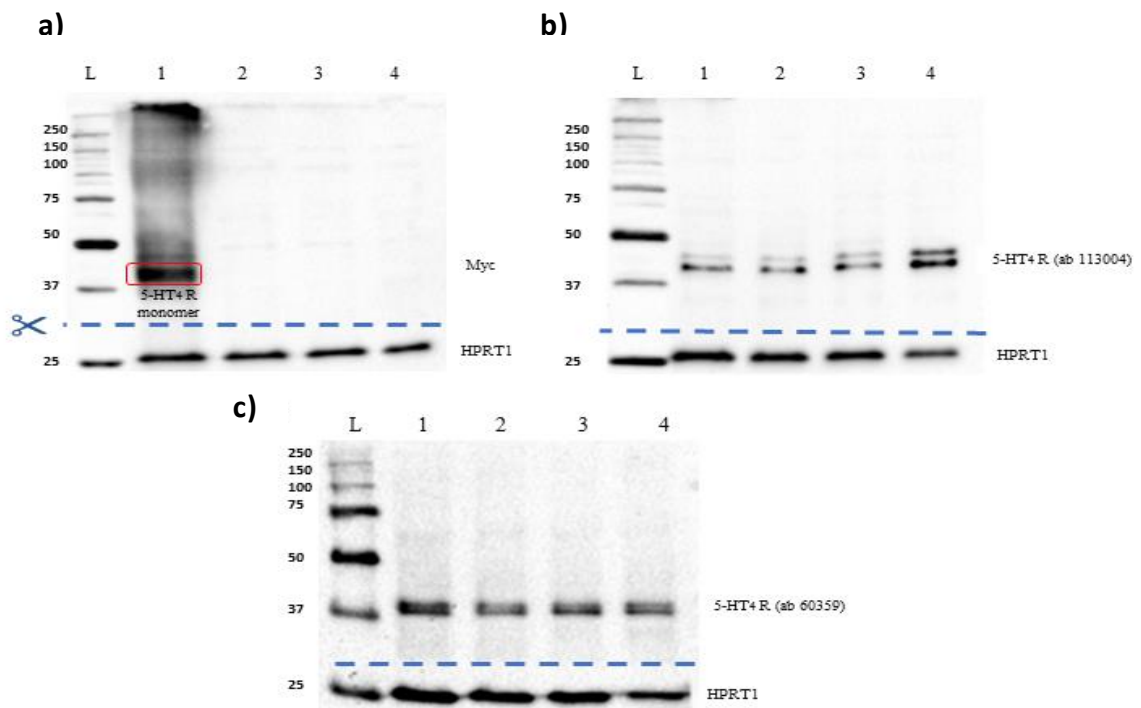
5-HT <sub>6</sub> R transfected cells	23.540 ± 0.119	26.265 ± 0.054	-2.725 ± 0.131	-12.778 ± 0.131	7025.831 ± 0.913
--	----------------	----------------	----------------	-----------------	------------------

### **3.5. The re-analysis of the protein expression of 5-HT<sub>4</sub> and 5-HT<sub>6</sub> receptors in both the SH-SY5Y and HEK293 cell lines using recombinant proteins as controls**

This step was conducted to generate positive controls for protein expression analysis, and most importantly to validate the antibodies' sensitivity and specificity. As previously shown in **Section 3.2**, faint immunoreactive bands were observed for the human hippocampus lysates when immunoblotted against the 5-HT<sub>4</sub> and 5-HT<sub>6</sub> antibodies. However, these bands were faint thus making it difficult to determine if they corresponded to the target receptors. Therefore, some of the transiently transfected HEK293 cells used in the qPCR experiment (**section 3.4**) were lysed and run alongside the tested samples.

At 48 hr post-transfection, cells were harvested, and the whole cell lysates were loaded and probed with antibodies against either Myc tag or the 5-HT receptors. The results revealed that the HEK293 cells expressed the Myc-tagged 5-HT<sub>4</sub> receptors by showing the immunoreactive band at approximately 41 kDa. This band was absent in mock-transfected and un-transfected HEK293 cells as well as SH-SY5Y cells (**Figure 16a**). Nevertheless, the endogenously expressed 5-HT<sub>4</sub> receptor was assessed independently by reloading the same samples and then probing with 5-HT<sub>4</sub> antibodies. As previously demonstrated in **Section 3.2**, blotting with the anti-5-HT<sub>4</sub> antibody (ab113004) revealed two bands at the 41 and 43 kDa sizes which were prevalent in all cell lysates but more apparent in SH-SY5Y cells than HEK293 cells. However, there are no detectable differences in terms of signal intensity between the

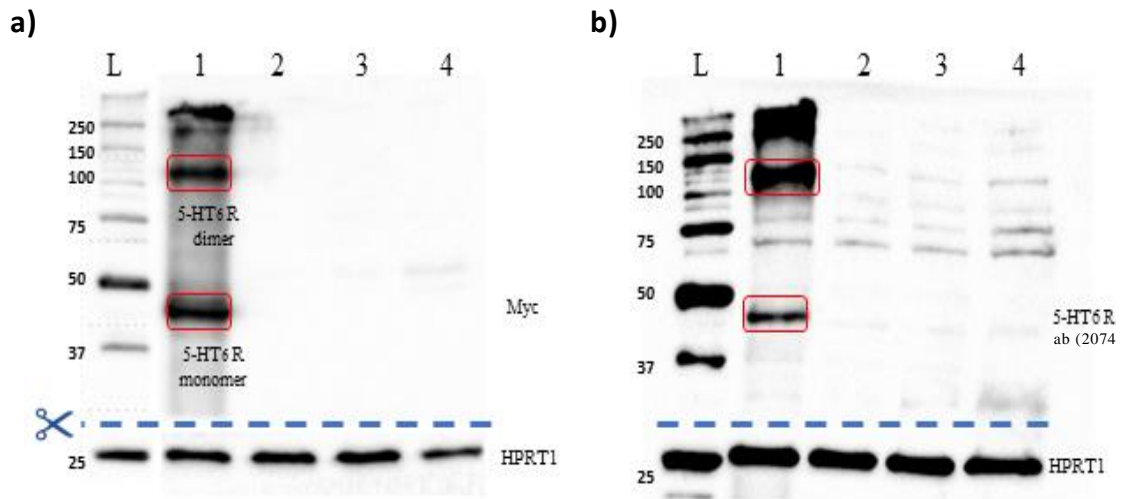
transfected and untransfected HEK293 cells as illustrated in **Figure 16b**. Likewise, the blot of the 5-HT<sub>4</sub> antibody (ab60359) showed positive bands at the expected protein size in all cell lines, but its detection of the recombinant protein was not achieved. A small increase in the signal intensity between the 5-HT<sub>4</sub> receptor transfected and untransfected HEK293 cells was detected which was more likely to be due to the loading instead of the actual protein level (**Figure 16c**). In agreement with the gene expression results, both cell lines were deemed positive for the 5-HT<sub>4</sub> receptor.



**Figure 16. Characterisation of the 5-HT<sub>4</sub> receptor expression in the HEK293 and SH-SY5Y cell lines**

*Western blot immunoreactivity of (a) anti-Myc, (b) anti-5-HT<sub>4</sub> R (ab113004) and (c) anti-5-HT<sub>4</sub> R (ab60359) antibodies. The transient overexpression of 5-HT<sub>4</sub> receptors (which are Myc-tagged at its C-terminus) in HEK293 cells was used as a positive control (Lane 1), together with mock-transfected HEK293 cells (Lane 2), untransfected HEK293 cells (Lane 3) and SH-SY5Y cells (Lane 4). The predicted*

*protein size for the 5-HT<sub>4</sub> receptors was 44 kDa (n = 3). The dashed lines indicate the sites where the membranes were cut and incubated with two different antibodies.* Regarding 5-HT<sub>6</sub> receptors expression, the recombinant receptor contained a Myc tag at its N-terminus and was found to be overexpressed in the HEK293 cells. Myc immunoreactivity revealed two distinct bands corresponding to the 5-HT<sub>6</sub> receptors in a monomeric size (approximately 47 kDa) and a dimeric size (approximately 110 kDa) but not in the mock transfected, untransfected HEK293 cells or the SH-SY5Y cells as shown in **Figure 17a**. When the same samples were loaded in the same order and probed with the 5-HT<sub>6</sub> receptor antibody (Ab207400), the positive control revealed bands similar to those that appeared in the Myc blot, but neither the monomeric nor dimeric bands appeared in the tested samples (**Figure 17b**). This indicated that the tested cell lines do not express the 5-HT<sub>6</sub> receptor. This was inconsistent with the PCR result for the 5-HT<sub>6</sub> receptor transcripts. Multiple non-specific faint bands were also visible in all samples.



**Figure 17. Characterisation of the 5-HT<sub>6</sub> receptor expression in both the HEK293 and SH-SY5Y cell lines**

*Western blot reactivity of cell lysates probed with (a) Myc and (b) 5-HT<sub>6</sub> receptor (ab207400) antibodies. The transient expression of Myc-tagged receptors in HEK293 cells was used as a positive control (Lane 1), mock transfection in HEK293 cells (Lane 2), un-transfected HEK293 cells (Lane 3) and the SH-SY5Y cell lysate (Lane 4). The predicted band size for the 5-HT<sub>6</sub> receptors was 47 kDa ( $n = 3$ ). The dashed lines indicate the sites where the membranes were cut to incubate with two different antibodies.*



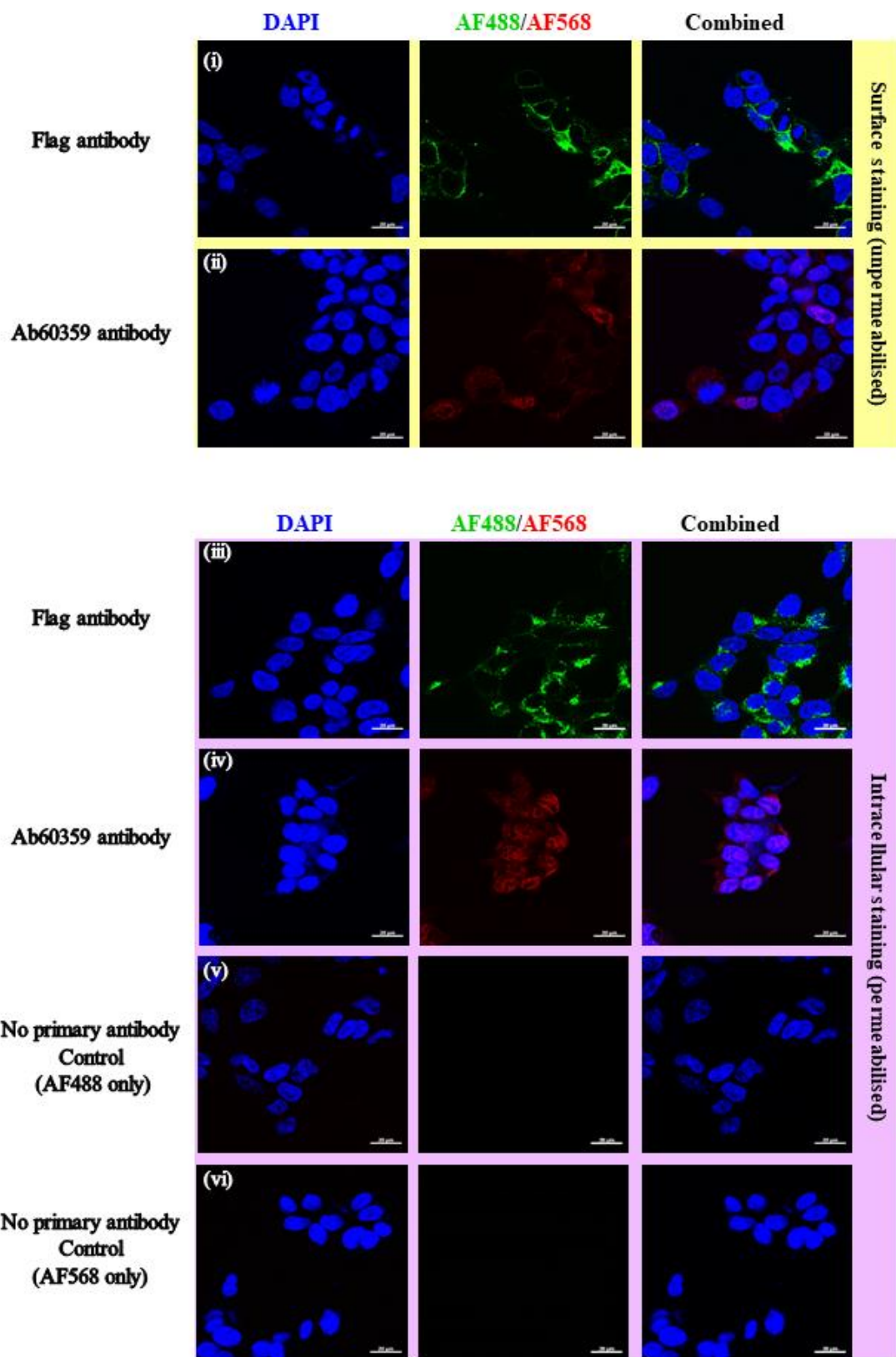
### **3.6. Cellular localisation of exogenous and endogenous expressed 5-HT<sub>4</sub> and 5-HT<sub>6</sub> receptors**

Immunofluorescence was performed to confirm Western blotting findings and to determine the cellular localisation of these receptors. Constructs encoding the N-Flag-5-HT<sub>4</sub> receptor or N-Myc-5-HT<sub>6</sub> receptor were transfected into HEK293 cells to be used as controls. Next, to specify protein localisation, staining was performed with and without permeabilisation.

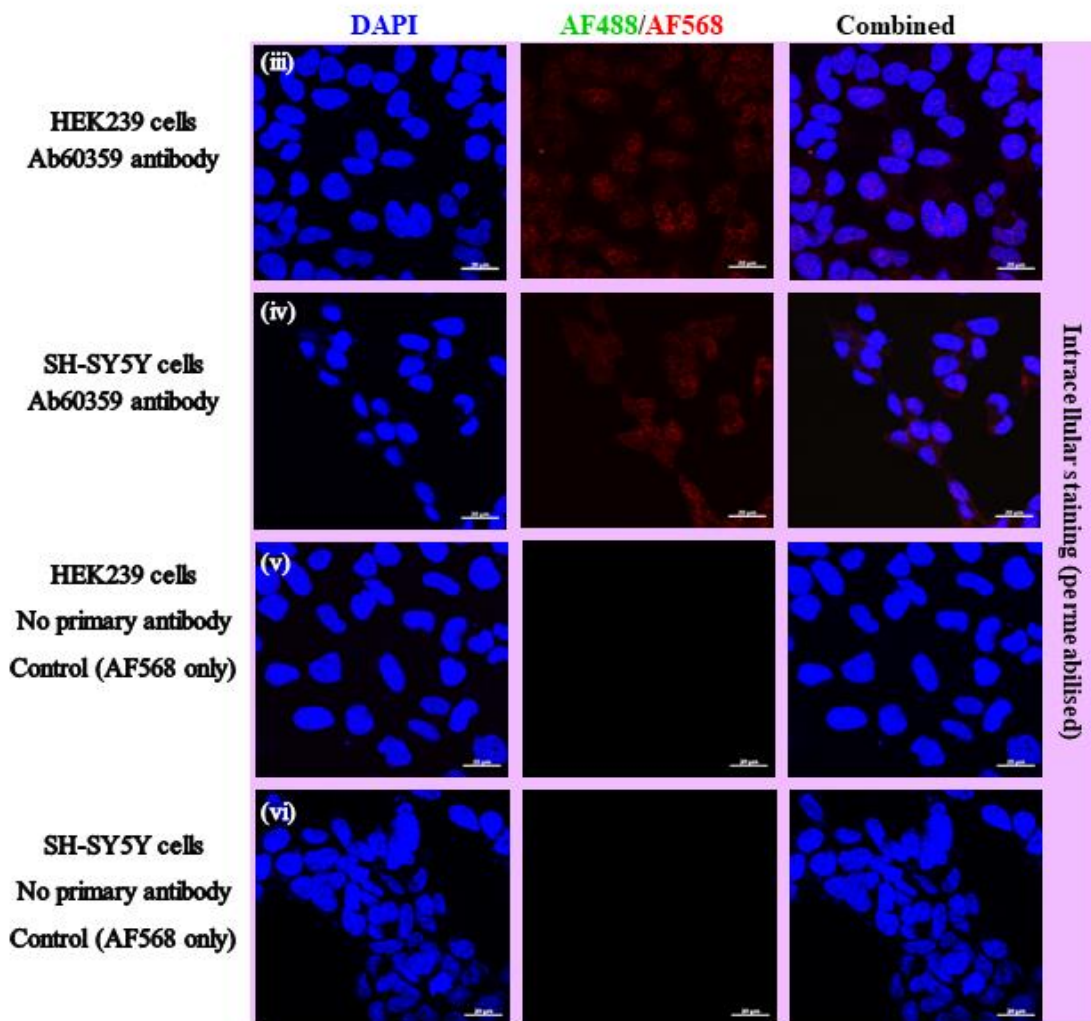
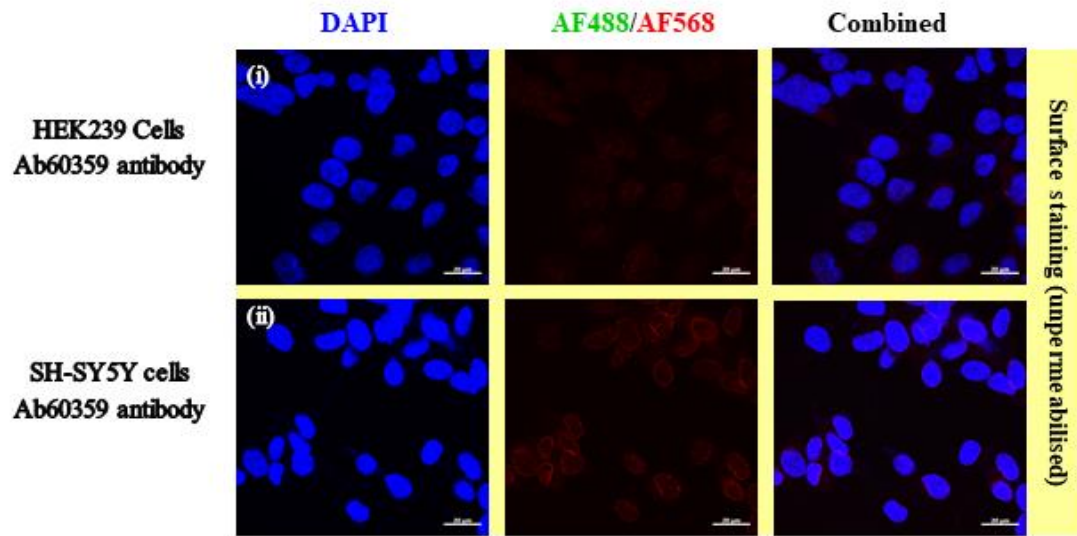
For the purposes of discrimination, green fluorescence secondary antibody (AF488) was used with a monoclonal Flag or Myc antibodies while red fluorescence secondary antibody (AF568) was used with 5-HT receptor antibodies. Probing against the Flag or Myc epitopes revealed a positive signal in transfected HEK293 cells. The immunoreactivities of these epitopes were detected in the cell membrane and the peri-nuclear organelles including the ER and Golgi apparatus where protein synthesis takes place prior to its migration to the cell membrane as in **Figure 18a** and **Figure 19a**.

In agreement with the Western blot results, the endogenous 5-HT<sub>4</sub> receptor was present in HEK293 and SH-SY5Y cells (**Figure 18b**), while, the endogenous expression of the 5-HT<sub>6</sub> receptor in both cell lines was absent (**Figure 19b**). It is noteworthy that omitting the primary antibodies during the staining procedure did not result in the detection of any fluorescent signal in all cells even with cell permeabilisation. Thus, the secondary fluorophore-conjugated antibodies were target specific.

a) HEK293 cells expressed exogenous N-Flag5-HT<sub>4</sub> receptor



**b) HEK293 and SH-SY5Y cells expressed endogenous 5-HT<sub>4</sub> receptor**

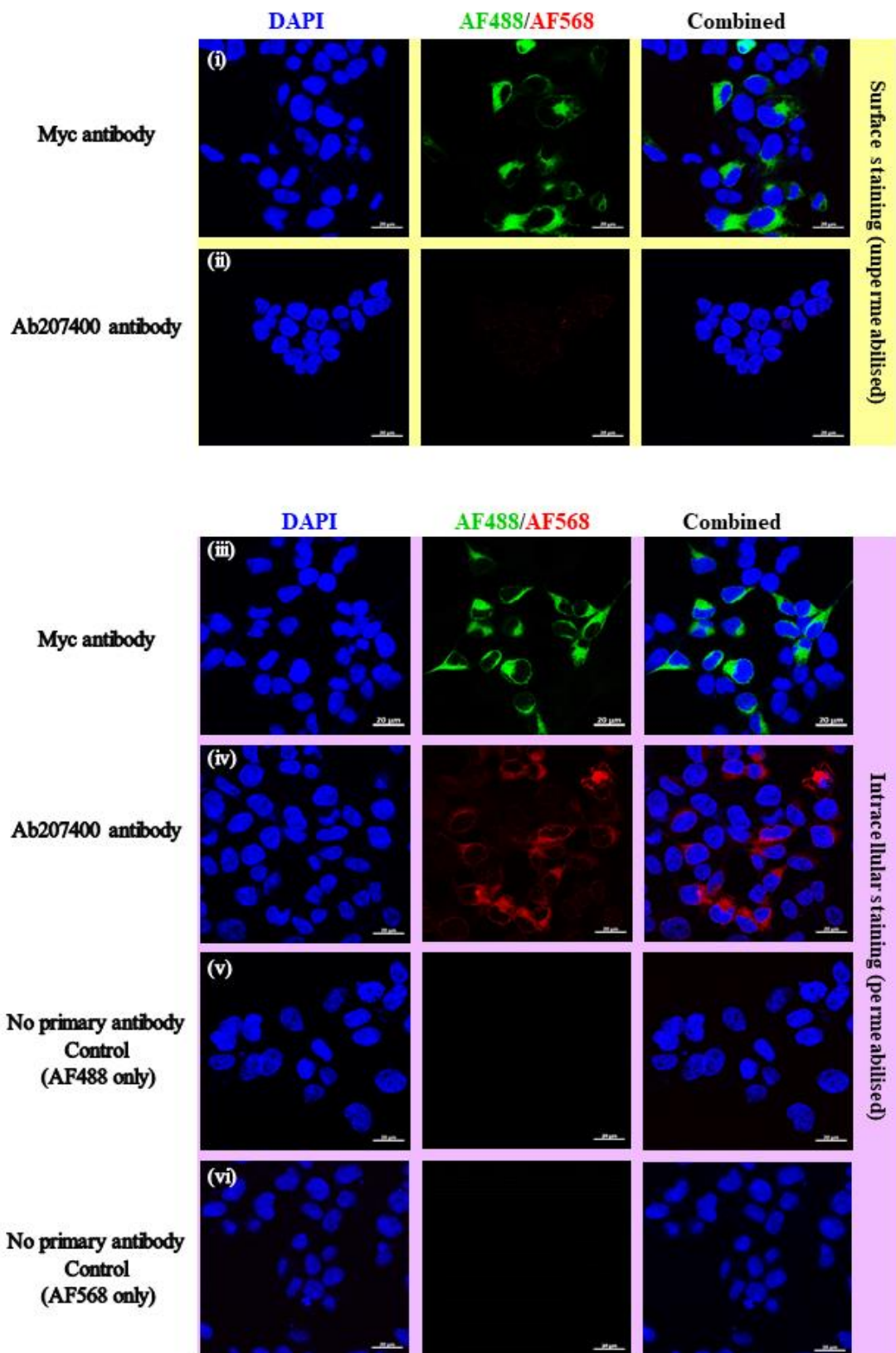


**Figure 18. Immunofluorescence of the 5-HT<sub>4</sub> receptors and its cellular localisation**

*(a) Unpermeabilised transfected HEK293 cells showed positive green immunofluorescence (AF488) in the extracellular surface of the cell membrane against (i) the N-terminal Flag 5-HT<sub>4</sub> receptors (iii) as well as intracellularly. Upon staining the same set of cells with the anti-5-HT<sub>4</sub> receptor (ab60359), a positive red signal was detected (ii) in the cell surface (iv) but stronger intracellularly. Negative controls were included in the experiment in which the cells were subjected to a similar staining procedure but without the primary antibody (secondary only, AF488 or AF568, v, vi).*

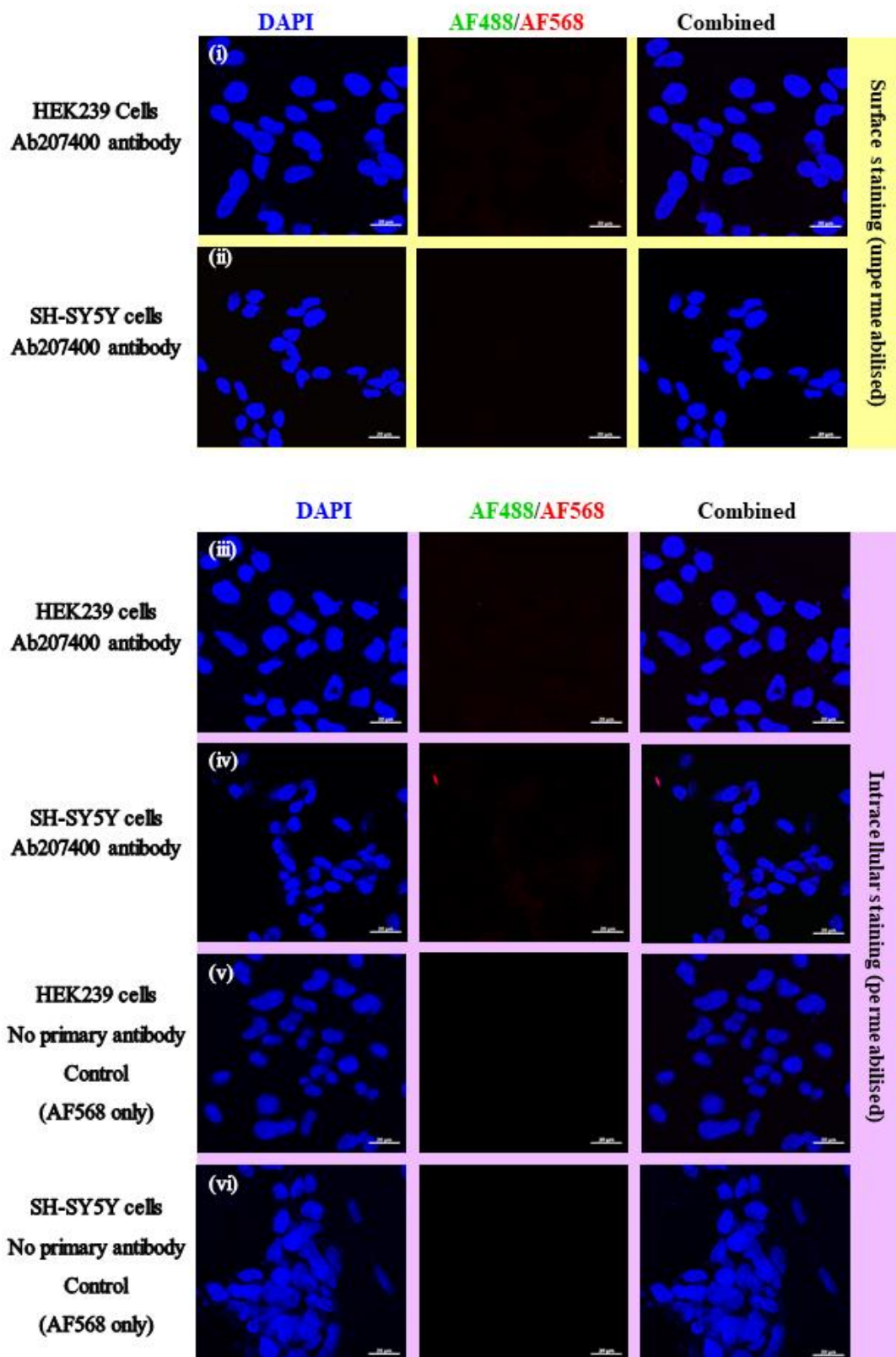
*(b) Unpermeabilised HEK293 and SH-SY5Y cells showed a positive red signal (i, ii) against 5-HT<sub>4</sub> receptors in the cell surface (iii, iv) but the intracellular signal was more intense and localised in the cytoplasm and perinuclear regions. The intensity of this signal was comparable to the one observed in the HEK293 cells that exogenously expressed the recombinant 5-HT<sub>4</sub> receptors. (v, vi) No primary controls were negative for both cell lines. These representative images of 3 independent experiments which were obtained by confocal microscopy. Nuclei were counterstained by DAPI (blue channel). Scale bar 20 µm.*

a) HEK293 cells expressed exogenous N-Myc 5-HT<sub>6</sub> receptor





**b) HEK293 and SH-SY5Y cells did not express endogenous 5-HT<sub>6</sub> receptor**



**Figure 19. Immunofluorescence of the 5-HT<sub>6</sub> receptors and its cellular localisation**

*(a) Unpermeabilised HEK293 cells transiently transfected with 5-HT<sub>6</sub> construct showed positive green immunofluorescence (AF488) in (i) the extracellular surface of the cell membrane against N-terminal Myc 5-HT<sub>6</sub> receptors and (iii) when the cell permeabilised, more cells with positive green signal were detected. The localisation pattern of the receptor was similar in both conditions, i.e. with and without permeabilisation. (ii) Upon staining the same set of cells with ab207400 antibody without permeabilisation, no or very weak signal was detected since the antibody was designed to recognise the C-terminus of the 5-HT<sub>6</sub> receptor. (iv) In contrast, a strong red signal was revealed with cell permeabilisation. (v, vi) Neither the AF488 nor AF568 negative control staining showed fluorescence immunoreactivity in these transfected cells.*

*(b) HEK293 and SH-SY5Y cells were (i, ii) negative for 5-HT<sub>6</sub> receptors in the cell surface and (iii, iv) intracellularly. (v, vi) no primary controls were negative for both cell lines. These images were obtained by confocal microscopy of 3 independent experiments. Scale bar 20  $\mu$ m.*

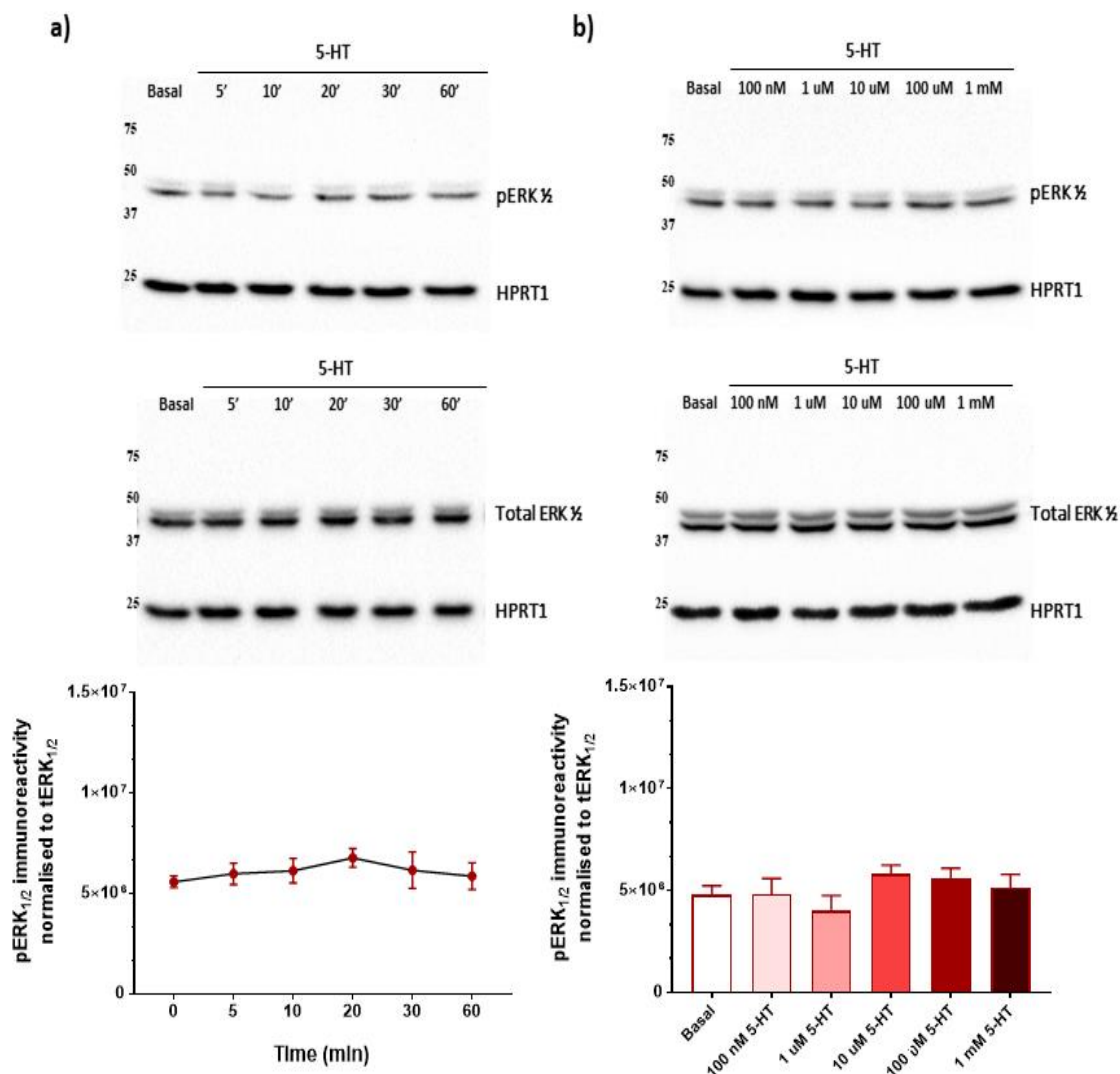
### **3.7. Functional characterisation of the endogenous 5-HT<sub>4</sub> receptor in HEK293 and SH-SY5Y cell lines via ERK<sub>1/2</sub> phosphorylation**

Previous work of Barthet et al. (2007) showed that 5-HT mediated dose- and time-dependent increases in ERK<sub>1/2</sub> phosphorylation at threonine and tyrosine residues in HEK293 cells transiently transfected with the 5-HT<sub>4</sub> receptor. The ERK<sub>1/2</sub> signalling pathway involves in many cell processes. In the neurones, it promotes neuroplasticity as it activates many growth factors such as BDNF (Peng et al., 2010). In addition, measuring the level of pERK<sub>1/2</sub> as a functional readout for GPCR activation required less protocol optimisation than measuring the cAMP level.

To assess whether the endogenously expressed 5-HT<sub>4</sub> receptors in HEK293 and SH-SY5Y cells were responsive to 5-HT and whether they increased the level of ERK<sub>1/2</sub> phosphorylation, the cells were serum starved for 16 hr before being stimulated by 10  $\mu$ M of 5-HT for 5, 10, 20, 30 and 60 min. Unexpectedly, this stimulation failed to evoke time-dependent changes in ERK<sub>1/2</sub> activation (indicated by immunoreactivity of phosphorylated ERK<sub>1/2</sub> form, pERK<sub>1/2</sub>) (**Figure 20a** and **Figure 21a**). The immunoreactivities of pERK<sub>1/2</sub> at these time points were not significantly different from the basal level without any stimulant ( $P > 0.05$ ).

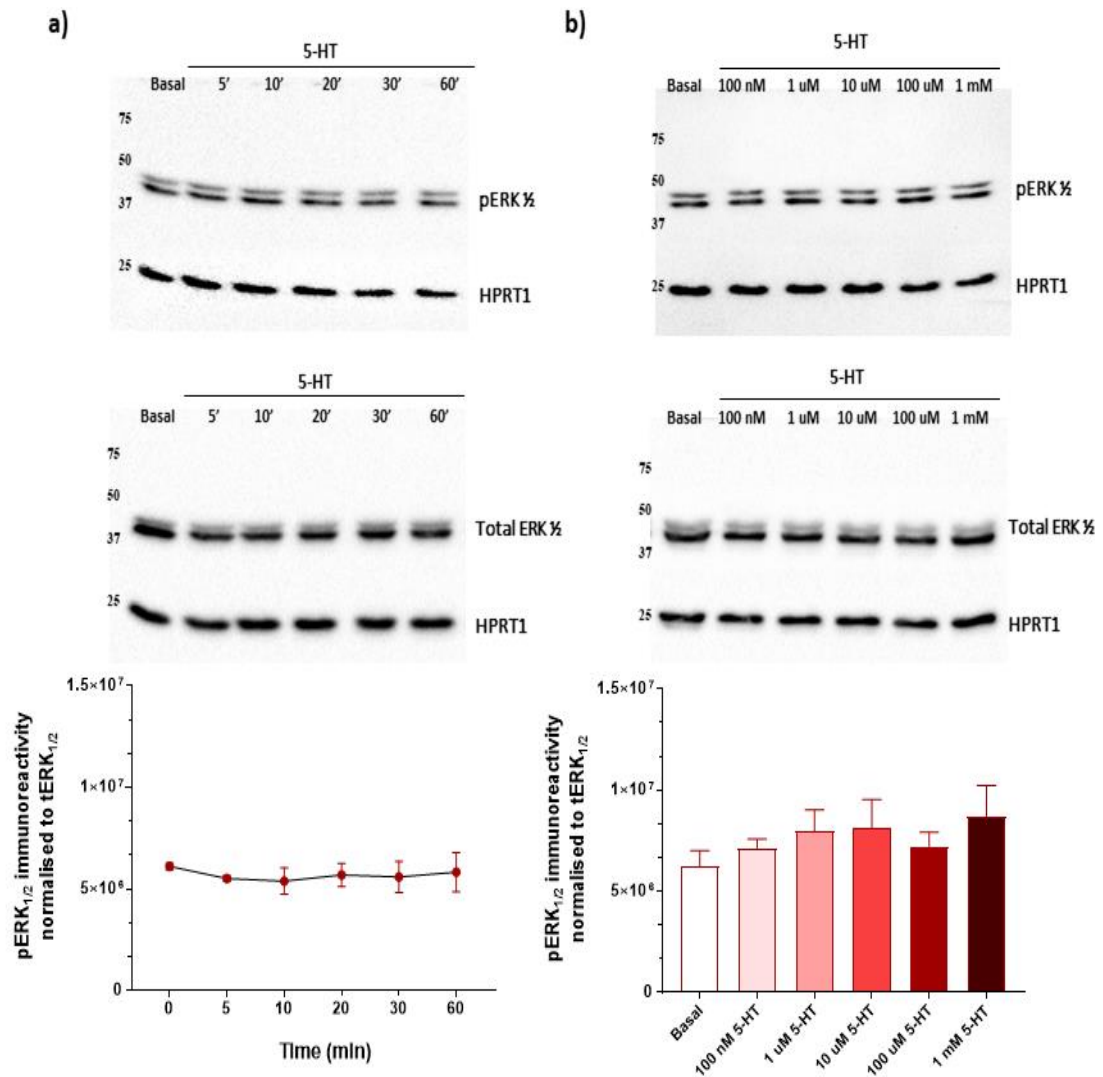
Likewise, stimulation of the HEK293 and SH-SY5Y cell lines by increasing concentrations of 5-HT ( $1 \times 10^{-7}$  to  $1 \times 10^{-3}$  M) for 5 min did not reveal any difference in the pERK<sub>1/2</sub> immunoreactivity ( $P > 0.05$ ) as illustrated in **Figures 20b** and **21b**. The immunoreactivity of pERK<sub>1/2</sub> was quantified by densitometry and normalised by the total ERK<sub>1/2</sub> immunoreactivity of the same cell lysates for each experiment.





**Figure 20. A representative blot revealing the time dependent and the dose dependent effects of 5-HT on pERK<sub>1/2</sub> in the HEK293 cell line**

Following overnight serum-starvation, HEK293 cells were treated with (a) 10 μM of 5-HT for the indicated periods, or (b)  $1 \times 10^{-7}$  to  $1 \times 10^{-3}$  M of 5-HT for 5 min at 37°C. The pERK<sub>1/2</sub> level was detected by immunoblotting with an antibody that specifically recognised the phosphorylated sites. Total ERK<sub>1/2</sub> and HPRT1 were used as loading controls. Data are denoted as mean ± SEM which is calculated from 3 independent experiments and plotted in graphs below each panel ( $P > 0.05$ , one-way ANOVA test).

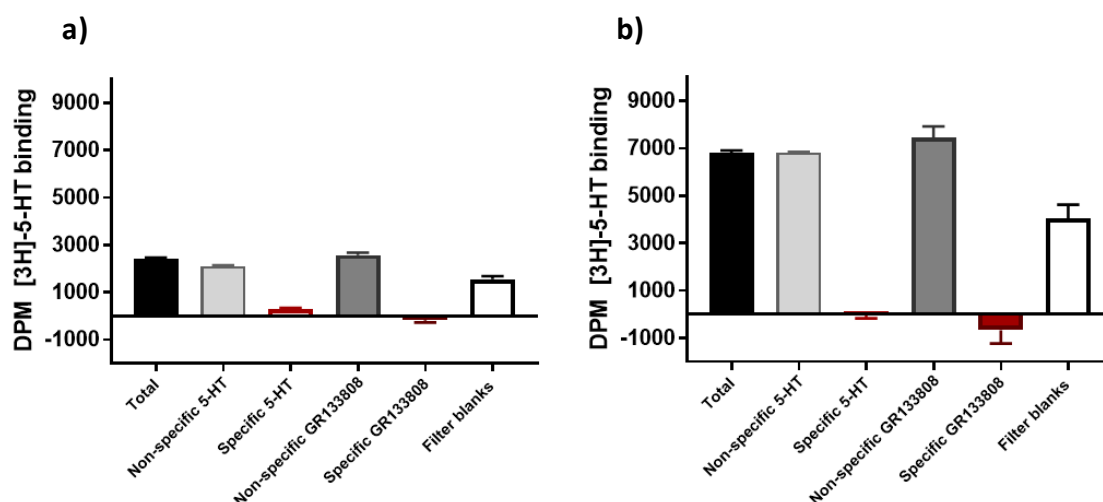


**Figure 21. A representative blot illustrated the time-dependent and the dose-dependent effects of 5-HT on pERK<sub>1/2</sub> in the SH-SY5Y cell line**

Following overnight serum-starvation, SH-SY5Y cells were treated with (a) 10  $\mu$ M of 5-HT for the indicated periods, or (b)  $1 \times 10^{-7}$  to  $1 \times 10^{-3}$  M of 5-HT for 5 min at 37°C. The pERK<sub>1/2</sub> level was detected by immunoblotting. Total ERK<sub>1/2</sub> and HPRT1 were used as loading controls. Data are represented as mean  $\pm$  SEM from 3 independent experiments and plotted in graphs below each panel ( $P > 0.05$ , one-way ANOVA test).

### **3.8. Assessment of the radioligand binding affinity of the 5-HT<sub>4</sub> receptor in HEK293 cells**

This assessment was performed in parallel with each RLB experiment and acted as an endogenous control for the transfected HEK293 cells. HEK293 cells stably expressing the 5-HT<sub>7</sub> receptor was used in every RLB experiment as a positive control. Competitive ligands for the 5-HT<sub>4</sub> receptor either 5-HT or GR113808 in a 10  $\mu$ M concentration were utilised to calculate the specifically bound radioligand [<sup>3</sup>H]-5-HT. The results revealed that there was no specific binding affinity of radioligand to the membrane fraction of these cells, even when high concentrations of the radioligand or membrane fraction protein were used and as depicted in **Figure 22**. This supported the previous negative findings of the 5-HT<sub>4</sub> receptor functionality assays in HEK293 cells.



**Figure 22. The lack of specific binding affinity of [<sup>3</sup>H]-5-HT to the 5-HT<sub>4</sub> receptor in HEK293 cells**

*Representative data from two separate preparations using (a) 5 nM of [<sup>3</sup>H]-5-HT and 0.1 mg/ml of protein, and (b) 10 nM of [<sup>3</sup>H]-5-HT and 1 mg/ml of protein. Disintegrations per minute (DPM) of the radioligand were measured by a Tri-carb counter. The columns represent mean  $\pm$  SD of three technical repeats.*

### **3.9. Summary**

The finding of this chapter showed that the HEK293 and SH-SY5Y cell lines are expressing a very low level of the 5-HT<sub>4</sub> receptors which was insufficient to produce any detectable difference in the pERK<sub>1/2</sub> level. In addition, both cells were negative for 5-HT<sub>6</sub> receptor, therefore, the experiments were directed to overexpress the recombinant 5-HT receptors either singly or simultaneously in order to study the interaction of two receptors as will be shown in the following chapter.

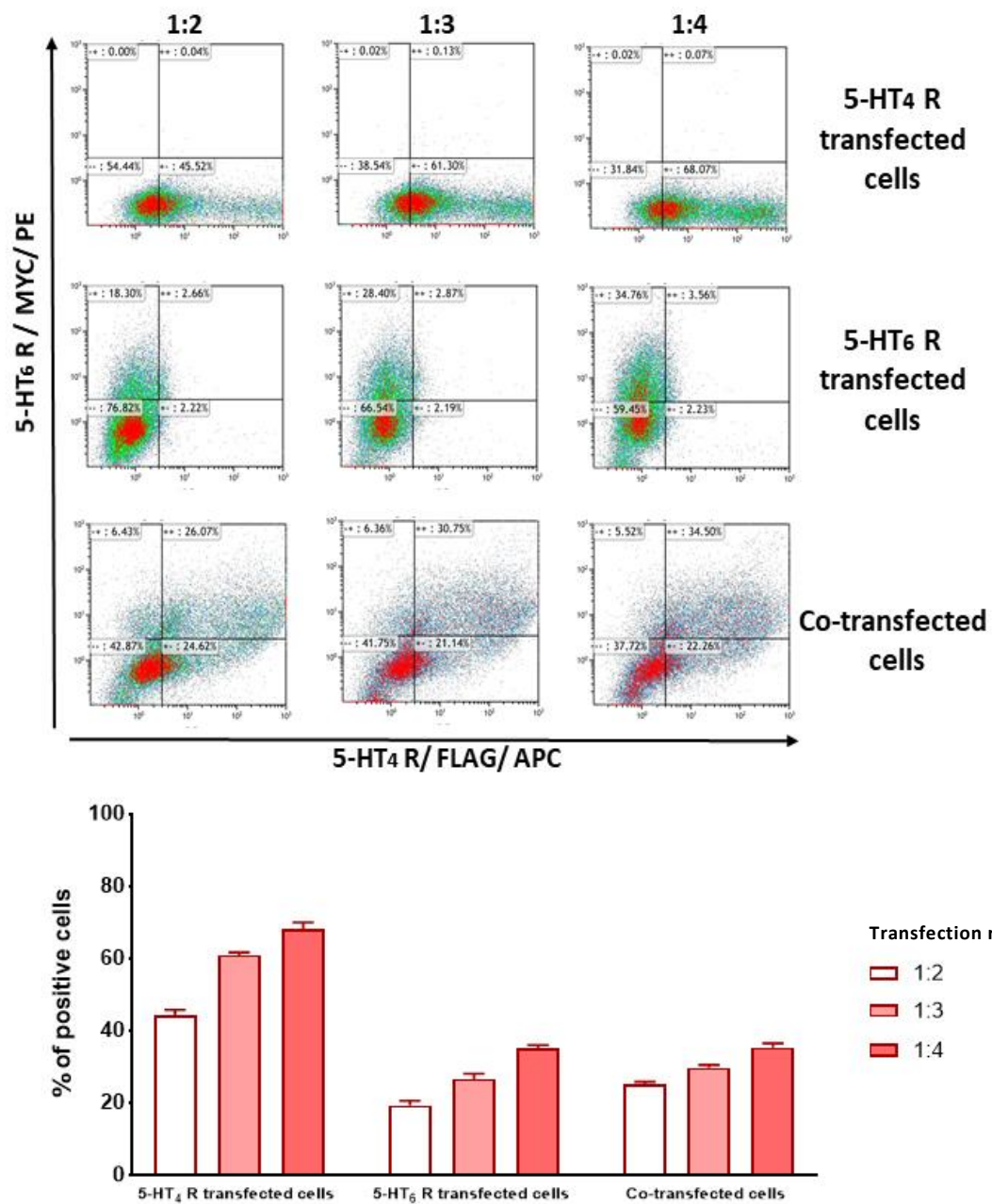
## **Chapter 4. Evaluation of the 5-HT<sub>4</sub> and 5-HT<sub>6</sub> receptors' interaction by measuring the pERK<sub>1/2</sub> level**

## **4. Evaluation of the 5-HT<sub>4</sub> and 5-HT<sub>6</sub> receptors' interaction by measuring the pERK<sub>1/2</sub> level**

### **4.1. Optimisation of transfection ratio**

The HEK293 cells were seeded in 6 well plates and grown to reach 70% confluency. The plasmid and PEI were mixed in SFM before being added to the cells to allow the complex formation. Three different ratios of DNA to PEI were assessed; 1:2, 1:3 and 1:4 for each plasmid separately, and when combined together in co-transfected cells. The optimum ratio that possessed high protein level and good cell tolerability was selected for subsequent experiments. This was achieved by staining the cells, 48 hr post-transfection, against the tag in each plasmid and determining the percentage of fluorescence positive cells by flow cytometry.

**Figure 23** revealed that the 5-HT<sub>4</sub> receptor was expressed at a higher level than the 5-HT<sub>6</sub> receptor and this was consistent in the three transfection ratios. In cotransfected cells, and based on using the same gating strategy, the percentage of double positive cells reflected a similar percentage of the 5-HT<sub>6</sub> receptor transfected cells because it had lower transfectability. Increasing the PEI amount was associated with higher percentages of positive cells with both plasmids. Although the 1:4 ratio had the highest positive cells, however, it is associated with more cell death (detected by the detachment of the cells under the microscope), and this was obvious in co-transfected cells. Usually higher transfection efficiency is associated with a decrease in cell viability (de Los Milagros Bassani Molinas et al., 2014). Hence, the complex ratio was kept at 1:3 because it produced high percentage of positive cells with the accepted level of cell tolerability.



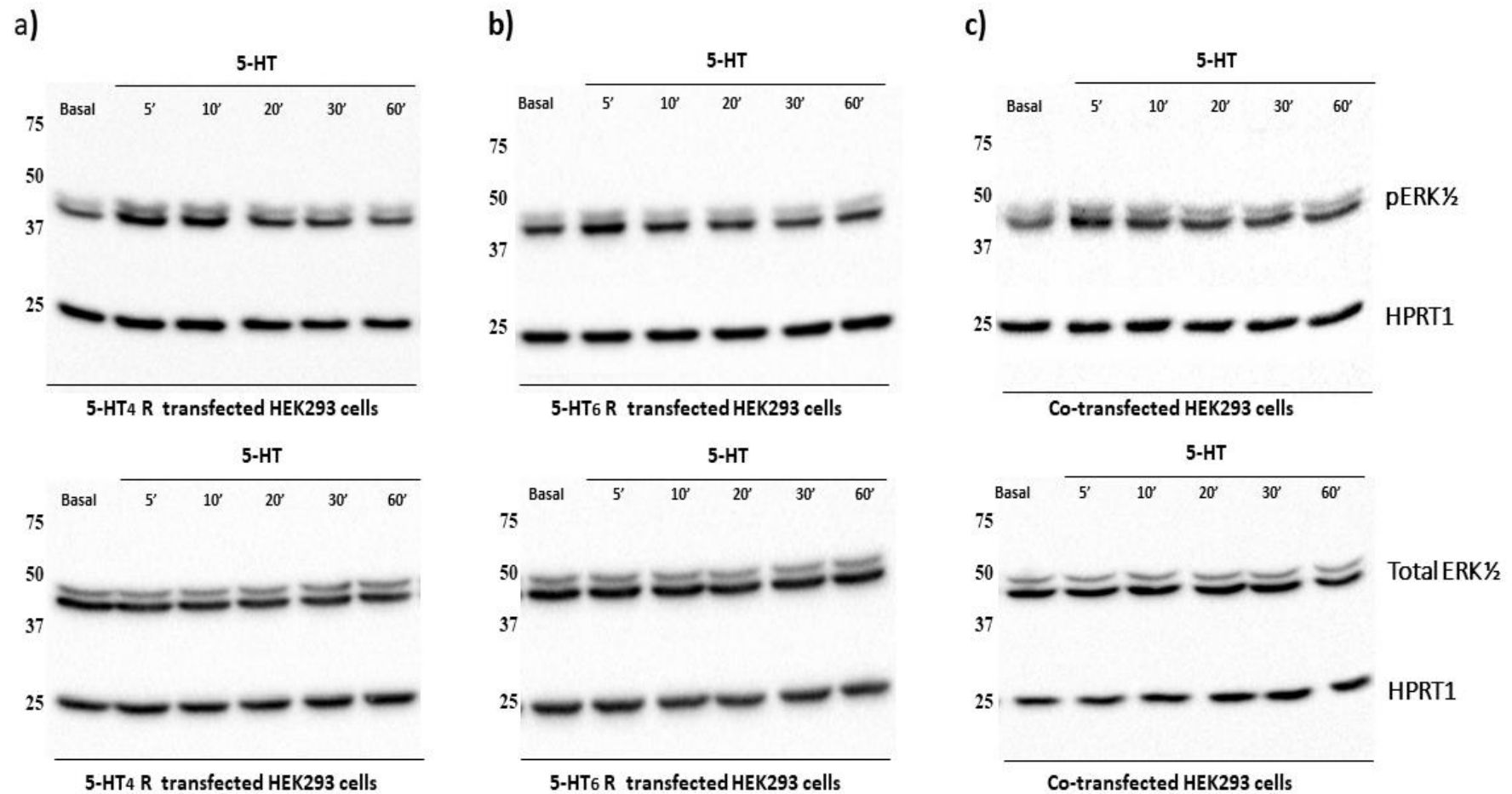
**Figure 23. Titration of DNA: PEI transfection ratio of plasmids encoding 5-HT<sub>4</sub> and 5-HT<sub>6</sub> receptors**

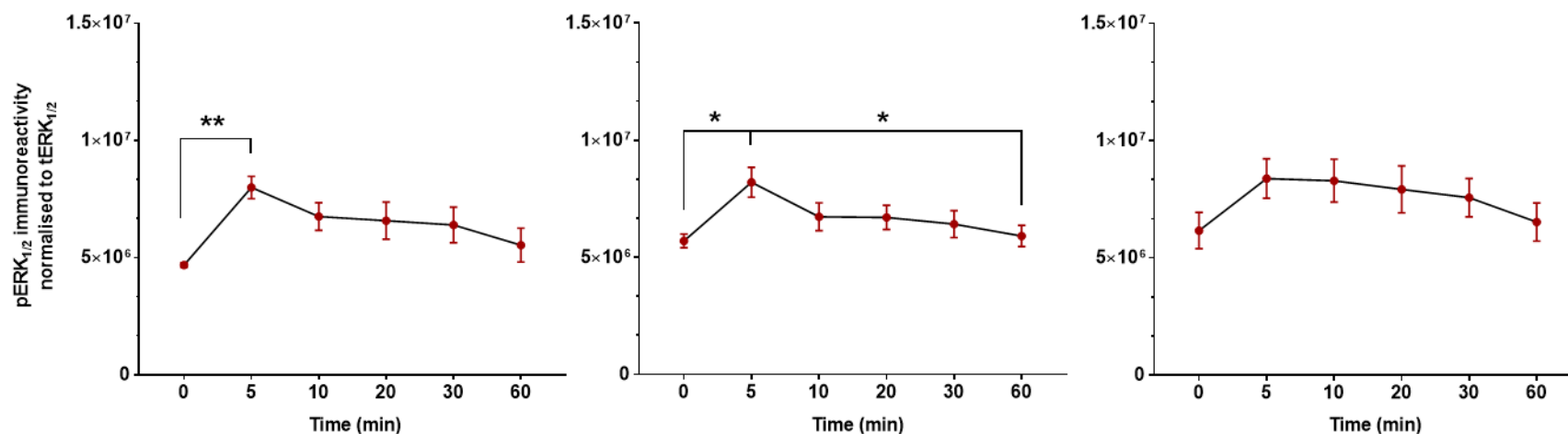
*Small-scale transfection of HEK293 cells was conducted by different complex ratios to select the optimum ratio for subsequent experiments. Two days post-transfection, the cells were stained, and the percentages of positive cells were determined. Data are mean  $\pm$  SD, n = 3.*

#### **4.2. Time-dependent effect of 5-HT-induced ERK<sub>1/2</sub> phosphorylation in transfected HEK293 cells**

In an effort to determine the time point at which 5-HT-induced maximum ERK phosphorylation, HEK293 cells were transiently transfected with constructs of either 5-HT<sub>4</sub> receptor alone, 5-HT<sub>6</sub> receptor alone or both concurrently in a 1:3 pre-optimised DNA: PEI ratio. Activation of the serotonin receptor in response to 10  $\mu$ M of 5-HT produced transient phosphorylation of ERK<sub>1/2</sub> kinases which significantly peaked early on after 5 min. The immunoreactivity was increased above basal by;  $70 \pm 9\%$  in 5-HT<sub>4</sub> transfected cells,  $44 \pm 10\%$  in 5-HT<sub>6</sub> receptor transfected cells and  $41 \pm 12\%$  in co-transfected cells. Prolonged stimulation of these cells by the same concentration of 5-HT returned the pERK<sub>1/2</sub> immunoreactivity level close to the basal level notably after 60 min of stimulation (see the representative blots and the time point graphs in **Figure 24**). This pattern of time-dependent changes in ERK<sub>1/2</sub> phosphorylation was similar in either the single activation of the 5-HT receptor or in coactivation of both receptors. Contrary to expectations, the stimulation of both receptors in co-transfected cells by a single agonist, 5-HT, did not reveal any further increases in pERK<sub>1/2</sub> immunoreactivity as in **Figure 24c**. This might be due to the difference in the level of the recombinant receptors in the single transfected and co-transfected HEK293 cells. To exclude the presence of this difference, the protein lysates used in the ERK<sub>1/2</sub> experiment were reloaded in the same order and probed with monoclonal Flag and Myc tag antibodies to detect the recombinant 5-HT<sub>4</sub> receptor and 5-HT<sub>6</sub> receptor, respectively. There was no significant difference in the tag immunoreactivity between the single or co-transfected cells as shown in **Figure 25**.

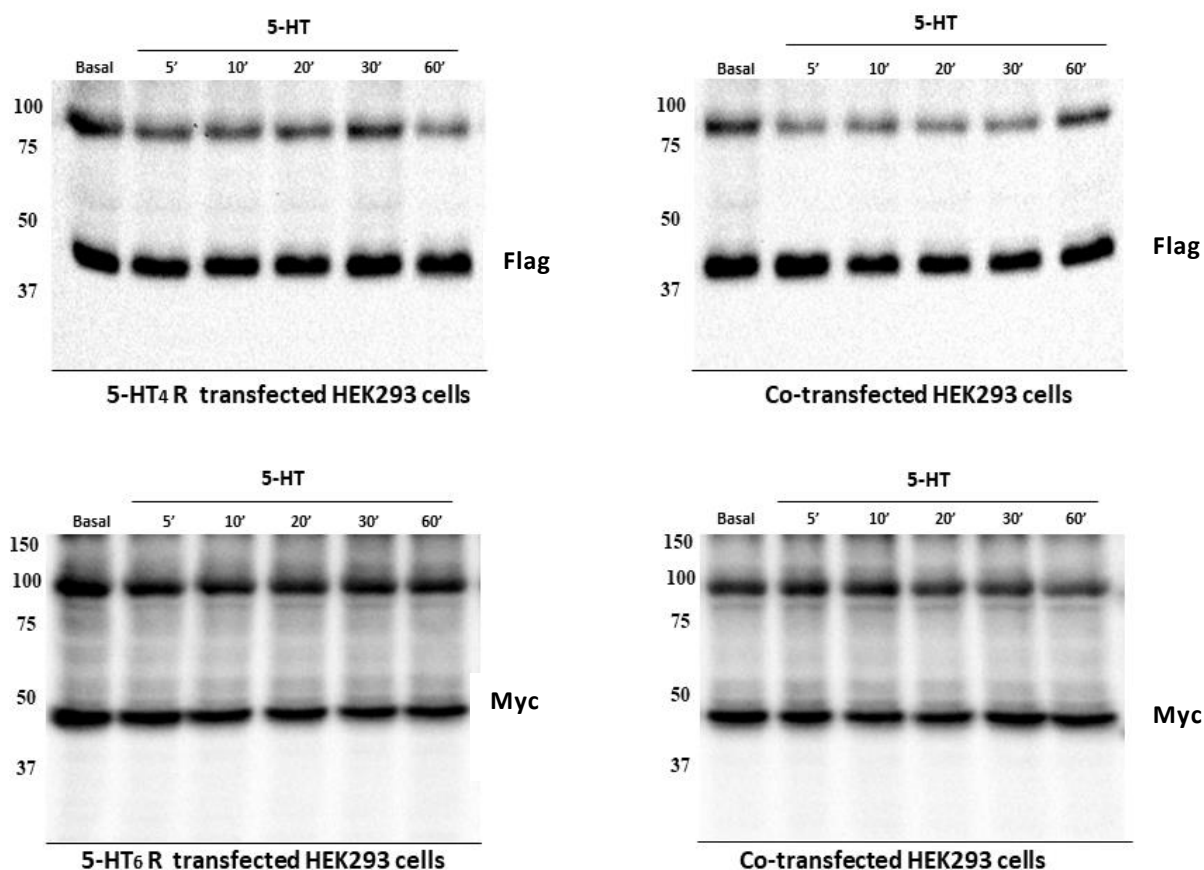






**Figure 24. Time-dependent effect of 5-HT-mediated ERK<sub>1/2</sub> phosphorylation in transiently transfected HEK293 cells**

HEK293 cells were transiently transfected with the constructs of (a) 5-HT<sub>4</sub> receptor, (b) 5-HT<sub>6</sub> receptor and (c) both. Forty-eight hours post-transfection, the cells were stimulated with 5-HT (10 μM) for 5, 10, 20, 30 and 60 min at 37°C. Representative blots showed 5-HT inducing transient phosphorylation of ERK<sub>1/2</sub> which peaked after 5 min. Total ERK<sub>1/2</sub> was used as a loading control and for normalisation of pERK<sub>1/2</sub> immunoreactivity. Time course graphs were plotted below each panel. The data are represented as mean ± SEM (n=7) and analysed by one-way ANOVA followed by Tukey's multiple comparison test, \*P < 0.05, \*\*P < 0.01.



**Figure 25. The immunoreactivity of monoclonal Flag and Myc antibodies in transfected HEK293 cells at different time point stimulation**

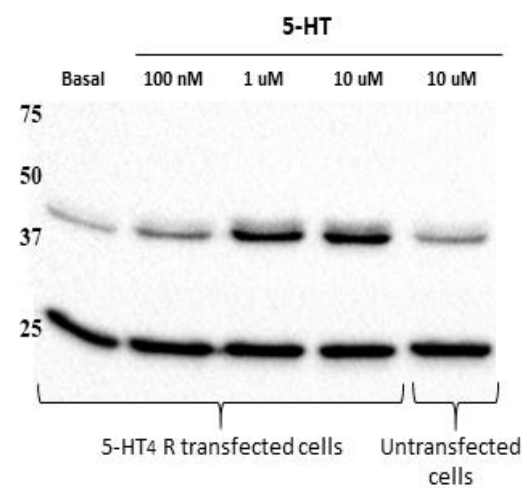
*HEK293 cells were transiently transfected with constructs of the 5-HT<sub>4</sub> receptor, 5-HT<sub>6</sub> receptor or both. Two days post-transfection, the cells were stimulated with 5-HT (10  $\mu$ M) for the indicated time points. The level of recombinant proteins in each condition was detected by Flag epitope for the 5-HT<sub>4</sub> receptor and Myc epitope for the 5-HT<sub>6</sub> receptor in single transfected (left panel) or co-transfected (right panel) cells (n=4).*

#### **4.3. Dose-dependent effect of 5-HT-induced ERK<sub>1/2</sub> phosphorylation in transfected HEK293 cells**

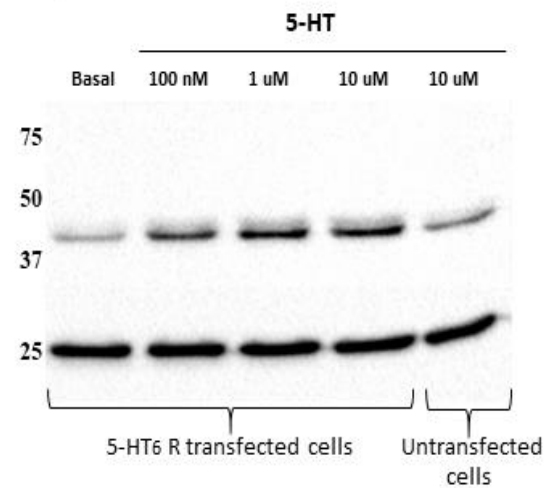
To investigate further the effect of 5-HT on ERK<sub>1/2</sub> activation and to determine whether 5-HT<sub>4</sub> and 5-HT<sub>6</sub> receptors can produce additive or synergistic effects on ERK<sub>1/2</sub> activation, three different doses of 5-HT (100 nM, 1  $\mu$ M and 10  $\mu$ M) were used for cell stimulation within 5 min period. Untransfected HEK293 cells were also stimulated with 10  $\mu$ M of 5-HT, and these were used as an endogenous control to be run alongside the transfected cells.

The results reported in **Figure 26** revealed that 5-HT-induced a dose-dependent increase in ERK<sub>1/2</sub> phosphorylation as indicated by its immunoreactivity. The highest immunoreactivity of pERK<sub>1/2</sub> was seen with the 5-HT<sub>4</sub> receptor stimulation at which 10  $\mu$ M of 5-HT produced approximately a  $3.7 \pm 0.6$  fold increase while the stimulation of 5-HT<sub>6</sub> receptor produced a  $2.7 \pm 0.5$  fold increase over the basal level. The presence of both receptors in co-transfected HEK293 cells produced only  $1 \pm 0.13$  fold increase over the basal with the same dose, and thus it did not reveal any further increase in pERK<sub>1/2</sub> immunoreactivity as in **Figure 26c**. Furthermore, no significant differences in the immunoreactivity of the recombinant proteins were detected as illustrated in **Figure 27**. These results further support the lack of synergistic effect between the 5-HT<sub>4</sub>, and 5-HT<sub>6</sub> receptors which was measured though ERK phosphorylation in HEK293 cells that co-expressed both receptors.

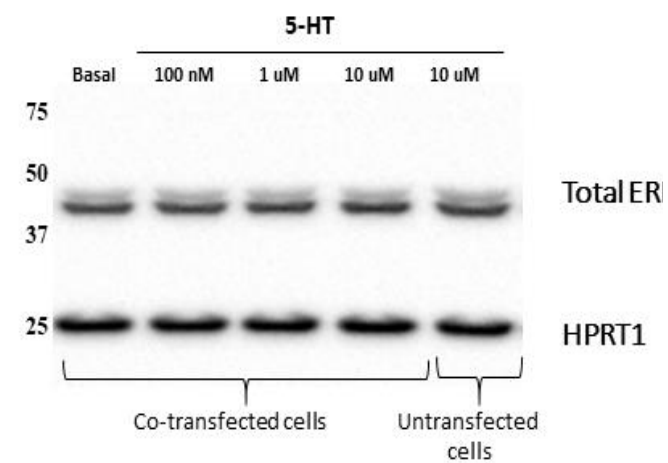
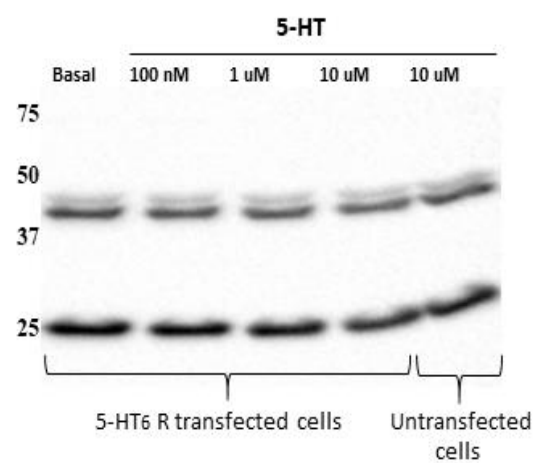
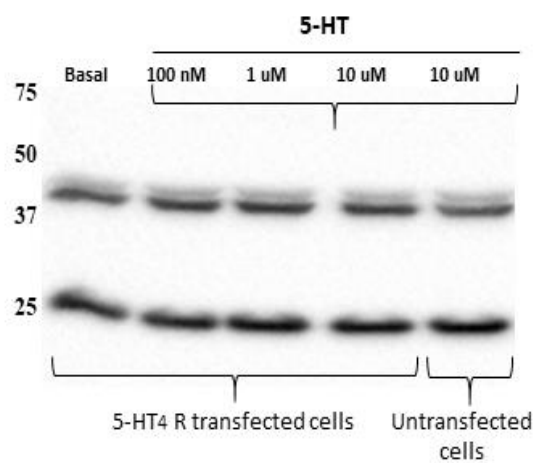
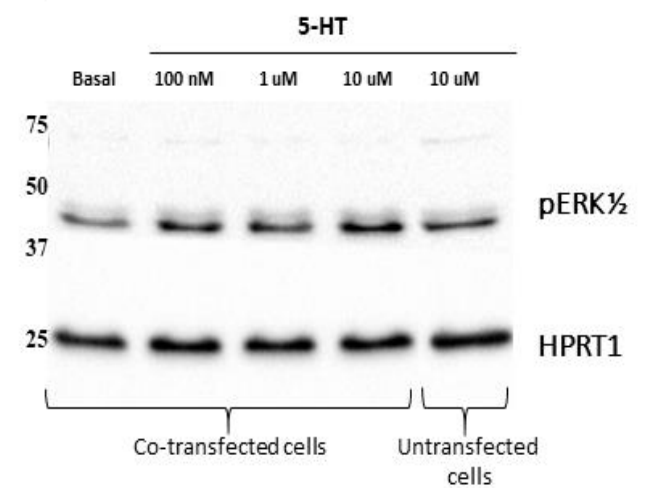
a)

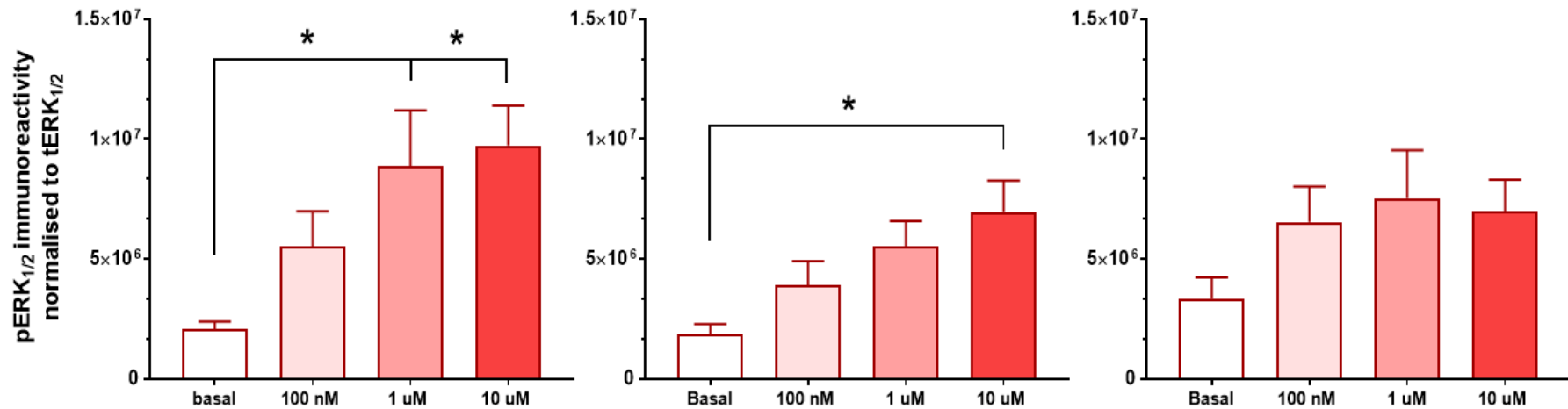


b)



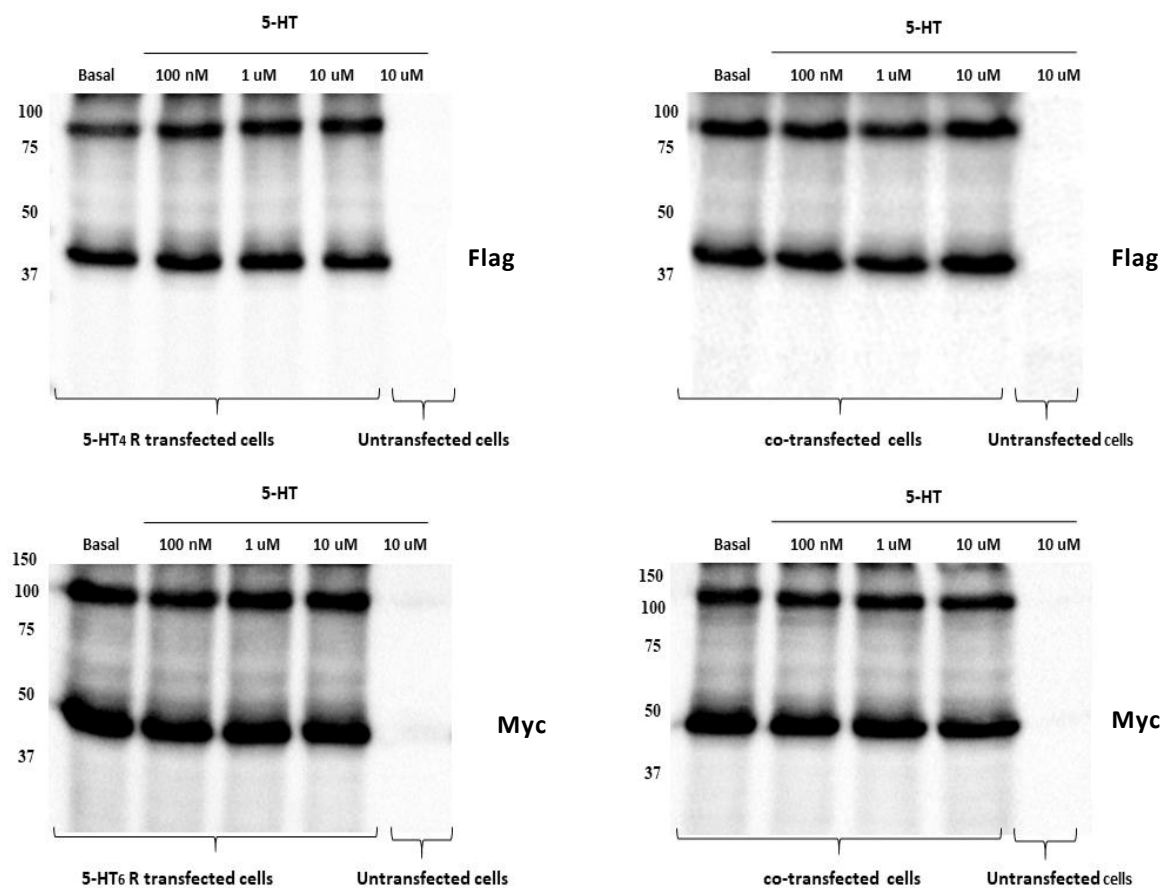
c)





**Figure 26. Dose-dependent effect of 5-HT-mediated ERK<sub>1/2</sub> phosphorylation in transiently transfected HEK293 cells**

*HEK293 cells were transiently transfected with constructs of (a) 5-HT<sub>4</sub> receptor, (b) 5-HT<sub>6</sub> receptor and (c) both. Forty-eight hours post-transfection, the cells were stimulated with three doses of 5-HT for 5 min. Untransfected HEK293 cells were used as an endogenous control. HPRT1 and total ERK<sub>1/2</sub> were used as loading controls. The data are represented as mean  $\pm$  SEM (n=5) and the statistical analysis is performed by one-way ANOVA followed by Tukey's multiple comparison test \*  $P < 0.05$ .*



**Figure 27. The immunoreactivity of monoclonal Flag and Myc antibodies of transfected HEK293 cells following treatment with different doses of 5-HT**

*Forty-eight hours post-transfection, the cells were treated with three doses of 5-HT for 5 min. The level of recombinant proteins in each condition was detected by identification of the Flag epitope for the 5-HT<sub>4</sub> receptor and the Myc epitope for the 5-HT<sub>6</sub> receptor in single transfected cells (left panel) or co-transfected cells (right panel). These blots are representative of three repeats.*

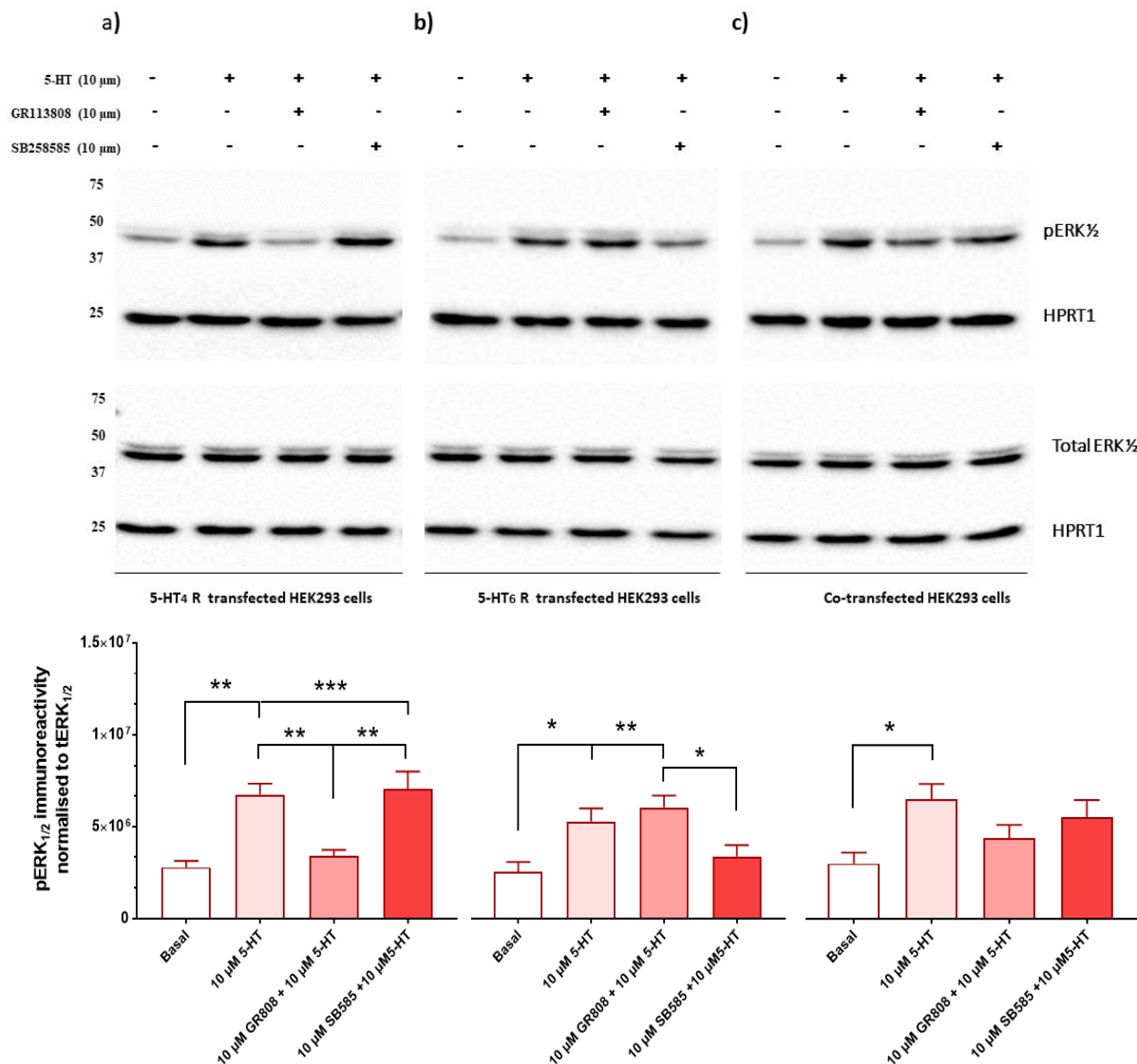
#### **4.4. The 5-HT-mediated ERK<sub>1/2</sub> phosphorylation was specific to 5-HT<sub>4</sub> and 5-HT<sub>6</sub> receptors**

Potent and selective antagonists; GR-113808 for 5-HT<sub>4</sub> receptors and SB-258585 for 5-HT<sub>6</sub> receptors were utilised to test whether the increase in ERK<sub>1/2</sub> activation was specific to the overexpressed receptors by comparing the pERK<sub>1/2</sub> level in the presence or absence of the antagonists. Forty-eight hours post-transfection, the antagonist was added in a final concentration of 10  $\mu$ M and incubated for 30 min at 37°C prior to challenging the cells with 10  $\mu$ M of 5-HT for 5 min. As demonstrated in **Figure 28**, GR-113808 abolished the 5-HT-mediated ERK<sub>1/2</sub> phosphorylation and significantly reduced it by  $79 \pm 8\%$  ( $P=0.007$ ) in the 5-HT<sub>4</sub> receptor transfected cells. Preincubation of 5-HT<sub>6</sub> receptor transfected cells with SB-258585 caused reduction of  $72 \pm 10\%$  of the pERK<sub>1/2</sub> immunoreactivity ( $P=0.186$ ). These percentages were calculated relative to the 5-HT-induced pERK<sub>1/2</sub> after removal to the basal level. This highlighted that the activation of the 5-HT<sub>4</sub> receptor was involved in ERK<sub>1/2</sub> activation more than the 5-HT<sub>6</sub> receptor.

When both receptors were concurrently overexpressed, the antagonists showed less inhibition of ERK<sub>1/2</sub> phosphorylation in comparison to the singly expressed receptor in which GR-113808 and SB-258585 caused inhibition by  $53 \pm 14\%$  and  $24 \pm 18\%$ , respectively. These percentages were lower than those obtained each time in the presence of one type of receptor. However, it was clear that the ERK<sub>1/2</sub> activation had resulted from the activation of both receptors, as blocking of the 5-HT<sub>4</sub> receptor, for example, still showed the effect of the 5-HT<sub>6</sub> receptor activation and vice versa. Overall, these findings thus need to be interpreted with caution because the interactions of 5-HT<sub>4</sub> and 5-HT<sub>6</sub> receptors could be influenced by the presence of



heterogeneous cell populations following transient transfections or by more complex signalling mechanisms that might interfere with the synergy between the two receptors.

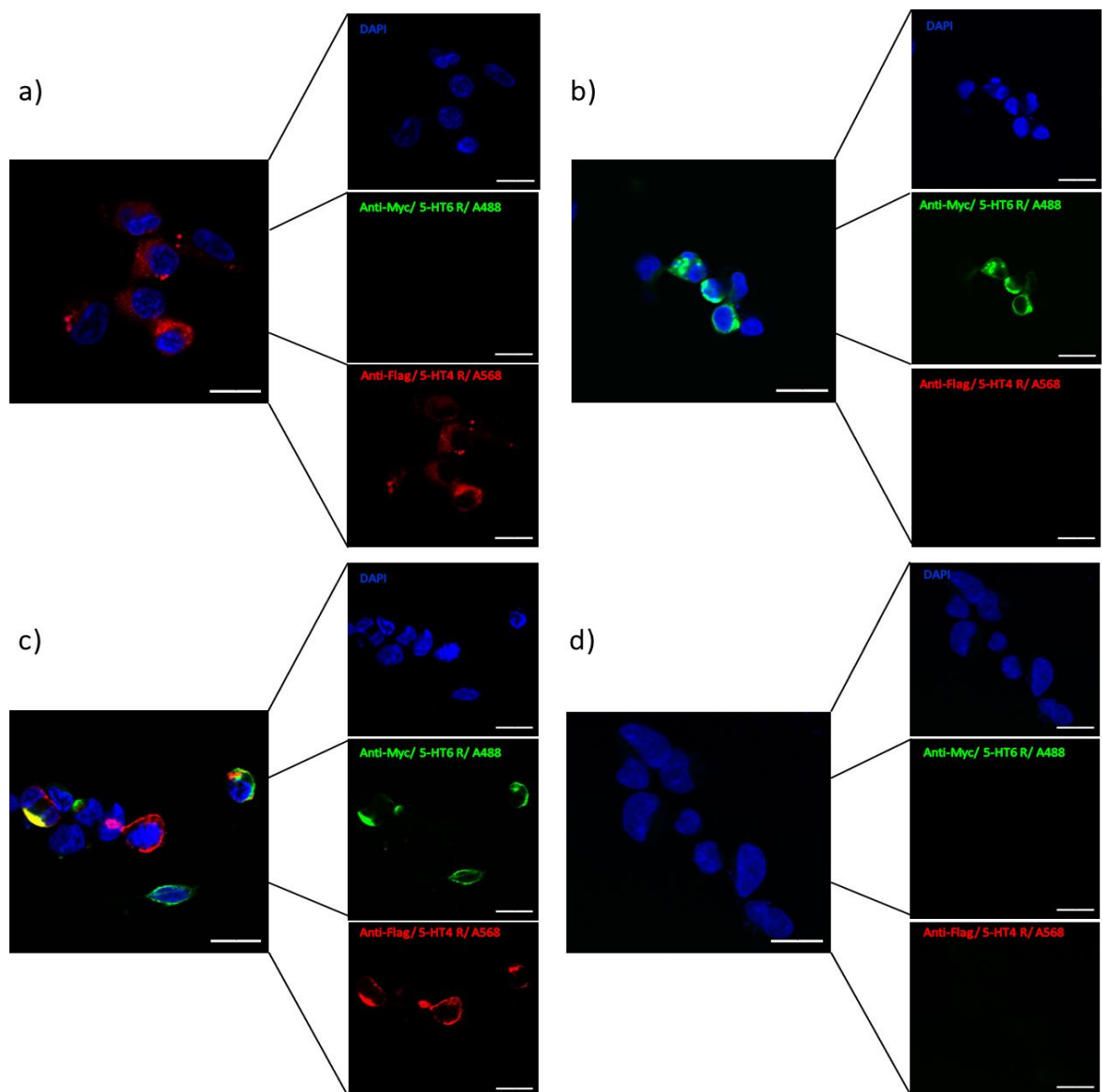


**Figure 28. The effect of 5-HT receptor antagonists on the ERK<sub>1/2</sub> phosphorylation**

The antagonist (10  $\mu$ M) was added 48 hr post-transfection and maintained in the medium for 30 min then 10  $\mu$ M of 5-HT was added for 5 min. The pERK<sub>1/2</sub> immunoreactivity was normalised to total ERK<sub>1/2</sub> immunoreactivity. HPRT1 was used as a loading control. Data are represented as a mean  $\pm$  SEM (n=5) and was analysed by one-way ANOVA and Tukey's multiple comparison test \*  $P < 0.05$ , \*\*  $P < 0.01$ , \*\*\*  $P < 0.001$ .

#### **4.5. Heterogeneity of the cell population of the co-transfected HEK293 cells**

Immunofluorescence analysis of single and double transfected cells showed positive signal in some but not all the cells (**Figure 29**). Visualisation of the cell populations following transient co-expression of the 5-HT<sub>4</sub> and 5-HT<sub>6</sub> receptors showed the expected mixed cell populations; single positive for either receptor, double positive for both receptors, as well as untransfected double negative cells (**Figure 29c**). This might influence the 5-HT receptors-mediated ERK<sub>1/2</sub> activation. Therefore, stabilising clonal cell lines, which expressed the target receptors individually and in combination, through permanent integration of the target gene in the mammalian cell genome should provide a more homogenous cell population for studying the interaction of both receptors.



**Figure 29.** Immunofluorescent imaging showed the cell populations following transient transfection with constructs of the 5-HT<sub>4</sub> and 5-HT<sub>6</sub> receptor

*The HEK293 cells were transiently transfected with the constructs of (a) 5-HT<sub>4</sub> receptor, (b) 5-HT<sub>6</sub> receptor (c) both receptors or (d) untransfected cells. Forty-eight hours following transfection, the cells were fixed and incubated with antibodies against the tagged receptors then with fluorophore-labelled secondary antibodies. The yellow fluorescence indicated co-localised protein (double positive cells). The transfection and staining were repeated twice, and similar results obtained. Scale bar 20  $\mu$ m.*

#### **4.6. Attempts to generate stable cell lines expressing each of the 5-HT<sub>4</sub> receptor and 5-HT<sub>6</sub> receptors alone and in combination**

Many attempts were performed to generate clonal and stable cell lines expressing the 5-HT<sub>4</sub> and 5-HT<sub>6</sub> receptors. This entailed many months of antibiotic selection, clonal cell expansion, and screenings of each cell line separately by Western blotting, flow cytometry and RLB assay. The cell clones were picked at least 3 weeks after transfection then allowed to expand in the presence of antibiotic selection for 2 weeks. Some of these clones did not show any positive bands by Western blotting, indicating the absence of the receptors, while others showed a truncated form of the protein, as in the case of the 5-HT<sub>6</sub> receptor. In addition, some cell lines were positive for the target receptor which had the correct protein size but were not fortunate enough to show binding affinity to [<sup>3</sup>H]-5-HT by RLB assay. This might be due to the low expression level of the target receptor; thus, all these cell lines were excluded (See **Supplementary Figures 1-5** in the **Appendices**).

#### **4.7. Summary**

The work in this chapter revealed that the overexpression of 5-HT<sub>4</sub> or 5-HT<sub>6</sub> receptors activated the ERK<sub>1/2</sub> transiently and in a dose-dependent manner. However, there is no evidence of synergy between the two receptors when they expressed together. Stabilisation of these receptors was performed to obtain more homogenous cell lines. Finally, successful stabilisation of the 5-HT<sub>4</sub> receptor in HEK293 cells was achieved, and evaluation of the 5-HT<sub>4</sub> receptor expression, radioligand affinity and *N*-glycosylation pattern will be discussed in the following chapter.

**Chapter 5. Determination of the potential  
*N*-glycosylation sites in the 5-HT<sub>4</sub> receptor  
and their role in the receptor trafficking**

## **5. Determination of potential *N*-glycosylation sites in the 5-HT<sub>4</sub> receptor and their role in receptor trafficking**

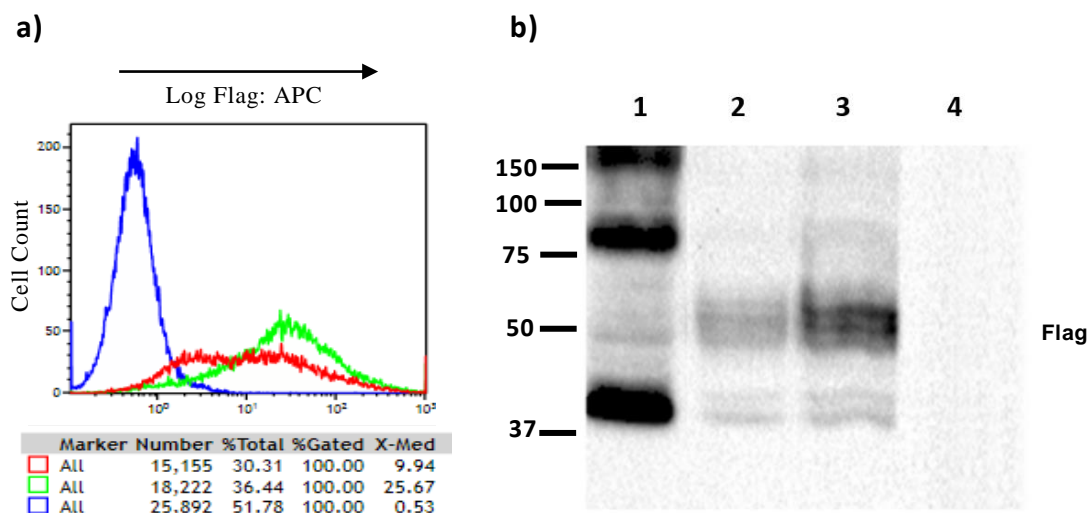
### **5.1. Stable expression of the 5-HT<sub>4</sub> receptor in HEK293 cells**

The Flag-5-HT<sub>4</sub> receptor containing plasmid was transfected into HEK293 cells. At 24 hr post-transfection, the cells were harvested and split into two portions. The first portion was seeded at a low seeding density (1:10 splitting ratio) in a culture dish and allowed to stabilise the receptor for several weeks under hygromycin selection as described in **Section 2.7**. The second portion was lysed for use as a positive control for Flag antibody during the screening for positive clones by Western blotting. Forty clones were individually picked and grown until they reached acceptable confluency.

The initial screening by flow cytometry indicated that only two clones; C24 and C31, were stably expressing the 5-HT<sub>4</sub> receptor in the cell surface since they showed positive immunoreactive cells for Flag antibody (**Figure 30a**). The immunoreactivity was detected as a fluorescence signal for APC conjugated secondary antibody. Overlay histograms were used to compare the level of protein expression in both clones. The C31 clone, denoted as a green histogram, had higher MFI than the C24 clone denoted as a red histogram. Therefore, the C31 clonal cell line possessed a higher protein expression level and was consequently selected for further experiments.

In agreement with the flow cytometry results, Western blotting confirmed that both cell lines were positive against Flag antibody and the intensity of the C31 band was higher than that of C24 as shown in **Figure 30b**. Transient Flag-5-HT<sub>4</sub> receptor

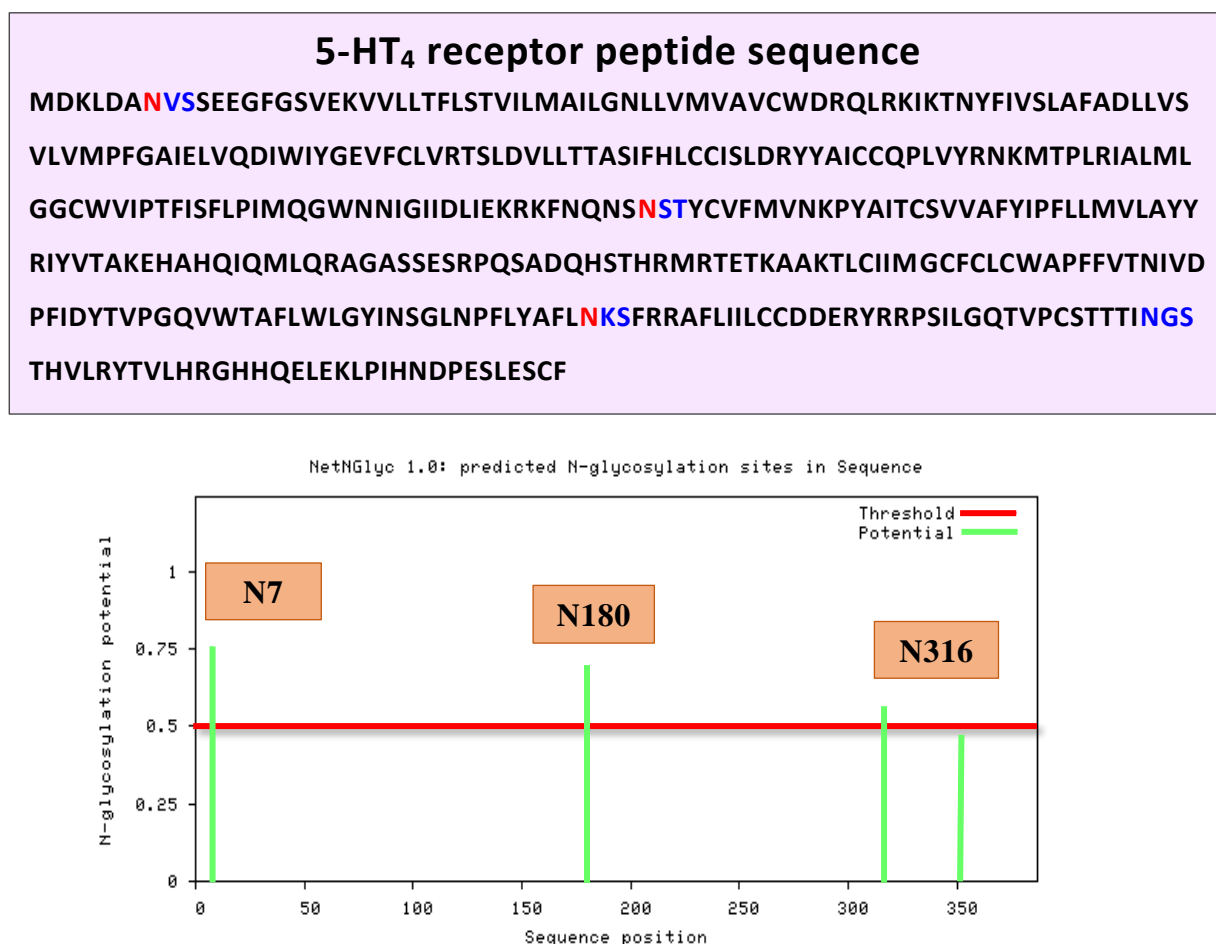
protein (the positive control), showed a band at approximately 41 kDa (monomer) and higher bands at sizes equivalent to dimer and possibly tetramer species. Interestingly, and unlike the transiently expressed Flag-5-HT<sub>4</sub> receptor, the stable receptor protein in C24 and C31 showed multiple smeared bands ranging between approximately 49 and 56 kDa, and a couple of faint bands at approximately 41 and 43 kDa. Therefore, the stable 5-HT<sub>4</sub> receptor predominantly had larger bands than those of the transient receptor (**Figure 30b**). This could be attributed to glycosylation of the 5-HT<sub>4</sub> receptor during its translation.



**Figure 30. Stable expression of the 5-HT<sub>4</sub> receptor in HEK293 cells**

*a) The flow cytometry overlay histograms of surface staining of Flag-tagged receptor in clones 24 and 31 which are denoted as red and green histograms, respectively. Untransfected HEK293 cells are negative (blue histogram). b) Immunoblot of the 5-HT<sub>4</sub> receptor which probed against Flag antibody and displaying the difference in the migration of the transiently expressed receptor (lane 1) and the stably expressed receptor (clone 24 and 31 in lanes 2 and 3, respectively). Untransfected HEK293 cells are negative in lane 4.*

The most prevalent form of glycosylation is *N*-linked glycosylation. According to the NetNGlyc online server, the 5-HT<sub>4</sub> receptor sequence has four sites on the N-X-S/T motif but only three of them—namely N7, N180 and N316—are putative sites for glycosylation because their potential scores are above the 0.5 threshold (**Figure 31**).



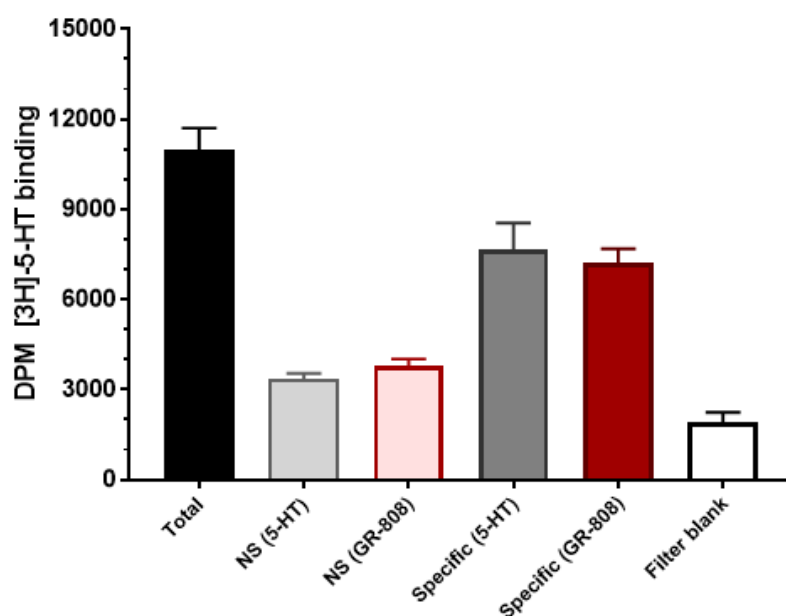
**Figure 31. The potential glycosylation motifs in the 5-HT<sub>4</sub> receptors**

*The cropped figure illustrates the potential sites of N-glycosylation highlighted in red and the glycosylation motifs in blue. Any site with the N-X-S/T motif and a potential above the 0.5 threshold represents a predicted glycosylated site. The x-axis shows the position of the putative N-glycosylation motifs in the protein sequence. The y-axis represents the N-glycosylation potential scores averaged from nine neural networks which are calculated based on the position of the motifs within the protein structure. Adapted from Gupta et al. (2017).*



## **5.2. Radioligand binding assay of the 5-HT<sub>4</sub> receptor stable cell line**

Membrane fraction of the 5-HT<sub>4</sub> receptor stable cell line (clone 31) was used to assess the ability of the radiolabelled agonist [<sup>3</sup>H]-5-HT to bind to the receptor. This fraction was incubated with 5 nM of the radioligand either in the absence or presence of a high concentration (10  $\mu$ M) of competing ligands. The results confirmed that the overexpressed Flag-5-HT<sub>4</sub> receptor had a specific binding affinity ranging from 60-80% of the total binding (**Figure 32**). The approximate density of the recombinant receptor was  $1763 \pm 72$  fmol/mg of membrane protein which was reflected from the specific binding of 4.6-5.2 nM of [<sup>3</sup>H]-5-HT.

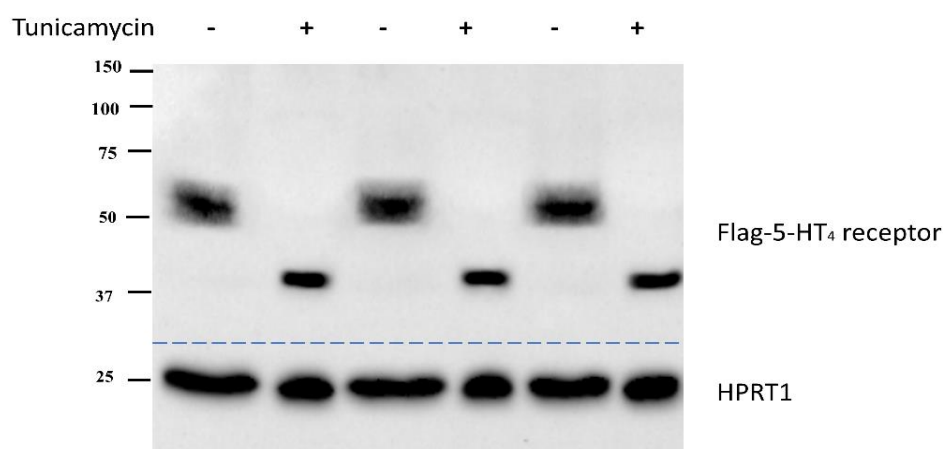


**Figure 32. Radioligand binding for the 5-HT<sub>4</sub> receptor stable cell line**

*The radioligand [<sup>3</sup>H]-5-HT concentration is 5 nM and nonspecific (NS) binding is determined by 10  $\mu$ M of 5-HT or GR113808. The protein concentration of the membrane fraction is 0.1 mg/ml. DPM of the radioligand were measured by a Tri-carb counter. The experiment shown is representative of four independent experiments each consisting of three technical repeats. Data are represented as mean  $\pm$  SD.*

### **5.3. The effect of tunicamycin on the size of the Flag-5-HT<sub>4</sub> receptors**

Tunicamycin is a mixture of antibiotics that induce protein deglycosylation by inhibiting the N-acetylglucosamine 1-phosphate transferase which is essential in glycoprotein synthesis (Heifetz et al., 1979). Therefore, this drug was used to test whether the increase in the size of the stable 5-HT<sub>4</sub> receptor was due to *N*-glycosylation (**Figure 30b**). Cells stably expressing the 5-HT<sub>4</sub> receptor were seeded in a 6 well plate at a density of  $3 \times 10^5$  cell per well. Tunicamycin was added to the medium at a final concentration of 1  $\mu\text{g/ml}$  and incubated for 48 hr. As expected, the presence of tunicamycin consistently reduced the size of the stable 5-HT<sub>4</sub> receptor by condensing the smeared bands to a single sharp band which migrated faster in the SDS-PAGE due to its lower size ~ 41 kDa as illustrated in **Figure 33**.



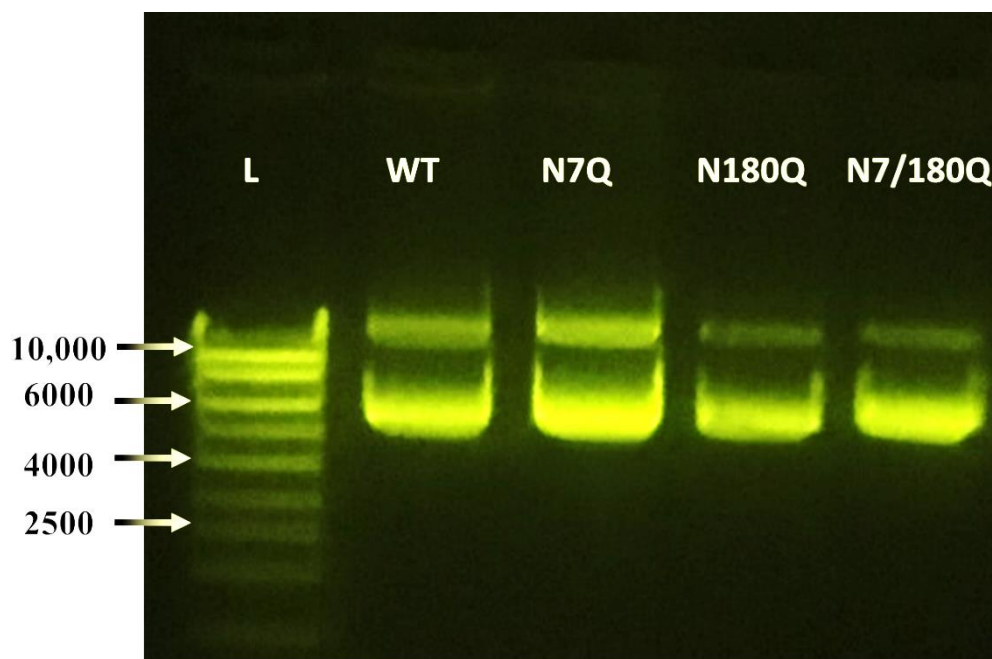
**Figure 33. Enzymatic inhibition of *N*-glycosylation of the 5-HT<sub>4</sub> receptor by tunicamycin**

*HEK293 cells stably expressing the 5-HT<sub>4</sub> receptor were maintained for 48 hr with (+) and without (-) tunicamycin (1  $\mu\text{g/ml}$ ). The size of the glycosylated receptor species was reduced to 41 kDa following tunicamycin treatment. HPRT1 was used as a loading control. This is a representative blot of 4 independent repeats with similar results.*

#### **5.4. Generating single and double mutant constructs of N7 and N180 glycosylation sites of the 5-HT<sub>4</sub> receptor.**

Based on the NetNglyc online server, three sites have potential glycosylation scores above the 0.5 threshold. The asparagine residues N7 and N180 are located on the extracellular side of the receptor while N316 is located intracellularly. According to Salom et al. (2012), the human 5-HT<sub>4b</sub> receptor was potentially *N*-glycosylated at N7 and N180 when heterologously expressed in rod cells of transgenic mice.

Most of the potential *N*-glycosylation sites are located extracellularly, and the frequency of authentic sites is lower towards the C terminus (Gavel and Heijne, 1990) and thus N316 was excluded. Therefore, SDM was used to substitute two asparagine residues (N7 and N180) of the wild 5-HT<sub>4</sub> receptor sequence with glutamine (Q) residues. Glutamine has a similar chemical structure to asparagine but has no tendency for glycosylation. The two sites were either mutated individually by the aid of PCR to form two single mutant constructs or mutated simultaneously to form the double mutant construct. These constructs were amplified inside the bacteria and then isolated for sequencing. All plasmid constructs were intact and of the correct size (**Figure 34**). The sequencing chromatogram confirmed the individual mutations of N7 and N180 as shown in **Figures 35a and b**, respectively. The double mutant construct exhibited both mutation sites.



**Figure 34. Blue-light image of agarose gel electrophoresis of the wild type and mutant 5-HT<sub>4</sub> receptor plasmids**

*Following maxi-prep plasmid isolation, the plasmids were loaded onto a 1% agarose gel to determine their integrity and size prior to sequencing. Most plasmids appearing in the supercoiled form were observed at ~ 5500 bp, and the nicked circular form was observed at a higher size. L: DNA ladder, WT: wild type, N7Q, N180Q: single mutants and N7/180Q: Double mutant of 5-HT<sub>4</sub> receptor plasmids.*

a)

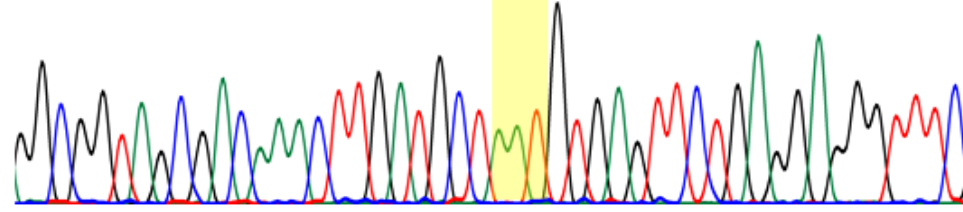
Wild type (5-HT<sub>4</sub>R in pCMV3-N-FLAG)

ATG GAT TAC AAG GAT GAC GAC GAT AAG GGT GGA GGC GGT AGC GAC AAA CTT GAT GCT AAT GTG AGT TCT GAG GAG GGT TTC  
M D Y K D D D D K G G G G S D K L D A N V S S E E G F  
TAC CTA ATG TTC CTA CTG CTG CTA TTC CCA CCI CCG CCA TCG CTG TTT GAA CTA CGA TTA CAC TCA AGA CTC CTC CCA AAG

Start codon      Flag tag      Short link      5-HT<sub>4</sub>R N-terminus

GGCGGTAGCGACAAACTTGTATGCTAATGTGAGTTCTGAGGAGGGTTTC

CMV Forward



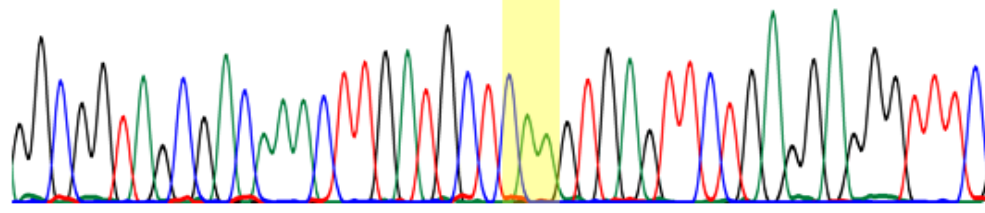
Mutant clone of 1<sup>st</sup> glycosylation site (5-HT<sub>4</sub>R -N7Q)

ATG GAT TAC AAG GAT GAC GAC GAT AAG GGT GGA GGC GGT AGC GAC AAA CTT GAT GCT CAA GTG AGT TCT GAG GAG GGT TTC  
M D Y K D D D D K G G G G S D K L D A Q V S S E E G F  
TAC CTA ATG TTC CTA CTG CTG CTA TTC CCA CCI CCG CCA TCG CTG TTT GAA CTA CGA GTT CAC TCA AGA CTC CTC CCA AAG

Start codon      Flag tag      Short link      5-HT<sub>4</sub>R N-terminus

GGCGGTAGCGACAAACTTGTATGCTCAAGTGAGTTCTGAGGAGGGTTTC

CMV Forward



b)



**Figure 35. The sequence chromatogram showing the wild type, N7Q and N180Q mutants of the 5-HT<sub>4</sub> receptor**

*The mutated sites a) N7 and b) N180 are highlighted in yellow, and the chromatogram shows the forward sequence indicated by the blue rectangle.*

### **5.5. The differences in the glycosylation pattern of the wild type and mutant 5-HT<sub>4</sub> receptor following transient and stable protein expression**

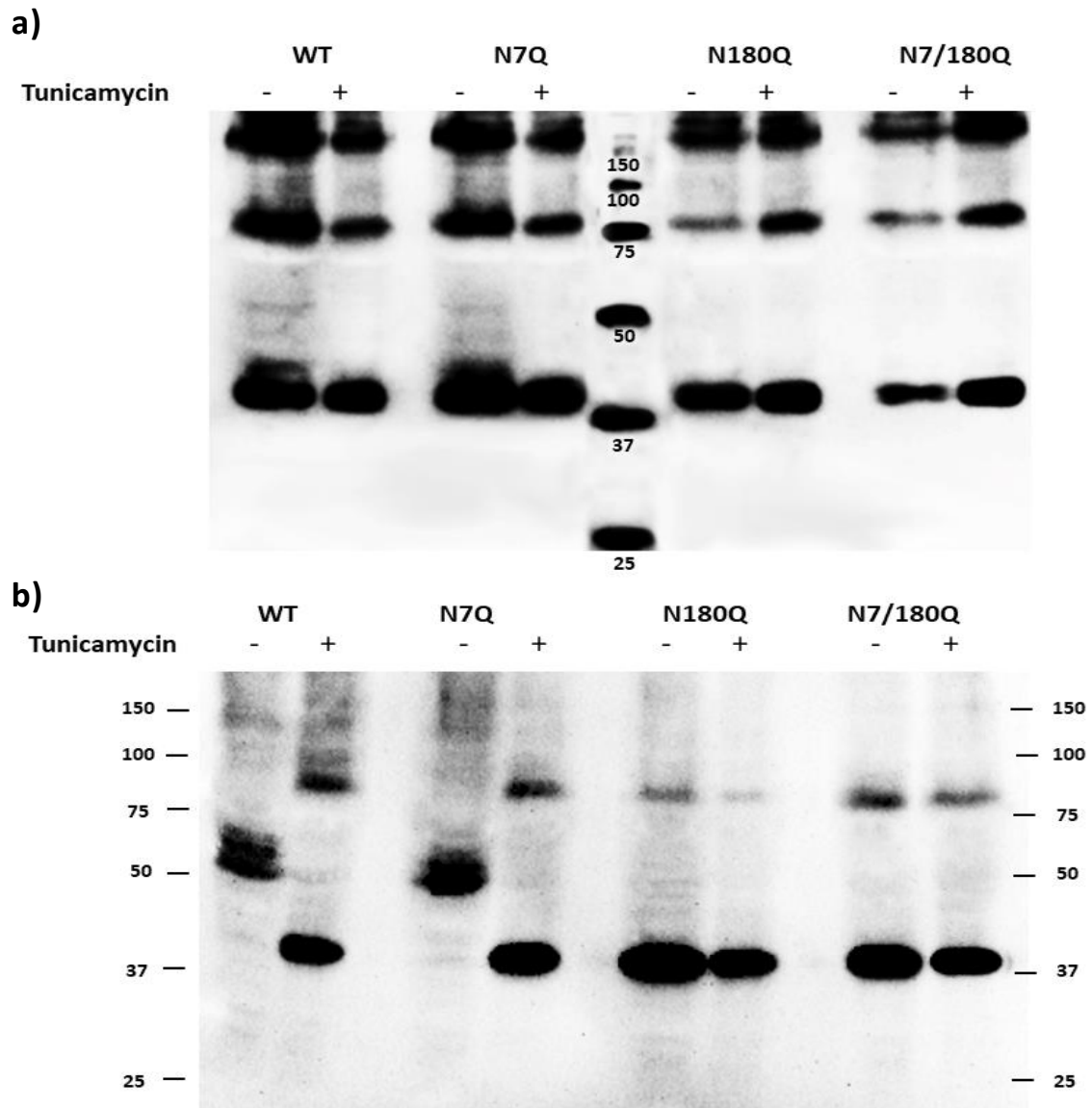
The plasmid constructs generated and verified in the previous section were first transiently transfected into HEK293 cells using Lipofectamine 3000 as described in the Method. Four hours post-transfection, the transfection mixture was removed, and the cells were incubated in complete medium with and without 1 µg/ml of tunicamycin for 48 hr. Next, the cells were harvested, and the whole cell lysates were immunoblotted against Flag antibody.

The blot demonstrated predominant receptor bands (unglycosylated species) at approximately 41 kDa, and less predominant bands at approximately 43-44 kDa (glycosylated species) in the wild type and the N7Q mutated receptors. Other faint bands appeared at approximately 50 kDa. This indicated that the disruption of the N7 residue did not influence the glycosylation pattern of the transiently expressed 5-HT<sub>4</sub> receptor since the immunoreactive bands in the N7Q mutant were similar to those of the wild type. Tunicamycin, however, deglycosylated the high size receptor species in both wild type and N7Q mutant. In contrast, disruption of the N180 residue did not show any higher bands above the deglycosylated one. This was also the case for the double mutant receptor. Thus, the addition of tunicamycin to the growth medium did not change the band migration of N180Q mutant and double mutant receptors (**Figure 36a**).

Owing to the difference in the receptor size between the transient and the stable expressions, the Flag-5-HT<sub>4</sub> receptor wild and mutant constructs were transfected individually in HEK293 cells to generate stable cell lines with hygromycin selection. From each transfection, 24-30 clones were grown in multi-well plates, and only Flag

positive clones were retained for further experiments. Four stable clones from each transfection were grown with and without tunicamycin as previously described. Next, the cells were lysed for Western blot analysis. As indicated in **Figure 36b**, the high size glycosylated bands were observed between approximately 49 and 56 kDa were in the wild type and N7Q mutant 5-HT<sub>4</sub> receptors. The size of these bands was reduced to approximately 41 kDa with tunicamycin treatment. The N180Q and N7/180Q mutants appeared as unglycosylated bands as they were treated with tunicamycin. Therefore, these findings support the online prediction for N180, but not for N7, as a site of glycosylation.



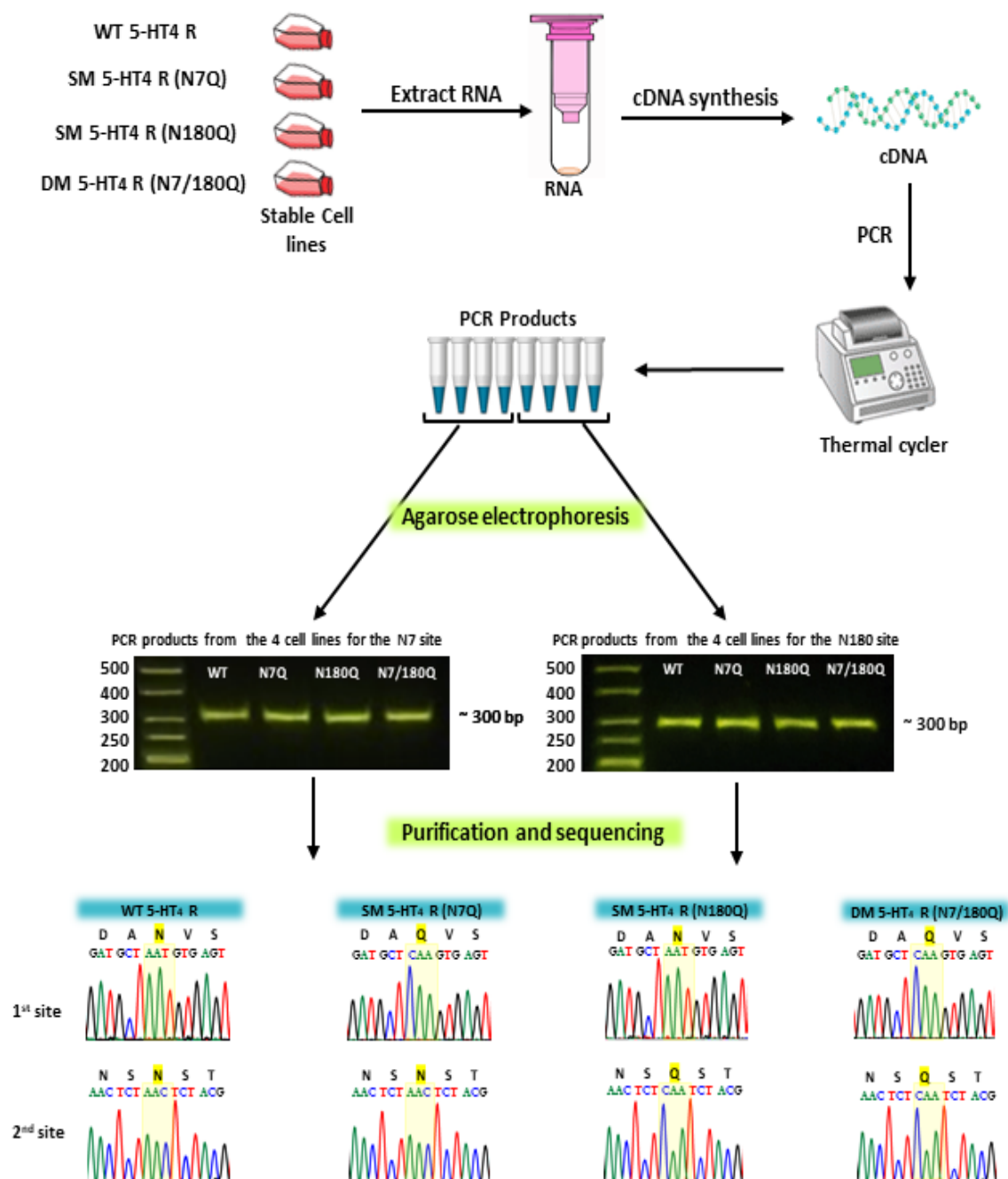


**Figure 36. The differences in 5-HT<sub>4</sub> receptor migration due to N-glycosylation**

*HEK293 cells with either **a)** transient or **b)** stable expression of wild type and mutant Flag-5-HT<sub>4</sub> receptors, with and without tunicamycin treatment, were immunoblotted using Flag antibody. In the transient expression, the glycosylated bands of wild type and N7Q mutant appear predominantly at the lower size (~ 43-44 kDa) while in the stable expression, they appear predominantly at the higher size (~ 49-56 kDa). The N180Q and N7/180Q mutants exhibit similar sizes (~ 41 kDa) of the unglycosylated 5-HT<sub>4</sub> receptor. These are representative images of 4 independent experiments each has the same result.*

### **5.6. Stable integration of the 5-HT<sub>4</sub> receptor coding sequence in the cell genome**

To confirm the stable integration of the WT and mutant 5-HT<sub>4</sub> receptor coding sequence without any change in their nucleotide sequence, total RNA of the stable cell line was individually isolated, and cDNA was synthesised as described in the **Method**. Primers were designed to flank the N7 and N180 residues and the PCR was performed. A small part of the PCR products (10 µl) was loaded in agarose gel to ensure the presence of fragments at the correct sizes which were appeared around 300 bp (The predicted sizes are 287 bp and 288 bp for the N7 and N180 spanning fragments, respectively). The remaining PCR products were purified and sequenced. The chromatogram of the DNA traces confirmed the stable integration of the exogenous DNA in the cell genome with preservation of the mutated and the non-mutated sites as they present in the transfected plasmids as shown in **Figure 37**.



**Figure 37. Confirmation of the stable integration of the CDS of the wild-type and mutant 5-HT<sub>4</sub> receptor in cells chromosome**

*Following RNA extraction and reverse transcription, two pairs of primers flanking the mutation sites were used to amplify the DNA. The actual sizes of PCR products were 287 bp for the N7 site and 288 bp for the N180 site (observed close to 300 bp). Sequencing of the PCR products showed the presence of the mutations at the desired site only. WT: Wild type, SM: Single mutant and DM: Double mutant.*

### **5.7. The role of *N*-linked glycosylation on 5-HT<sub>4</sub> receptor trafficking and cell surface expression**

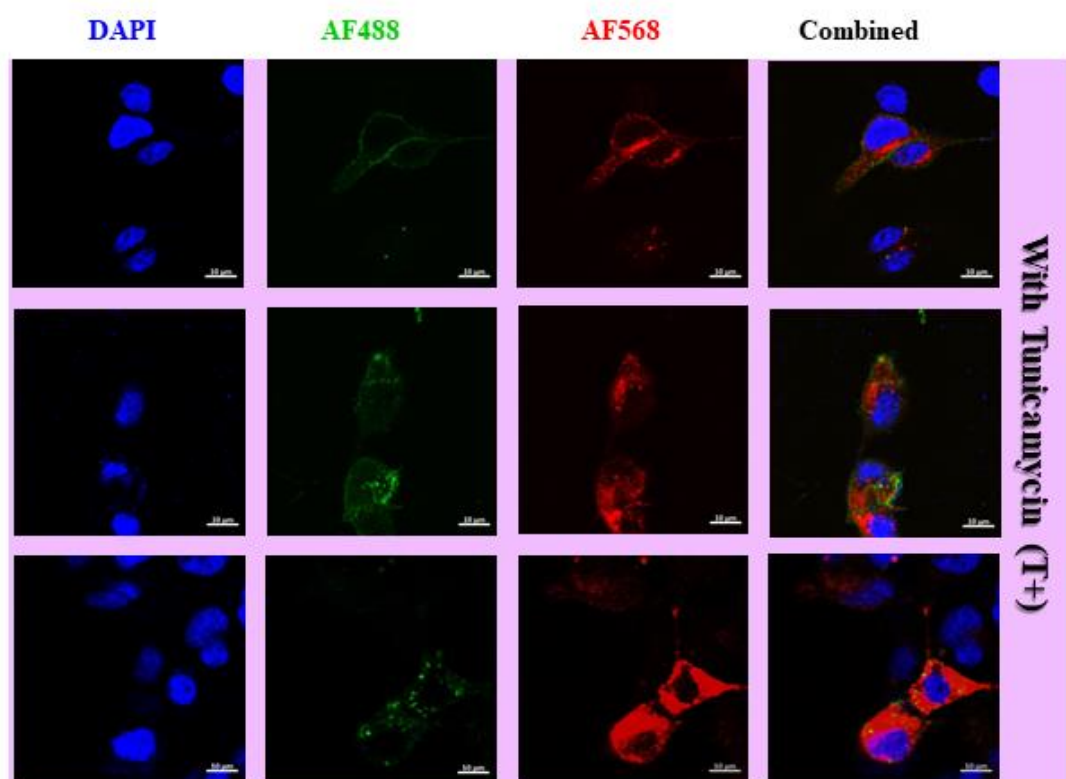
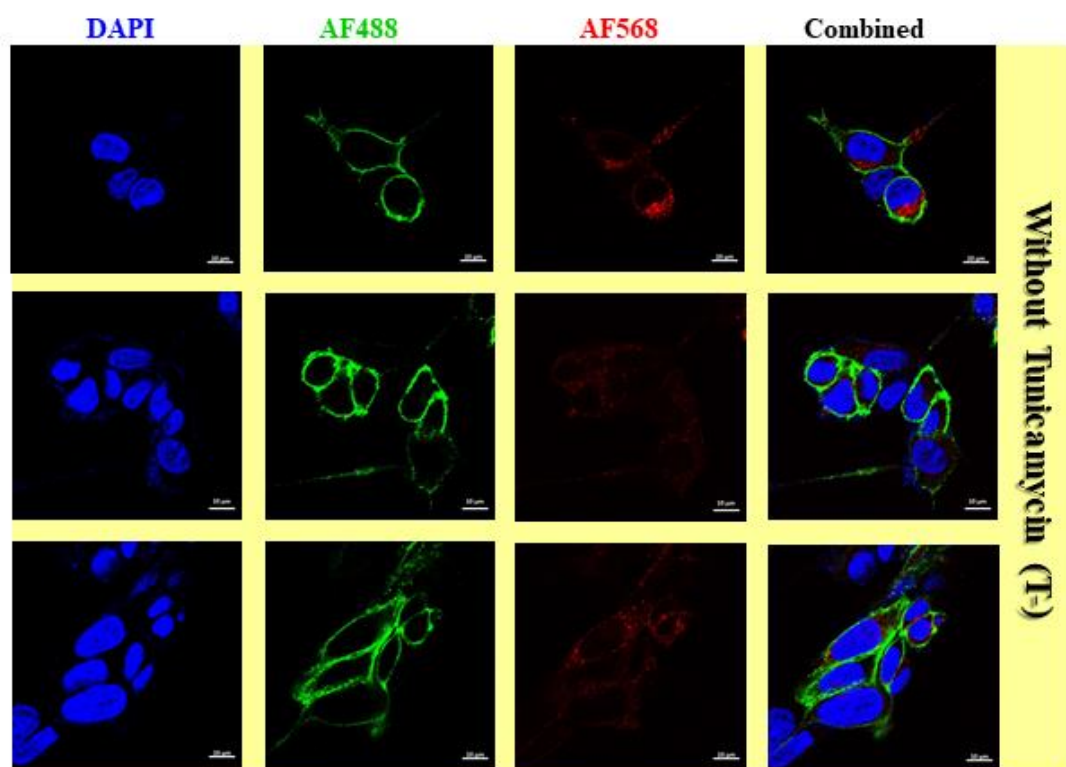
Cells with stable expression of wild type or mutant 5-HT<sub>4</sub> receptors were used to determine the role of *N*-glycosylation in protein trafficking. Two staining techniques were subsequently performed to discriminate between the cell membrane and the intracellular localisations of the receptors. The first staining was conducted without permeabilisation. Rabbit anti-Flag primary antibody was used to probe the Flag epitope located on the extracellular N-terminus of the receptor. This was followed by incubation with goat anti-rabbit secondary antibody (AF 488, green) to label the receptor localised in the cell surface. The second staining, however, required permeabilisation of the cell to label the intracellular receptor with mouse anti-Flag primary antibody followed by goat anti-mouse secondary antibody (AF 568, red).

Confocal images revealed that the wild type Flag-5-HT<sub>4</sub> receptor was mostly localised in the plasma membrane with strong green fluorescence. Some cytoplasmic red fluorescence was also detected. Tunicamycin reduced the plasma membrane protein expression as indicated by the reduction of the green fluorescence (**Figure 38a**). Cells expressing the N7Q mutant receptors displayed a similar pattern of protein localisation to the wild type with no reduction in protein expression in the cell membrane. Thus, the N7 residue was not glycosylated when the 5-HT<sub>4</sub> receptor was heterologously expressed in HEK293 cells (**Figure 38b**).

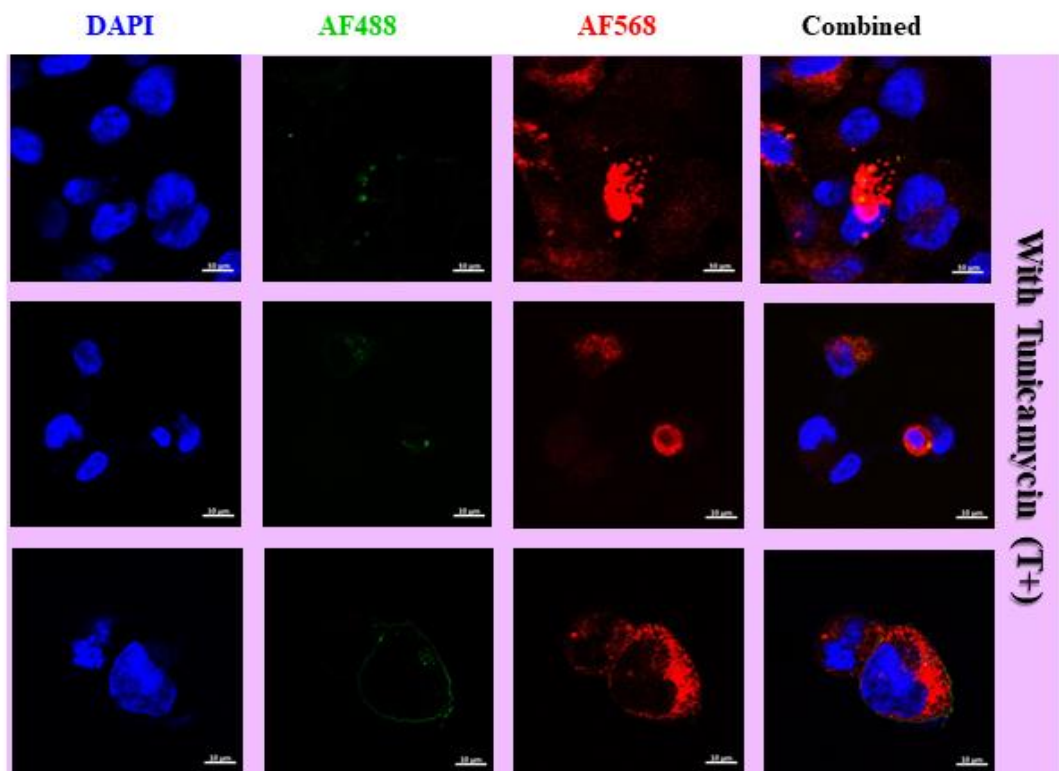
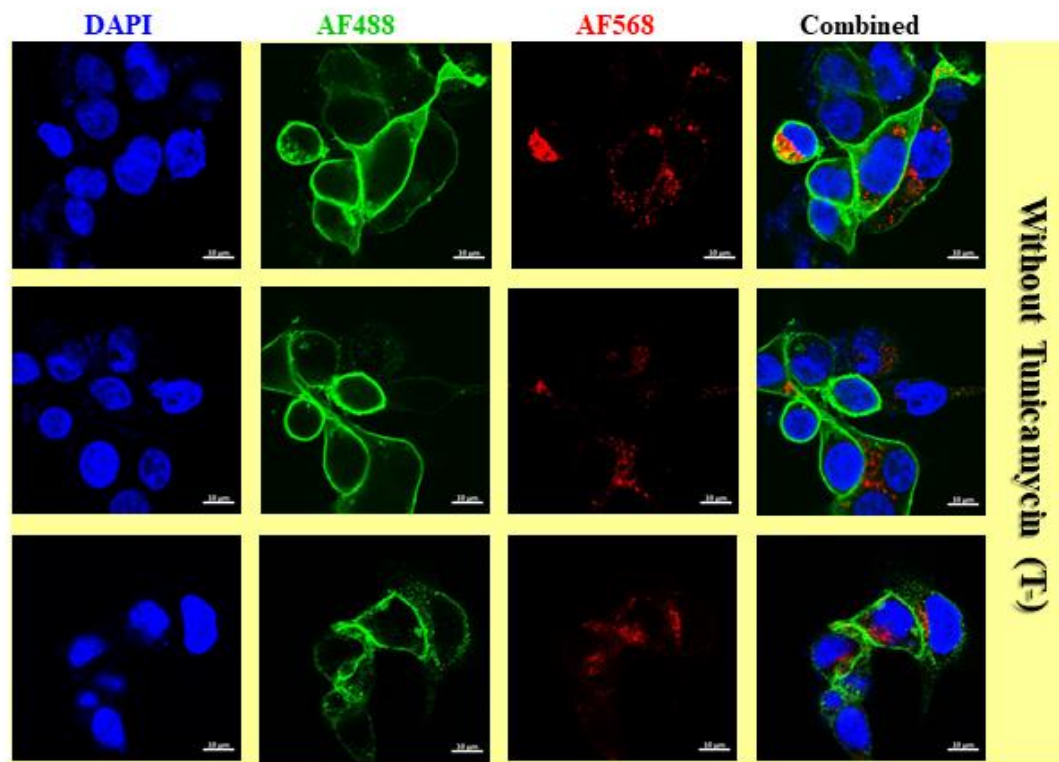
Unlike the N7Q mutant, the N180 mutant and the double mutant cell lines displayed a low level of green fluorescence on the cell surface. Most of the immunoreactivity was detected inside the cells as indicated by the red fluorescence. Thus, mutation of N180 of the 5-HT<sub>4</sub> receptor had a detrimental effect on receptor trafficking to the

cell membrane. The presence of tunicamycin did not change the cell surface expression of N180Q and N7/180Q receptors as they already had low cell surface expression (**Figure 38c and d**). Untransfected HEK293 cells were stained to ensure that the antibodies used were target specific. This was confirmed by the absence of fluorescence signals in them (**Figure 38e**).

a) Wild type Flag-5-HT<sub>4</sub>receptor

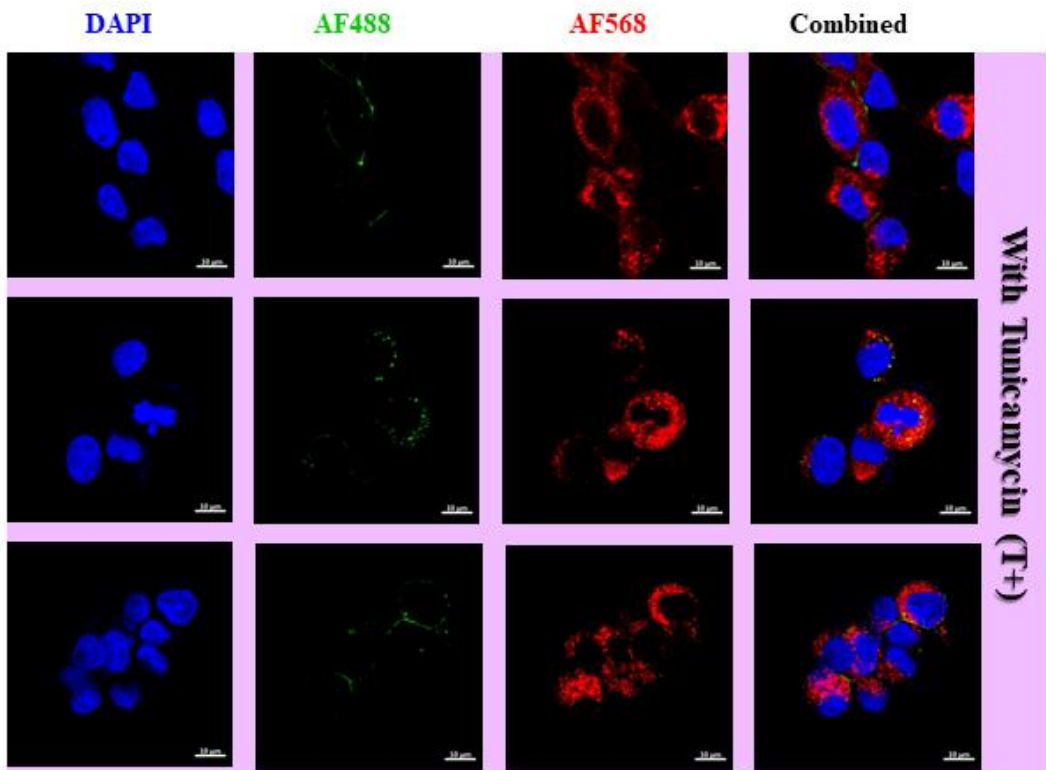
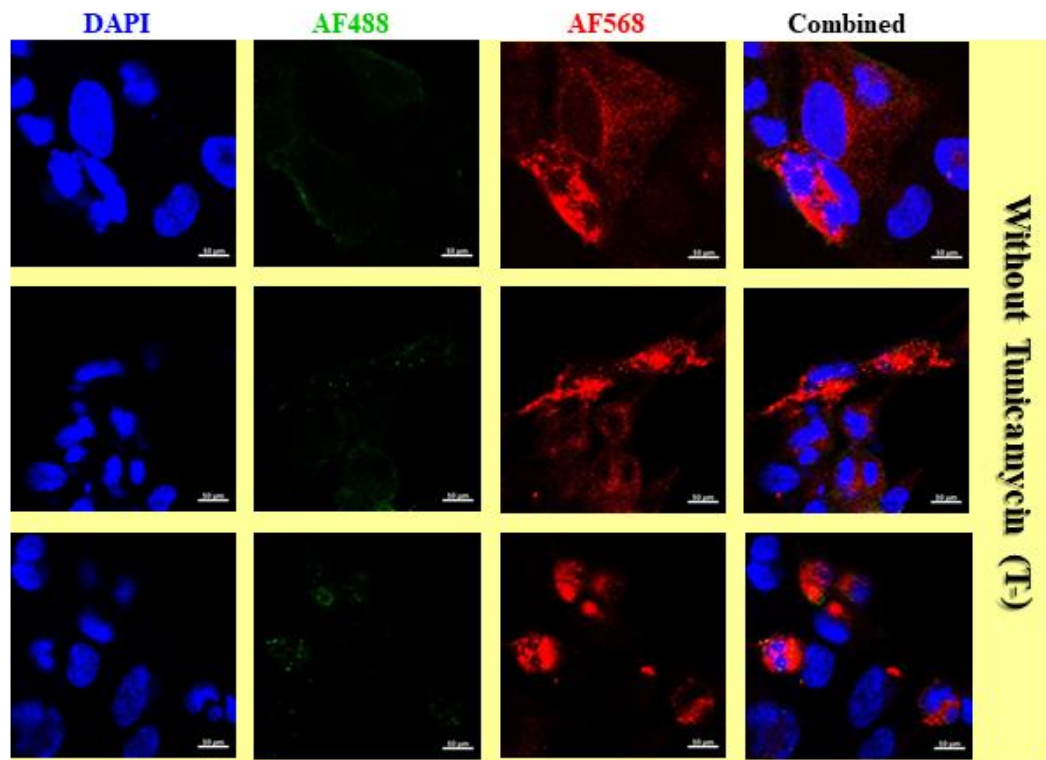


## b) Mutant N7Q Flag-5-HT<sub>4</sub>receptor



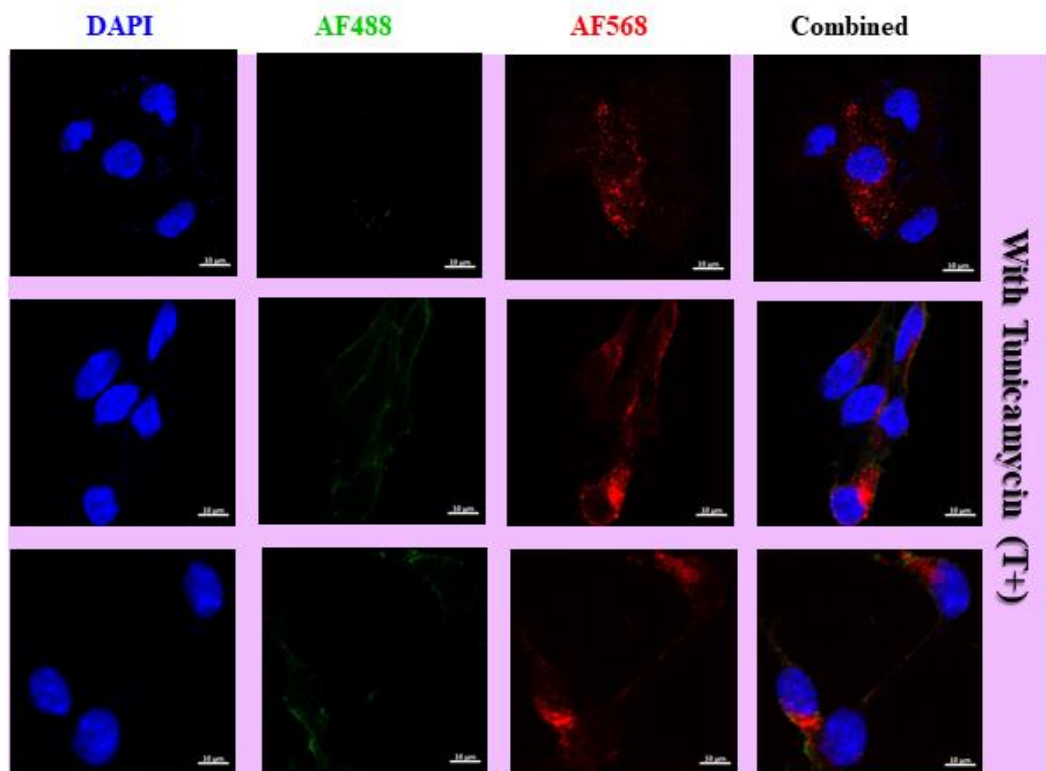
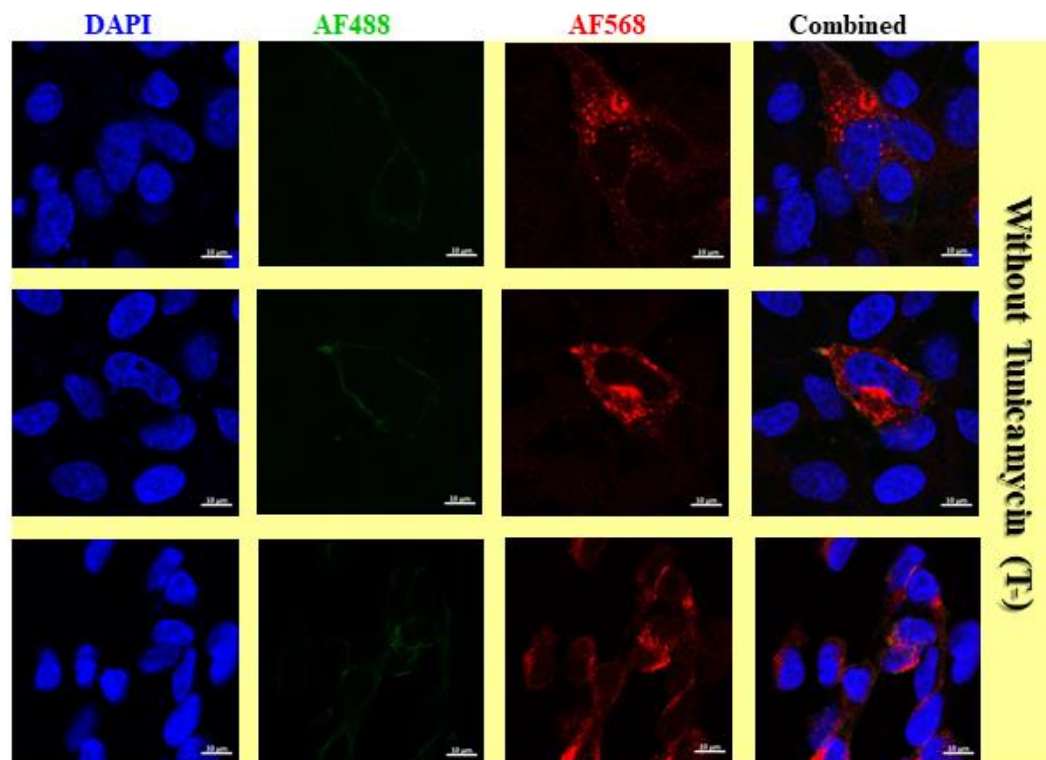


c) Mutant N180Q Flag-5-HT<sub>4</sub> receptor

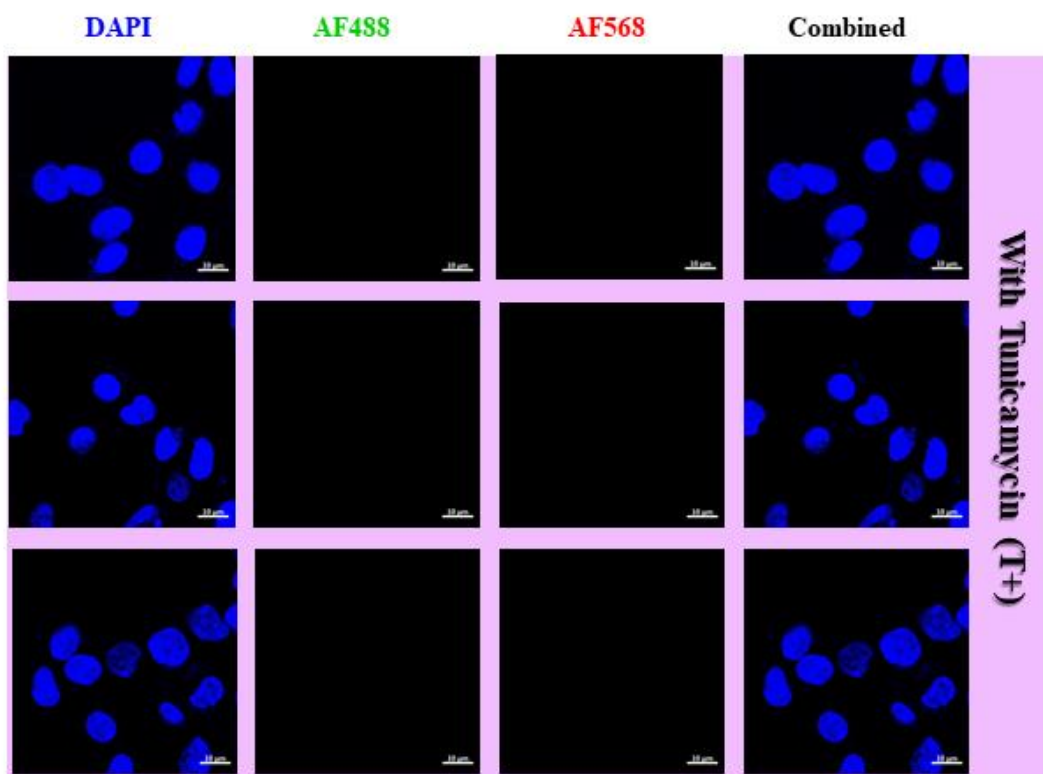
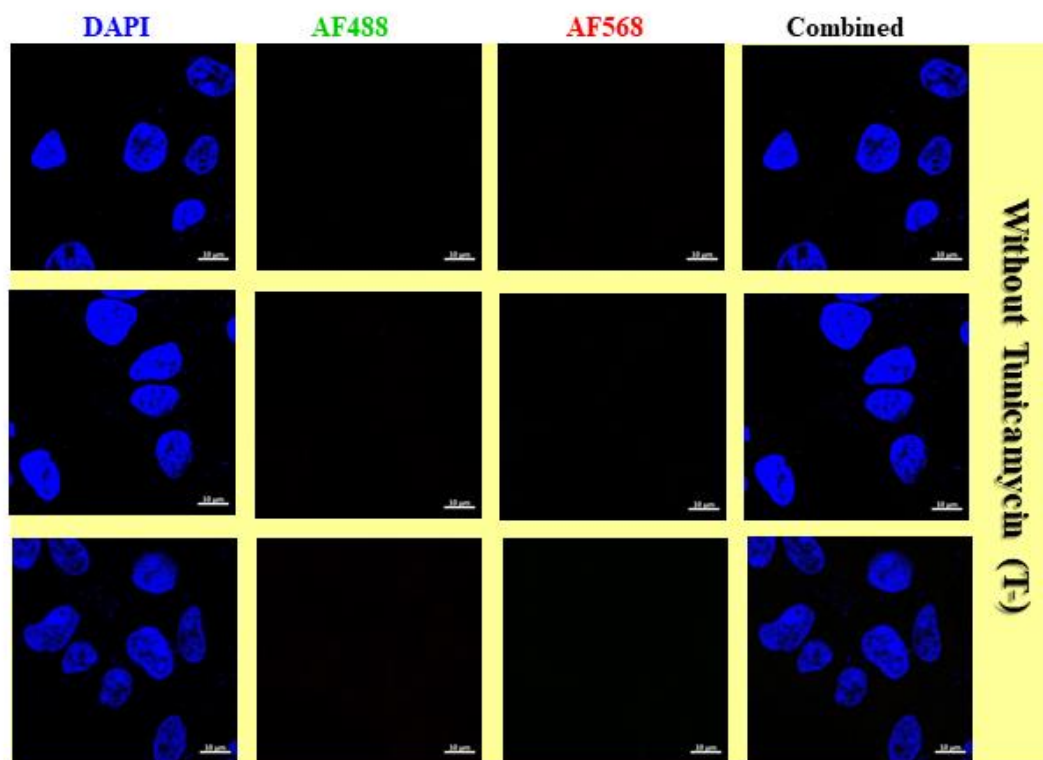




**d) Mutant N7/180Q Flag-5-HT<sub>4</sub> receptor**



e) Untransfected HEK293 cells



**Figure 38. The impact of N-glycosylation on Flag-5-HT<sub>4</sub> receptor localisation**

*Stable expression of wild type and mutants of the Flag-5-HT<sub>4</sub> receptors in HEK293 cells revealed an immunoreactive signal which was colour coded to discriminate between cell surface and intracellular localisation. Green fluorescence indicates the transmembrane receptor and red fluorescence indicates the intracellular receptor. Without tunicamycin, wild-type and N7Q mutant receptors are localised mainly in the cell surface. However, tunicamycin reduces the receptor expression in the cell membrane, thereby reducing the intensity of green fluorescence. The cell surface immunoreactivities of the N180Q and N7/180Q mutant receptors are markedly reduced in comparison to the wild-type receptor but they were still detected inside the cells. Untransfected HEK293 cells were subjected to a similar staining procedure, and no signal was detected in these cells. Nuclei were counterstained, thus appearing blue. These are representative images of at least 3 independent experiments. Scale bar 10 µm.*

## **5.8. Summary**

This chapter illustrated some novel findings on the *N*-linked glycosylation of the 5-HT<sub>4</sub> receptor heterologously expressed in HEK293 cells. The 5-HT<sub>4</sub> receptor was glycosylated at N180, but not the N7, and had a significance for the receptor trafficking to the final destination. During the protein synthesis, any mutations or changes in glycosylation which detected in AD-related proteins could lead to protein aggregation, misfolded proteins and potentially affecting the neuronal stability and viability.

The following chapter will assess the changes in the expression of 5-HT<sub>4</sub> and 5-HT<sub>6</sub> receptors during AD progression and provide a link between the cognitive functions and risk factors and the expression of serotonin proteins.

**Chapter 6. Investigating the expression of  
5-HT<sub>4</sub> and 5-HT<sub>6</sub> receptors and SERT in  
mild and advanced stages of AD relative to  
healthy age-matched controls**

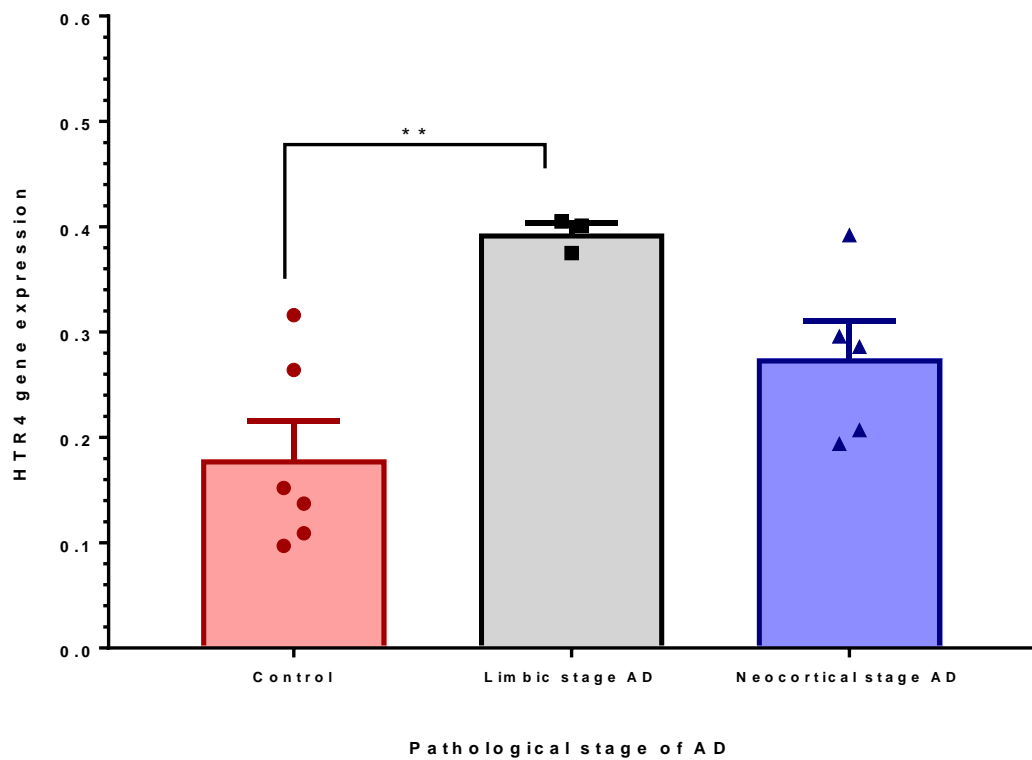
## **6. Assessment of the 5-HT<sub>4</sub> and 5-HT<sub>6</sub> receptors and SERT expression in mild and advanced stages of AD relative to healthy age-matched controls.**

### **6.1. Receptors quantitative gene expression assay**

#### **6.1.1. 5-HT<sub>4</sub> receptor**

Studying the gene expression of 5-HT<sub>4</sub> receptors in AD patients was measured using quantitative PCR. For normalisation, *EIF4A2* was selected to be the reference gene because its expression was stable in the post-mortem brains of AD patients relative to  $\beta$ -actin and other housekeeping genes which are commonly employed (Penna et al., 2011). Standard curves of at least 5 log scales were generated for each gene using transfected HEK293 cells (see **Supplementary figure 6**). The Ct values for the cases and controls were then used to interpolate the DNA amount from the curve for each gene.

Interestingly, by following the pattern of *HTR4* gene expression during AD progression, **Figure 39** showed a significant up-regulation in the early stage of AD (limbic) in comparison with the age-matched controls ( $P=0.0063$ ). However, this significant increase was lost when comparing the advanced stage of the disease (neocortical) with the controls ( $P=0.1482$ ). In addition, the difference in gene expression between the early and late stages of AD was also non-significant ( $P=0.1359$ ).



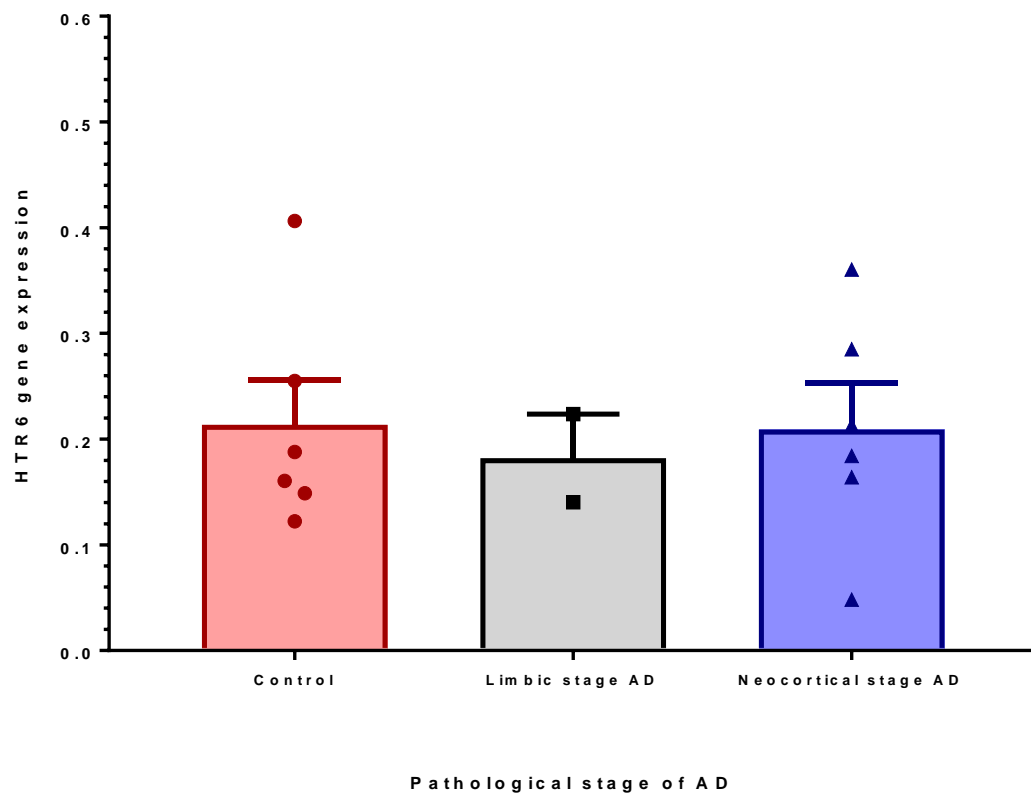
**Figure 39. 5-HT<sub>4</sub> receptor gene expression in control, and limbic and neocortical stages of AD**

*The vertical axis represents the HTR4 gene expression normalised with EIF4A2 (housekeeping gene). The statistical comparison was performed using the one-way ANOVA test, followed by Tukey's multiple comparisons test (\*\*  $P < 0.01$ ).*

### 6.1.2. 5-HT<sub>6</sub> receptor

The 5-HT<sub>6</sub> receptor gene expression was assessed in the AD patients and compared with age-matched controls. The results show that there was no difference between the disease and control groups (**Figure 40**). In the limbic stage of AD, only two of the six DNA samples showed amplification within the linear range of the standard curves. Furthermore, and due to the low gene expression in those samples (a Ct value of 39 or above), which was beyond the highest Ct values of 37 or 38 obtained from the lowest amount of the DNA standard (not within the linear range), a wider-standard curve DNA of 50 ng to  $5 \times 10^{-5}$  ng was used to encompass these values. However, the standard curve showed less accurate values (DNA amount), particularly at the last two dilution points,  $5 \times 10^{-4}$  ng and  $5 \times 10^{-5}$  ng, after comparing the actual and the obtained DNA amounts, which were back-calculated from the trendline equation. Since the gene expression could be drastically affected by PMD, the assessment of protein level might be useful. FFPE sections were used to provide more conclusive results by assessing the receptor expression in the protein level, which is more stable than the DNA.



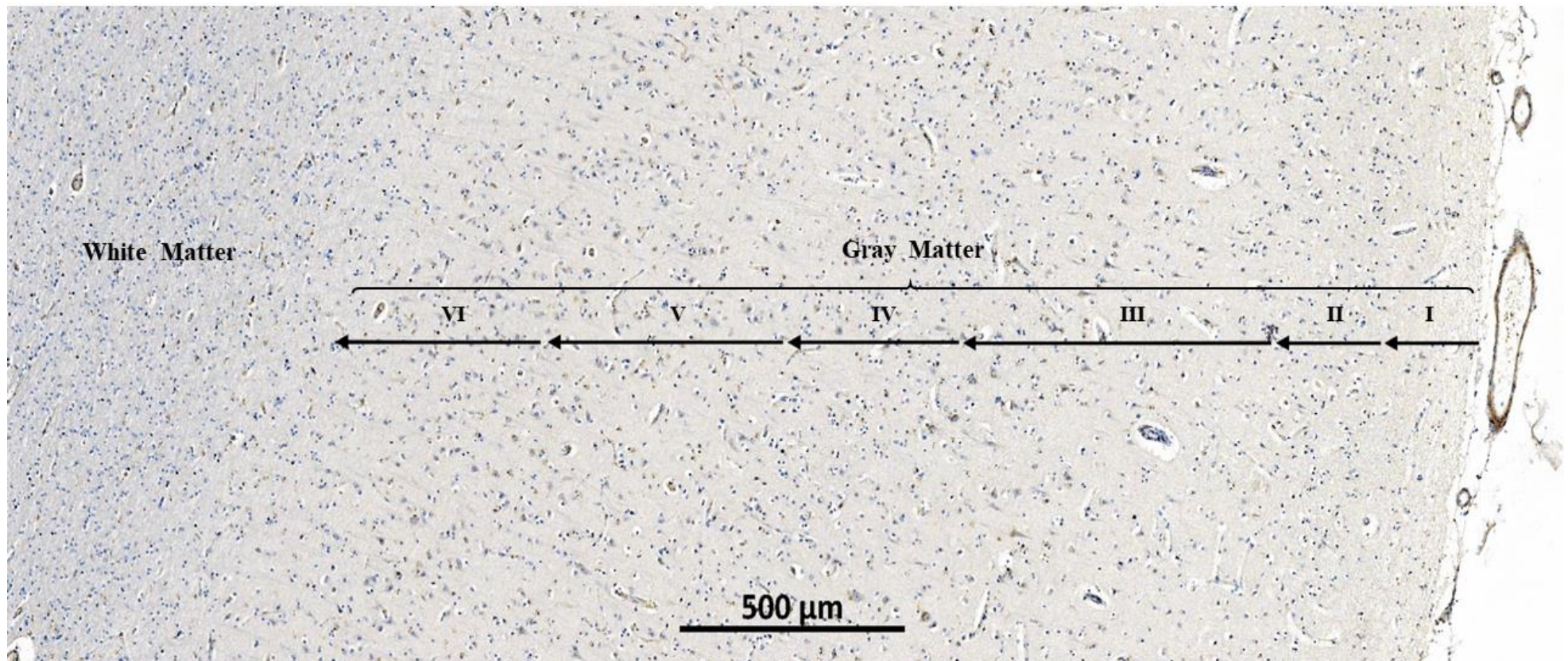


**Figure 40. 5-HT<sub>6</sub> receptor gene expression in control, and limbic and neocortical stages of AD**

*The vertical axis represents HTR6 gene expression normalised with EIF4A2 (housekeeping gene).*

## **6.2. Area selection for IHC quantification**

The outer pyramidal layer III of the prefrontal cortex (BA09) was chosen as a region of interest for three reasons: first, serotonergic 5-HT<sub>4</sub> and 5-HT<sub>6</sub> receptors are expressed in pyramidal neurones, which are abundant in this layer (King et al., 2008); second, this layer is highly affected by the pathological lesions of Alzheimer's disease (Braak and Braak, 1991); and third, it is thicker than the inner pyramidal layer (layer V), which usually has less dense scattered large pyramidal neurones (Rockland, 2017) as shown in **Figure 41**, and thus a larger area was used for IHC quantification. The two adjacent layers (II and IV) have a granular appearance and are packed with dense and small neuronal cells, thus helping in layer III discrimination. Images of 3 or 6 areas of layer III from each section were quantified for positive DAB staining, followed by calculation of the mean. The scanned surface area was, in all slides, very similar: 240,000  $\mu\text{m}^2$ , 600  $\mu\text{m}$  wide and 400  $\mu\text{m}$  high. Differences in the nuclei count between the sections were considered, as they were used to normalise the total DAB signal in all the sections.

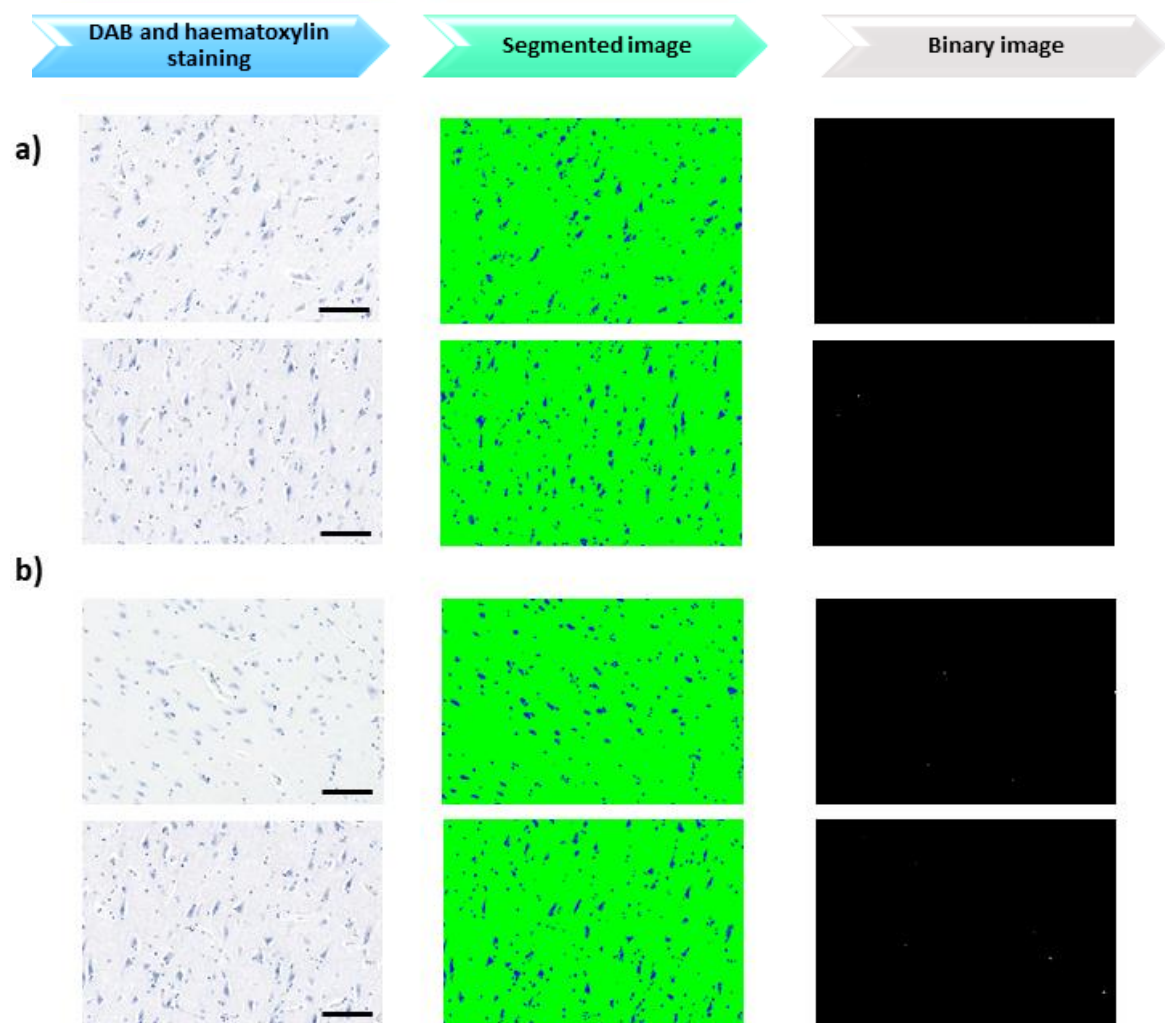


**Figure 41. Neocortical layers of human brain stained with DAB and haematoxylin**

*Human neocortex consists of six layers from the outer pial surface to the inner white matter and are labelled layers I to VI. These layers differ in their cellular composition, density, and layer thickness throughout the gyri and sulci of the brain. Brodmann area 9 was used to assess the expression of 5-HT<sub>4</sub> and 5-HT<sub>6</sub> receptors and SERT, particularly in cortical layer III. Scale bar 500 μm.*

### **6.3. Evaluation of the specificity of the 5-HT<sub>4</sub> and 5-HT<sub>6</sub> receptors antibodies by isotype control**

To obtain reliable results from the IHC study of 5-HT receptor expression and localisation, tissue was stained with isotype control rabbit IgG. The antibodies of both receptors have the same isotype class. Isotype control ensures that the detected immunoreactive signal is due to the primary antibody binding the target antigen and not due to non-specific binding of the antibody IgG to the tissue which can cause background staining. Isotype control staining was conducted in parallel with the experimental sample staining with the primary antibodies for the target receptors, the resulting immunoreactive signals were then compared against each other. No background staining was detected in isotype control sections and thus confirmed the specificity of the primary antibody used (**Figure 42**).



**Figure 42. Example of isotype control staining and colour segmentation**

*Two representative images of isotype control staining of human prefrontal cortex show no brown DAB signal when the DAB was incubated for **a)** 10 min in parallel with 5-HT<sub>4</sub> primary antibody staining or for **b)** 4 min in parallel with 5-HT<sub>6</sub> primary antibody staining. The DAB, nuclei and background are segmented to red, blue and green channels, respectively. The binary image represents the red channel only. Scale bar 100  $\mu$ m.*

#### **6.4. Changes in the 5-HT<sub>4</sub> and 5-HT<sub>6</sub> receptor immunoreactivities with AD progression**

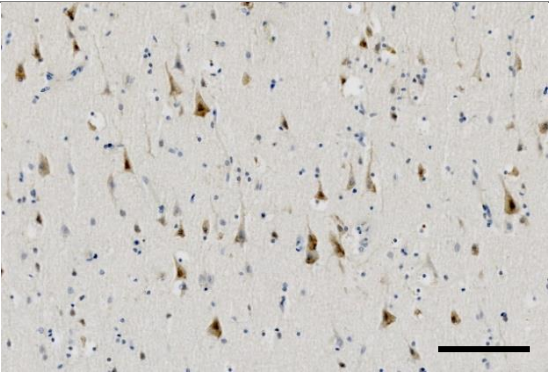
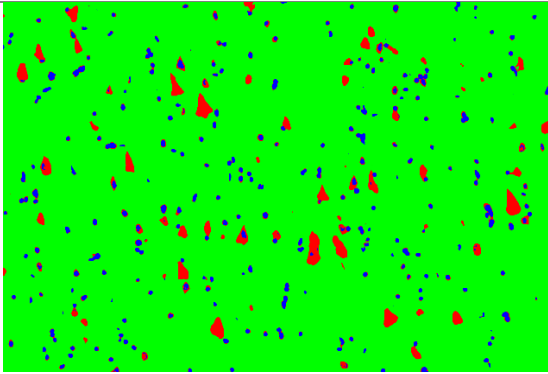
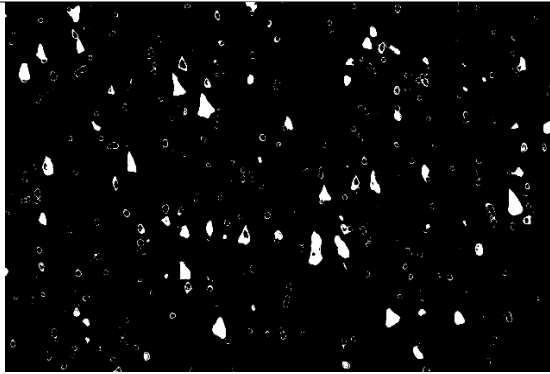
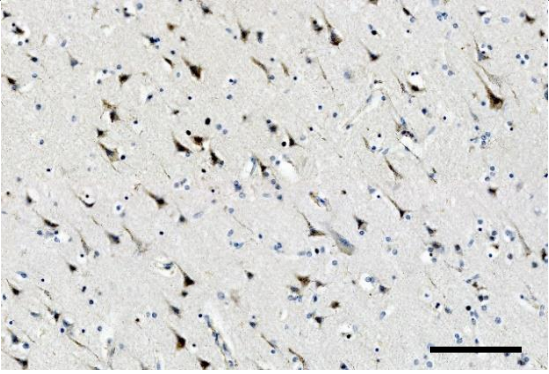
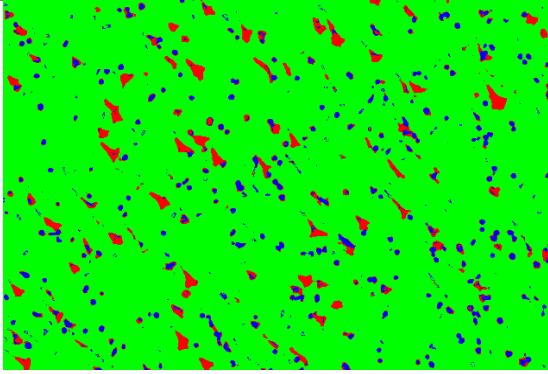
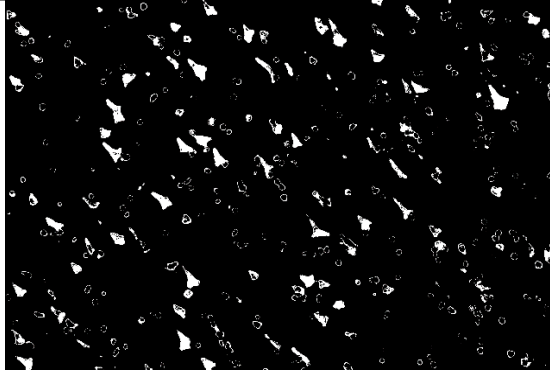
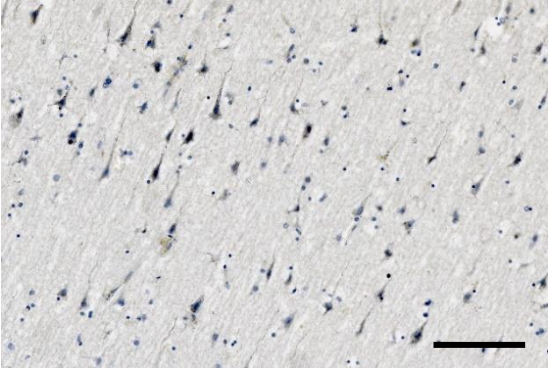
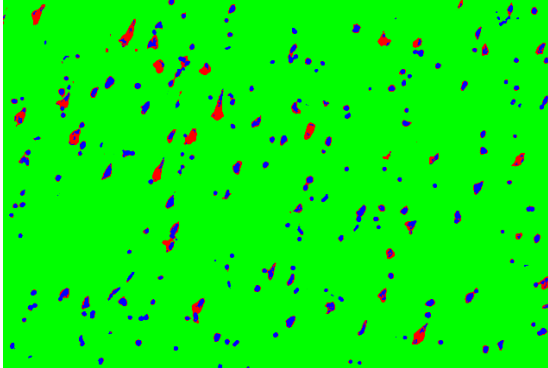

The staining protocol was optimised by assessing the immunoreactivity of the target receptors in the FFPE hippocampi of normal post-mortem controls. The hippocampus is extensively innervated by serotonergic neurones, and it expresses all 5-HT receptors that modulate neuronal functions (Berumen et al., 2012, Dale et al., 2016). To visualise the cellular structures and provide orientation with respect to specific staining, haematoxylin counter-staining was conducted. After selecting the best staining condition and dilution for each antibody, the staining was performed blindly on the disease and control brain sections.

##### **6.4.1. 5-HT<sub>4</sub> receptor**

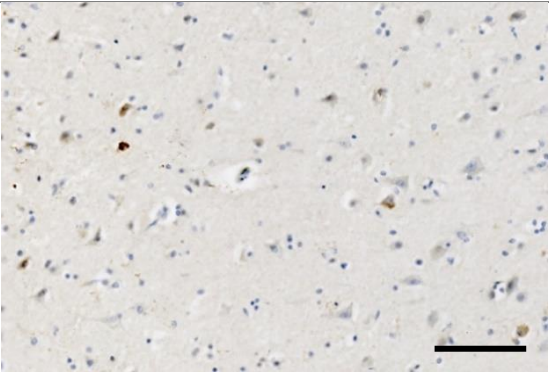
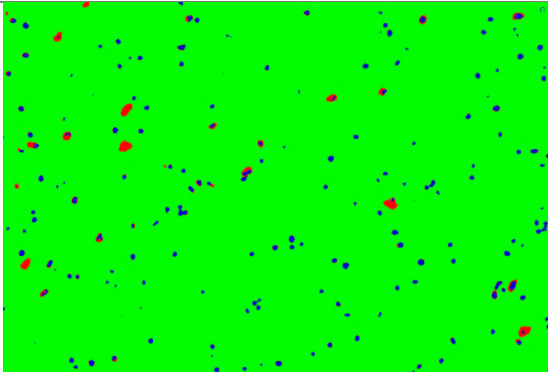
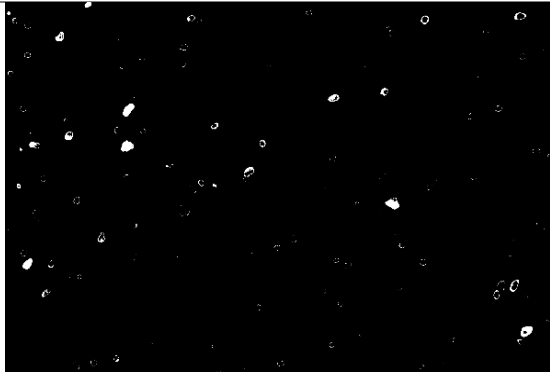
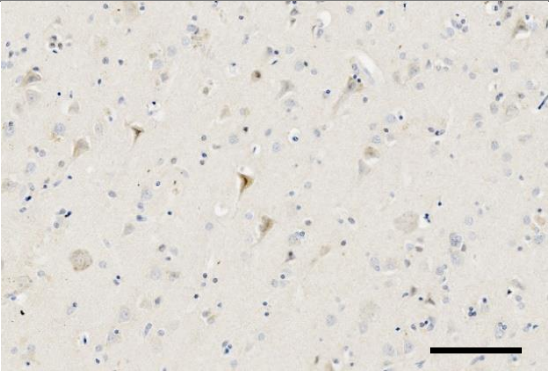
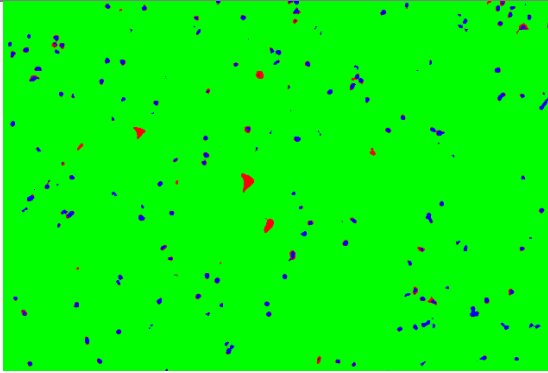
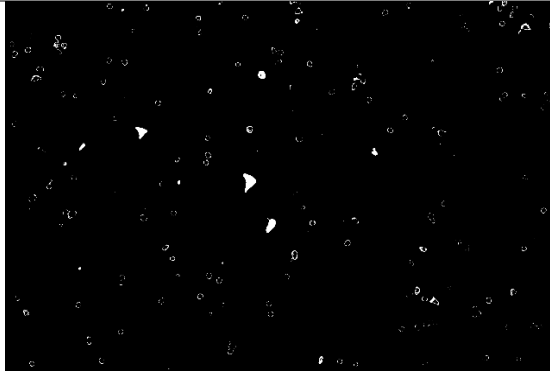
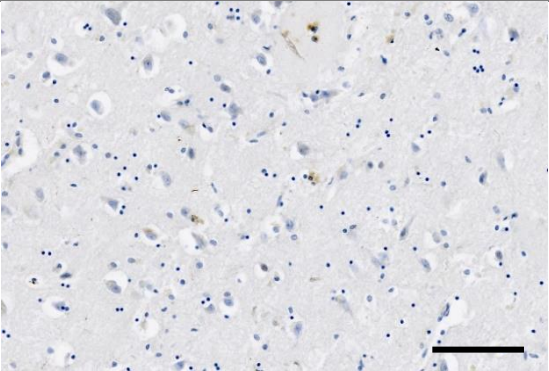
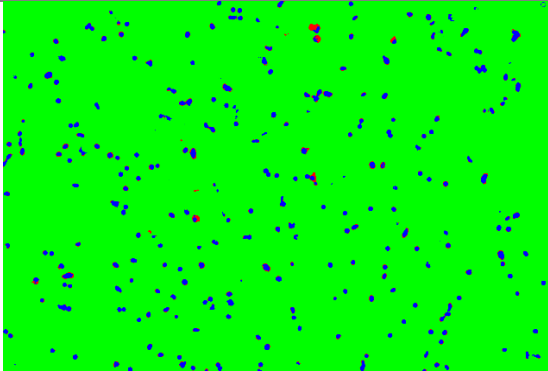
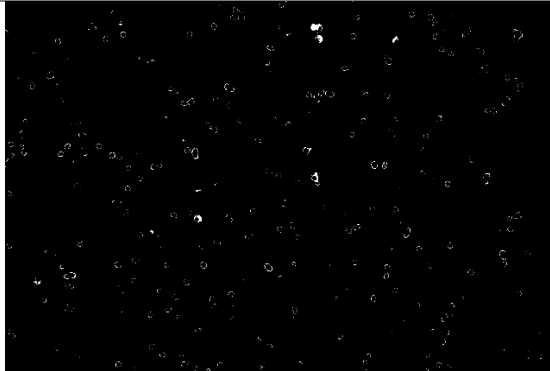
Immunoreactivity of 5-HT<sub>4</sub> receptors was assessed in early and advanced stages of AD and compared with age-matched controls. Apparent 5-HT<sub>4</sub> receptor immunoreactivity was predominantly detected in pyramidal neurones, particularly in the cell bodies, and sometimes in neuronal projected axons, as in **Figure 43** which showed representative images of some cases and the segmented images. The identification of pyramidal neurones is based on their distinctive cell morphology. As the disease progressed, 5-HT<sub>4</sub> receptor expression was down-regulated gradually in the early and late stages of the disease, as shown in **Figure 44**. Nevertheless, this reduction did not reach the significance level when the total area was quantified without considering the total number of nuclei ( $P > 0.05$ ). In **Figure 44b**, the nuclei count was used to normalise the total positive area. The pattern of receptor expression was relatively consistent, as in **Figure 44a**, but the difference between the control and the limbic stage of the disease was statistically significant

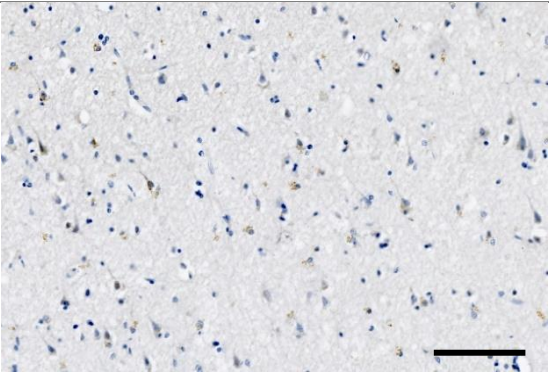
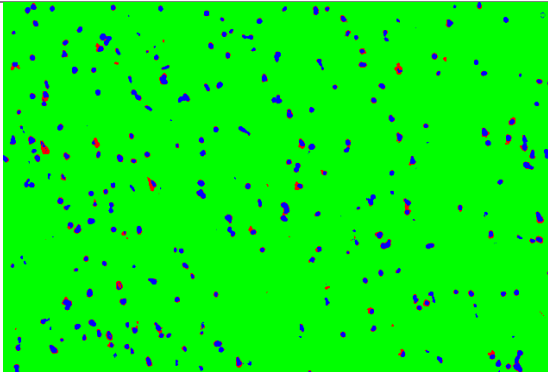
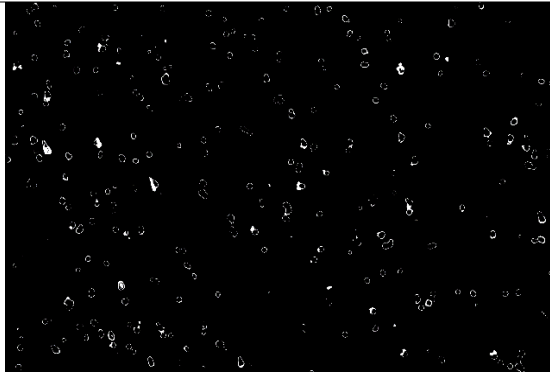
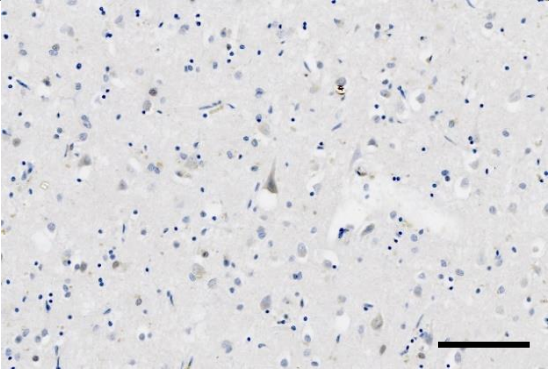
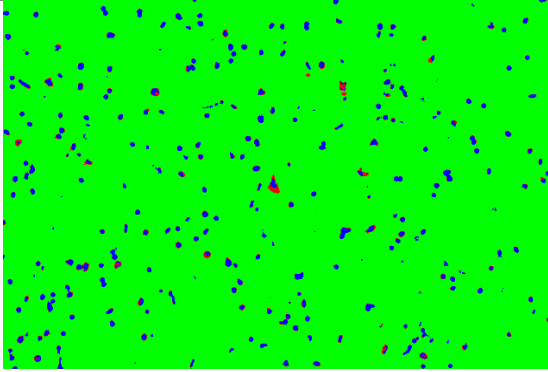

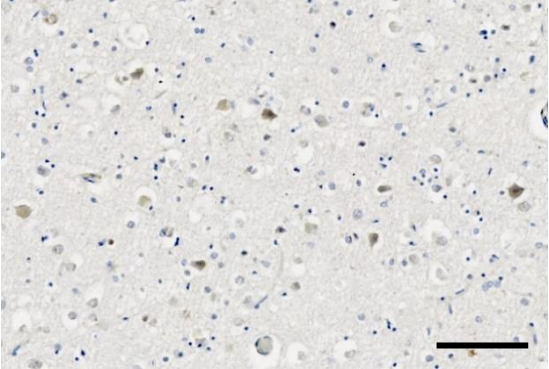
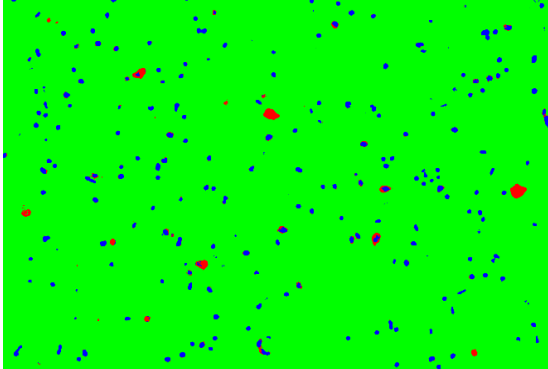
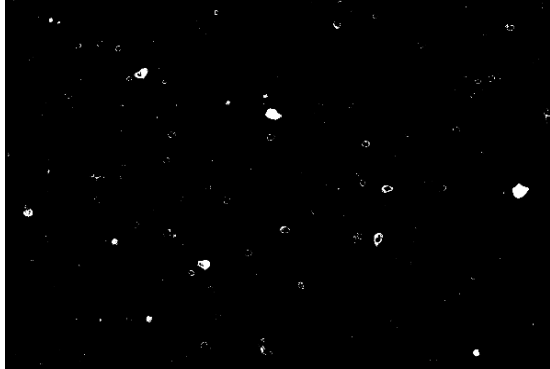
( $P=0.0316$ ). The neocortical stage showed a further reduction in 5-HT<sub>4</sub> receptor immunoreactivity relative to control ( $P=0.0034$ ). This was expected because the prefrontal cortex is less affected by pathological lesions in the early stage than in the late stage of the disease.

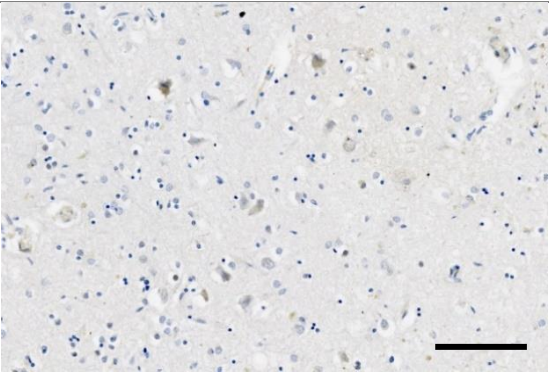
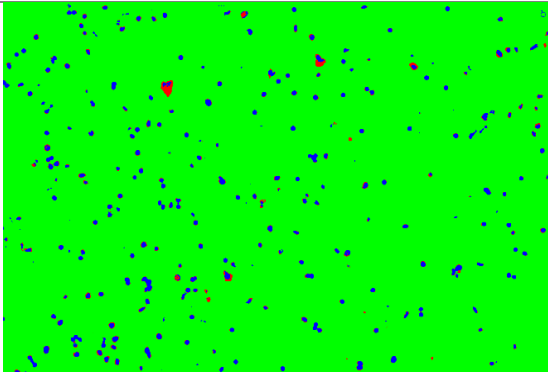
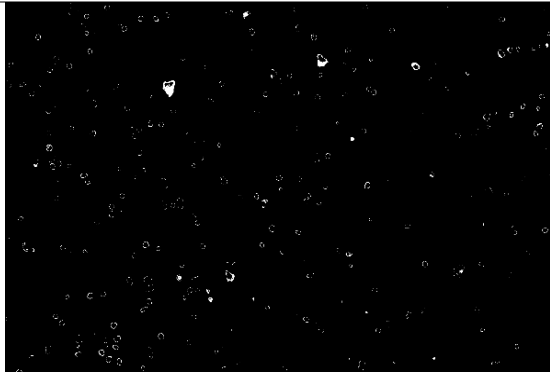
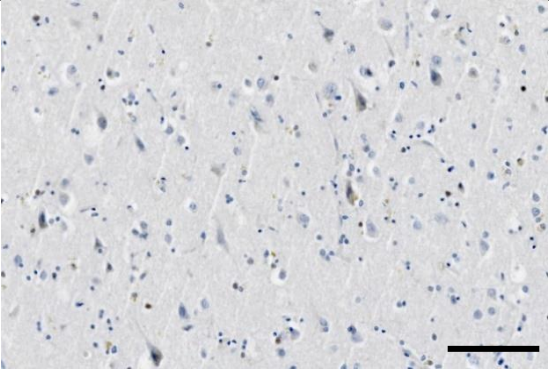
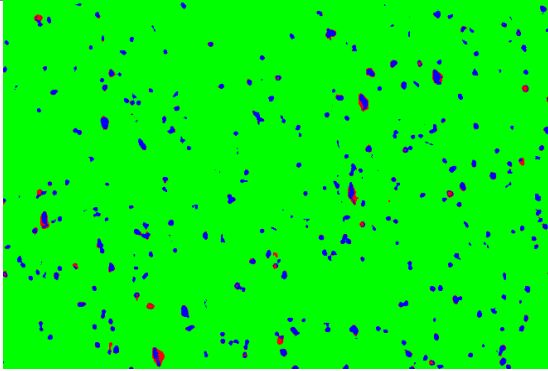



Case ID	Stage	DAB and haematoxylin staining	Segmented image	Binary image for DAB staining
RI95 1385	C			
RI03 0211	C			
RI02 0054	C			



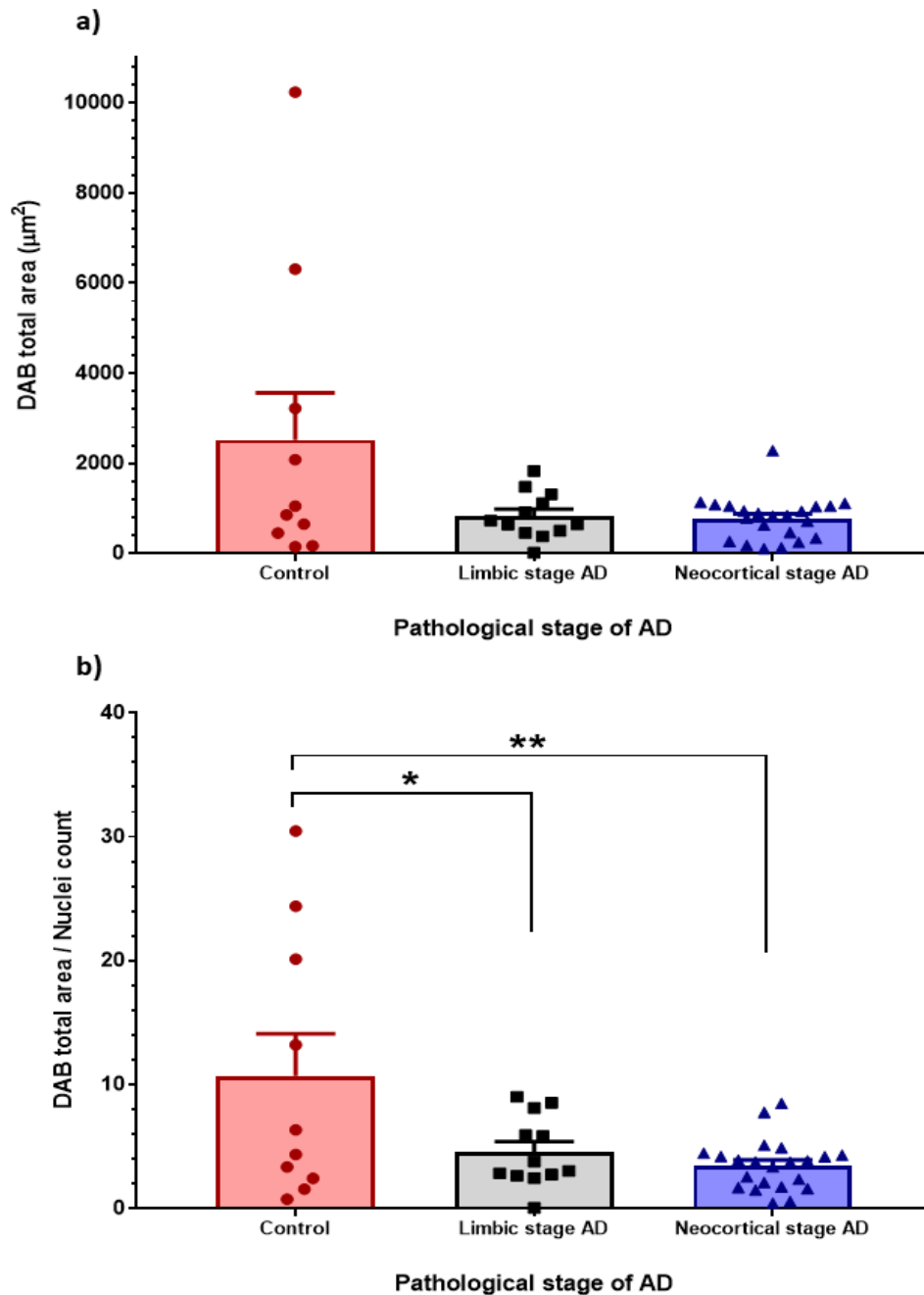
Case ID	Stage	DAB and haematoxylin staining	Segmented image	Binary image for DAB staining
RI96 1058	L			
RI99 1160	L			
RI95 1214	L			

Case ID	Stage	DAB and haematoxylin staining	Segmented image	Binary image for DAB staining
RI95 1334	L			
RI97 1001	N			
RI96 1018	N			

Case ID	Stage	DAB and haematoxylin staining	Segmented image	Binary image for DAB staining
RI95 1302	N			
RI02 0046	N			

**Figure 43. Illustration of signal decomposition from DAB and haematoxylin stained-images for 5-HT<sub>4</sub> receptors**

*The positive brown signals indicate the expression of serotonin receptors (red channel). The nuclei and background are segmented to blue and green channels, respectively. The binary image represents the red channel only. C: control, L: limbic stage, N: neocortical stage. Scale bar 100  $\mu$ m.*



**Figure 44. Differences in 5-HT<sub>4</sub> receptor expression in the control, and limbic and neocortical stages of AD**

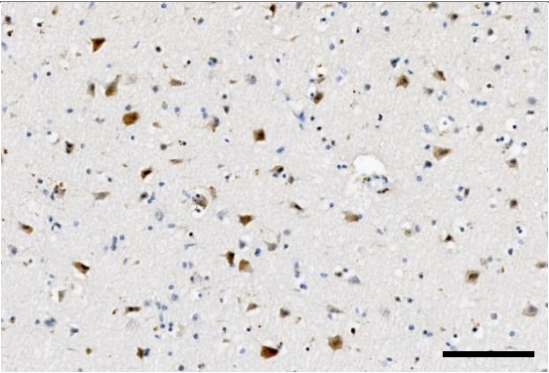
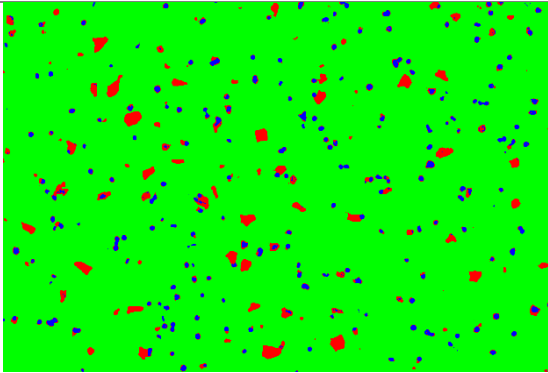
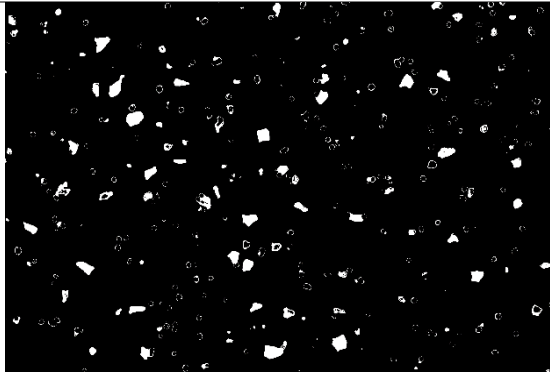
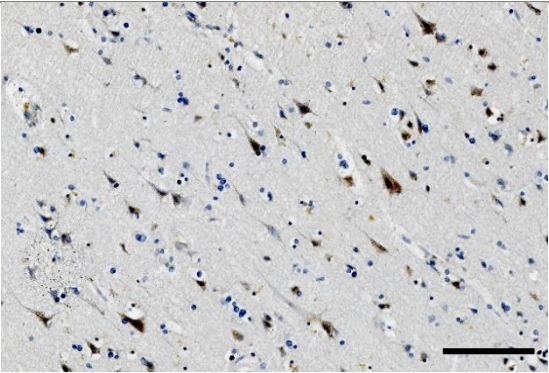
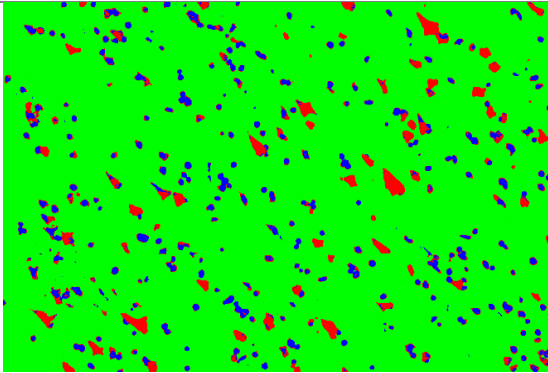
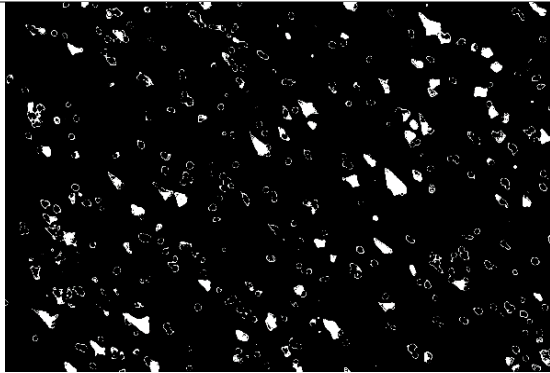
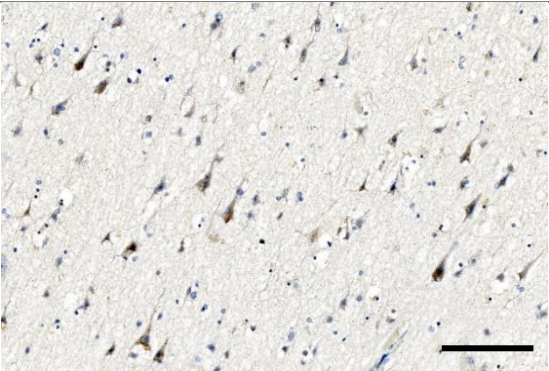
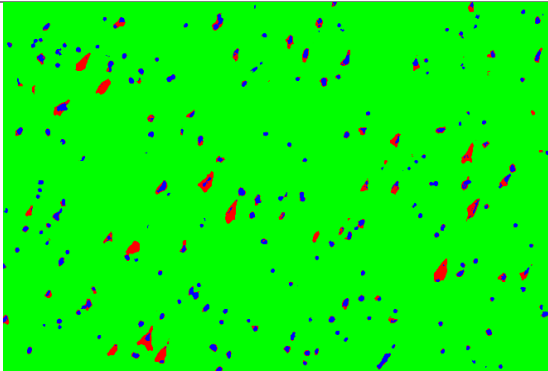
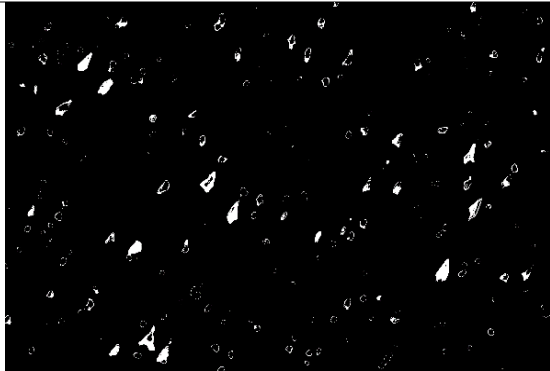
*a) Quantification of DAB total area per field of 0.24 mm<sup>2</sup>. b) DAB area is normalised to the nuclei count. Data are represented by the mean  $\pm$  SEM and analysed using one-way ANOVA, followed by the Tukey post hoc test (\* $P < 0.05$ , \*\* $P < 0.01$ ).*

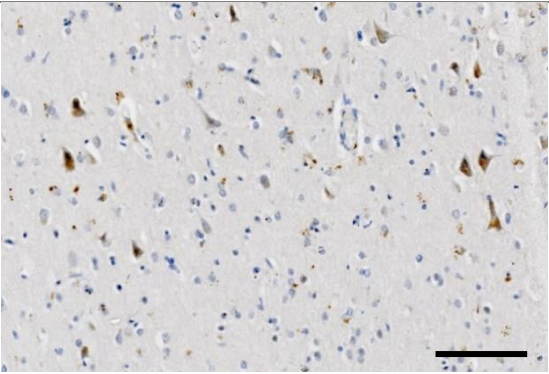
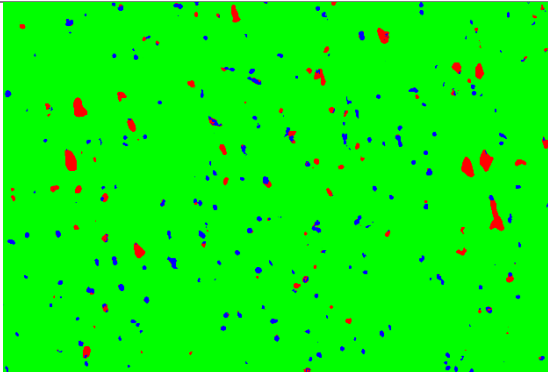
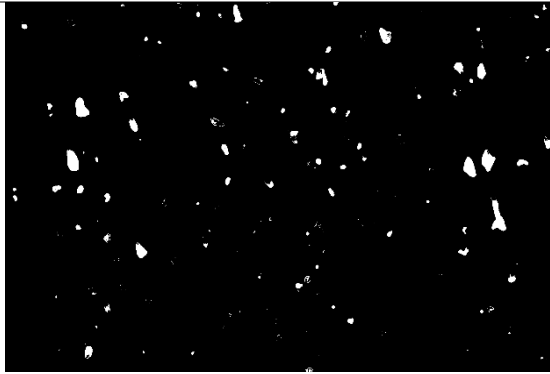
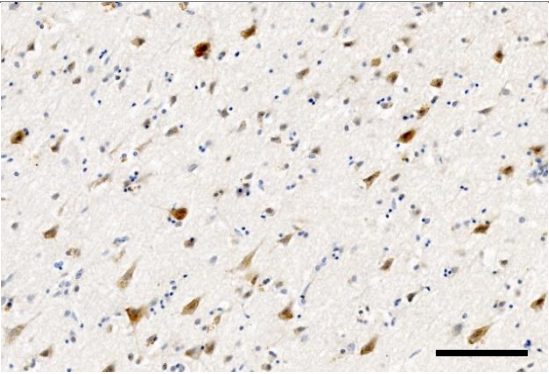
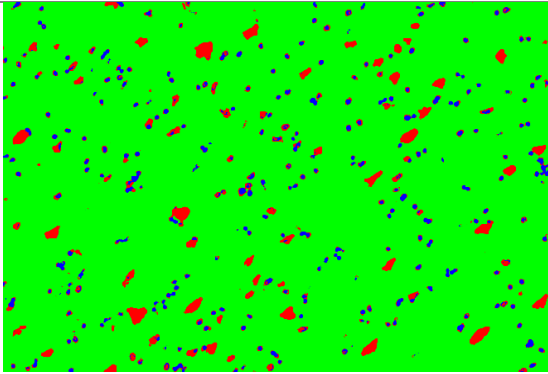
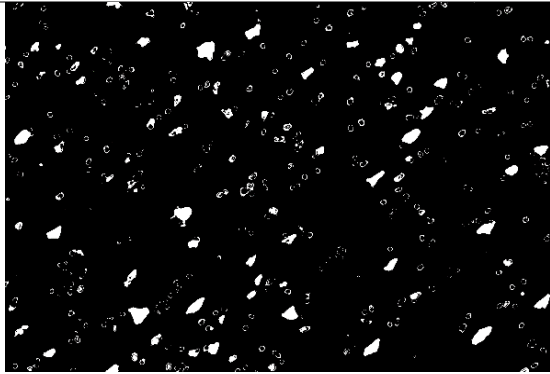
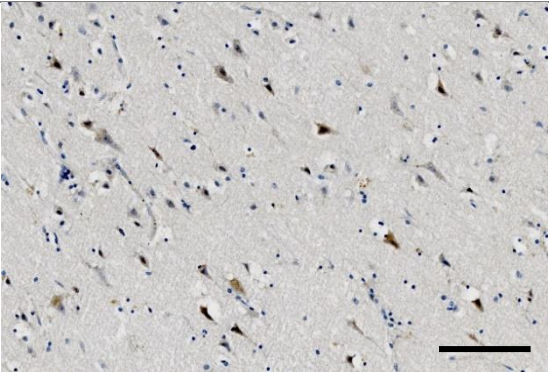
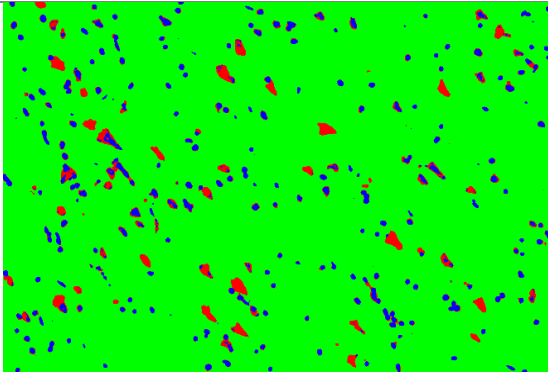
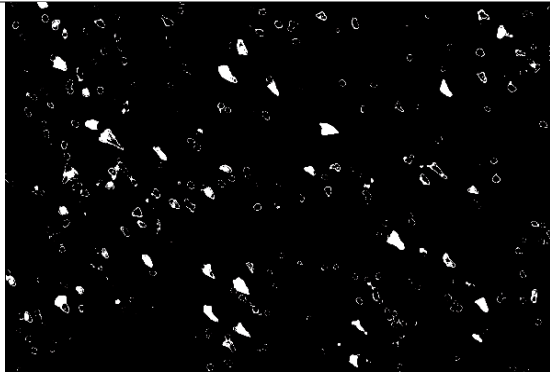
#### 6.4.2. 5-HT<sub>6</sub> receptor

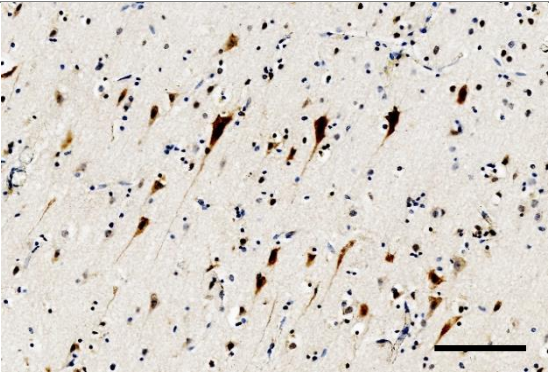
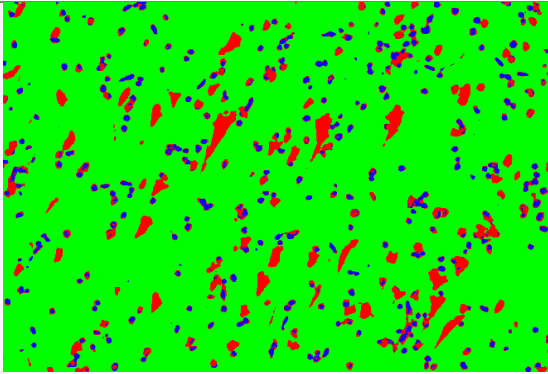
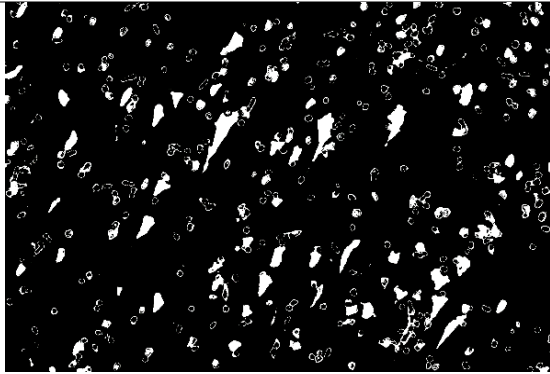
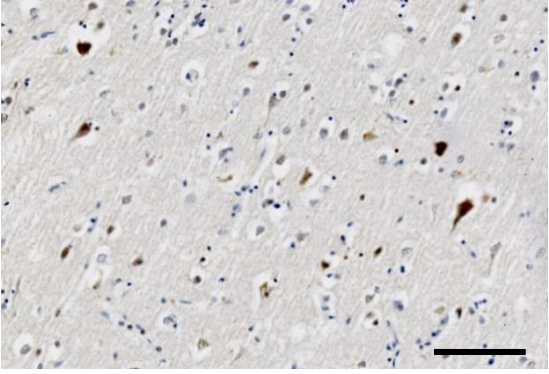
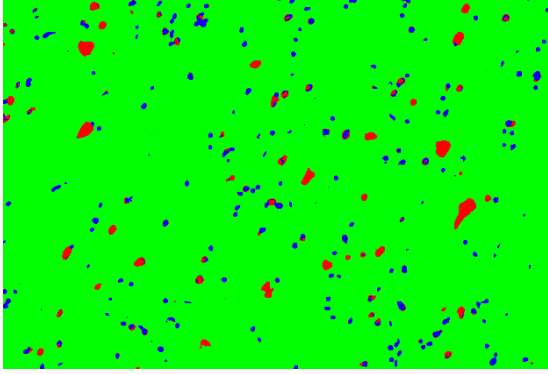
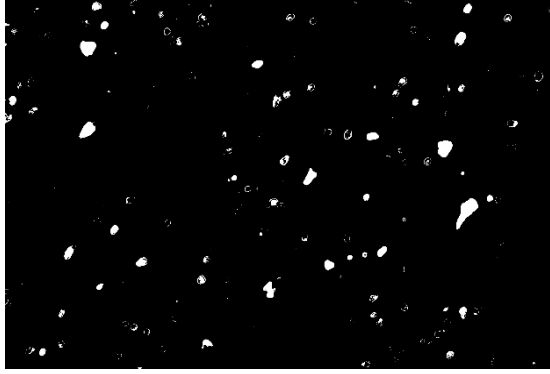
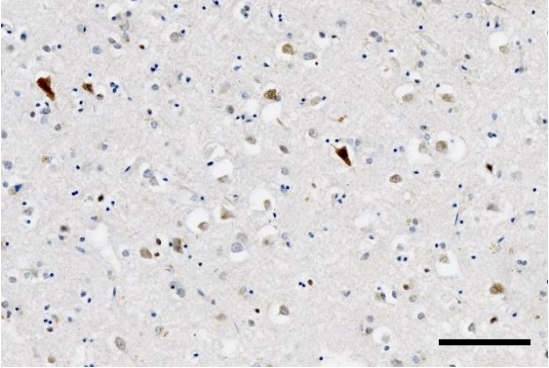
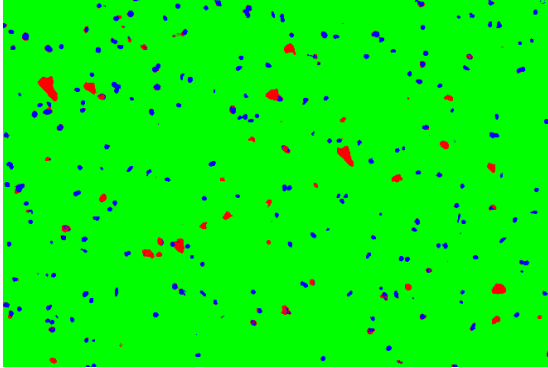
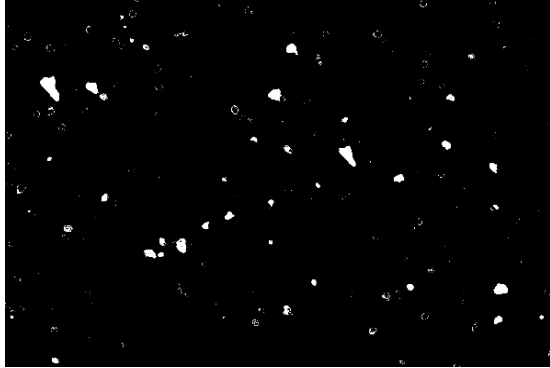
With regard to 5-HT<sub>6</sub> receptor expression, a positive immunoreactive signal was detected in the pyramidal neurones of cortical layer III. Similar to 5-HT<sub>4</sub> receptors, this was located in the cell bodies and the axons of the neurones (see the representative images in **Figure 45**). In terms of signal intensity, 5-HT<sub>6</sub> immunoreactivity was stronger than the 5-HT<sub>4</sub> receptor immunoreactivity. The expression pattern of the 5-HT<sub>6</sub> receptors in the early and late stages of the disease was interesting because there was a small receptor up-regulation in the limbic stage but then the level reduced below that of the controls when the neocortex was affected at the neocortical stage. However, none of these changes reached the statistical significance level ( $P > 0.05$ , **Figure 46a**).

Normalisation of the total positive area with the number of cells as in **Figure 46b** showed the same pattern of receptor expression as the one without normalisation. The immunoreactivity showed no statistical difference between the control and either limbic stage or neocortical stage of AD, however; there was a reduction in the 5-HT<sub>6</sub> receptor immunoreactivity in the neocortical stage relative to the limbic stage ( $P=0.0106$ ). Notably, the limbic cases exhibited a slight but not significant increase in the cortical 5-HT<sub>6</sub> receptor immunoreactivity which might be a compensatory mechanism to overcome early neuronal degeneration and pathological lesions in the limbic area of the brain.

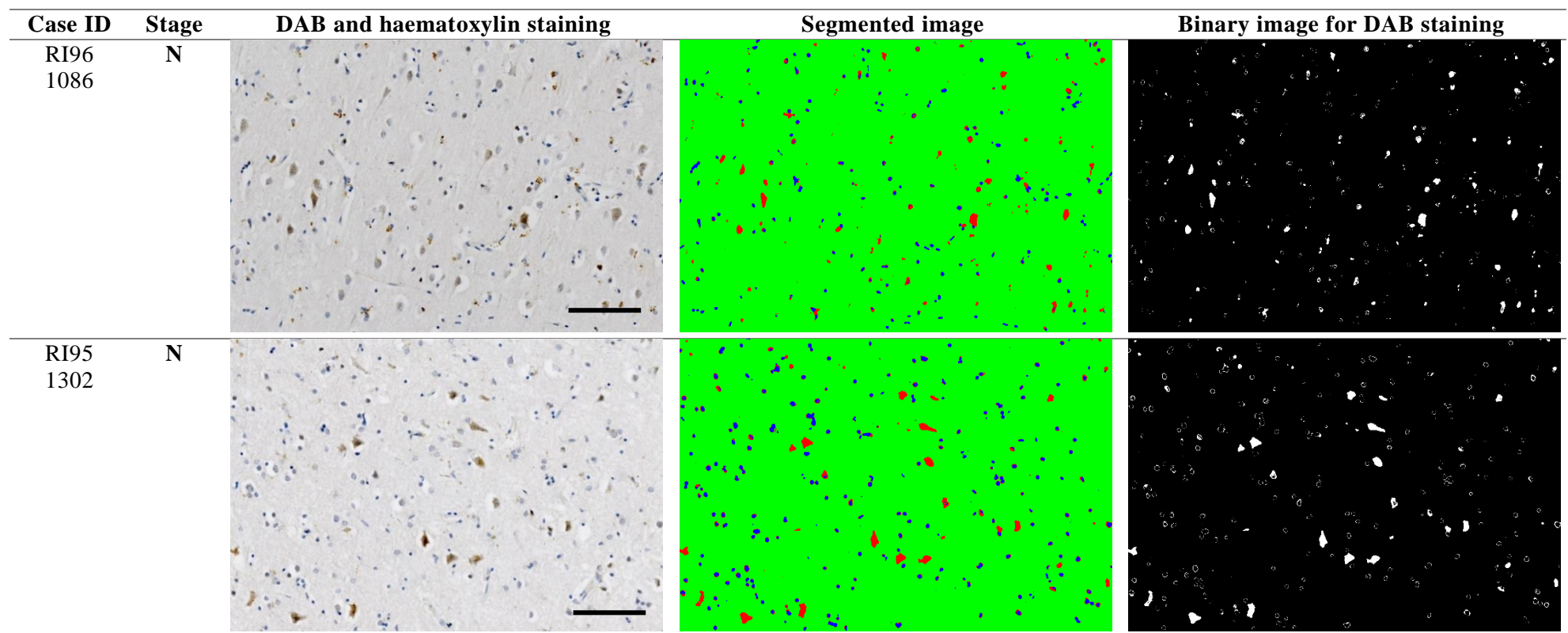


Case ID	Stage	DAB and haematoxylin staining	Segmented image	Binary image for DAB staining
RI95 1385	C			
RI03 0211	C			
RI02 0054	C			

Case ID	Stage	DAB and haematoxylin staining	Segmented image	Binary image for DAB staining
RI96 1058	L			
RI96 1287	L			
RI01 0173	L			

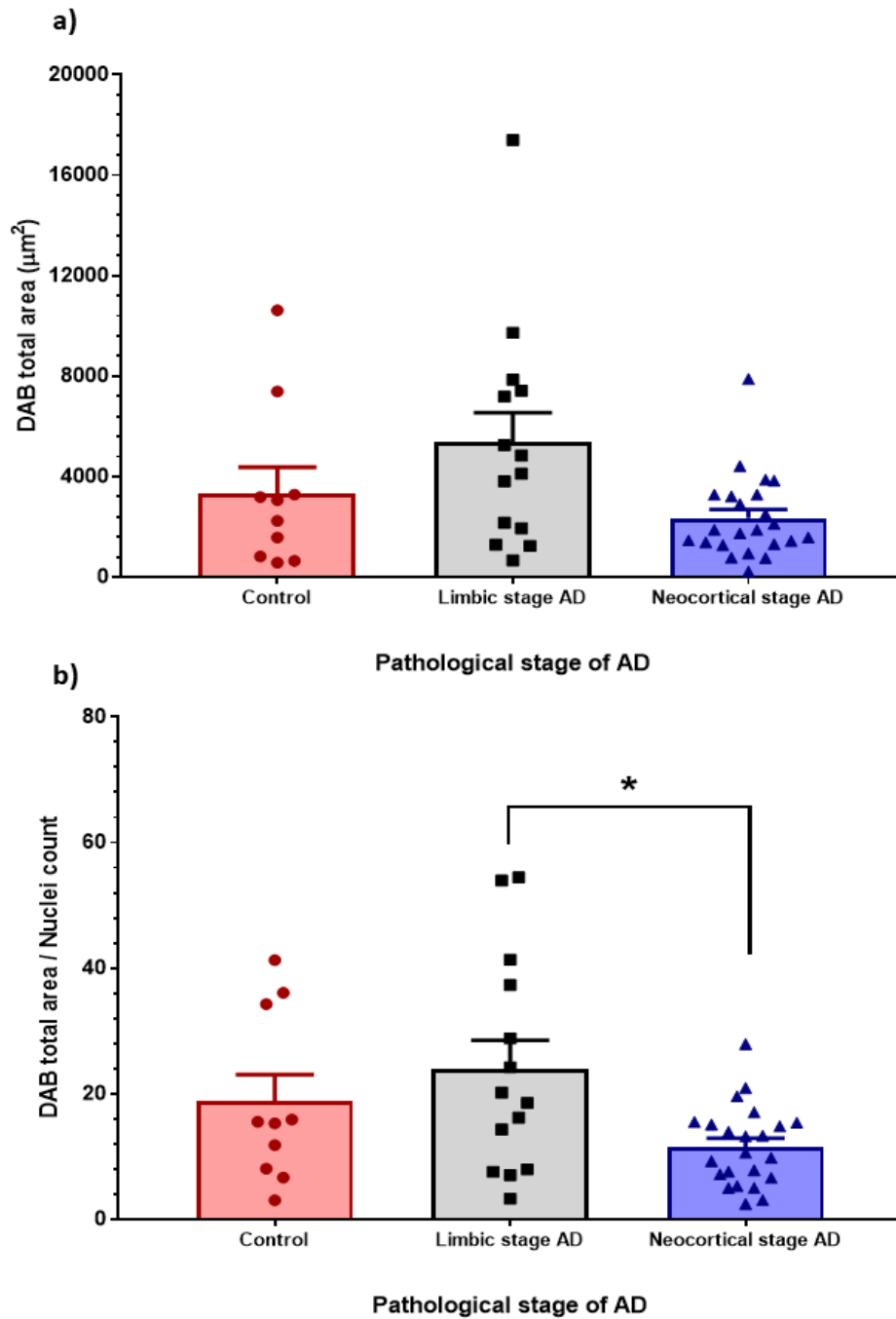
Case ID	Stage	DAB and haematoxylin staining	Segmented image	Binary image for DAB staining
C 2567	L			
RI99 1002	N			
RI96 1018	N			





**Figure 45. Illustration of signal decomposition from DAB and haematoxylin stained-images for 5-HT<sub>6</sub> receptor**

*The positive brown signals indicate the expression of serotonin receptors (red channel). The nuclei and background are segmented to blue and green channels, respectively. The binary image represents the red channel only. C: control, L: limbic stage, N: neocortical stage. Scale bar 100  $\mu$ m.*



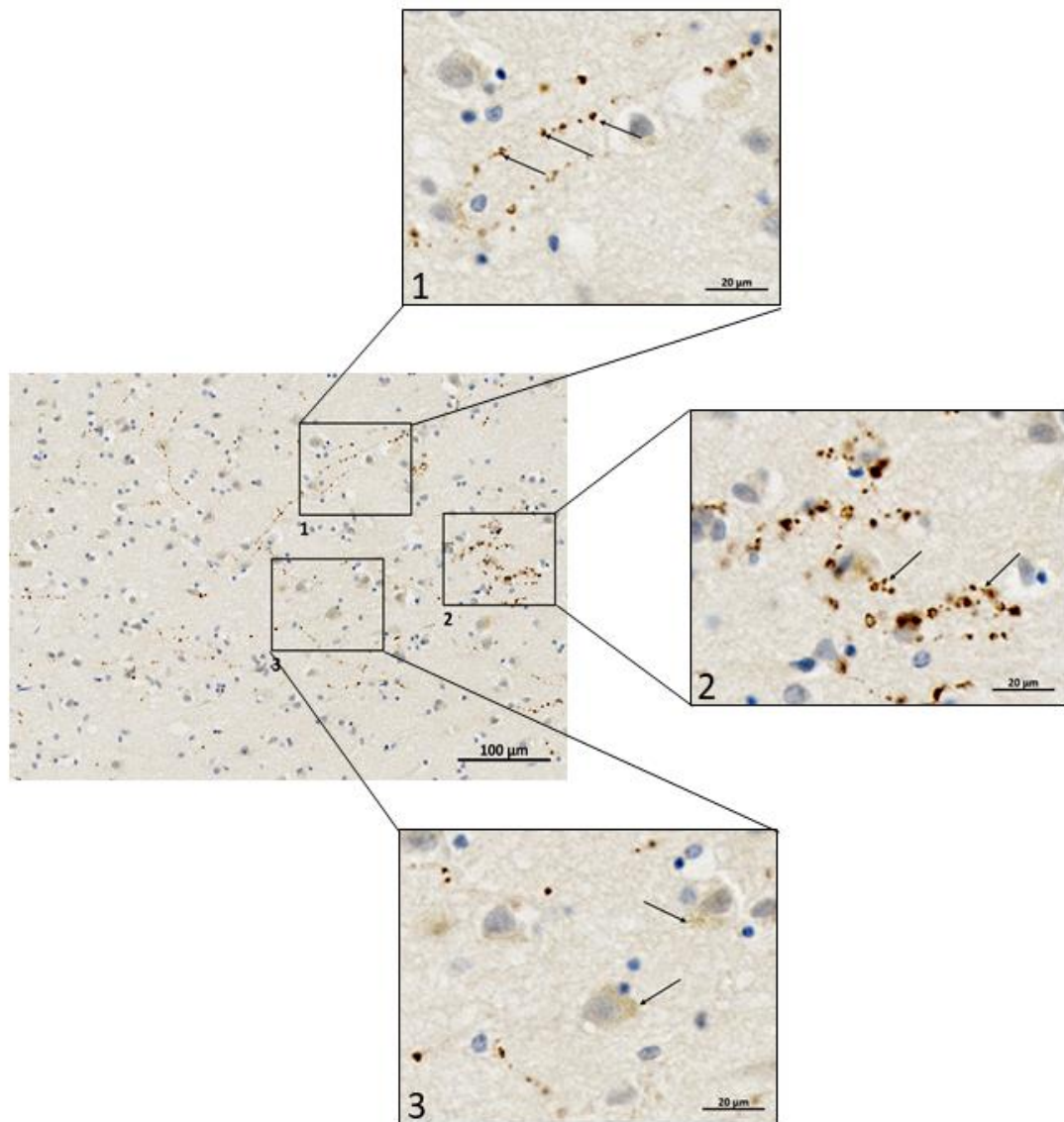
**Figure 46. Differences in 5-HT<sub>6</sub> receptor expression in the control, and limbic and neocortical stages of AD**

*a) Quantification of DAB-positive area per 0.24 mm<sup>2</sup>. b) DAB area was normalised to the nuclei count. Data are represented by the mean  $\pm$  SEM and analysed using one-way ANOVA, followed by the Tukey post hoc test (\* $P < 0.05$ ).*

### **6.5. Changes in SERT immunoreactivity in different AD stages**

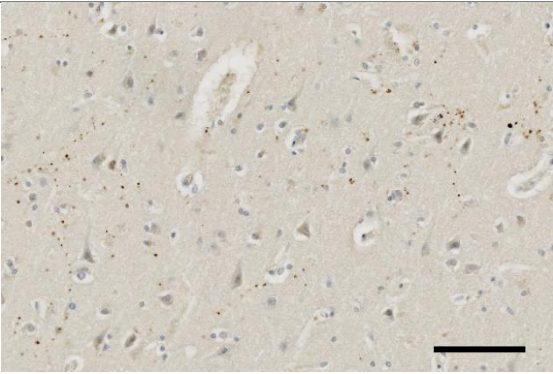
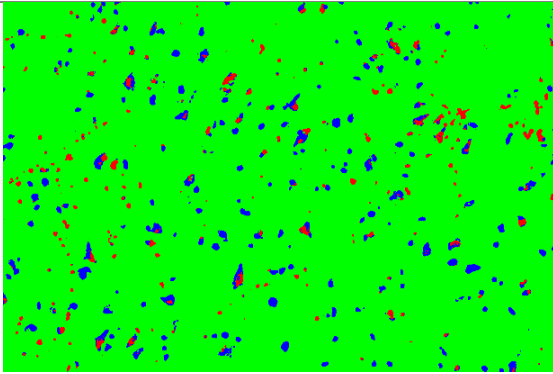
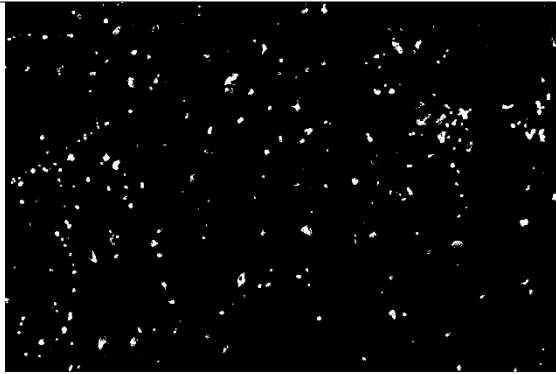
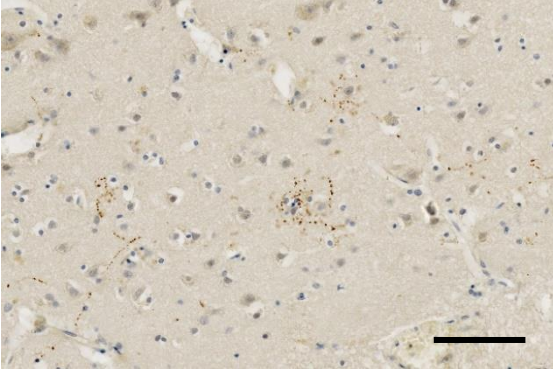
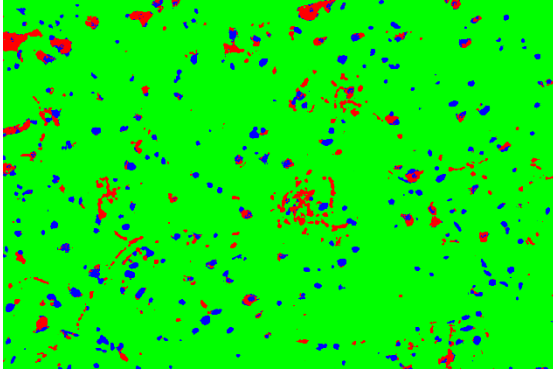
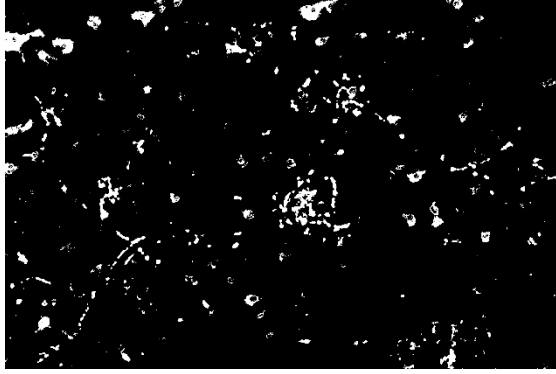
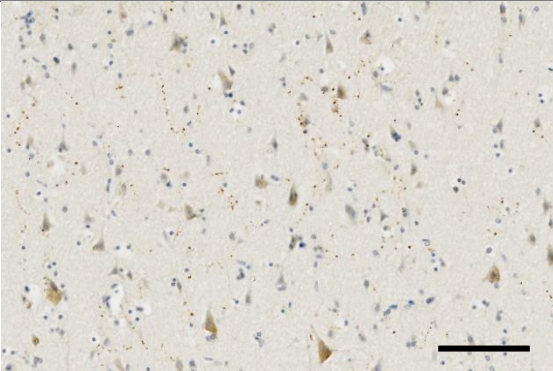
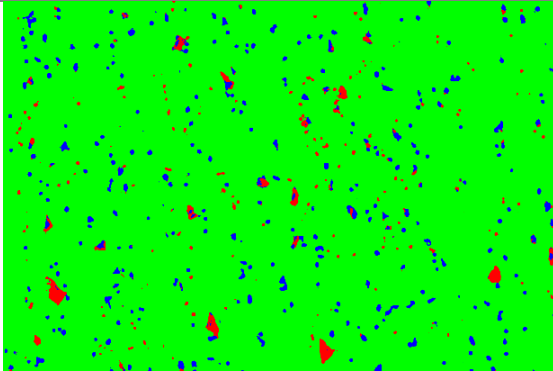
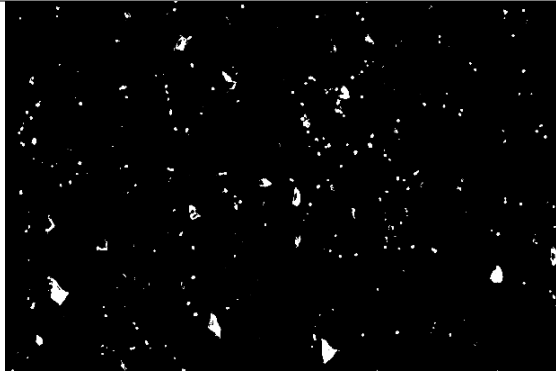
Unlike serotonin receptors, SERT immunoreactivity was widely distributed throughout the cortical layers. SERT immunoreactivity appeared mainly as diffused and clustered processes with numerous varicosities along the length of these fibres. Some neuronal cell bodies had little immune-reactive staining as shown in **Figure 47**.

Regardless of the tissue variability, the staining was low in the neocortical AD cases stage compared to controls or limbic AD cases, fewer varicosities and cell bodies appeared positively stained (**Figure 48**). **Figure 49a** elucidated the differences in the SERT immunoreactivities in which the total expression area was significantly down-regulated in the late stage of AD relative to control and early stage of AD with P-value of 0.005 and 0.0210, respectively. There was no significant difference between the control and the early stage of AD ( $P=0.7128$ ). When the cell count was considered, the pattern of the expression was consistent and showed significant differences between the control and late AD ( $P=0.0104$ ), and the early stage of AD and late stage of AD ( $P=0.0426$ ) but not between the control and the early stage of AD ( $P=0.7199$ ) (**Figure 49b**).

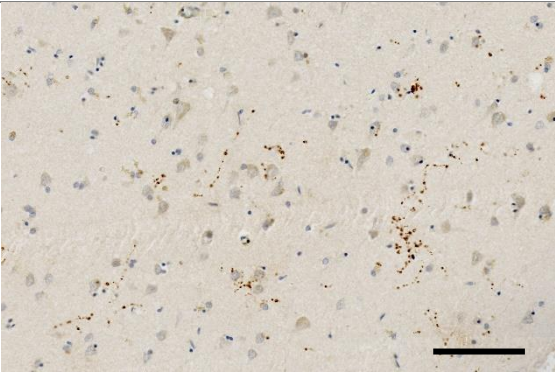
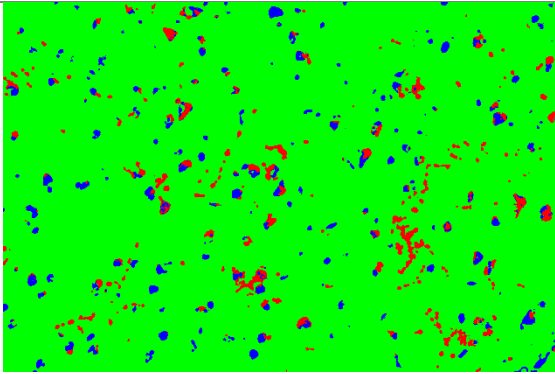
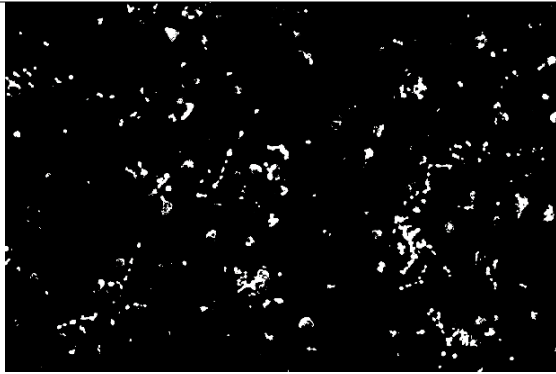
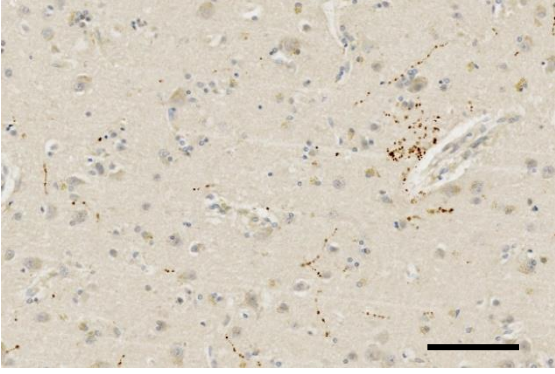
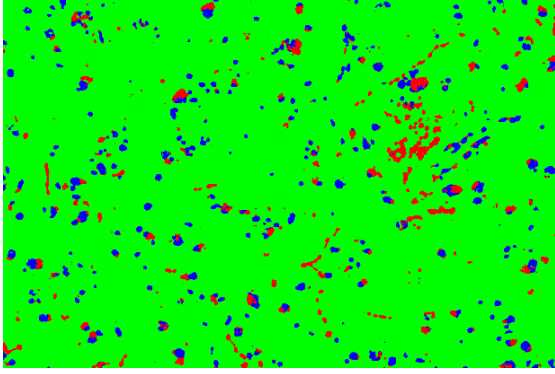
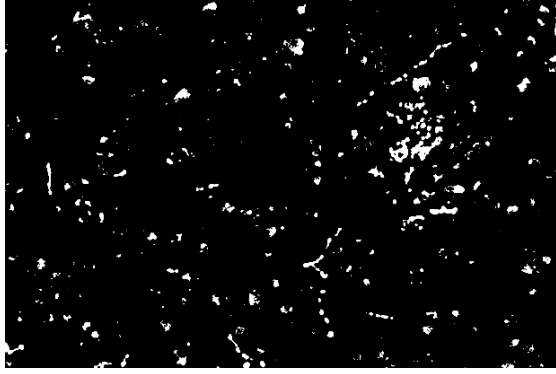
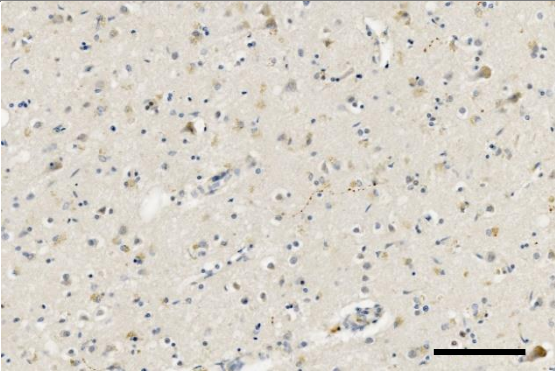
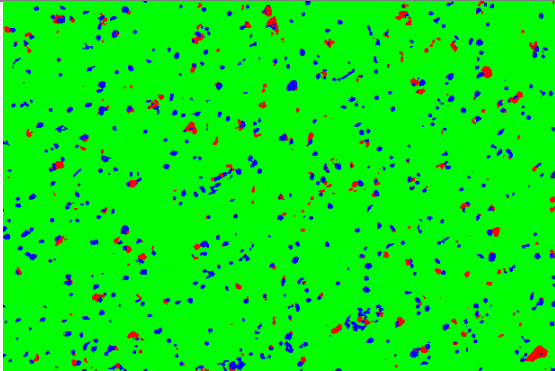
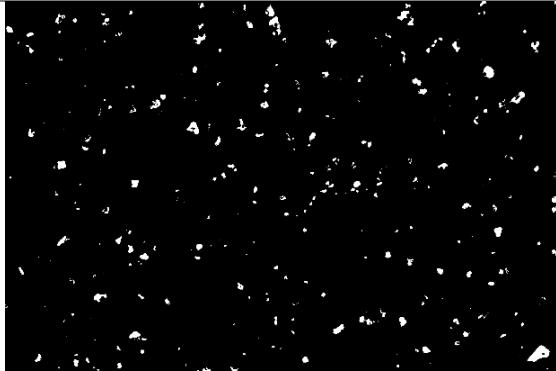


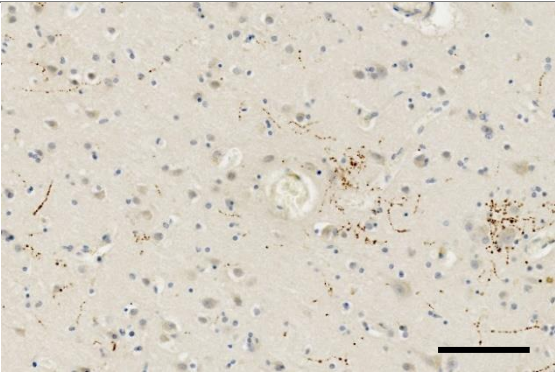
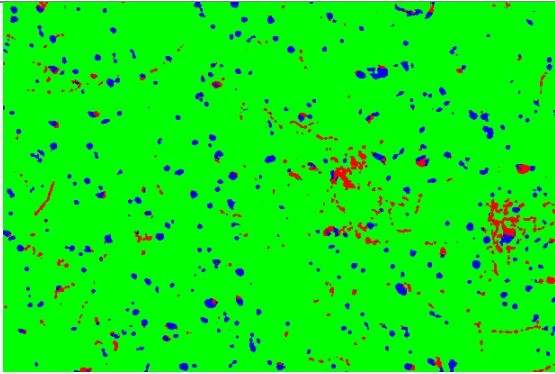
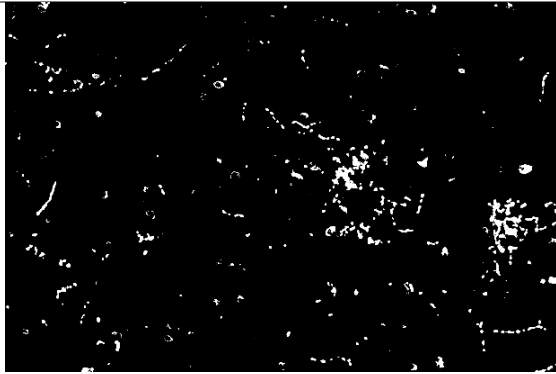
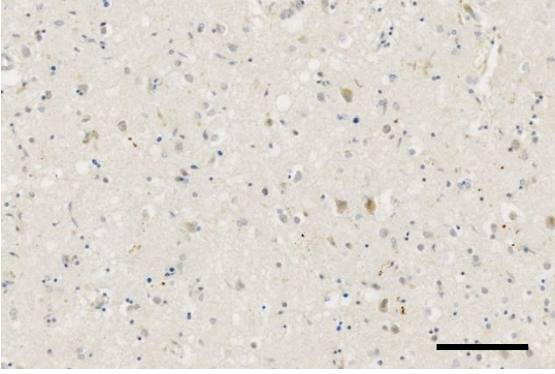
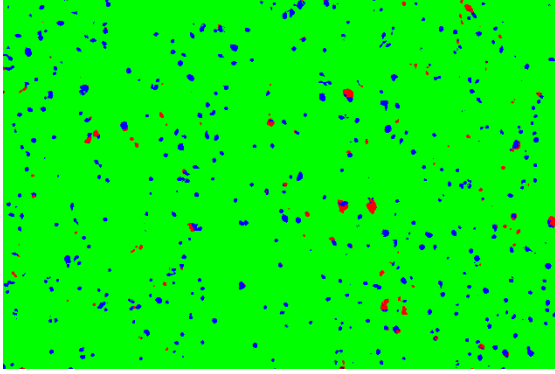
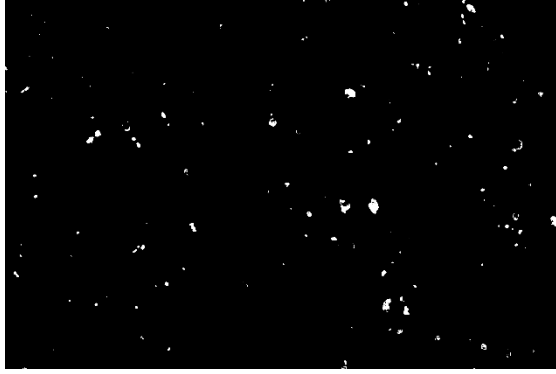
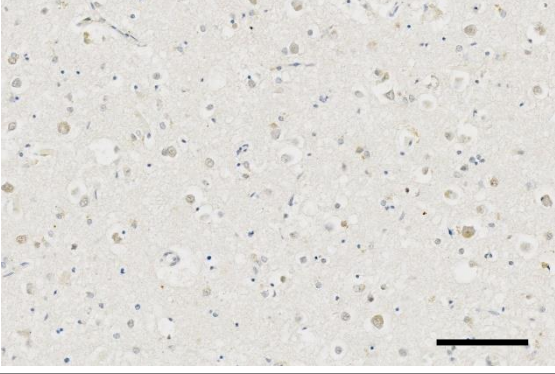
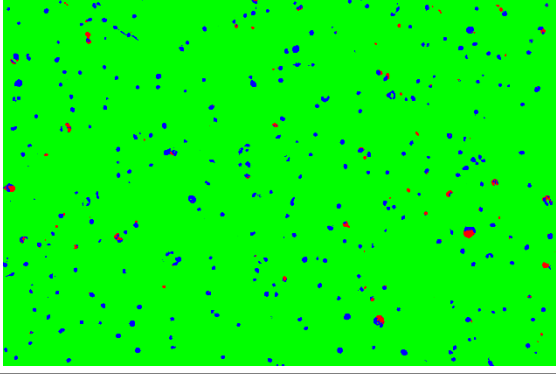

**Figure 47. SERT immunoreactivity and its neuronal distributions in layer III of the cortex**

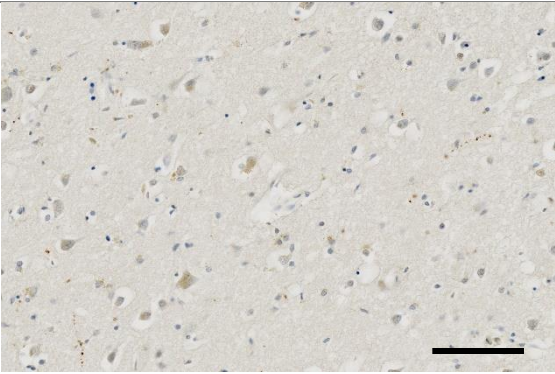
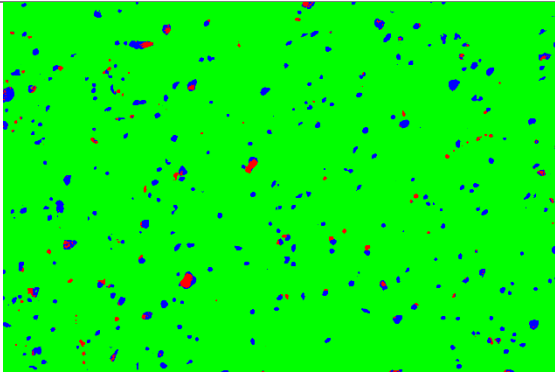
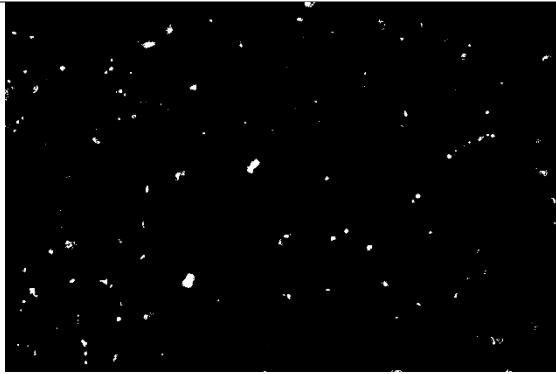
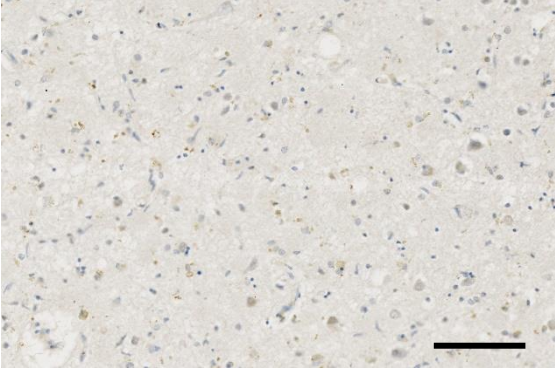
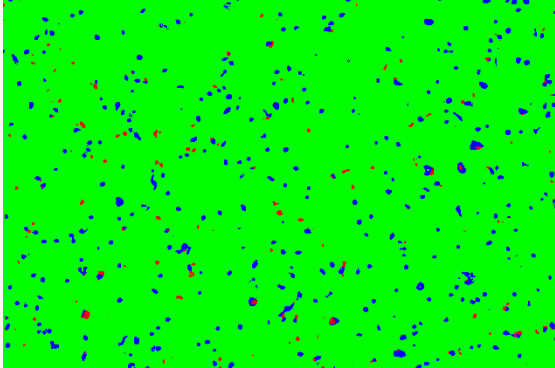

*SERT positive DAB signal, indicated by arrows, was more intense in neuronal processes appeared as (1) diffused or (2) cluster varicosities (beaded fibres). Some cell bodies as in (3) showed less intense signal.*

Case ID	Stage	DAB and haematoxylin staining	Segmented image	Binary image for DAB staining
RI03 0128	C			
RI97 1288	C			
RI95 1385	C			



Case ID	Stage	DAB and haematoxylin staining	Segmented image	Binary image for DAB staining
RI96 1102	L			
RI99 1121	L			
RI95 1334	L			

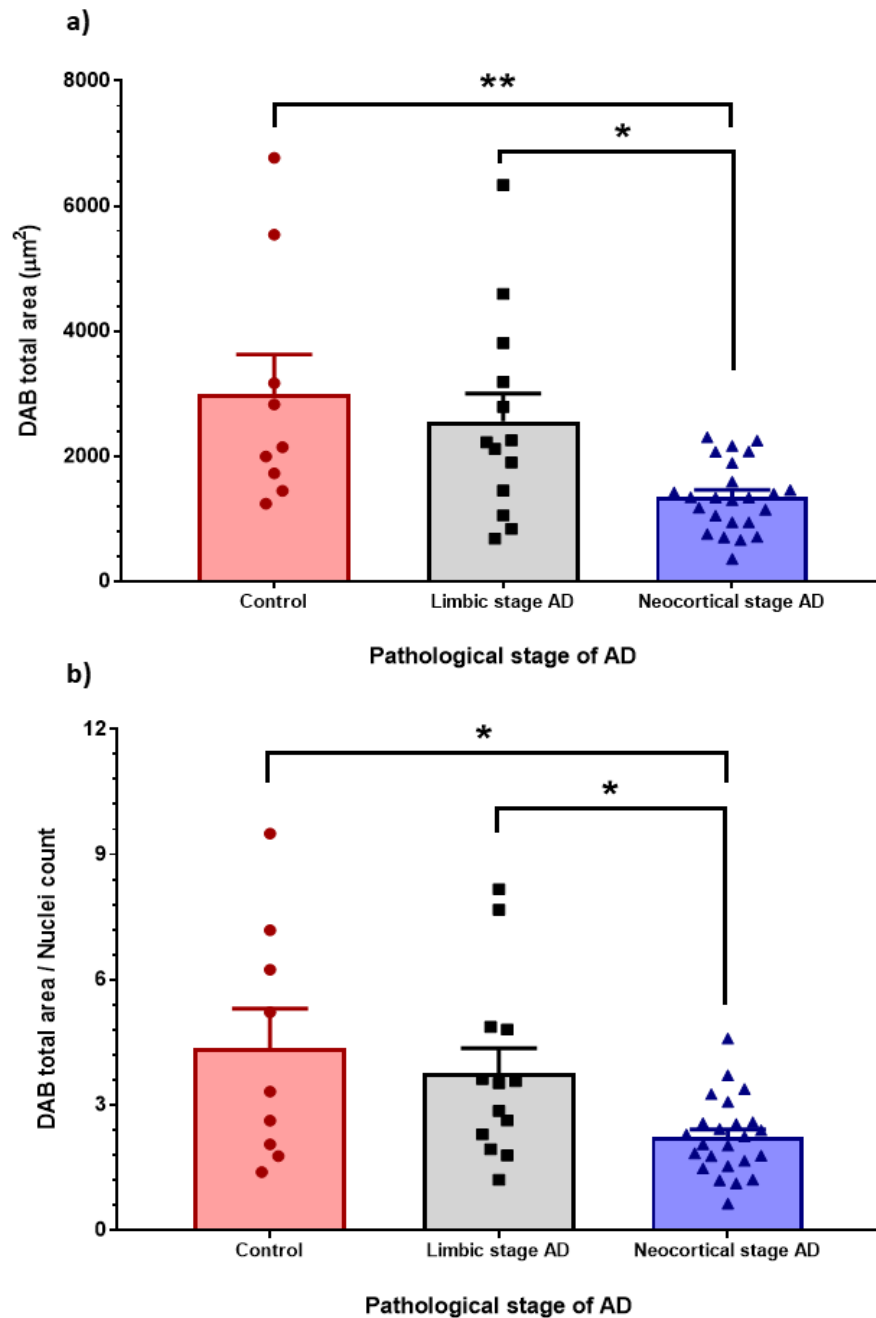
Case ID	Stage	DAB and haematoxylin staining	Segmented image	Binary image for DAB staining
C 2567	L			
RI98 1004	N			
RI96 1018	N			

Case ID	Stage	DAB and haematoxylin staining	Segmented image	Binary image for DAB staining
RI96 1089	N			
RI02 0036	N			

**Figure 48. Illustration of signal decomposition from DAB and haematoxylin stained-images for SERT**

*The positive brown signals indicate the expression of serotonin transporter (red channel). The nuclei and background are segmented to blue and green channels, respectively. The binary image represents the red channel only. C: control, L: limbic stage, N: neocortical stage. Scale bar 100  $\mu$ m.*





**Figure 49. Changes in SERT immunoreactivity in the control, and limbic and neocortical stages of AD**

*a) Quantification of DAB-positive area per 0.24 mm<sup>2</sup>. b) DAB area was normalised to the nuclei count. Data are represented by the mean  $\pm$  SEM and analysed using one-way ANOVA, followed by the Tukey post hoc test (\* $P < 0.05$ , \*\* $P < 0.01$ ).*

### **6.6. Effects of demographics and PMD on 5-HT<sub>4</sub> and 5-HT<sub>6</sub> receptors immunoreactivity**

The study individuals consisted of a maximum of 10 controls, 14 AD patients in the limbic stage and 24 AD patients in the neocortical stage. These numbers were varied for each protein target based on the sample availability, and the actual (n) number was presented as scattered points in the column graphs. In fact, studying the receptor expression during AD can overlap with the normal ageing process in which most of these receptors are changing in the same direction but the extent is more evident in AD relative to normal ageing (Avramopoulos et al., 2011, Rodriguez et al., 2012). In this study, well matched demographics of the study groups were used in which there were no significant differences in the mean values of age, sex distribution and PMD between controls, limbic and neocortical AD patients (**Table 22**, ANOVA test for the age and PMD and Chi-square test for sex distribution,  $P > 0.05$ ). In addition, there were no significant correlations between age, PMD and 5-HT<sub>4</sub> and 5-HT<sub>6</sub> receptors or SERT immunoreactivities in the study groups (Spearman's correlations  $P > 0.05$ ). Thus, none of these variables were counted as a covariate in the subsequent analysis.

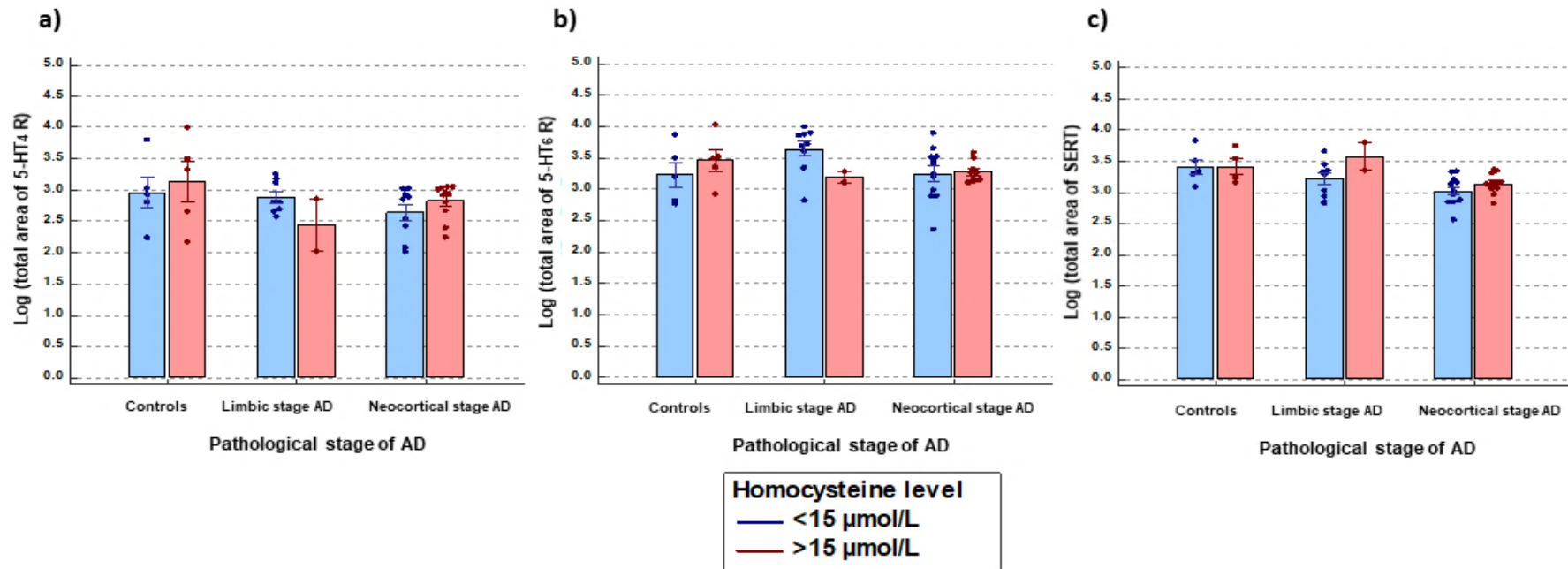
**Table 22. Demographic variables of controls and AD patients.**

<b>Variables</b>	<b>Control</b>	<b>Limbic stage</b>	<b>Neocortical stage</b>	<b>P-value</b>
<b>Age (years)</b>	82 ± 2	82 ± 2	76 ± 2	0.0927
<b>Sex (% male)</b>	60%	57%	48%	0.7618
<b>PMD (hr)</b>	56 ± 9	55 ± 6	56 ± 6	0.9935

### **6.7. Elevated homocysteine level did not influence the protein expression of 5-HT<sub>4</sub> and 5-HT<sub>6</sub> receptors and SERT**

To assess whether elevation in the plasma Hcy level can influence the expression of serotonin 5-HT<sub>4</sub> and 5-HT<sub>6</sub> receptors or transporter at different disease stages, pre-existing clinical and pathology data for the patients (obtained from the OPTIMA cohort study) were used to determine the effect of AD risk factors on receptor expression. In addition to demographics, these data included categorical variables such as disease severity, ApoE genotype and Hcy level and AD-related proteins namely,  $\beta$ -amyloid, APP and two forms of phosphorylated tau (recognised by AT8 and DC11 epitopes), neuronal proteins: growth-associated protein 43 (GAP-43), neuronal specific nuclear protein (NeuN) and synaptophysin, oxidative stress products: 4-HN and 8-HG as well as cell cycle regulating kinases and inhibitors; CDK4, CDK5, CDK2 and p16, p21, p27, p57, respectively.

For the sake of simplicity and to facilitate studying the interactions between pathological severity and the homocysteine level, as well as their influence on receptor expression, the homocysteine level was categorised as a discrete (dichotomous) variable: either  $> 15 \mu\text{mol/L}$  or  $< 15 \mu\text{mol/L}$ . The results showed that homocysteine level *per se* did not relate to 5-HT<sub>4</sub> or 5-HT<sub>6</sub> receptor expression, as well as SERT expression even when disease severity was considered, as shown in **Figure 50** ( $P > 0.05$ , not significant).



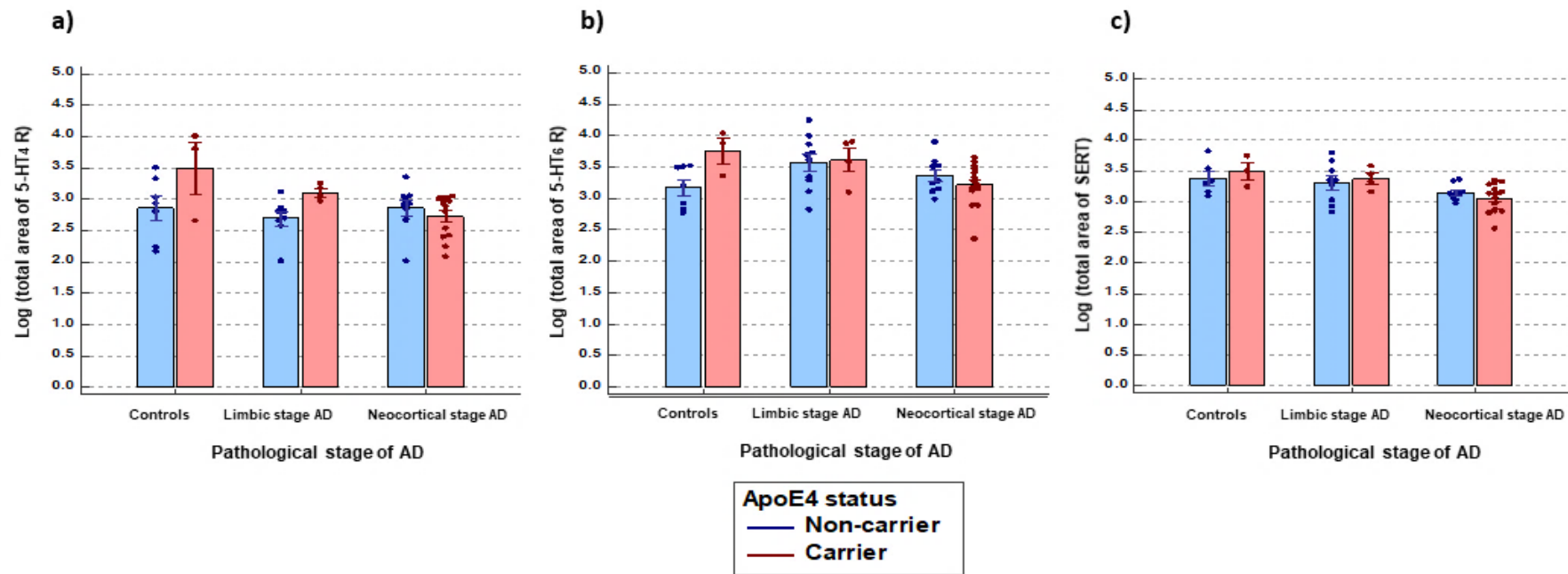
**Figure 50. Effect of homocysteine level on the expression of 5-HT<sub>4</sub> and 5-HT<sub>6</sub> receptors and SERT in different AD stages**

*Categorising individuals according to their plasma homocysteine level and disease severity did not affect the expression of either receptor. Data are analysed using two-way ANOVA.*

### **6.8. Effect of ApoE genotype on the expression of serotonin receptors and transporter**

To determine whether the ApoE genotype influenced 5-HT<sub>4</sub> receptors in different disease stages, the AD patients and controls were allocated according to categorical variables: ApoE genotype and disease severity. Individuals who had one or two copies of the ApoE  $\epsilon$ 4 allele depicted a higher level of 5-HT<sub>4</sub> receptors when compared with those who had none ( $P=0.034$ ). This difference was clear in the controls and in the limbic stage of AD but not in the neocortical stage, as shown in **Figure 51a** below.

With regard to 5-HT<sub>6</sub> receptors, the results revealed that the ApoE genotype had no significant effect on 5-HT<sub>6</sub> receptor level ( $P=0.192$ ) but it is very close to significance when the disease severity was considered ( $P=0.052$ ) as demonstrated in **Figure 51b**. The same was found with SERT expression in which the ApoE genotype *per se* or with disease severity depicted no significant effect on SERT immunoreactivity ( $P > 0.05$ , **Figure 51c**).



**Figure 51. Effect of ApoE genotype and disease evolution on the expression of 5-HT<sub>4</sub> and 5-HT<sub>6</sub> receptors and SERT in different AD stages**

*The presence of the ApoE  $\epsilon 4$  allele was significantly associated with higher 5-HT<sub>4</sub> receptor immunoreactivity, particularly in the control and the limbic stage ( $P=0.034$ ) but not associated with the 5-HT<sub>6</sub> receptor or SERT immunoreactivities. Data are analysed using two-way ANOVA.*

### **6.9. Correlation between serotonin receptors and cognitive functions**

An evaluation of the cognitive status of the cohort of AD patients and age-matched controls had been longitudinally assessed by the clinical team of the OPTIMA project during life. Two cognitive tests were used: MMSE and CAMCOG. The scores of these tests were correlated with the level of 5-HT<sub>4</sub> and 5-HT<sub>6</sub> receptors and SERT and AD pathological proteins, namely,  $\beta$ -amyloid, APP and phosphorylated tau. In addition, neuronal outgrowth and synaptic density markers, GAP-43 and synaptophysin, were also considered. Multiple regression analysis and backward elimination were used. The results showed that the variation of the cognitive test scores could be predicted by the level of AT8, 5-HT<sub>4</sub> and 5-HT<sub>6</sub> receptors and SERT. Interestingly, and similar to the tau protein, AT8, the correlation direction of 5-HT<sub>6</sub> receptors with cognitive functions was negative; indicating that individuals who have a higher receptor level of these proteins tended to have a lower cognitive score and vice versa. The correlation coefficient and the P-values are, summarised in **Table 23**.

**Table 23. Regression analysis of the relationship between cognitive function, the level of serotonin proteins and AD-pathological proteins.**

	<b>MMSE</b>			<b>CAMCOG</b>		
<b>Predictors</b>	<b>Coefficient</b>	<b>Std. Error</b>	<b>P-value</b>	<b>Coefficient</b>	<b>Std. Error</b>	<b>P-value</b>
<b>5-HT<sub>4</sub> receptor</b>	0.002995	0.001329	0.0422*	0.01122	0.004588	0.0294*
<b>5-HT<sub>6</sub> receptor</b>	-0.001970	0.0008398	0.0355*	-0.006896	0.002898	0.0333*
<b>SERT</b>	0.001604	0.0009031	0.0991	0.006928	0.003116	0.0445*
<b>AT8</b>	-12.3206	2.2266	0.0001***	-37.7715	7.6837	0.0003***
	Adjusted R <sup>2</sup> = 0.7825 (P-value =0.0001***)			Adjusted R <sup>2</sup> = 0.7683 (P-value =0.0001***)		



### **6.10. Summary**

The expression of the 5-HT<sub>4</sub> receptor, 5-HT<sub>6</sub> receptor and SERT, at the protein level, was reduced at neocortical AD stage when the frontal cortex was affected by the AD pathology but only 5-HT<sub>4</sub> receptor was reduced at the limbic stage. In addition, the 5-HT<sub>4</sub> receptor expression was influenced by ApoE carrier status but this was dependent on the AD stage. Variations in the expression of serotonergic proteins contributed significantly to the cognitive status of those patients besides the strong effect of the AD-related phospho-tau.

## **Chapter 7. Discussion**

## **7. Discussion**

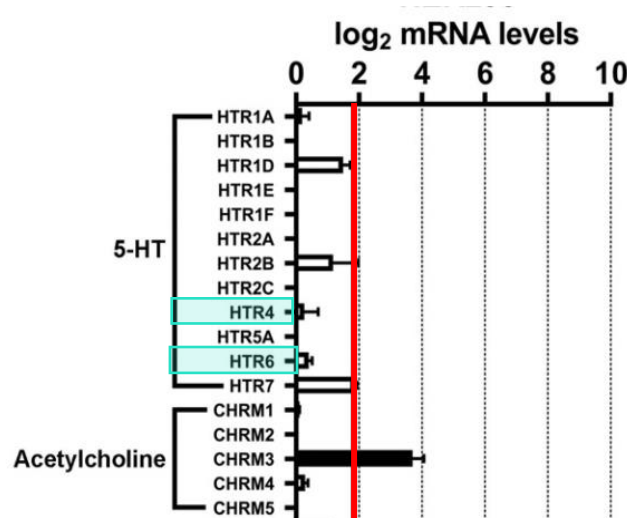
### **7.1. Expression profile of 5-HT<sub>4</sub> and 5-HT<sub>6</sub> receptors in SH-SY5Y and HEK293 cell lines**

Searching for a cell line that natively expresses the 5-HT<sub>4</sub> and 5-HT<sub>6</sub> receptors to study their pharmacological interactions was challenging due to the plethora of cell lines and the low native expression of these GPCRs (Reeves et al., 2002). Although many studies characterised the relevance of 5-HT<sub>4</sub> and 5-HT<sub>6</sub> receptors to AD by overexpressing these receptors in cell lines such as HEK293 and SH-SY5Y, limited studies have shown their native expression profile in such cell lines. This work aims to evaluate the expression of serotonin 5-HT<sub>4</sub> and 5-HT<sub>6</sub> receptors in these cell lines which are commonly used for studying signalling and interactions of recombinant 5-HT receptors with other proteins related to AD.

#### **7.1.1. The transcript and protein expressions of the 5-HT receptors**

Determining the transcript and protein profiles can complement each other resulting in a better assessment of the expression on the target proteins in the tested cell or tissue. In this work, gene expression analysis of 5-HT<sub>4</sub> and 5-HT<sub>6</sub> receptors showed that both cell lines endogenously expressed the transcripts of both 5-HT receptors at different levels. The results obtained from the neuroblastoma cell line showed relatively similar levels of the 5-HT<sub>4</sub> and 5-HT<sub>6</sub> receptor transcripts. In the HEK293 cell line, however, the mRNA of the 5-HT<sub>6</sub> receptor was more abundant than the 5-HT<sub>4</sub> receptor. This difference is not attributed to technical variation because the mRNA of  $\beta$ -actin showed a relatively stable level in both cell lines. A study conducted by Atwood et al. (2011) used unbiased microarray analysis to quantify

the transcripts of non-chemosensory GPCRs including 5-HT and Ach receptors in the HEK293 cell line. In agreement with the findings of this study, Atwood et al. found that the HEK293 cells expressed the transcripts of 5-HT<sub>4</sub> and 5-HT<sub>6</sub> receptors but at a low level, whereas the mRNA of the 5-HT<sub>7</sub> receptor was the highest among other 5-HT receptors (**Figure 52**). On the contrary, Johnson et al. (2003) confirmed the native presence of mRNA of 5-HT<sub>6</sub> and 5-HT<sub>7</sub> receptors in HEK293 cells but not of 5-HT<sub>4</sub> and 5-HT<sub>2A</sub> receptors. Despite the lack of agreement in the mRNA expression of the 5-HT<sub>4</sub> receptor, the findings of this study are comparable with Johnson et al. (2003) where 30 amplification cycles were used, while this study used 40 cycles. On employment of 30 cycles; no PCR product was detected in the agarose gel (data not shown).



**Figure 52. The mRNA expression profile of 5-HT and Ach receptors in HEK293 cells**

*Microarray analysis showing the levels of mRNA for 5-HT and Ach receptors in the HEK293 cell line. The red vertical line indicates the threshold of statistical significance. The genes below the threshold are represented with white bars while the black bar represents the gene encoding the muscarinic M<sub>3</sub> receptor which is expressed at a statistically significant level in HEK293 cells (Adapted from Atwood et al., 2011).*

Regarding the protein expression of these receptors, two positive controls were used. The first was the human hippocampus lysate and the second included recombinant protein lysates to assess the antibodies for each receptor. As confirmed in **Section 3.2**, the immunoreactive signal detected in the hippocampus lysate was faint and positioned at higher sizes than the expected sizes for the 5-HT<sub>4</sub> and 5-HT<sub>6</sub> receptors which might indicate native glycosylated forms of the receptors. The blots showed approximately a 6 kDa increase in the 5-HT<sub>4</sub> receptor's size and approximately a 3 kDa increase in the 5-HT<sub>6</sub> receptor's size. The increase in the size of endogenously expressed GPCRs is probably due to PTMs such as glycosylation which slow protein migration through SDS-PAGE. Also, the faint signal in hippocampus lysates might be attributed to the low expression of these receptors or post-mortem protein degradations.

As the signals detected in the hippocampus lysate were low, Myc-tagged recombinant receptors were used. The Myc immunoreactive blots confirmed the expression of the recombinant Myc-tagged 5-HT<sub>4</sub> and 5-HT<sub>6</sub> receptors at the expected sizes, hence these proteins were utilised as positive controls when probing with antibodies against the 5-HT<sub>4</sub> and 5-HT<sub>6</sub> receptors *per se*. Immunoreactivity of the 5-HT<sub>4</sub> receptor showed that HEK293 and SH-SY5Y cells constitutively express the 5-HT<sub>4</sub> receptor in agreement with transcript expression. This technique potentially detected two receptor isoforms as it revealed two bands with very close molecular weights. However, both 5-HT<sub>4</sub> receptor antibodies used in this work did not show an increase in the immunoreactive signal in proportion to the overexpressed 5-HT<sub>4</sub> receptor. No difference in the band density was detected between the wild-type and transfected HEK293 cells. The reason behind the antibodies' inability to recognise the recombinant protein is not known.

Theoretically, these antibodies should recognise the peptide sequence of the 5-HT<sub>4</sub> receptor which is identical in both the recombinant and the native receptor. In a reducing environment, the proteins typically unfold or demonstrate a low level of folding, which consequently increases their ability to migrate appropriately in the gel. Therefore, any difference in the folding between the endogenous and exogenous proteins should also be excluded. Notably, the Myc tag of the recombinant receptor was located in the C-terminus while the anti-5-HT<sub>4</sub> receptor antibodies detected peptides close to the N-terminus, therefore, the tag should not interfere with the 5-HT<sub>4</sub> receptor antibody.

Concerning the 5-HT<sub>6</sub> receptor, probing the overexpressed 5-HT<sub>6</sub> receptor with Myc and 5-HT<sub>6</sub> receptor antibodies exhibited two bands. The upper band was approximately double the size of the lower band, indicating the presence of receptor dimerisation. Metabotropic serotonin receptors can form homodimers (identical subunits) or heterodimers (distinct subunits) with other GPCRs when expressed in the native and the recombinant forms (Herrick-Davis, 2013). Analysis of the 5-HT<sub>6</sub> receptor immunoblot revealed that neither the SH-SY5Y cells nor the HEK293 cells natively expressed 5-HT<sub>6</sub> receptors, even though the endpoint PCR indicated the presence of mRNA corresponding to 5-HT<sub>6</sub> receptors in both cell lines. This discrepancy in the transcript and protein expression is not uncommon, considering that mRNA production does not necessarily lead to protein synthesis. Li et al. (2015) found that the 5-HT<sub>6</sub> receptor expression was confirmed at the transcript level, but the protein was not detectable in the human lower oesophageal sphincter. Complex gene-regulation processes can occur post-transcription, including the impact of mRNA half-life, translation rate and efficiency, PTMs of the translated proteins and protein degradation (Shankavaram et al., 2007, Vogel and Marcotte, 2012).

Therefore, evaluation of protein expression is preferred over transcript expression and thus, a PCR gene expression assay must be run alongside, rather than instead of, a protein expression assay.

Moreover, the immunocytochemistry finding demonstrated the presence and localisation of 5-HT receptors and supported the expression data obtained by Western blotting. Positive controls showed receptor expression in the cell membrane and cytoplasm. The 5-HT<sub>4</sub> receptor antibody detected only the endogenous 5-HT<sub>4</sub> receptor in HEK293 and SH-SY5Y cell lines—the signal, however, was detected in all cell compartments. The signal intensity was increased upon cell permeabilisation. The 5-HT<sub>6</sub> receptor antibody detected the exogenous 5-HT<sub>6</sub> receptor and produced a fluorescent signal on the cell surface and cytoplasm. However, no signal was detected in HEK293 and SH-SY5Y cell lines. This provided further evidence for the lack of expression of the endogenous 5-HT<sub>6</sub> receptor in both cell lines.

#### **7.1.2. Functionality and radioligand binding to the endogenous 5-HT<sub>4</sub> receptor**

Activation of 5-HT<sub>4</sub> receptors can stimulate several downstream molecules depending on the type of protein expression system (Bockaert et al., 2008). Previous studies confirmed that 10 µM of 5-HT could induce a transient increase in pERK<sub>1/2</sub> expression in HEK293 cells transfected with 5-HT<sub>4</sub> receptors as well as in colliculi neurones natively expressed 5-HT<sub>4</sub> receptors (Barthet et al., 2007, Norum et al., 2003). In this work, ERK<sub>1/2</sub> phosphorylation was used as a functional readout for the endogenous 5-HT<sub>4</sub> receptors in HEK293, and SH-SY5Y cells since the phospho-ERK<sub>1/2</sub> antibody was available in Barnes's laboratory. ERK<sub>1/2</sub> phosphorylation is a generic and alternative readout for Gs-coupled receptor activation (Leroy et al., 2007).

The design of this experiments usually involved cell serum starvation prior to any drug application and this is due to the presence of 5-HT in the serum which might interfere with the results. Additionally, serum starvation of the cells can synchronise their cycles and minimise the growth variability (Pirkmajer and Chibalin, 2011). Therefore, the cells were serum starved overnight before agonist stimulation. Unexpectedly, the results showed that the stimulation of endogenous receptor with different doses of 5-HT at different time points was not capable of inducing any phosphorylation in ERK<sub>1/2</sub> in both cells. This could be due to the low expression level of the 5-HT<sub>4</sub> receptor in these cells which was insufficient to mediate intracellular signalling by showing differences in the pERK<sub>1/2</sub> level. Other endogenously expressed GPCRs showed more convincing results in terms of ERK<sub>1/2</sub> activation in which challenging of these cells with 100 µM of carbachol, a muscarinic agonist, showed ERK<sub>1/2</sub> activation at 5 min (see **Supplementary Figure 7**). Carbachol mediated its action through the activation of muscarinic (M<sub>3</sub>) receptors in HEK293 and SH-SY5Y cells (Atwood et al., 2011, Greenwood and Dragunow, 2002, Rosethorne et al., 2008). These receptors might be more abundantly expressed in these cells than the 5-HT<sub>4</sub> receptors.

Likewise, the radioligand binding assay for the endogenous 5-HT<sub>4</sub> receptor in HEK293 cells revealed negative results even with high concentrations of the [<sup>3</sup>H]-5-HT or the membrane protein. This assay was conducted during the testing of the binding affinity of the recombinant 5-HT<sub>4</sub> and 5-HT<sub>6</sub> receptors when overexpressing them in HEK293 cells and the untransfected cells were used as an endogenous control.



It is well known that Western blotting is a very sensitive method for detecting low abundant proteins at nM to pM concentration range. This refers to the ability of the secondary antibody to amplify the immunoreactive signal since several secondary antibodies can interact with a single primary antibody (Bass et al., 2017). This might suggest that the level of 5-HT<sub>4</sub> receptors in HEK293 and SH-SY5Y cells can be detected by Western blotting but that it is inadequate to show functionality or radioligand binding. Also, these cells did not express the 5-HT<sub>6</sub> receptor. Therefore, the work is directed to overexpress both receptors in the HEK293 cell line to study the receptors interactions and to achieve positive results.

### **7.1.3. Future work**

Despite the apparent detection of endogenous 5-HT<sub>4</sub> expression in these cell lines, further experiments should be conducted to fully confirm the antibody specificity potentially by elucidation of the peptide sequence via liquid chromatography-mass spectrometry (LC-MS/MS). This, however, will require access to costly equipment and expertise. Alternatively, knock-down of the receptor gene in these cells, followed by comparison of the receptor level before and after the knock-down could help in determining band specificity.

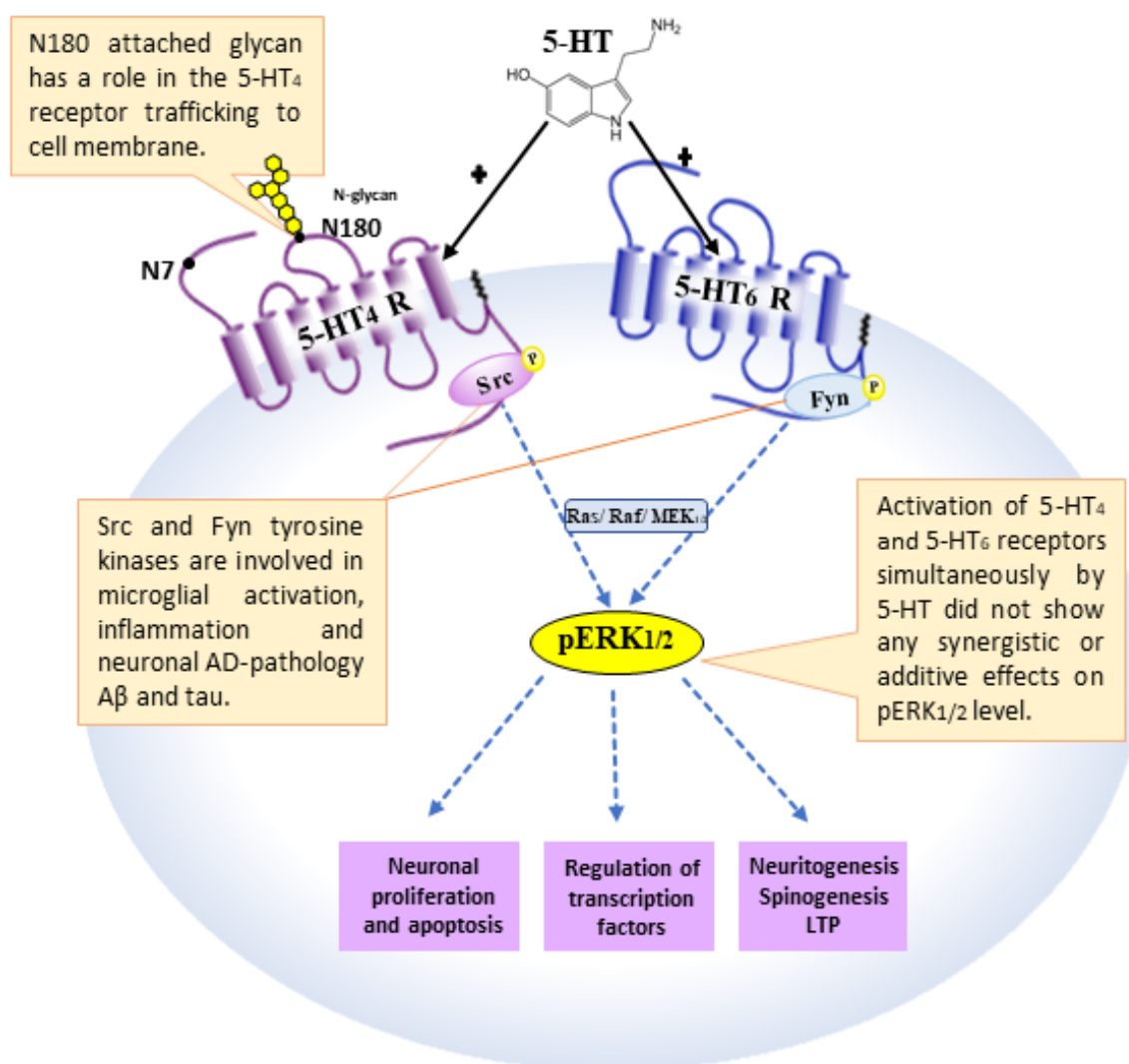
The low native expression of the 5-HT<sub>4</sub> receptors on the cell surface of the SH-SY5Y and HEK293 cell lines described in this work could provide a reason for the negative readout of any attempts to functionally characterise the receptors present. Further optimisation of the 5-HT<sub>4</sub> receptor stimulation protocol should not be excluded as it could show positive results when other selective agonists are used. Furthermore, the use of functional assessment methodologies with high sensitivity, such as the cAMP assay, might help to achieve positive results. Overall, searching for a cell line that

natively co-expresses the two receptors can be time-consuming and is beyond the main scope of this study. However, generating a stable cell line that expresses the recombinant receptors might be necessary to study the functional interaction of 5-HT<sub>4</sub> and 5-HT<sub>6</sub> receptors.

## **7.2. Evaluation of the 5-HT<sub>4</sub> and 5-HT<sub>6</sub> receptors interaction by measuring the pERK<sub>1/2</sub> level**

The HEK293 cell line was utilised as a heterologous expression system because it is widely used to study GPCR signalling since it expresses most of the downstream effectors (Atwood et al., 2011, Huang et al., 2005). Additionally, it exhibits good doubling time and relatively higher transfection efficiency in comparison to the SH-SY5Y cell line. Based on the literature concerning the roles of 5-HT<sub>4</sub> and 5-HT<sub>6</sub> receptors in the context of learning and memory, these receptors have many similarities in their signalling cascades; even though certain discrepancies have also been noted. They share converging signalling pathways through coupling to G<sub>s</sub> protein and activation of the cAMP/PKA/pCREB and RAS/RAF/MEK/ERK pathways which control gene expression and are implicated in LTP as shown in **Figure 53** (Ahmad and Nirogi, 2011, Gelinas et al., 2008).

Previous studies reported that challenging HEK293 cells that overexpressed 5-HT<sub>4</sub> or 5-HT<sub>6</sub> receptors by 5-HT or other agonists produced transient ERK<sub>1/2</sub> activation (Barthet et al., 2007, Riccioni et al., 2011). This work aimed to investigate the interaction between 5-HT<sub>4</sub> and 5-HT<sub>6</sub> receptors and whether the simultaneous stimulation of these receptors can produce synergistic or additive effects, particularly on ERK<sub>1/2</sub> activation.



**Figure 53. Illustration of the interaction between the 5-HT<sub>4</sub> and 5-HT<sub>6</sub> receptors and their effect on ERK<sub>1/2</sub> activation**

*The pERK<sub>1/2</sub> has a critical importance in many cells including neurones. The 5-HT-mediated ERK<sub>1/2</sub> activation occurs upon stimulation of both receptors but without any augmentation response. Sequestration of ERK<sub>1/2</sub> up-stream signalling proteins may cause the lack of augmentation response. The glycosylation of 5-HT<sub>4</sub> receptor at N180 is essential for cell surface expression and function.*

### **7.2.1. Overexpressed 5-HT<sub>4</sub> and 5-HT<sub>6</sub> receptors are functional**

Following selection of the optimum transfection complex ratio, HEK293 cells were transiently transfected with 5-HT<sub>4</sub> or 5-HT<sub>6</sub> receptors which allowed their expression of the receptors for 48-72 hr. The results confirmed the findings of previous studies and recreated the 5-HT-mediated ERK<sub>1/2</sub> activation in HEK293 cells overexpressing either receptor (Barthet et al., 2007, Riccioni et al., 2011). It also indicated that both 5-HT<sub>4</sub> and 5-HT<sub>6</sub> receptors were functional and expressed at the cell surface since the cells responded to 5-HT which binds to the extracellular domains of these receptors. The 5-HT mediated a dose-dependent ERK<sub>1/2</sub> activation but at relatively high doses ( $\geq 10^{-7}$  M) whereas, the cAMP assay exhibits greater sensitivity, attaining the maximum cAMP level at  $10^{-8}$  M of 5-HT (Barthet et al., 2007).

In terms of enzyme kinetics, ERK<sub>1/2</sub> phosphorylation was transient, peaked at 5 min, and subsequently decreased with longer periods of 5-HT incubation. Such a response occurred after stimulation of the overexpressed 5-HT<sub>4</sub> or 5-HT<sub>6</sub> receptors. Regarding the 5-HT<sub>4</sub> receptor, previous work conducted by Barthet et al. (2007) reported that stimulation of the native 5-HT<sub>4</sub> receptor in primary colliculus neurones by 10  $\mu$ M of selective 5-HT<sub>4</sub> agonist produced the maximum ERK<sub>1/2</sub> phosphorylation after 5 min of time course stimulation and this supported the finding of this study. The signalling cascades arising in primary colliculus neurones was similar to that in HEK293 cells that heterologously expressed the 5-HT<sub>4</sub> receptor. ERK<sub>1/2</sub> phosphorylation was independent of the canonical Gs/cAMP/PKA signalling cascade and  $\beta$ -arrestin, instead of being mediated through Src tyrosine kinase activation (Barthet et al., 2007). Src kinase and the downstream pathway is

contributed to microglial activation and inflammation associated with AD (Dhawan and Combs, 2012). The use of Src kinase inhibitor dasatinib in APP/PS1 mice attenuated the active Src, reactive microglia, and reduced TNF $\alpha$  levels in the hippocampus and temporal cortex (Dhawan and Combs, 2012, Nygaard, 2018).

The transient ERK<sub>1/2</sub> activation was also indicated by Norum et al. (2003) study in COS-7 and HEK293 cell lines transiently expressing the 5-HT<sub>4</sub> receptors. For the 5-HT<sub>6</sub> receptor, simulation of the overexpressed 5-HT<sub>6</sub> receptor in HEK293 cells was performed by Riccioni et al. (2011) using ST1936, a 5-HT<sub>6</sub> receptor agonist. This produced dose-dependent ERK<sub>1/2</sub> phosphorylation which peaked at 5 min and was mostly mediated via Fyn kinase activation. This kinase has been involved in neuronal pathology associated with A $\beta$  and tau (Ittner et al., 2010). Overexpression of Fyn in the neurones of hAPP mice deteriorates the A $\beta$ -dependent cognitive impairments, neuronal abnormalities, and causes depletion of calbindin, Fos, and pERK (Chin et al., 2004). Fyn also modulates NMDA receptor transmission and function via its association with the postsynaptic density protein 95 (PSD-95) which responsible for anchoring many proteins essential for cell signalling and LTP (Nygaard, 2018, Salter and Kalia, 2004).

### **7.2.2. Concomitant stimulation of overexpressed 5-HT<sub>4</sub> and 5-HT<sub>6</sub> receptors provides no evidence of functional synergy in ERK<sub>1/2</sub> phosphorylation**

To answer the question of whether the presence of 5-HT<sub>4</sub> and 5-HT<sub>6</sub> receptors could augment each other on ERK<sub>1/2</sub> activation, HEK293 cells were transiently transfected with these receptors simultaneously. Unlike the control cells singly expressing the 5-HT<sub>4</sub> or 5-HT<sub>6</sub> receptors, dual receptors expressing cells did not show any

significant increase in ERK<sub>1/2</sub> phosphorylation in response to dose- or time-dependent 5-HT stimulation (**Figure 53**). The lack of synergy was unexpected as individual receptors increased the pERK<sub>1/2</sub> to a significant level. Moreover, the level of the receptors did not significantly differ between the single or co-transfected cells.

Many mechanisms potentially cause this observation; the mixed expression patterns of the receptors among the cells create distinct subpopulations which might mask the presence of an action synergy between the 5-HT receptors. Moreover, these receptors stimulate converging proteins which might lead to sequestration of the upstream signalling proteins in the ERK<sub>1/2</sub> pathway from the signalling pool and interference with full ERK<sub>1/2</sub> activation. Although such a phenomenon is yet to be proven for ERK, Tubio et al. (2010) identified a similar effect on cAMP level in which overexpressing human histamine H<sub>2</sub> receptors, that are also coupled to Gs protein, resulted in a reduction in the cAMP level below the maximal response following agonist stimulation of other endogenously and transiently expressed GPCRs that signal through the same subfamily of G protein. This reduction was proportional to the expression level of the H<sub>2</sub> receptor, and it was also reproduced with overexpressed  $\beta_2$  adrenoreceptors suggesting this is not specific to the H<sub>2</sub> receptor but rather considers a more general phenomenon. Other speculated possibilities may be ascribed to the inability to detect such synergistic responses including, receptor internalisation, cross-desensitisation and physical inhibition following receptor overexpression. Differences in the expression level of these receptors should also be considered as they may require further optimisation.

As further details about the extent and specificity at which each receptor had contributed to ERK<sub>1/2</sub> activation, particularly in co-transfected cells, selective

antagonists for 5-HT<sub>4</sub> and 5-HT<sub>6</sub> receptors GR-113808 and SB-258585, respectively were used. The phosphorylation of ERK<sub>1/2</sub> was specific to the overexpressed receptor as it was reduced significantly in the presence of the antagonists. The 5-HT mediated-ERK<sub>1/2</sub> activation was more profound with the 5-HT<sub>4</sub> compared to the 5-HT<sub>6</sub> receptor. This result is directly associated with the number of positive cells in the flow cytometry optimisation plots. Pre-treating the co-transfected cells with either antagonist showed that both receptors contributed to ERK<sub>1/2</sub> activation. Indeed, and based on these results, it seems that the signalling of the 5-HT receptors does not result from the simple sequential activation of several proteins, but rather from a complex network activation which is hard to predict.

### **7.2.3. Future prospects to enhance this work**

This work sought to elucidate the interactions between the 5-HT<sub>4</sub> and 5-HT<sub>6</sub> receptors; however, studying the interaction of GPCRs is far more complex and unpredictable. Further optimisation of the transfection ratio could help achieve relatively equal percentages of positive cells. Moreover, using another provider for the 5-HT<sub>6</sub> receptor construct might help to stabilise a cell line with full, non-truncated and highly expressed protein and in doing so achieving greater levels of homogeneity. The inclusion of more selective agonists for each receptor in the ERK<sub>1/2</sub> activation assay could give rise to more arguments in support of the lack of synergy between the two receptors. In future experiments, it would be worthwhile to investigate whether overexpressing upstream signalling proteins (see **Figure 53**) in the ERK pathway such as Src and Fyn tyrosine kinases could influence ERK<sub>1/2</sub> activation and show augmentation response following activation of both receptors.



### **7.3. The presence and impact of *N*-linked glycosylation of the human 5-HT<sub>4</sub> receptor**

*N*-glycosylation is a common post-translational modification which has an essential role in the structural maturation of many GPCRs during the stages of synthesis and secretion. It is also involved in protein folding, stability, localisation and trafficking, as well as ligand-receptor interactions (Jones et al., 2005, Wheatley and Hawtin, 1999). This modification is initiated in the ER and finalised in the Golgi apparatus. From this location, the proteins are either transported to the lysosomes or integrated into the cellular membrane. The second form of glycosylation is *O*-glycosylation which primarily takes place in the Golgi apparatus by the linking of a glycan to the serine or threonine residues but without a well-known consensus sequence (Jones et al., 2005, Nilsson et al., 2013).

Unlike RNA transcription or protein translation, *N*-glycosylation is a non-templated process. It involves different steps including glycan linkage, trimming and chain elongation or branching during every glycosylation event. This creates highly diverse glycoproteins in a given expressing system. Like many other transmembrane proteins, the 5-HT<sub>4</sub> receptor is subjected to glycosylation during protein synthesis at the putative asparagine residues (Salom et al., 2012).

While the consensus sequence (N-X-Serine/Threonine) appears to be a prerequisite for *N*-glycosylation, it is not always apparent that this type of modification ensues. Moreover, it also appears to be influenced by consensus accessibility and location, protein's properties, enzyme kinetics, substrate concentrations and even the type of expressing cells (Gupta and Brunak, 2002, Jones et al., 2005, Nilsson et al., 2013). It has been noted, however, that the glycosylation of the asparagine residue can

occur in an unusual consensus sequence (N-X-Cysteine) (Gavel and Heijne, 1990).

In addition, in order for glycosylation to take place, the consensus sequences must be positioned towards the anterior side of the ER. Thus, not all of them are suitable to function as an acceptor site for glycosylation. This variation in site occupancy with *N*-glycans is denoted as macroheterogeneity where certain asparagine residues in potential consensus are authentically glycosylated while others are not in any one protein (Jones et al., 2005). Another variation referred to as a microheterogeneity is one where the type of the attached glycans may differ down to a single glycosylation site (Jones et al., 2005). There are three common types of *N*-glycans: high-mannose which consists of two N-acetylglucosamine (GlcNAc) and five to nine mannose molecules, a complex type containing GlcNAc, galactose, sialic acid, and/or fucose molecules, and a hybrid type which has shared molecules of the former two types (Wheatley and Hawtin, 1999).

To allow understanding of how the *N*-glycosylation for this receptor is proceeding, it would be useful to briefly review the processes by which proteins are modified during their synthesis to attach the oligosaccharide to the putative asparagine residues. Moreover, the significance of such modifications on the protein structure, secretion and function may also be understood.

### **7.3.1. *N*-glycosylation from protein synthesis to the final destination**

*N*-glycosylation is a complex multi-step process which begins as a co-translational event in the ER (reviewed by Wheatley and Hawtin, 1999), where a dolichol pyrophosphate carries a core oligosaccharide consisting of two N-acetylglucosamine, nine mannose and three glucose molecules (GlcNAc<sub>2</sub>-Man<sub>9</sub>-Glc<sub>3</sub>). This oligosaccharide is assembled through the addition of these sugars in a

step-wise manner. Subsequently, this pre-assembled oligosaccharide is transferred *en bloc* via oligosaccharide transferase from the dolichol carrier to the nitrogen in the amide group of an asparagine residue once the consensus site is recognised inside the lumen of the ER. This forms a covalent N-glycosidic bond between the oligosaccharide and the protein (Wheatley and Hawtin, 1999).

During the whole process, there are continuous quality control steps included to ensure proper protein folding before exiting the ER. These steps involve the trimming and elaboration of glucose sequentially until the final protein confirmation is achieved. Initially, two glucose residues are trimmed by glucosidase which makes the protein detectable to two ER resident lectins; calnexin and calreticulin. These lectins can fold the protein and form a disulphide bridge (Caramelo and Parodi, 2008). Trimming of the last glucose residue prevents this recognition and allows the protein transfer to the Golgi. Any misfolded or unfolded protein is usually recognised by UDP-glucose: glycoprotein. This is a glucosyltransferase which adds one glucose residue and returns the protein to the calnexin/calreticulin cycle for refolding. Failure of proper folding within a time limit will force the protein towards proteolytic degradation (Jones et al., 2005).

In addition, it has been suggested that glucose trimming is essential for effective transfer of the glycoproteins from the ER to the Golgi (Kornfeld and Kornfeld, 1985). Subsequently, the glycoproteins traverse via vesicles from the cis to the trans cisternae. During this process, a wide variety of sugar molecules are added to produce the mature protein form. These sugars include mannose, galactose, N-acetyl galactosamine (GalNAc), fucose and sialic acid (Wheatley and Hawtin, 1999).

As little is known about the *N*-glycosylation of the 5-HT<sub>4</sub> receptor, this work investigated the presence of *N*-glycan in the 5-HT<sub>4</sub> receptor via enzyme inhibition and mutation approaches. The potential impact of *N*-glycosylation on receptor trafficking to the cell surface was also tested using a combination of immunoreactive techniques such as Western blotting and ICC. The human Flag-tagged 5-HT<sub>4</sub> receptor was stabilised in HEK293 cells. The single-point radioligand binding assay revealed that the [<sup>3</sup>H]-5-HT bound explicitly to the overexpressed 5-HT<sub>4</sub> receptor at a detectable level. This was in contrast to the endogenously expressed 5-HT<sub>4</sub> receptor in HEK293 cells which showed negative RLB results. This confirms that the expression level of the receptor can influence the detection of receptor functionality or binding affinity to the radioligand.

### **7.3.2. The human 5-HT<sub>4</sub> receptor is *N*-glycosylated in HEK293 cells**

The stable Flag-tagged human 5-HT<sub>4</sub> receptor showed multiple ‘smeared’ immunoreactive bands at higher molecular weights than expected. This shift in the electrophoretic mobility could be due to *N*-linked glycosylation of this receptor. To confirm this, *de novo* *N*-glycosylation inhibitor tunicamycin was added to the growth medium. Tunicamycin caused reduction of the high size receptor species and compressed the multiple bands to a single band at a lower molecular weight. Accordingly, an enzyme inhibition approach by tunicamycin confirmed the presence of *N*-glycosylation in the human 5-HT<sub>4</sub> receptor which was stabilised heterologously in HEK293 cells.

However, such a large increase in the 5-HT<sub>4</sub> receptor size implies glycosylation of multiple asparagine sites or attaching of a complex polysaccharide chain. Indeed, the 5-HT<sub>4</sub> receptor has two possible sites for *N*-glycosylation located at position 7

of the N-terminal domain and at position 180 of ECL2 (Salom et al., 2012). To assess whether one or both sites were glycosylated, a mutation approach was used by generating constructs with disrupted asparagine residues, and then determine their electrophoretic mobility in SDS-PAGE.

### **7.3.3. The N180 of the 5-HT<sub>4</sub> receptor is the only site of glycosylation in HEK293 cells**

Disruptions of the glycosylation consensus sequence at position 7 and 180 either individually or together were utilised to determine the exact glycosylation site. Western blot analysis revealed that N180 was the only authentic glycosylated site, particularly in the employed cell line. In contrast, N7 did not show any sign of glycosylation. These findings were similar in all the clonal cell lines expressing the N7Q or N180Q mutant receptors. The presence of the Flag tag close to N7 is unlikely to cause any steric hindrance that might have interfered with the glycosylation of this site because there were ten amino acids between the tag and N7.

In addition to position difference, N7 and N180 also differ in the third amino acid of the consensus sequence with N7 containing a serine (N7-V-S) and N180 a threonine (N180-S-T). This simple difference could describe the macroheterogeneity of 5-HT<sub>4</sub> receptor glycosylation. In Gavel and Heijne (1990) study, the frequency analysis of different glycoproteins showed that the N-X-T sites had been reported to be glycosylated three times more often than the N-X-S sites as the former was more rapidly glycosylated. In addition, a study on rabies virus glycoprotein, which is well known to be inefficiently glycosylated at N37 (Shakin-Eshleman et al., 1992), revealed that substitution of the third serine to threonine at position 39 significantly increased the core glycosylation efficiency and enhanced

the cell surface expression (Kasturi et al., 1995). The results of both these studies, therefore, support the data obtained from this study.

Of particular relevance to this study, Salom et al. (2012) estimated the tendency of glycosylation of the human 5-HT<sub>4</sub> receptor expressed in mouse rod cells as 75% for the N7 site and nearly 100% for the N180 site based on the deglycosylation rate of PNGase F. However, they did not verify the effects of single and double mutations of these sites on the electrophoretic mobility or the trafficking of the receptor. Therefore, it seems that the glycosylation pattern of the 5-HT<sub>4</sub> receptor overexpressed in mouse rod cells was glycosylated more homogeneously (i.e. both sites were glycosylated) than the HEK293 cell line which showed one site of glycosylation.

The *N*-glycosylation occurs solely in the extracellular domains of the GPCRs including the N-terminus and the extracellular loops (ECLs). Screening of the GPCR database revealed that approximately 66% of the human non-orphan GPCRs are preferentially *N*-glycosylated on the second extracellular loop (ECL2), 14% on ECL1 and 20% on ECL3 (Lancot et al., 2005). No studies, however, had compared the percentages of glycosylated GPCRs in the N-terminus to the extracellular loops.

A few discrepancies were identified in the extent and the pattern of glycosylation between the transient and the stably expressed 5-HT<sub>4</sub> receptor. Both transfection conditions showed immunoreactive species at approximately 41 and 50 kDa which represented the unglycosylated and glycosylated receptors, respectively. The signal intensity of these species had achieved highly opposing levels of expression with a high level of the 41 kDa species detected in the transient expression but a low level detected in the stable expression. The 50 kDa species was expressed at a very low

level in transient expression but at a high level in stable expression and appeared as a diffused band—most likely due to heterogeneity in the *N*-glycans attached. The reasons behind these differences could be related to the duration and the level of expression in which the transiently overexpressed 5-HT<sub>4</sub> receptor in HEK293 cells is produced for a short time, 3 days maximum, which is not enough for the glycosylation machinery to glycosylate all the translated proteins, therefore resulting in only a small portion being glycosylated. Alternatively, the high level of the translated proteins during transient expression may exert stress on such machinery and produce heterogeneity in glycosylation. The outcome changed following the stable incorporation of the receptor into the chromosome (a rare event), which resulted in an increase in the duration of receptor expression albeit at a lower level than that of the transient expression. Therefore, protein stabilisation may aid the glycosylation machinery in attaching the *N*-glycan to the majority of the translated proteins. Sadeghi et al. (1997) found a similar pattern of protein expression during their work on the vasopressin V2 receptor. They revealed that the transient expression of this receptor produced high levels of immature proteins (unglycosylated) and low levels of fully mature proteins (glycosylated) and the opposite was true upon protein stabilisation.

In addition, the size increase of the stabilised 5-HT<sub>4</sub> receptor (glycosylated species) to approximately 49-56 kDa from the unglycosylated receptor size of approximately 41 kDa, is considered novel because such an increase for one glycosylation site (N180) indicated that the sizes of the attached *N*-glycans ranged from approximately 8-15 kDa. Detection of such a significant shift in protein size by SDS-PAGE indicates the presence of multiple glycosylation sites. This, however, does not hold true for the 5-HT<sub>4</sub> receptor in this expression system where only one site is truly

glycosylated based on mutation results. To confirm whether the stable cell lines incorporated the coding sequence of the 5-HT<sub>4</sub> receptor in their cell chromosome while maintaining the mutation sites, RNAs were extracted, reverse-transcribed and amplified by primers flanking the consensus sequence at the N7 and N180 sites. The sequencing data showed that each cell line expressed the correct transcripts corresponding to the target protein sequence as expected. Therefore, this makes it highly likely that a very complex glycan was attached at the N180 site. Occasionally, *N*-glycans may undergo several elaborating steps after being bound to proteins to form large and extensively branched glycans. To our knowledge, no previous studies showed that one site glycosylation of GPCRs could produce an approximately 8-15 kDa size increase. Usually, the increase in receptor size is expected to be between 2-4 kDa per one *N*-glycosylation site. Many GPCRs exhibited a corresponding increase in their size after transient expressions such as the human 5-HT<sub>5A</sub> receptor which possessed a 3-4 kDa increase per each glycosylated site positioned at N6 and N21 (Dutton et al., 2008). The angiotensin II receptor subtype I (AT1) also exhibited a close size range for each of the glycosylated species at N4, N176, and N188 (Lancot et al., 1999). Indeed, such small size shifts (2-4 kDa) occur with the commonly attached *N*-glycans. Glycomic profiles of the *N*-glycans showed that some complex types contained sugar molecules of 13 kDa size or even larger in glycosylation mutant CHO cells (North et al., 2010). Based on these data, future analysis of the composition of this glycan is required to determine whether it meets the expected size.



#### **7.3.4. N180 is important for 5-HT<sub>4</sub> membrane integration**

The capability of certain GPCRs to reach the final destination on the cell surface membrane is dependent at least, in part, on the presence of *N*-glycosylation. For instance, the surface expression level of the de-glycosylated AT1 receptor mutant was significantly reduced, and the protein was distributed more intracellularly in HEK293 cells (Lancot et al., 1999). Likewise, the impact of disruption of the *N*-glycosylation site on protein trafficking to the cell surface expression was also detected with other GPCRs such as the 5-HT<sub>2A</sub> receptor (Maginnis et al., 2010), glucagon-like peptide 1 (GLP-1) receptor (Chen et al., 2010),  $\beta_2$  adrenoreceptor (Mialet-Perez et al., 2004), P2Y<sub>2</sub> purine receptor (Nakagawa et al., 2017), and bradykinin B2 receptor (Michineau et al., 2004). Nonetheless, there are several GPCRs where the mutation induced deglycosylation did not alter their membrane expression; such as the GPR61 orphan receptor following the substitution of asparagine (N12) with serine (Kozielewicz et al., 2017). To this day, the reason behind these inconsistencies is not known. It may, however, be related to the variability of the receptor secretion process or the expressing cells.

An immuno-localisation assay of the wild-type and mutant 5-HT<sub>4</sub> receptors indicated that disruption of the N7 site did not affect the trafficking of the receptor to the cell surface as it was actually not the site of glycosylation as shown by Western blotting. Whereas, the disruption of N180 markedly affects the receptor cell surface expression with most of the receptor primarily localising to the area surrounding the nucleus. This mutation trapped the receptor within intracellular compartments; specifically, the ER and Golgi apparatus. Double mutation at N7 and N180 showed a similar localisation pattern of the N180 mutant. This provided evidence

demonstrating that a 5-HT<sub>4</sub> receptor with N180Q point mutant being capable of impacting receptor activity as it would hinder the receptor's integration into the plasma membrane when compared to the wild-type 5-HT<sub>4</sub> receptor. In addition, and based on NCBI database, SNPs have not been found in the 5-HT<sub>4</sub> receptor gene particularly at the position coding for N180.

In addition to *N*-glycosylation, there are several other proteins capable of influencing 5-HT<sub>4</sub> receptor trafficking to the target cellular compartments and offering a tuning of their downstream signalling pathways (Bockaert et al., 2006). These intracellular proteins are known as GPCR-interacting proteins (GIPs) (Bockaert et al., 2006, Joubert et al., 2004). In this work, specifically, isoform a of the 5-HT<sub>4</sub> receptor was used. This isoform has a class I post-synaptic density-95/disc-large/zonula-occludens-1 (PDZ) binding domain present at the end of the C-terminus (Joubert et al., 2004). Among GIPs that bind specifically to this domain are the Na<sup>+</sup>/H<sup>+</sup> exchanger regulatory factor (NHERF) and sorting nexin 27 (SNX27). NHERF recruits the 5-HT<sub>4</sub> receptor to the membrane microvilli and regulates cytoskeleton remodelling, while SNX27 promotes receptor trafficking to early endosomes, thereby reducing membrane expression (Joubert et al., 2004).

#### **7.3.5. Further studies on the role of *N*-glycosylation of the 5-HT<sub>4</sub> receptors; future prospects**

Besides the receptor trafficking to the cell membrane, the role of *N*-glycosylation with respect to 5-HT<sub>4</sub> receptor functionality, binding affinity and protein degradation had not yet been investigated. Therefore, further studies are required to perform in-depth analysis of the other implications of *N*-glycosylation on this receptor. It will be interesting to study the effect of overexpression of SNX27 and

NHERF on the cell surface expression of the N180 mutant receptor. These studies should ultimately increase understanding of the interactions between these proteins and the 5-HT<sub>4</sub> receptor. Of further interest would be the analysis of the structure of the unusual *N*-glycan attached to the N180 site of the 5-HT<sub>4</sub> receptor heterologously expressed in HEK293 cells using detailed mass spectroscopy.

#### **7.4. Differential expression of 5-HT<sub>4</sub> and 5-HT<sub>6</sub> receptors in accordance with the pathological severity of AD**

The pathological severity of AD is classified according to topographical distribution of tau lesions in the entorhinal, limbic and neocortical regions. These distinct brain regions may exhibit different and region-specific changes in the expression of 5-HT receptors. Many studies have shown how AD is associated with changes in the serotonergic neurotransmission which primarily results in the behavioural and psychological symptoms of this disease. Serotonin 5-HT<sub>4</sub> and 5-HT<sub>6</sub> receptors have become a focus of a concerted research effort because modulation of these receptors in pre-clinical studies shows beneficial outcomes in terms of memory and cognition while also resulting in improvement of disease symptoms. Evaluation of the expression of these receptors during disease progression is necessary because it can provide further insights into the gradient changes of receptor expression, and thus the regulation of 5-HT neurotransmission. In addition, the correlation of the expression of these receptors to the cognitive functions and risk factors of AD can help in specifying the best time and strategies for therapeutic interventions.

#### **7.4.1. Changes in the expression of the 5-HT receptors in the frontal cortex of AD patients at different disease stages**

The expression of 5-HT<sub>4</sub> and 5-HT<sub>6</sub> receptors was quantitatively investigated by measuring the gene and the protein expressions in the frontal cortex of AD patients and healthy controls. This was accomplished to determine whether changes in the expression of these serotonin receptors exists early in the course of the disease since limited studies confirmed the reduction of these serotonin targets at the late AD stage (Lorke et al., 2006, Reynolds et al., 1995). To the best of our knowledge, no study had assessed the expression of these receptors in the frontal cortex at the early AD stage. Surprisingly, no studies investigating the expression differences in the mRNA of 5-HT<sub>4</sub> and 5-HT<sub>6</sub> receptors in AD have been reported.

##### ***7.4.1.1. The mRNA expression of 5-HT<sub>4</sub> and 5-HT<sub>6</sub> receptors***

The absolute qPCR quantification method was used in this work, thereby allowing the comparison of the transcript levels of the 5-HT<sub>4</sub> and 5-HT<sub>6</sub> receptors. Both receptors had been normalised to the same housekeeping gene and denoted as a normalised ratio. Despite the small number of cases in each group, no difference existed between the expression levels of the two receptors in the different stages of the disease. Regarding *HTR4* expression, the analysis showed significant up-regulation of this gene in the early AD stage (limbic stage) relative to controls while no difference was detected with the late AD stage (neocortical stage). This increase in *HTR4* gene expression might be an evoked compensatory response to overcome the reduction in the protein expression of the 5-HT<sub>4</sub> receptor in the limbic AD stage as detected by its immunoreactivity in the frontal cortex. Alternatively, a reduction of the interstitial level of 5-HT might cause feedback up-regulation of the 5-HT<sub>4</sub>

receptor transcription to restore its serotonergic tone through this post-synaptic receptor prior to it being lost at later stages of the disease.

Compensatory mechanisms during the early phases of AD are common phenomena with other neurotransmitter systems. Counts et al. (2007) found an up-regulation of the mRNA of  $\alpha 7$  nicotinic receptor in the cholinergic neurones of the nucleus basalis in mild to moderate AD cases compared to those who had mild or no cognitive impairment. In addition, the mRNA of the  $M_1$  muscarinic receptor was significantly increased in the temporal cortex as a response to the deficit in the cholinergic system (Harrison et al., 1991). Moreover, transcript up-regulation can also accompany the late stage of AD as in the case of the glutamatergic kainate receptor in the hippocampus (Jacob et al., 2007).

Notably, the qPCR results generated reflected the expression of all the splice variants of the 5-HT<sub>4</sub> receptors since the TaqMan primer/probe set (5-HT<sub>4pan</sub> primers) did not discriminate between them. An earlier study quantified *HTR4* expression in various human brain regions (Medhurst et al., 2001). This revealed that the pan *HTR4* expression was highest in the basal ganglia tissues of the caudate and putamen, followed by the amygdala and hippocampus and less abundant in the temporal cortex. Each individual transcript was expressed at various densities within the brain. The 5-HT<sub>4b</sub> isoform was the most abundant followed by 5-HT<sub>4a, c</sub> then 5-HT<sub>4g</sub>, but the 5-HT<sub>4d</sub> isoform was not detected (Medhurst et al., 2001). To date, none of these isoforms have been linked to any neuropsychological disorders as it would be difficult to distinguish between isoforms in such studies.

On the other hand, the expression of the 5-HT<sub>6</sub> receptor transcript was less conclusive due to the limited number of AD cases in the limbic stage group but,

regardless of this drawback, there were no differences detected in the relative gene expression of 5-HT<sub>6</sub> receptors throughout disease progression between the controls and that of advanced AD. PMD or agonal status of certain study individuals can reduce the mRNA stability which could be the reason behind the lack of proper gene amplification.

#### ***7.4.1.2. The protein expression of 5-HT<sub>4</sub> and 5-HT<sub>6</sub> receptors***

It cannot be assumed that the changes in the transcript levels of 5-HT<sub>4</sub> and 5-HT<sub>6</sub> receptors are accompanied by equivalent changes in the receptor proteins, since alterations in the protein translation efficiency and mechanisms may occur in AD. These receptors are the functional molecules in the neurones and the ones most likely to be targeted for drug discovery. Therefore, evaluation of the receptor expression at the protein level can provide more stable readout than at the transcript level.

For measurement of DAB immunoreactive signals that reflected the expression of serotonin receptors and transporter, a quantitative image analysis-based method was used. This approach can provide a good measurement for the DAB positive area per cell despite the variance of the obtained brain tissue samples. This automated approach was used instead of the traditional visual scoring technique as it resulted in less visual bias. Moreover, the results obtained can be presented as continuous values rather than as discrete scores. Quantification of the results by colour intensity was also avoided because DAB is a non-linear chromogen (van der Loos, 2008); thus the surface area was used instead. According to Dickerson et al. (2009) study, the reduction of the temporal cortex in AD patients was primarily due to the thinning of these regions. For these reasons, the disease-associated changes in the gray matter

were also considered in the quantification by normalising the positive immunoreactive area to the neuronal cell count. However, in this study, there was no discrimination between the phenotypes of the DAB positive cells, and the results indicated the total DAB immunoreactivity.

The overall expression of the 5-HT<sub>4</sub> receptor is relatively low in the human brain in comparison with non-human brains (Reynolds et al., 1995). In terms of cellular localisation, the immunoreactivity of the 5-HT<sub>4</sub> receptor in the prefrontal cortex was detectable mainly in the soma of pyramidal neurones of the cortical layer III and V. This observed receptor localisation corroborates the result of the previous dual-label *in situ* hybridisation study showing positive 5-HT<sub>4</sub> receptor expression in the rat hippocampal and cortical pyramidal neurones (Penas-Cazorla and Vilaro, 2015).

Interestingly, the immunoreactivity of the 5-HT<sub>4</sub> receptor in the prefrontal cortex was gradually and significantly reduced with AD progression. This reduction began in the early stage and continued through to the late stage of AD. The prefrontal cortex, at the early AD stage, is less likely to be affected by the pathological tau lesions but A $\beta$  plaques can accumulate at this stage or even before the appearance of clinical symptoms (Morris and Price, 2001). Therefore, the down-regulation of the 5-HT<sub>4</sub> receptor might be related to early A $\beta$  accumulation and not tau lesions. Many studies emphasised the role of the 5-HT<sub>4</sub> receptor on the A $\beta$  level in the cell lines and cortical neurones (Cho and Hu, 2007, Cochet et al., 2013, Robert et al., 2005) and *in vivo* (Giannoni et al., 2013). Activation of the 5-HT<sub>4</sub> receptors can reduce A $\beta$  accumulation by regulating APP processing towards the non-amyloidogenic pathway. On the other hand, the early accumulation of A $\beta$  in a transgenic mouse model of AD can cause gradual axonal degeneration of 5-HT

afferent neurones in the cortex and hippocampus (Liu et al., 2008). This degeneration is due to A $\beta$  accumulation which also occurs in the pyramidal neurones (Revett et al., 2013). Accordingly, bidirectional regulation appears to exist between the 5-HT<sub>4</sub> receptor and A $\beta$ , but this definitely needs further investigation.

Most of the expression analysis studies of this receptor stemmed from RLB assays which usually overlooked the different stages of AD. Reynolds et al. (1995) reported that the 5-HT<sub>4</sub> receptor binding density was decreased in the hippocampus, temporal cortex and prefrontal cortex in post-mortem AD brains which supported the findings of this study. Contrastingly, by using [<sup>11</sup>C]-SB-207145 PET scan, Madsen and others (2011) found no difference in 5-HT<sub>4</sub> receptors binding between AD patients and the controls. In addition, the affinity and density of [<sup>3</sup>H]-GR113808 were unchanged in AD compared to controls in frontal and temporal cortices (Lai et al., 2003). So far, there are no pre-clinical studies showing variations in 5-HT<sub>4</sub> receptor expression in AD animal models (Rebholz et al., 2018).

Regarding the 5-HT<sub>6</sub> receptor, the immunoreactivity was apparently detected in the cell bodies, axons and the dendrites of pyramidal neurones of layer III and V, which were distinguished based on morphology. It was also detected in the granular cells in layers II and IV. This immune-localisation was in agreement with Lorke et al. (2006) study in which IHC had been used to determine the cellular expression of the 5-HT<sub>6</sub> receptor in the frontal cortex of AD patients and controls. Also, Marazziti et al. (2013) studied 5-HT<sub>6</sub> receptor distribution in the prefrontal cortex of post-mortem human controls. They used double immunofluorescence staining to characterise the 5-HT<sub>6</sub> receptor positive cells by their phenotypic antigens: neuronal nuclear antigen (NeuN, neuronal cell marker) and glial fibrillary acidic protein



(GFAP, glial cell marker). Their results revealed the co-localisation of 5-HT<sub>6</sub> receptors with the NeuN in pyramidal neurones of layer III, and this was consistent with the findings of this study. They also showed the receptor co-localisation with the GFAP in astrocytes of layer I (Marazziti et al., 2013).

The quantification analysis of 5-HT<sub>6</sub> receptor expression following normalisation to the nuclei count showed no significant difference in the immunoreactivity between the controls and the other AD stages in the frontal cortex, nevertheless; there was a slight increase in the immunoreactivity in the limbic AD stage. In the limbic stage, the cortex is usually intact and probably responds to the pathological proteins accumulated in the limbic region by modulation of the expression of the serotonin receptor. However, this hypothesis needs further studies involving parallel staining of the brain section from the limbic regions with the frontal cortex at different stages of the disease. This increase in 5-HT<sub>6</sub> immunoreactivity in the limbic stage resulted in the difference between limbic and neocortical AD stages being statistically significant as the immunoreactivity in the later stage was reduced.

Furthermore, Lorke et al. (2006) revealed a 40% significant reduction in the numerical density of 5-HT<sub>6</sub> receptor immunoreactive neurones in BA10 cortical regions of AD patients relative to controls. The total quantification area of Lorke et al. study was 0.21 mm<sup>2</sup>, whereas this study used a relatively larger area (0.24 mm<sup>2</sup> which was averaged from 3 images) and more study cases than those used in Lorke et al. study. This may explain why no significant reductions between the controls and AD cases were detected in this study. Indeed, interpretation of the 5-HT<sub>6</sub> receptor expression requires additional tissue samples in the control and limbic

groups to determine whether the difference between the early and late stages of AD could be detected between the controls and the late stage of AD.

#### **7.4.2. Changes in SERT expression in the frontal cortex of AD patients at different disease stages**

Assessment of SERT immunoreactivity in the prefrontal cortex during AD evolution can extend insights into the AD-associated changes on the serotonergic fibres since SERT is considered a stable marker for these fibres. In accordance with Raghanti et al. (2007) finding, SERT immunoreactive fibres were widely distributed through the cortical layers. The two morphological forms of serotonergic fibres “axons” were clearly distinguished; they either appeared as diffused fibres with small and regularly spaced varicosities or as clustered fibres with irregularly spaced varicosities.

Interestingly, some neuronal cell bodies, apparently pyramidal neurones, had little immune-reactive staining but in the cortices of AD patients more than in controls. This observation is unexpected because the SERT immunoreactive cell bodies are typically found in the raphe nuclei in the adult brain. However, in early life, during brain development, SERT can be detected in non-serotonergic neurones in humans (Verney et al., 2002). In postnatal mouse brains, SERT can be found transiently in glutamatergic pyramidal neurones in the cortex (Soiza-Reilly et al., 2018). This transient expression enables these neurones to uptake 5-HT for the formation of a neuronal circuit between the dorsal raphe nuclei and the prefrontal cortex (Soiza-Reilly et al., 2018). However, it could be argued that the presence of SERT immunoreactivity in these neurones was not transient and possibly disease-related

since it was consistently detected mostly in the AD brains. Thus, further investigations are needed to understand this equivocal observation.

The quantitative analysis of SERT immunoreactivity in cortical layer III revealed that these transporters were reduced significantly at the neocortical stage of the disease only and not changed at the limbic stage. This reduction was detected even before normalisation. This change in SERT expression at the late stage of the disease can affect the extracellular 5-HT levels and consequently influence its action through 5-HT receptors. Similarly, the density of SERT in the prefrontal cortex of post-mortem controls and AD patients with and without depression was assessed by Thomas et al. (2006) using autoradiography. They found that the density of the transporter was significantly reduced in AD regardless of the presence of comorbid depression. It should be noted that neither of the protein expression results could be explained by the putative demographic differences in demographics between the control and the disease groups as they were not significant.

#### **7.4.3. The influence of AD risk factors on the expression of serotonin proteins**

The two most common AD risk factors namely Hcy and ApoE4 were considered in this study. Comparing the immunohistochemistry results obtained to the clinical categorical variables would provide an insight into the clinical-biological associations between ante-mortem and post-mortem data. In this study, categorising the study AD cases and controls according to their plasma Hcy level did not show any association with the expression of 5-HT<sub>4</sub> and 5-HT<sub>6</sub> receptors and SERT transporter even when disease severity was considered. This lack of significant association may be the result of low patient numbers (study underpowered).

Depressed patients with high Hcy levels had significantly low serotonin metabolites in the cerebrospinal fluid which has been implicated in the pathology of depression (Bottiglieri et al., 2000). Nevertheless, the serum Hcy level was found to be positively correlated with behavioural and psychological symptoms of AD (Kim and Lee, 2014), and negatively correlated with the plasma level of 5-HT at postpartum depression (Aishwarya et al., 2013).

Categorising the study AD cases and controls according to the ApoE 4 genotype showed that the presence of one or two alleles of ApoE 4 was significantly associated with higher 5-HT<sub>4</sub> receptor immunoreactivity, particularly in the control and the limbic AD stage. The pattern of high 5-HT<sub>4</sub> receptor expression in the gene carriers was also observed with the 5-HT<sub>6</sub> receptor expression in the control group but not at a statistically significant level. The influence of the ApoE 4 genotype on these receptors might reflect one of many adaptive changes that may take place prior to the initiation of any symptoms. Several studies confirmed that the ApoE4 carrier exhibited various anatomical and metabolic changes in the brains even in asymptomatic cognitively intact adults relative to non-carriers. Examples of these changes include lower gray matter density (Wishart et al., 2006), lower glucose metabolism in late-middle-aged carriers (Small et al., 2000) and in the young adult (Reiman et al., 2004) but increased brain activity measured by oxygen and blood perfusion at rest and during memory encoding task (Filippini et al., 2009). In the ApoE gene-targeted replacement mouse model, Chhibber and Zhao (2017) demonstrated that the cortical expression of the 5-HT<sub>2A</sub> receptor, but not the 5-HT<sub>1A</sub>, was higher in the ApoE4 carrier relative to ApoE2 and ApoE3 carrier brains. The mechanism by which this gene-phenotype influenced the serotonin receptor expression is not known and needs further investigation.

#### **7.4.4. Association between the expression of serotonin receptors in the prefrontal cortex and cognitive functions**

The regression analysis in this study showed the contribution of the expression of serotonin proteins in addition to the AD-related tau pathology to the cognitive functions. Variation of cognitive functions could be predicted by the level of AT8 tau protein, 5-HT<sub>4</sub> and 5-HT<sub>6</sub> receptors and SERT. However, the directions of this association are varied for each protein. As expected the AT8 tau is the primary contributor on the cognitive scores; as tau increases, it causes deterioration of the cognitive status of the AD patients (Mitchell et al., 2000). Both 5-HT<sub>4</sub> receptor and SERT expressions are directly associated with the cognitive function because the level of these proteins is reduced with AD evolution that usually accompanies gradual cognitive decline.

Interestingly, and similar to the AT8 (although not as strong) the correlation direction of 5-HT<sub>6</sub> receptors with cognitive functions was negative in both cognitive tests; MMSE and CAMCOG, indicating that individuals who have a higher receptor level of this protein tend to have lower cognitive scores. This negative correlation between the expression of 5-HT<sub>6</sub> receptors with cognitive function can be supported by Mitchell et al. (2006) findings in rats. The overexpression of the 5-HT<sub>6</sub> receptor in rat dorsomedial striatum interfered with the acquisition or consolidation of reward habituated instrumental learning which is site-specific for the striatum. This learning impairment might be due to the strengthening of the GABAergic inhibitory effect on the glutamatergic and cholinergic transmissions (Mitchell et al., 2006). Moreover, and based on the physical interaction of the 5-HT<sub>6</sub> receptor and the mTOR which is reported in the Meffre et al. (2012) study, the increase in the expression of

the 5-HT<sub>6</sub> receptor might cause dysregulation of the mTOR pathway which had a negative consequence on cognition (Oddo, 2012, Yates et al., 2013). Other serotonin receptors were previously measured in post-mortem cortices of controls and AD patients. For example, the 5-HT<sub>2A</sub> receptor expression was assessed by [<sup>3</sup>H]-ketanserin binding. The results achieved demonstrated that AD-related loss of this receptor was directly associated with the cognitive decline without consideration for ChAT activity or disease severity (Lai et al., 2005). Taken together the increase in 5-HT<sub>6</sub> receptor did not necessarily lead to improvement in the cognitive status. This observation makes the 5-HT<sub>6</sub> receptor different from the 5-HT<sub>2A</sub> and 5-HT<sub>4</sub> receptors.

#### **7.4.5. Future directions**

As protein expression analysis was only determined through IHC, alternative techniques, such as Western blotting and RLB experiments, will have to be conducted to support the IHC results. This can be achieved by using frozen cortical brain samples from AD patients and controls at different disease stages, but these samples were not available at the time of this study. Another significant step forward would be studying the impact of the AD evolution on the serotonin receptors expressed in other brain regions such as the hippocampus, striatum and temporal cortex to compare the level of the serotonin proteins in different brain regions, by using IHC, RLB and autoradiography. Further longitudinal cohort studies are essential to determine the relationship between the 5-HT<sub>6</sub> receptor/ mTOR pathway and the cognitive status of AD patients.

### **7.5. Limitations and critique**

Although this study has addressed its main aims, it encountered some limitations. The short time frame for the lab work was the main restraint. Some experiments showed negative results which changed the direction of the lab work, from the search for endogenously expressed 5-HT receptors in cell lines to overexpression of these receptors. While receptor overexpression is a good option to study the receptor interaction and signalling, it might not act as a true representation of the native receptor condition in primary cells which are hard to maintain. Different screening methods were used; including Western blotting, flow cytometry and RLB during the attempts to stabilise the 5-HT<sub>6</sub> receptor in HEK293 cells and none of the stabilised clones were expressing the protein as required. The difference in the percentage of positive cells transfected with either the 5-HT<sub>4</sub> receptor or the 5-HT<sub>6</sub> receptor can be minimised by further optimisation and repetition, and this also requires more time.

Assessment of the mRNA expression by qPCR was completed with only a few samples showed amplification, particularly in the limbic AD group, and this is due to potential DNA degradation. In the IHC staining, the number of cases in each study group was different; the neocortical cases were almost double the controls and the limbic cases; this was solely related to tissue availability. Although the comparison between the study groups has been made, adequate assessment requires comparable numbers in each group.

The AD post-mortem studies, in addition to this study, have disease- and method-related limitations. AD pathological diagnosis and stage are confirmed after death. The individual variabilities, ante-mortem and post-mortem variabilities and

variations in tissue storage times can all influence the final results. Furthermore, the possible effects of polypharmacy and comorbidities in elderly patients which might directly or indirectly change serotonin transmission cannot be excluded.



## **7.6. Conclusion**

AD is a multifactorial neurodegenerative disease associated with many neurochemical and biological disturbances that cause cognitive decline and behavioural symptoms. Limited non-curative AD therapies and multiple clinical trial failures following a decade of research transform this disease into a growing problem. Serotonin dysregulation during AD is evidenced in molecular, pre-clinical and clinical studies. Most attention is currently directed towards the 5-HT<sub>4</sub> and 5-HT<sub>6</sub> receptors as they hold the potential to be new druggable targets for AD. Nevertheless, the interaction and expression of these receptors during disease evolution are yet to be addressed.

Initially, individual activation of 5-HT<sub>4</sub> and 5-HT<sub>6</sub> receptors showed dose and time-dependent increase in ERK<sub>1/2</sub> phosphorylation. However, this study provides no evidence of receptor synergy on ERK phosphorylation upon co-activation of both 5-HT<sub>4</sub> and 5-HT<sub>6</sub> receptors, but this does not rule out that these receptors may functionally interact by activating other signalling proteins.

As *N*-glycosylation can influence the cell surface expression of many GPCRs, this study assessed the impact of this modification on the cell surface expression of the 5-HT<sub>4</sub> receptor. Consequently, this demonstrated that only the N180 residue, and not the N7 residue, was *N*-glycosylated in the expressing cells. Moreover, *N*-glycosylation was identified as an essential step for receptor trafficking to the cell membrane to allow functional engagement with extracellular 5-HT.

Finally, this study also revealed that the expression of the 5-HT<sub>4</sub> and 5-HT<sub>6</sub> receptors in the prefrontal cortex were reduced in the advanced AD stage, but only the 5-HT<sub>4</sub> receptor was reduced in the early AD stage. These IHC results were relevant to the

cognitive status of those patients besides the strong effect of the AD-related AT8 positive phospho-tau.

Taken together, the results presented in this thesis can extend the view on the fundamental changes of serotonin receptors and neurotransmission in AD and provide a rationale to further understanding of the neurochemical mechanisms of AD, and thus select the best time for therapeutic intervention. Furthermore, designing more compounds for dual targeting of these receptors may offer new approaches for the future treatment of AD pathology and symptoms which will hopefully lead to more positive outcomes in clinical trials.

## **Chapter 8. References**

## 8. References

- Ahmad, I. & Nirogi, R. 2011. 5-HT<sub>4</sub> Receptor Agonists for the Treatment of Alzheimer's Disease. *Neuroscience & Medicine*, 02, 87-92.
- Aishwarya, S., Rajendiren, S., Kattimani, S., Dhiman, P., Haritha, S. & Ananthanarayanan, P. H. 2013. Homocysteine and serotonin: association with postpartum depression. *Asian J Psychiatr*, 6, 473-7.
- Albasanz, J. L., Dalfo, E., Ferrer, I. & Martin, M. 2005. Impaired metabotropic glutamate receptor/phospholipase C signaling pathway in the cerebral cortex in Alzheimer's disease and dementia with Lewy bodies correlates with stage of Alzheimer's-disease-related changes. *Neurobiol Dis*, 20, 685-93.
- Alvarez-Alvarez, M., Galdos, L., Fernandez-Martinez, M., Gomez-Busto, F., Garcia-Centeno, V., Arias-Arias, C., Sanchez-Salazar, C., Rodriguez-Martinez, A. B., Zarranz, J. J. & De Pancorbo, M. M. 2003. 5-Hydroxytryptamine 6 receptor (5-HT<sub>6</sub>) receptor and apolipoprotein E (ApoE) polymorphisms in patients with Alzheimer's disease in the Basque Country. *Neurosci Lett*, 339, 85-7.
- Alzheimer's Association 2018. 2018 Alzheimer's disease facts and figures. *Alzheimer's & Dementia*, 14, 367-429.
- Amemori, T., Jendelova, P., Ruzicka, J., Urdzikova, L. M. & Sykova, E. 2015. Alzheimer's Disease: Mechanism and Approach to Cell Therapy. *Int J Mol Sci*, 16, 26417-51.
- Anand, R., Gill, K. D. & Mahdi, A. A. 2014. Therapeutics of Alzheimer's disease: Past, present and future. *Neuropharmacology*, 76 Pt A, 27-50.
- Andrade, R., Barnes, N., Baxter, G., Bockaert, J., Branchek, T., Cohen, M. L., Dumuis, A., Eglen, R. M., Göthert, M., Hamblin, M., Hamon, M., R., P., Hartig, P. R., Hen, R., Herrick-Davis, K., Hills, R., Hoyer, D., Humphrey, P. A., Latté, K. P., Maroteaux, L., Martin, G. R., Middlemiss, D. N., Mylecharane, E., Peroutka, S. J., Saxena, P. R., Sleight, A., Villalon, C. M. & Yocca, F. 2016. 5-Hydroxytryptamine receptors: 5-HT<sub>4</sub> receptor. *IUPHAR/BPS Guide to Pharmacology* [Online]. Available: <http://www.guidetopharmacology.org/GRAC/ObjectDisplayForward?objectId=9>. [Accessed 5 April 2016].
- Applied Biosystems. 2008. *Guide to performing relative quantitation of gene expression using real-time quantitative PCR* [Online]. Available: [http://www3.appliedbiosystems.com/cms/groups/mcb\\_support/documents/generaldocuments/cms\\_042380.pdf](http://www3.appliedbiosystems.com/cms/groups/mcb_support/documents/generaldocuments/cms_042380.pdf) [Accessed 9 June 2017].
- Assal, F., Alarcon, M., Solomon, E. C., Masterman, D., Geschwind, D. H. & Cummings, J. L. 2004. Association of the serotonin transporter and receptor gene polymorphisms in neuropsychiatric symptoms in Alzheimer disease. *Arch Neurol*, 61.
- Attems, J., Quass, M., Jellinger, K. A. & Lintner, F. 2007. Topographical distribution of cerebral amyloid angiopathy and its effect on cognitive decline are influenced by Alzheimer disease pathology. *J Neurol Sci*, 257, 49-55.
- Atwood, B. K., Lopez, J., Wager-Miller, J., Mackie, K. & Straiker, A. 2011. Expression of G protein-coupled receptors and related proteins in HEK293, AtT20, BV2, and N18 cell lines as revealed by microarray analysis. *BMC genomics*, 12, 14-14.
- Avramopoulos, D., Szymanski, M., Wang, R. & Bassett, S. 2011. Gene expression reveals overlap between normal aging and Alzheimer's disease genes. *Neurobiology of aging*, 32, 2319.e27-2319.e2.319E34.
- Ballard, C. & Waite, J. 2006. The effectiveness of atypical antipsychotics for the treatment of aggression and psychosis in Alzheimer's disease. *Cochrane Database Syst Rev*, Cd003476.
- Ballatore, C., Lee, V. M. Y. & Trojanowski, J. Q. 2007. Tau-mediated neurodegeneration in Alzheimer's disease and related disorders. *Nat Rev Neurosci*, 8, 663-672.
- Barnes, N. M., Costall, B., Naylor, R. J., Williams, T. J. & Wischik, C. M. 1990. Normal densities of 5-HT<sub>3</sub> receptor recognition sites in Alzheimer's disease. *Neuroreport*, 1, 253-4.

- Barnes, N. M. & Neumaier, J. F. 2011. Neuronal 5-HT receptors and SERT. *Tocris bioscience scientific review series*, 34, 1-15.
- Barnes, N. M. & Sharp, T. 1999. A review of central 5-HT receptors and their function. *Neuropharmacology*, 38, 1083-1152.
- Bartels, C., Wagner, M., Wolfsgruber, S., Ehrenreich, H. & Schneider, A. 2018. Impact of SSRI Therapy on Risk of Conversion From Mild Cognitive Impairment to Alzheimer's Dementia in Individuals With Previous Depression. *Am J Psychiatry*, 175, 232-241.
- Barthet, G., Framery, B., Gaven, F., Pellissier, L., Reiter, E., Claeysen, S., Bockaert, J. & Dumuis, A. 2007. 5-hydroxytryptamine 4 receptor activation of the extracellular signal-regulated kinase pathway depends on Src activation but not on G protein or beta-arrestin signaling. *Mol Biol Cell*, 18, 1979-91.
- Barthet, G., Gaven, F., Framery, B., Shinjo, K., Nakamura, T., Claeysen, S., Bockaert, J. & Dumuis, A. 2005. Uncoupling and endocytosis of 5-hydroxytryptamine 4 receptors. Distinct molecular events with different GRK2 requirements. *J Biol Chem*, 280, 27924-34.
- Baschieri, F., Dayot, S., Elkhatib, N., Ly, N., Capmany, A., Schauer, K., Betz, T., Vignjevic, D. M., Poincloux, R. & Montagnac, G. 2018. Frustrated endocytosis controls contractility-independent mechanotransduction at clathrin-coated structures. *Nature Communications*, 9, 3825.
- Bass, J. J., Wilkinson, D. J., Rankin, D., Phillips, B. E., Szewczyk, N. J., Smith, K. & Atherton, P. J. 2017. An overview of technical considerations for Western blotting applications to physiological research. *Scand J Med Sci Sports*, 27, 4-25.
- Bateman, R. J., Xiong, C., Benzinger, T. L., Fagan, A. M., Goate, A., Fox, N. C., Marcus, D. S., Cairns, N. J., Xie, X., Blazey, T. M., Holtzman, D. M., Santacruz, A., Buckles, V., Oliver, A., Moulder, K., Aisen, P. S., Ghetti, B., Klunk, W. E., Mcdade, E., Martins, R. N., Masters, C. L., Mayeux, R., Ringman, J. M., Rossor, M. N., Schofield, P. R., Sperling, R. A., Salloway, S. & Morris, J. C. 2012. Clinical and biomarker changes in dominantly inherited Alzheimer's disease. *N Engl J Med*, 367, 795-804.
- Bear, M. F., Connors, B. W. & Paradiso, M. A. 2007. *Neuroscience: exploring the brain*. , Philadelphia, PA, Lippincott Williams & Wilkins.
- Bell, R. D. & Zlokovic, B. V. 2009. Neurovascular mechanisms and blood-brain barrier disorder in Alzheimer's disease. *Acta Neuropathol*, 118, 103-13.
- Benhamu, B., Martin-Fontecha, M., Vazquez-Villa, H., Pardo, L. & Lopez-Rodriguez, M. L. 2014. Serotonin 5-HT<sub>6</sub> receptor antagonists for the treatment of cognitive deficiency in Alzheimer's disease. *J Med Chem*, 57, 7160-81.
- Bentley, J. C., Bourson, A., Boess, F. G., Fone, K. C., Marsden, C. A., Petit, N. & Sleight, A. J. 1999. Investigation of stretching behaviour induced by the selective 5-HT<sub>6</sub> receptor antagonist, Ro 04-6790, in rats. *British journal of pharmacology*, 126, 1537-1542.
- Beranek, V., Reinkemeier, C. D., Zhang, M. S., Liang, A. D., Kym, G. & Chin, J. W. 2018. Genetically Encoded Protein Phosphorylation in Mammalian Cells. *Cell Chem Biol*, 25, 1067-1074.e5.
- Berger, M., Gray, J. A. & Roth, B. L. 2009. The expanded biology of serotonin. *Annu Rev Med*, 60.
- Berumen, L. C., Rodríguez, A., Miledi, R. & García-Alcocer, G. 2012. Serotonin Receptors in Hippocampus. *The Scientific World Journal*, 2012, 823493.
- Bimboim, H. C. & Doly, J. 1979. A rapid alkaline extraction procedure for screening recombinant plasmid DNA. *Nucleic Acids Research*, 7, 1513-1523.
- Blakely, R. D., Berson, H. E., Freneau, R. T., Jr., Caron, M. G., Peek, M. M., Prince, H. K. & Bradley, C. C. 1991. Cloning and expression of a functional serotonin transporter from rat brain. *Nature*, 354, 66-70.
- Bockaert, J., Claeysen, S., Becamel, C., Dumuis, A. & Marin, P. 2006. Neuronal 5-HT metabotropic receptors: fine-tuning of their structure, signaling, and roles in synaptic modulation. *Cell Tissue Res*, 326, 553-72.

- Bockaert, J., Claeysen, S., Compan, V. & Dumuis, A. 2008. 5-HT(4) receptors: history, molecular pharmacology and brain functions. *Neuropharmacology*, 55, 922-31.
- Bokare, A. M., Praveenkumar, A. K., Bhonde, M., Nayak, Y., Pal, R. & Goel, R. 2017. 5-HT<sub>6</sub> Receptor Agonist and Antagonist Against  $\beta$ -Amyloid-Peptide-Induced Neurotoxicity in PC-12 Cells. *Neurochemical Research*, 42, 1571-1579.
- Bonda, D. J., Evans, T. A., Santocanale, C., Llosa, J. C., Vina, J., Bajic, V., Castellani, R. J., Siedlak, S. L., Perry, G., Smith, M. A. & Lee, H. G. 2009. Evidence for the progression through S-phase in the ectopic cell cycle re-entry of neurons in Alzheimer disease. *Aging (Albany NY)*, 1, 382-8.
- Borsini, F., Bordi, F. & Riccioni, T. 2011. 5-HT<sub>6</sub> pharmacology inconsistencies. *Pharmacol Biochem Behav*, 98, 169-72.
- Bottiglieri, T., Laundry, M., Crellin, R., Toone, B. K., Carney, M. W. P. & Reynolds, E. H. 2000. Homocysteine, folate, methylation, and monoamine metabolism in depression. *Journal of Neurology, Neurosurgery & Psychiatry*, 69, 228.
- Bourson, A., Borroni, E., Austin, R. H., Monsma, F. J., Jr. & Sleight, A. J. 1995. Determination of the role of the 5-HT<sub>6</sub> receptor in the rat brain: a study using antisense oligonucleotides. *J Pharmacol Exp Ther*, 274, 173-80.
- Boyle, P. A., Wilson, R. S., Aggarwal, N. T., Tang, Y. & Bennett, D. A. 2006. Mild cognitive impairment: risk of Alzheimer disease and rate of cognitive decline. *Neurology*, 67, 441-5.
- Braak, H. & Braak, E. 1991. Neuropathological staging of Alzheimer-related changes. *Acta Neuropathologica*, 82, 239-259.
- Bröer, S. 2018. Monoamine transporter subfamily: SERT. *IUPHAR/BPS Guide to Pharmacology* [Online]. Available: <http://www.guidetopharmacology.org/GRAC/ObjectDisplayForward?objectId=928>. [Accessed 16 January 2019].
- Brunton, L. L., Chabner, B. A. & Knollmann, B. C. 2011. *Goodman & Gilman's The Pharmacological Basis of Therapeutics*, New York, The McGraw-Hill Companies.
- Businaro, R., Scaccia, E., Bordin, A., Pagano, F., Corsi, M., Siciliano, C., Capovano, R., Procaccini, E., Salvati, B., Petrozza, V., Totta, P., Vietri, M. T., Frati, G. & De Falco, E. 2018. Platelet Lysate-Derived Neuropeptide  $\gamma$  Influences Migration and Angiogenesis of Human Adipose Tissue-Derived Stromal Cells. *Scientific Reports*, 8, 14365.
- Butterfield, D. A. & Pocernich, C. B. 2003. The glutamatergic system and Alzheimer's disease: therapeutic implications. *CNS Drugs*, 17, 641-52.
- Caramelo, J. J. & Parodi, A. J. 2008. Getting in and out from calnexin/calreticulin cycles. *The Journal of biological chemistry*, 283, 10221-10225.
- Celada, P., Puig, M. V. & Artigas, F. 2013. Serotonin modulation of cortical neurons and networks. *Front Integr Neurosci*, 7, 25.
- Chabrier, M. A., Cheng, D., Castello, N. A., Green, K. N. & Laferla, F. M. 2014. Synergistic effects of amyloid-beta and wild-type human tau on dendritic spine loss in a floxed double transgenic model of Alzheimer's disease. *Neurobiol Dis*, 64, 107-17.
- Chapin, E. M., Haj-Dahmane, S., Torres, G. & Andrade, R. 2002. The 5-HT<sub>4</sub> receptor-induced depolarization in rat hippocampal neurons is mediated by cAMP but is independent of I<sub>h</sub>. *Neuroscience letters*, 324, 1-4.
- Cheignon, C., Tomas, M., Bonnefont-Rousselot, D., Faller, P., Hureau, C. & Collin, F. 2018. Oxidative stress and the amyloid beta peptide in Alzheimer's disease. *Redox Biol*, 14, 450-464.
- Chen, C. P., Eastwood, S. L., Hope, T., McDonald, B., Francis, P. T. & Esiri, M. M. 2000. Immunocytochemical study of the dorsal and median raphe nuclei in patients with Alzheimer's disease prospectively assessed for behavioural changes. *Neuropathol Appl Neurobiol*, 26, 347-55.
- Chen, Q., Miller, L. J. & Dong, M. 2010. Role of N-linked glycosylation in biosynthesis, trafficking, and function of the human glucagon-like peptide 1 receptor. *American journal of physiology. Endocrinology and metabolism*, 299, E62-E68.

- Chen, Y., Huang, X., Zhang, Y. W., Rockenstein, E., Bu, G., Golde, T. E., Masliah, E. & Xu, H. 2012. Alzheimer's beta-secretase (BACE1) regulates the cAMP/PKA/CREB pathway independently of beta-amyloid. *J Neurosci*, 32, 11390-5.
- Chen, Y., Zhou, B., Xu, L., Fan, H., Xie, J. & Wang, D. 2017. MicroRNA-146a promotes gastric cancer cell apoptosis by targeting transforming growth factor beta-activated kinase 1. *Mol Med Rep*, 16, 755-763.
- Chhibber, A. & Zhao, L. 2017. ERbeta and ApoE isoforms interact to regulate BDNF-5-HT2A signaling and synaptic function in the female brain. *Alzheimers Res Ther*, 9, 79.
- Chin, J., Palop, J. J., Puolivali, J., Massaro, C., Bien-Ly, N., Gerstein, H., Searce-Levie, K., Masliah, E. & Mucke, L. 2005. Fyn kinase induces synaptic and cognitive impairments in a transgenic mouse model of Alzheimer's disease. *J Neurosci*, 25, 9694-703.
- Chin, J., Palop, J. J., Yu, G. Q., Kojima, N., Masliah, E. & Mucke, L. 2004. Fyn kinase modulates synaptotoxicity, but not aberrant sprouting, in human amyloid precursor protein transgenic mice. *J Neurosci*, 24, 4692-7.
- Cho, S. & Hu, Y. 2007. Activation of 5-HT4 receptors inhibits secretion of beta-amyloid peptides and increases neuronal survival. *Exp Neurol*, 203, 274-8.
- Cirrito, J. R., Disabato, B. M., Restivo, J. L., Verges, D. K., Goebel, W. D., Sathyan, A., Hayreh, D., D'angelo, G., Benzinger, T., Yoon, H., Kim, J., Morris, J. C., Mintun, M. A. & Sheline, Y. I. 2011. Serotonin signaling is associated with lower amyloid-beta levels and plaques in transgenic mice and humans. *Proc Natl Acad Sci U S A*, 108, 14968-73.
- Cochet, M., Donneger, R., Cassier, E., Gaven, F., Lichtenthaler, S. F., Marin, P., Bockaert, J., Dumuis, A. & Claeysen, S. 2013. 5-HT4 receptors constitutively promote the non-amyloidogenic pathway of APP cleavage and interact with ADAM10. *ACS Chem Neurosci*, 4, 130-40.
- Codony, X., Burgueno, J., Ramirez, M. J. & Vela, J. M. 2010. 5-HT6 receptor signal transduction second messenger systems. *Int Rev Neurobiol*, 94, 89-110.
- Codony, X., Vela, J. M. & Ramirez, M. J. 2011. 5-HT(6) receptor and cognition. *Curr Opin Pharmacol*, 11, 94-100.
- Constantinescu, R., Constantinescu, A., Reichmann, H. & Janetzky, B. 2007. Neuronal differentiation and long-term culture of the human neuroblastoma line SH-SY5Y. *J Neural Transm*.
- Cooper, J. P. 2003. Buspirone for anxiety and agitation in dementia. *Journal of Psychiatry and Neuroscience*, 28, 469-469.
- Counts, S. E., He, B., Che, S., Ikonomic, M. D., Dekosky, S. T., Ginsberg, S. D. & Mufson, E. J. 2007. Alpha7 nicotinic receptor up-regulation in cholinergic basal forebrain neurons in Alzheimer disease. *Arch Neurol*, 64, 1771-6.
- Coupar, I. M., Desmond, P. V. & Irving, H. R. 2007. Human 5-HT4 and 5-HT7 receptor splice variants: are they important? *Current neuropharmacology*, 5, 224-231.
- Cowen, P. J., Parry-Billings, M. & Newsholme, E. A. 1989. Decreased plasma tryptophan levels in major depression. *J Affect Disord*, 16, 27-31.
- Cummings, J., Lee, G., Ritter, A. & Zhong, K. 2018. Alzheimer's disease drug development pipeline: 2018. *Alzheimers Dement (N Y)*, 4, 195-214.
- D'souza, U. M. & Craig, I. W. 2010. CHAPTER 1.2 - Genetic Organization of the Serotonergic System. In: Müller, C. P. and Jacobs, B. L. (eds.) *Handbook of Behavioral Neuroscience*. Elsevier.
- Dale, E., Pehrson, A. L., Jeyarajah, T., Li, Y., Leiser, S. C., Smagin, G., Olsen, C. K. & Sanchez, C. 2016. Effects of serotonin in the hippocampus: how SSRIs and multimodal antidepressants might regulate pyramidal cell function. *CNS Spectrums*, 21, 143-161.
- Daubert, E. A. & Condon, B. G. 2010. Serotonin: a regulator of neuronal morphology and circuitry. *Trends Neurosci*, 33, 424-34.
- Davenport, A. P. 2012. *Receptor Binding Techniques*, Cambridge, UK, Humana Press.

- Dawson, L. A., Nguyen, H. Q. & Li, P. 2001. The 5-HT<sub>6</sub> receptor antagonist SB-271046 selectively enhances excitatory neurotransmission in the rat frontal cortex and hippocampus. *Neuropsychopharmacology*, 25, 662-668.
- De Los Milagros Bassani Molinas, M., Beer, C., Hesse, F., Wirth, M. & Wagner, R. 2014. Optimizing the transient transfection process of HEK-293 suspension cells for protein production by nucleotide ratio monitoring. *Cytotechnology*, 66, 493-514.
- Derkach, V. A., Oh, M. C., Guire, E. S. & Soderling, T. R. 2007. Regulatory mechanisms of AMPA receptors in synaptic plasticity. *Nat Rev Neurosci*, 8, 101-13.
- Desai, A. K. & Grossberg, G. T. 2003. Buspirone in Alzheimer's disease. *Expert Rev Neurother*, 3, 19-28.
- Dhawan, G. & Combs, C. K. 2012. Inhibition of Src kinase activity attenuates amyloid associated microgliosis in a murine model of Alzheimer's disease. *J Neuroinflammation*, 9, 117.
- Dickerson, B. C., Feczko, E., Augustinack, J. C., Pacheco, J., Morris, J. C., Fischl, B. & Buckner, R. L. 2009. Differential effects of aging and Alzheimer's disease on medial temporal lobe cortical thickness and surface area. *Neurobiology of aging*, 30, 432-440.
- Diniz, B. S. & Teixeira, A. L. 2011. Brain-derived neurotrophic factor and Alzheimer's disease: physiopathology and beyond. *Neuromolecular Med*, 13, 217-22.
- Dong, S., Duan, Y., Hu, Y. & Zhao, Z. 2012. Advances in the pathogenesis of Alzheimer's disease: a re-evaluation of amyloid cascade hypothesis. *Translational neurodegeneration*, 1, 1.
- Ducy, P. & Karsenty, G. 2010. The two faces of serotonin in bone biology. *The Journal of Cell Biology*, 191, 7-13.
- Dutton, A. C., Massoura, A. N., Dover, T. J., Andrews, N. A. & Barnes, N. M. 2008. Identification and functional significance of N-glycosylation of the 5-HT<sub>5A</sub> receptor. *Neurochem Int*, 52, 419-25.
- Feng, Y. & Wang, X. 2012. Antioxidant Therapies for Alzheimer's Disease. *Oxidative Medicine and Cellular Longevity*, 2012, 472932.
- Fernández-Mosquera, L., Diogo, C. V., Yambire, K. F., Santos, G. L., Luna Sánchez, M., Bénit, P., Rustin, P., Lopez, L. C., Milosevic, I. & Raimundo, N. 2017. Acute and chronic mitochondrial respiratory chain deficiency differentially regulate lysosomal biogenesis. *Scientific Reports*, 7, 45076.
- Ferrero, H., Solas, M., Francis, P. T. & Ramirez, M. J. 2016. Serotonin 5-HT<sub>6</sub> Receptor Antagonists in Alzheimer's Disease: Therapeutic Rationale and Current Development Status. *CNS Drugs*.
- Filippini, N., Macintosh, B. J., Hough, M. G., Goodwin, G. M., Frisoni, G. B., Smith, S. M., Matthews, P. M., Beckmann, C. F. & Mackay, C. E. 2009. Distinct patterns of brain activity in young carriers of the APOE-epsilon4 allele. *Proc Natl Acad Sci U S A*, 106, 7209-14.
- Foley, A. G., Murphy, K. J., Hirst, W. D., Gallagher, H. C., Hagan, J. J., Upton, N., Walsh, F. S. & Regan, C. M. 2004. The 5-HT<sub>6</sub> receptor antagonist SB-271046 reverses scopolamine-disrupted consolidation of a passive avoidance task and ameliorates spatial task deficits in aged rats. *Neuropsychopharmacology*, 29, 93-100.
- Fone, K. C. 2008. An update on the role of the 5-hydroxytryptamine<sub>6</sub> receptor in cognitive function. *Neuropharmacology*, 55, 1015-22.
- Frade, J. M. & Ovejero-Benito, M. C. 2015. Neuronal cell cycle: the neuron itself and its circumstances. *Cell Cycle*, 14, 712-720.
- Francis, P. T. 2003. Glutamatergic systems in Alzheimer's disease. *Int J Geriatr Psychiatry*, 18, S15-21.
- Francis, P. T., Palmer, A. M., Snape, M. & Wilcock, G. K. 1999. The cholinergic hypothesis of Alzheimer's disease: a review of progress. *J Neurol Neurosurg Psychiatry*, 66.
- Francis, P. T., Ramirez, M. J. & Lai, M. K. 2010. Neurochemical basis for symptomatic treatment of Alzheimer's disease. *Neuropharmacology*, 59, 221-9.



- Gao, J., Adam, B. L. & Terry, A. V., Jr. 2014. Evaluation of nicotine and cotinine analogs as potential neuroprotective agents for Alzheimer's disease. *Bioorg Med Chem Lett*, 24, 1472-8.
- Garcia-Alloza, M., Gil-Bea, F. J., Diez-Ariza, M., Chen, C. P., Francis, P. T., Lasheras, B. & Ramirez, M. J. 2005. Cholinergic-serotonergic imbalance contributes to cognitive and behavioral symptoms in Alzheimer's disease. *Neuropsychologia*, 43.
- Garcia-Alloza, M., Hirst, W. D., Chen, C. P., Lasheras, B., Francis, P. T. & Ramirez, M. J. 2004. Differential involvement of 5-HT(1B/1D) and 5-HT6 receptors in cognitive and non-cognitive symptoms in Alzheimer's disease. *Neuropsychopharmacology*, 29, 410-6.
- Garcia, M. L. & Cleveland, D. W. 2001. Going new places using an old MAP: tau, microtubules and human neurodegenerative disease. *Curr Opin Cell Biol*, 13, 41-8.
- Gaspar, P., Cases, O. & Maroteaux, L. 2003. The developmental role of serotonin: news from mouse molecular genetics. *Nat Rev Neurosci*, 4, 1002-12.
- Gavel, Y. & Heijne, G. V. 1990. Sequence differences between glycosylated and non-glycosylated Asn-X-Thr/Ser acceptor sites: implications for protein engineering. *Protein Engineering, Design and Selection*, 3, 433-442.
- Gelinas, J. N., Banko, J. L., Peters, M. M., Klann, E., Weeber, E. J. & Nguyen, P. V. 2008. Activation of exchange protein activated by cyclic-AMP enhances long-lasting synaptic potentiation in the hippocampus. *Learning & Memory*, 15, 403-411.
- Gella, A. & Durany, N. 2009. Oxidative stress in Alzheimer disease. *Cell Adhesion & Migration*, 3, 88-93.
- Gendron, T. F. & Petrucelli, L. 2009. The role of tau in neurodegeneration. *Mol Neurodegener*, 4, 13.
- Gerald, C., Adham, N., Kao, H. T., Olsen, M. A., Laz, T. M., Schechter, L. E., Bard, J. A., Vaysse, P. J., Hartig, P. R., Branchek, T. A. & Et Al. 1995. The 5-HT4 receptor: molecular cloning and pharmacological characterization of two splice variants. *Embo j*, 14, 2806-15.
- Gerard, C., El Mestikawy, S., Lebrand, C., Adrien, J., Ruat, M., Traiffort, E., Hamon, M. & Martres, M. P. 1996. Quantitative RT-PCR distribution of serotonin 5-HT6 receptor mRNA in the central nervous system of control or 5,7-dihydroxytryptamine-treated rats. *Synapse*, 23, 164-73.
- Gershon, M. D. 2004. Review article: serotonin receptors and transporters -- roles in normal and abnormal gastrointestinal motility. *Aliment Pharmacol Ther*, 20 Suppl 7, 3-14.
- Gershon, M. D. & Tack, J. 2007. The serotonin signaling system: from basic understanding to drug development for functional GI disorders. *Gastroenterology*, 132, 397-414.
- Giacobini, E. 2003. Cholinergic function and Alzheimer's disease. *Int J Geriatr Psychiatry*, 18.
- Giannoni, P., Gaven, F., De Bundel, D., Baranger, K., Marchetti-Gauthier, E., Roman, F. S., Valjent, E., Marin, P., Bockaert, J., Rivera, S. & Claeysen, S. 2013. Early administration of RS 67333, a specific 5-HT4 receptor agonist, prevents amyloidogenesis and behavioral deficits in the 5XFAD mouse model of Alzheimer's disease. *Front Aging Neurosci*, 5, 96.
- Godyn, J., Jonczyk, J., Panek, D. & Malawska, B. 2016. Therapeutic strategies for Alzheimer's disease in clinical trials. *Pharmacol Rep*, 68, 127-38.
- Gothert, M. 2013. Serotonin discovery and stepwise disclosure of 5-HT receptor complexity over four decades. Part I. General background and discovery of serotonin as a basis for 5-HT receptor identification. *Pharmacol Rep*, 65, 771-86.
- Grammas, P. 2011. Neurovascular dysfunction, inflammation and endothelial activation: implications for the pathogenesis of Alzheimer's disease. *J Neuroinflammation*, 8, 26.
- Grandoch, M., Roscioni, S. S. & Schmidt, M. 2010. The role of Epac proteins, novel cAMP mediators, in the regulation of immune, lung and neuronal function. *British Journal of Pharmacology*, 159, 265-284.

- Gray, N. A., Milak, M. S., Delorenzo, C., Ogden, R. T., Huang, Y.-Y., Mann, J. J. & Parsey, R. V. 2013. Antidepressant treatment reduces serotonin-1A autoreceptor binding in major depressive disorder. *Biological psychiatry*, 74, 26-31.
- Greenwood, J. M. & Dragunow, M. 2002. Muscarinic receptor-mediated phosphorylation of cyclic AMP response element binding protein in human neuroblastoma cells. *Journal of neurochemistry*, 82, 389-397.
- Guan, Z. Z., Miao, H., Tian, J. Y., Unger, C., Nordberg, A. & Zhang, X. 2001. Suppressed expression of nicotinic acetylcholine receptors by nanomolar beta-amyloid peptides in PC12 cells. *J Neural Transm (Vienna)*, 108, 1417-33.
- Guerreiro, R., Wojtas, A., Bras, J., Carrasquillo, M., Rogaeva, E., Majounie, E., Cruchaga, C., Sassi, C., Kauwe, J. S., Younkin, S., Hazrati, L., Collinge, J., Pocock, J., Lashley, T., Williams, J., Lambert, J. C., Amouyel, P., Goate, A., Rademakers, R., Morgan, K., Powell, J., St George-Hyslop, P., Singleton, A. & Hardy, J. 2013. TREM2 variants in Alzheimer's disease. *N Engl J Med*, 368, 117-27.
- Gupta, R. & Brunak, S. 2002. Prediction of glycosylation across the human proteome and the correlation to protein function. *Pac Symp Biocomput*, 310-22.
- Gupta, R., Jung, E. & Brunak, S. 2017. *Prediction of N-glycosylation sites in human proteins. DTU Bioinformatics. NetNglyc 1.0 server* [Online]. Available: <http://www.cbs.dtu.dk/services/NetNGlyc/> [Accessed 9 April 2018].
- Hardy, J. & Selkoe, D. J. 2002. The amyloid hypothesis of Alzheimer's disease: progress and problems on the road to therapeutics. *Science*, 297.
- Harmer, C. J. & Cowen, P. J. 2013. 'It's the way that you look at it'--a cognitive neuropsychological account of SSRI action in depression. *Philosophical transactions of the Royal Society of London. Series B, Biological sciences*, 368, 20120407-20120407.
- Harrison, P. J., Barton, A. J. L., Najlerahim, A., McDonald, B. & Pearson, R. C. A. 1991. Increased muscarinic receptor messenger RNA in Alzheimer's disease temporal cortex demonstrated by in situ hybridization histochemistry. *Molecular Brain Research*, 9, 15-21.
- Heifetz, A., Keenan, R. W. & Elbein, A. D. 1979. Mechanism of action of tunicamycin on the UDP-GlcNAc:dolichyl-phosphate GlcNAc-1-phosphate transferase. *Biochemistry*, 18, 2186-2192.
- Hendricksen, M., Thomas, A. J., Ferrier, I. N., Ince, P. & O'brien, J. T. 2004. Neuropathological study of the dorsal raphe nuclei in late-life depression and Alzheimer's disease with and without depression. *Am J Psychiatry*, 161, 1096-102.
- Hensler, J. G. 2006. Serotonergic modulation of the limbic system. *Neurosci Biobehav Rev*, 30, 203-14.
- Herr, N., Bode, C. & Duerschmied, D. 2017. The Effects of Serotonin in Immune Cells. *Frontiers in Cardiovascular Medicine*, 4, 48.
- Herrick-Davis, K. 2013. Functional Significance of Serotonin Receptor Dimerization. *Experimental brain research. Experimentelle Hirnforschung. Experimentation cerebrale*, 230, 375-386.
- Hirst, W. D., Stean, T. O., Rogers, D. C., Sunter, D., Pugh, P., Moss, S. F., Bromidge, S. M., Riley, G., Smith, D. R., Bartlett, S., Heidbreder, C. A., Atkins, A. R., Lacroix, L. P., Dawson, L. A., Foley, A. G., Regan, C. M. & Upton, N. 2006. SB-399885 is a potent, selective 5-HT<sub>6</sub> receptor antagonist with cognitive enhancing properties in aged rat water maze and novel object recognition models. *Eur J Pharmacol*, 553, 109-19.
- Hodge, E., Nelson, C. P., Miller, S., Billington, C. K., Stewart, C. E., Swan, C., Malarstig, A., Henry, A. P., Gowland, C., Melén, E., Hall, I. P. & Sayers, I. 2013. HTR4 gene structure and altered expression in the developing lung. *Respiratory research*, 14, 77-77.
- Hoeffer, C. A. & Klann, E. 2010. mTOR signaling: at the crossroads of plasticity, memory and disease. *Trends Neurosci*, 33, 67-75.

- Holsinger, R. M., Schnarr, J., Henry, P., Castelo, V. T. & Fahnstock, M. 2000. Quantitation of BDNF mRNA in human parietal cortex by competitive reverse transcription-polymerase chain reaction: decreased levels in Alzheimer's disease. *Brain Res Mol Brain Res*, 76, 347-54.
- Hornung, J. P. 2003. The human raphe nuclei and the serotonergic system. *J Chem Neuroanat*, 26, 331-43.
- Hrdina, P. D., Foy, B., Hepner, A. & Summers, R. J. 1990. Antidepressant binding sites in brain: autoradiographic comparison of [3H]paroxetine and [3H]imipramine localization and relationship to serotonin transporter. *J Pharmacol Exp Ther*, 252, 410-8.
- Hu, M., Retz, W., Baader, M., Pesold, B., Adler, G., Henn, F. A., Rösler, M. & Thome, J. 2000. Promoter polymorphism of the 5-HT transporter and Alzheimer's disease. *Neuroscience Letters*, 294, 63-65.
- Huang, W.-J., Zhang, X. I. A. & Chen, W.-W. 2016. Role of oxidative stress in Alzheimer's disease. *Biomedical Reports*, 4, 519-522.
- Huang, Z., Li, G., Pei, W., Sosa, L. A. & Niu, L. 2005. Enhancing protein expression in single HEK 293 cells. *J Neurosci Methods*, 142, 159-66.
- Inoue, H., Nojima, H. & Okayama, H. 1990. High efficiency transformation of *Escherichia coli* with plasmids. *Gene*, 96, 23-8.
- Ittner, L. M., Ke, Y. D., Delerue, F., Bi, M., Gladbach, A., Van Eersel, J., Wolfing, H., Chieng, B. C., Christie, M. J., Napier, I. A., Eckert, A., Staufenbiel, M., Hardeman, E. & Gotz, J. 2010. Dendritic function of tau mediates amyloid-beta toxicity in Alzheimer's disease mouse models. *Cell*, 142, 387-97.
- Jackson, R. J., Rudinskiy, N., Herrmann, A. G., Croft, S., Kim, J. M., Petrova, V., Ramos-Rodriguez, J. J., Pitstick, R., Wegmann, S., Garcia-Alloza, M., Carlson, G. A., Hyman, B. T. & Spires-Jones, T. L. 2016. Human tau increases amyloid beta plaque size but not amyloid beta-mediated synapse loss in a novel mouse model of Alzheimer's disease. *Eur J Neurosci*, 44, 3056-3066.
- Jacob, C. P., Koutsilieri, E., Bartl, J., Neuen-Jacob, E., Arzberger, T., Zander, N., Ravid, R., Roggendorf, W., Riederer, P. & Grunblatt, E. 2007. Alterations in expression of glutamatergic transporters and receptors in sporadic Alzheimer's disease. *J Alzheimers Dis*, 11, 97-116.
- Jeltsch-David, H., Koenig, J. & Cassel, J. C. 2008. Modulation of cholinergic functions by serotonin and possible implications in memory: general data and focus on 5-HT(1A) receptors of the medial septum. *Behav Brain Res*, 195, 86-97.
- Jenkins, T. A., Elliott, J. J., Ardis, T. C., Cahir, M., Reynolds, G. P., Bell, R. & Cooper, S. J. 2010. Tryptophan depletion impairs object-recognition memory in the rat: reversal by risperidone. *Behav Brain Res*, 208, 479-83.
- Johnson, M. S., Lutz, E. M., Firbank, S., Holland, P. J. & Mitchell, R. 2003. Functional interactions between native Gs-coupled 5-HT receptors in HEK-293 cells and the heterologously expressed serotonin transporter. *Cell Signal*, 15, 803-11.
- Jones, J., Krag, S. S. & Betenbaugh, M. J. 2005. Controlling N-linked glycan site occupancy. *Biochimica et Biophysica Acta (BBA) - General Subjects*, 1726, 121-137.
- Jonsson, T., Stefansson, H., Steinberg, S., Jonsdottir, I., Jonsson, P. V., Snaedal, J., Bjornsson, S., Huttenlocher, J., Levey, A. I., Lah, J. J., Rujescu, D., Hampel, H., Giegling, I., Andreassen, O. A., Engedal, K., Ulstein, I., Djurovic, S., Ibrahim-Verbaas, C., Hofman, A., Ikram, M. A., Van Duijn, C. M., Thorsteinsdottir, U., Kong, A. & Stefansson, K. 2013. Variant of TREM2 associated with the risk of Alzheimer's disease. *N Engl J Med*, 368, 107-16.
- Joubert, L., Hanson, B., Barthet, G., Sebben, M., Claeysen, S., Hong, W., Marin, P., Dumuis, A. & Bockaert, J. 2004. New sorting nexin (SNX27) and NHERF specifically interact with the 5-HT<sub>4</sub> receptor splice variant: roles in receptor targeting. *Journal of Cell Science*, 117, 5367-5379.

- Kametani, F. & Hasegawa, M. 2018. Reconsideration of Amyloid Hypothesis and Tau Hypothesis in Alzheimer's Disease. *Frontiers in Neuroscience*, 12.
- Kan, R., Wang, B., Zhang, C., Yang, Z., Ji, S. H. U. N., Lu, Z., Zheng, C., Jin, F. & Wang, L. 2004. Association of the HTR6 polymorphism C267T with late-onset Alzheimer's disease in Chinese. *Neurosci Lett*, 372.
- Kandimalla, R. & Reddy, P. H. 2017. Therapeutics of Neurotransmitters in Alzheimer's Disease. *Journal of Alzheimer's disease : JAD*, 57, 1049-1069.
- Karila, D., Freret, T., Bouet, V., Boulouard, M., Dallemagne, P. & Rochais, C. 2015. Therapeutic Potential of 5-HT<sub>6</sub> Receptor Agonists. *J Med Chem*, 58, 7901-12.
- Kasturi, L., Eshleman, J. R., Wunner, W. H. & Shakin-Eshleman, S. H. 1995. The hydroxy amino acid in an Asn-X-Ser/Thr sequon can influence N-linked core glycosylation efficiency and the level of expression of a cell surface glycoprotein. *J Biol Chem*, 270, 14756-61.
- Kendall, I., Sloten, H. A., Codony, X., Burgueno, J., Pauwels, P. J., Vela, J. M. & Fone, K. C. 2011. E-6801, a 5-HT<sub>6</sub> receptor agonist, improves recognition memory by combined modulation of cholinergic and glutamatergic neurotransmission in the rat. *Psychopharmacology (Berl)*, 213, 413-30.
- Kepe, V., Barrio, J. R., Huang, S. C., Ercoli, L., Siddarth, P., Shoghi-Jadid, K., Cole, G. M., Satyamurthy, N., Cummings, J. L., Small, G. W. & Phelps, M. E. 2006. Serotonin 1A receptors in the living brain of Alzheimer's disease patients. *Proc Natl Acad Sci U S A*, 103, 702-7.
- Kim, H. & Lee, K. J. 2014. Serum homocysteine levels are correlated with behavioral and psychological symptoms of Alzheimer's disease. *Neuropsychiatr Dis Treat*, 10, 1887-96.
- King, M., Marsden, C. & Fone, K. 2008. A role for the 5-HT<sub>1A</sub>, 5-HT<sub>4</sub> and 5-HT<sub>6</sub> receptors in learning and memory. *Trends in Pharmacological Sciences*, 29, 482-492.
- King, M. V., Sleight, A. J., Woolley, M. L., Topham, I. A., Marsden, C. A. & Fone, K. C. 2004. 5-HT<sub>6</sub> receptor antagonists reverse delay-dependent deficits in novel object discrimination by enhancing consolidation--an effect sensitive to NMDA receptor antagonism. *Neuropharmacology*, 47, 195-204.
- Kitagishi, Y., Nakanishi, A., Ogura, Y. & Matsuda, S. 2014. Dietary regulation of PI3K/AKT/GSK-3 $\beta$  pathway in Alzheimer's disease. *Alzheimers Res Ther*, 6, 35.
- Kohen, R., Fashingbauer, L. A., Heidmann, D. E., Guthrie, C. R. & Hamblin, M. W. 2001. Cloning of the mouse 5-HT<sub>6</sub> serotonin receptor and mutagenesis studies of the third cytoplasmic loop. *Brain Res Mol Brain Res*, 90, 110-7.
- Kohen, R., Metcalf, M. A., Khan, N., Druck, T., Huebner, K., Lachowicz, J. E., Meltzer, H. Y., Sibley, D. R., Roth, B. L. & Hamblin, M. W. 1996. Cloning, characterization, and chromosomal localization of a human 5-HT<sub>6</sub> serotonin receptor. *J Neurochem*, 66, 47-56.
- Kojro, E., Postina, R., Buro, C., Meiringer, C., Gehrig-Burger, K. & Fahrenholz, F. 2006. The neuropeptide PACAP promotes the alpha-secretase pathway for processing the Alzheimer amyloid precursor protein. *Faseb j*, 20, 512-4.
- Kornfeld, R. & Kornfeld, S. 1985. Assembly of asparagine-linked oligosaccharides. *Annu Rev Biochem*, 54, 631-64.
- Kozielewicz, P., Alomar, H., Yusof, S., Grafton, G., Cooper, A. J., Curnow, S. J., Ironside, J. W., Pall, H. & Barnes, N. M. 2017. N-glycosylation and expression in human tissues of the orphan GPR61 receptor. *FEBS Open Bio*, 7, 1982-1993.
- Laferla, F. M., Green, K. N. & Oddo, S. 2007. Intracellular amyloid-beta in Alzheimer's disease. *Nat Rev Neurosci*, 8, 499-509.
- Lai, M. K., Tsang, S. W., Alder, J. T., Keene, J., Hope, T., Esiri, M. M., Francis, P. T. & Chen, C. P. 2005. Loss of serotonin 5-HT<sub>2A</sub> receptors in the postmortem temporal cortex correlates with rate of cognitive decline in Alzheimer's disease. *Psychopharmacology (Berl)*, 179, 673-7.

- Lai, M. K., Tsang, S. W., Esiri, M. M., Francis, P. T., Wong, P. T. & Chen, C. P. 2011. Differential involvement of hippocampal serotonin<sub>1A</sub> receptors and re-uptake sites in non-cognitive behaviors of Alzheimer's disease. *Psychopharmacology (Berl)*, 213, 431-9.
- Lai, M. K., Tsang, S. W., Francis, P. T., Esiri, M. M., Hope, T., Lai, O. F., Spence, I. & Chen, C. P. 2003. [<sup>3</sup>H]GR113808 binding to serotonin 5-HT<sub>4</sub> receptors in the postmortem neocortex of Alzheimer disease: a clinicopathological study. *J Neural Transm (Vienna)*, 110, 779-88.
- Lancôt, K. L., Herrmann, N. & Mazzotta, P. 2001. Role of serotonin in the behavioral and psychological symptoms of dementia. *J Neuropsychiatry Clin Neurosci*, 13.
- Lancot, P. M., Leclerc, P. C., Clément, M., Auger-Messier, M., Escher, E., Leduc, R. & Guillemette, G. 2005. Importance of N-glycosylation positioning for cell-surface expression, targeting, affinity and quality control of the human AT<sub>1</sub> receptor. *The Biochemical journal*, 390, 367-376.
- Lancot, P. M., Leclerc, P. C., Escher, E., Leduc, R. & Guillemette, G. 1999. Role of N-glycosylation in the expression and functional properties of human AT<sub>1</sub> receptor. *Biochemistry*, 38, 8621-7.
- Laske, C., Stransky, E., Leyhe, T., Eschweiler, G. W., Maetzler, W., Wittorf, A., Soekadar, S., Richartz, E., Koehler, N., Bartels, M., Buchkremer, G. & Schott, K. 2007. BDNF serum and CSF concentrations in Alzheimer's disease, normal pressure hydrocephalus and healthy controls. *J Psychiatr Res*, 41, 387-94.
- Lecoutey, C., Hedou, D., Freret, T., Giannoni, P., Gaven, F., Since, M., Bouet, V., Ballandonne, C., Corvaisier, S., Malzert Freon, A., Mignani, S., Cresteil, T., Boulouard, M., Claeysen, S., Rochais, C. & Dallemagne, P. 2014. Design of donecopride, a dual serotonin subtype 4 receptor agonist/acetylcholinesterase inhibitor with potential interest for Alzheimer's disease treatment. *Proc Natl Acad Sci U S A*, 111, E3825-30.
- Lee, H. G., Casadesus, G., Zhu, X., Castellani, R. J., McShea, A., Perry, G., Petersen, R. B., Bajic, V. & Smith, M. A. 2009a. Cell cycle re-entry mediated neurodegeneration and its treatment role in the pathogenesis of Alzheimer's disease. *Neurochem Int*, 54, 84-8.
- Lee, J. G., Shin, B. S., You, Y. S., Kim, J. E., Yoon, S. W., Jeon, D. W., Baek, J. H., Park, S. W. & Kim, Y. H. 2009b. Decreased serum brain-derived neurotrophic factor levels in elderly Korean with dementia. *Psychiatry Investig*, 6, 299-305.
- Lehmann, O., Jeltsch, H., Lazarus, C., Tritschler, L., Bertrand, F. & Cassel, J. C. 2002. Combined 192 IgG-saporin and 5,7-dihydroxytryptamine lesions in the male rat brain: a neurochemical and behavioral study. *Pharmacol Biochem Behav*, 72, 899-912.
- Lehmann, O., Jeltsch, H., Lehnardt, O., Pain, L., Lazarus, C. & Cassel, J. C. 2000. Combined lesions of cholinergic and serotonergic neurons in the rat brain using 192 IgG-saporin and 5,7-dihydroxytryptamine: neurochemical and behavioural characterization. *Eur J Neurosci*, 12, 67-79.
- Leroy, D., Missotten, M., Waltzinger, C., Martin, T. & Scheer, A. 2007. G protein-coupled receptor-mediated ERK1/2 phosphorylation: towards a generic sensor of GPCR activation. *J Recept Signal Transduct Res*, 27, 83-97.
- Lesch, K. P., Bengel, D., Heils, A., Sabol, S. Z., Greenberg, B. D., Petri, S., Benjamin, J., Muller, C. R., Hamer, D. H. & Murphy, D. L. 1996. Association of anxiety-related traits with a polymorphism in the serotonin transporter gene regulatory region. *Science*, 274, 1527-31.
- Lesch, K. P. & Waider, J. 2012. Serotonin in the modulation of neural plasticity and networks: implications for neurodevelopmental disorders. *Neuron*, 76, 175-91.
- Levin, E. D., Mcclernon, F. J. & Rezvani, A. H. 2006. Nicotinic effects on cognitive function: behavioral characterization, pharmacological specification, and anatomic localization. *Psychopharmacology (Berl)*, 184, 523-39.

- Lezoualc'h, F. 2007. 5-HT<sub>4</sub> receptor and Alzheimer's disease: the amyloid connection. *Exp Neurol*, 205, 325-9.
- Lezoualc'h, F. & Robert, S. J. 2003. The serotonin 5-HT<sub>4</sub> receptor and the amyloid precursor protein processing. *Experimental gerontology*, 38, 159-166.
- Li, H. F., Liu, J. F., Zhang, K. & Feng, Y. 2015. Expression of serotonin receptors in human lower esophageal sphincter. *Exp Ther Med*, 9, 49-54.
- Li, Y., Rinne, J. O., Mosconi, L., Pirraglia, E., Rusinek, H., Desanti, S., Kemppainen, N., Nagren, K., Kim, B. C., Tsui, W. & De Leon, M. J. 2008. Regional analysis of FDG and PIB-PET images in normal aging, mild cognitive impairment, and Alzheimer's disease. *Eur J Nucl Med Mol Imaging*, 35, 2169-81.
- Liu, C.-C., Kanekiyo, T., Xu, H. & Bu, G. 2013. Apolipoprotein E and Alzheimer disease: risk, mechanisms, and therapy. *Nature reviews. Neurology*, 9, 106-118.
- Liu, Q., Kawai, H. & Berg, D. K. 2001. beta -Amyloid peptide blocks the response of alpha 7-containing nicotinic receptors on hippocampal neurons. *Proc Natl Acad Sci U S A*, 98, 4734-9.
- Liu, Y., Yoo, M. J., Savonenko, A., Stirling, W., Price, D. L., Borchelt, D. R., Mamounas, L., Lyons, W. E., Blue, M. E. & Lee, M. K. 2008. Amyloid pathology is associated with progressive monoaminergic neurodegeneration in a transgenic mouse model of Alzheimer's disease. *J Neurosci*, 28, 13805-14.
- Livak, K. J. & Schmittgen, T. D. 2001. Analysis of relative gene expression data using real-time quantitative PCR and the 2<sup>(-Delta Delta C(T))</sup> Method. *Methods*, 25.
- Lorke, D. E., Lu, G., Cho, E. & Yew, D. T. 2006. Serotonin 5-HT<sub>2A</sub> and 5-HT<sub>6</sub> receptors in the prefrontal cortex of Alzheimer and normal aging patients. *BMC Neuroscience*, 7, 1-8.
- Madsen, K., Neumann, W. J., Holst, K., Marner, L., Haahr, M. T., Lehel, S., Knudsen, G. M. & Hasselbalch, S. G. 2011. Cerebral serotonin 4 receptors and amyloid-beta in early Alzheimer's disease. *J Alzheimers Dis*, 26, 457-66.
- Maes, M., Leonard, B. E., Myint, A. M., Kubera, M. & Verkerk, R. 2011. The new '5-HT' hypothesis of depression: cell-mediated immune activation induces indoleamine 2,3-dioxygenase, which leads to lower plasma tryptophan and an increased synthesis of detrimental tryptophan catabolites (TRYCATs), both of which contribute to the onset of depression. *Prog Neuropsychopharmacol Biol Psychiatry*, 35, 702-21.
- Maginnis, M. S., Haley, S. A., Gee, G. V. & Atwood, W. J. 2010. Role of N-linked glycosylation of the 5-HT<sub>2A</sub> receptor in JC virus infection. *J Virol*, 84, 9677-84.
- Maher-Edwards, G., Watson, C., Ascher, J., Barnett, C., Boswell, D., Davies, J., Fernandez, M., Kurz, A., Zanetti, O., Safirstein, B., Schronen, J. P., Zvartau-Hind, M. & Gold, M. 2015. Two randomized controlled trials of SB742457 in mild-to-moderate Alzheimer's disease. *Alzheimer's & Dementia: Translational Research & Clinical Interventions*, 1, 23-36.
- Maillet, M., Robert, S. J., Cacquevel, M., Gastineau, M., Vivien, D., Bertoglio, J., Zugaza, J. L., Fischmeister, R. & Lezoualc'h, F. 2003. Crosstalk between Rap1 and Rac regulates secretion of sAPP $\alpha$ . *Nature cell biology*, 5, 633-639.
- Manocha, M. & Khan, W. I. 2012. Serotonin and GI Disorders: An Update on Clinical and Experimental Studies. *Clinical and Translational Gastroenterology*, 3, e13.
- Marazziti, D., Baroni, S., Pirone, A., Giannaccini, G., Betti, L., Schmid, L., Vatteroni, E., Palego, L., Borsini, F., Bordini, F., Piano, I., Gargini, C., Castagna, M., Catena-Dell'osso, M. & Lucacchini, A. 2012. Distribution of serotonin receptor of type 6 (5-HT<sub>6</sub>) in human brain post-mortem. A pharmacology, autoradiography and immunohistochemistry study. *Neurochem Res*, 37, 920-7.
- Marazziti, D., Baroni, S., Pirone, A., Giannaccini, G., Betti, L., Testa, G., Schmid, L., Palego, L., Borsini, F., Bordini, F., Piano, I., Gargini, C., Castagna, M., Catena-Dell'osso, M. & Lucacchini, A. 2013. Serotonin receptor of type 6 (5-HT<sub>6</sub>) in human prefrontal cortex and hippocampus post-mortem: an immunohistochemical and immunofluorescence study. *Neurochem Int*, 62, 182-8.

- Marner, L., Frokjaer, V. G., Kalbitzer, J., Lehel, S., Madsen, K., Baare, W. F., Knudsen, G. M. & Hasselbalch, S. G. 2012. Loss of serotonin 2A receptors exceeds loss of serotonergic projections in early Alzheimer's disease: a combined [<sup>11</sup>C]DASB and [<sup>18</sup>F]altanserin-PET study. *Neurobiol Aging*, 33, 479-87.
- Martinowich, K. & Lu, B. 2008. Interaction between BDNF and serotonin: role in mood disorders. *Neuropsychopharmacology*, 33, 73-83.
- Matlock, B. 2015. Assessment of nucleic acid purity. USA: Thermo Fisher Scientific.
- Mattson, M. P. 2004. Pathways towards and away from Alzheimer's disease. *Nature*, 430, 631-639.
- Mattson, M. P., Maudsley, S. & Martin, B. 2004. BDNF and 5-HT: a dynamic duo in age-related neuronal plasticity and neurodegenerative disorders. *Trends Neurosci*, 27, 589-94.
- Maurer-Spurej, E. 2005. Serotonin reuptake inhibitors and cardiovascular diseases: a platelet connection. *Cell Mol Life Sci*, 62, 159-70.
- Mccorvy, J. D. & Roth, B. L. 2015. Structure and Function of Serotonin G protein Coupled Receptors. *Pharmacology & therapeutics*, 150, 129-142.
- Medhurst, A. D., Lezoualc'h, F., Fischmeister, R., Middlemiss, D. N. & Sanger, G. J. 2001. Quantitative mRNA analysis of five C-terminal splice variants of the human 5-HT<sub>4</sub> receptor in the central nervous system by TaqMan real time RT-PCR. *Brain Res Mol Brain Res*, 90, 125-34.
- Meffre, J., Chaumont-Dubel, S., Mannoury La Cour, C., Loiseau, F., Watson, D. J., Dekeyne, A., Seveno, M., Rivet, J. M., Gaven, F., Deleris, P., Herve, D., Fone, K. C., Bockaert, J., Millan, M. J. & Marin, P. 2012. 5-HT<sub>6</sub> receptor recruitment of mTOR as a mechanism for perturbed cognition in schizophrenia. *EMBO Mol Med*, 4, 1043-56.
- Mendelsohn, D., Riedel, W. J. & Sambeth, A. 2009. Effects of acute tryptophan depletion on memory, attention and executive functions: a systematic review. *Neurosci Biobehav Rev*, 33, 926-52.
- Mesulam, M., Shaw, P., Mash, D. & Weintraub, S. 2004. Cholinergic nucleus basalis tauopathy emerges early in the aging-MCI-AD continuum. *Ann Neurol*, 55, 815-28.
- Mialet-Perez, J., Green, S. A., Miller, W. E. & Liggett, S. B. 2004. A primate-dominant third glycosylation site of the beta<sub>2</sub>-adrenergic receptor routes receptors to degradation during agonist regulation. *J Biol Chem*, 279, 38603-7.
- Michineau, S., Muller, L., Pizard, A., Alhenc-Gelas, F. & Rajerison, R. M. 2004. N-linked glycosylation of the human bradykinin B<sub>2</sub> receptor is required for optimal cell-surface expression and coupling. *Biol Chem*, 385, 49-57.
- Millan, M. J., Marin, P., Bockaert, J. & Mannoury La Cour, C. 2008. Signaling at G-protein-coupled serotonin receptors: recent advances and future research directions. *Trends Pharmacol Sci*, 29, 454-64.
- Mitchell, E. S., Sexton, T. & Neumaier, J. F. 2006. Increased Expression of 5-HT<sub>6</sub> Receptors in the Rat Dorsomedial Striatum Impairs Instrumental Learning. *Neuropsychopharmacology*, 32, 1520.
- Mitchell, T. W., Nissanov, J., Han, L. Y., Mufson, E. J., Schneider, J. A., Cochran, E. J., Bennett, D. A., Lee, V. M., Trojanowski, J. Q. & Arnold, S. E. 2000. Novel method to quantify neuropil threads in brains from elders with or without cognitive impairment. *J Histochem Cytochem*, 48, 1627-38.
- Mnie-Filali, O. & Piñeyro, G. 2012. Desensitization and internalization mechanisms of the 5-HT<sub>4</sub> receptors. *Wiley Interdisciplinary Reviews: Membrane Transport and Signaling*, 1, 779-788.
- Moh, C., Kubiak, J. Z., Bajic, V. P., Zhu, X., Smith, M. A. & Lee, H. G. 2011. Cell cycle deregulation in the neurons of Alzheimer's disease. *Results Probl Cell Differ*, 53, 565-76.
- Mohammad-Zadeh, L. F., Moses, L. & Gwaltney-Brant, S. M. 2008. Serotonin: a review. *J Vet Pharmacol Ther*, 31, 187-99.

- Monsma, F. J., Jr., Shen, Y., Ward, R. P., Hamblin, M. W. & Sibley, D. R. 1993. Cloning and expression of a novel serotonin receptor with high affinity for tricyclic psychotropic drugs. *Mol Pharmacol*, 43, 320-7.
- Morris, J. C. & Price, J. L. 2001. Pathologic correlates of nondemented aging, mild cognitive impairment, and early-stage Alzheimer's disease. *J Mol Neurosci*, 17, 101-18.
- Morris, M. S. 2003. Homocysteine and Alzheimer's disease. *Lancet Neurol*, 2, 425-8.
- Moser, P. C., Bergis, O. E., Jegham, S., Lochead, A., Duconseille, E., Terranova, J. P., Caille, D., Berque-Bestel, I., Lezoualc'h, F., Fischmeister, R., Dumuis, A., Bockaert, J., George, P., Soubrie, P. & Scatton, B. 2002. SL65.0155, a novel 5-hydroxytryptamine(4) receptor partial agonist with potent cognition-enhancing properties. *J Pharmacol Exp Ther*, 302, 731-41.
- Mowla, A., Mosavinasab, M., Haghshenas, H. & Borhani Haghighi, A. 2007. Does serotonin augmentation have any effect on cognition and activities of daily living in Alzheimer's dementia? A double-blind, placebo-controlled clinical trial. *J Clin Psychopharmacol*, 27, 484-7.
- Nagy, Z. 2005. The last neuronal division: a unifying hypothesis for the pathogenesis of Alzheimer's disease. *J Cell Mol Med*, 9, 531-41.
- Nagy, Z. 2007. The dysregulation of the cell cycle and the diagnosis of Alzheimer's disease. *Biochim Biophys Acta*, 1772, 402-8.
- Nagy, Z., Esiri, M. M. & Smith, A. D. 1998. The cell division cycle and the pathophysiology of Alzheimer's disease. *Neuroscience*, 87, 731-9.
- Nakagawa, T., Takahashi, C., Matsuzaki, H., Takeyama, S., Sato, S., Sato, A., Kuroda, Y. & Higashi, H. 2017. N-glycan-dependent cell-surface expression of the P2Y2 receptor and N-glycan-independent distribution to lipid rafts. *Biochem Biophys Res Commun*, 485, 427-431.
- Nelson, P. T., Jicha, G. A., Schmitt, F. A., Liu, H., Davis, D. G., Mendiondo, M. S., Abner, E. L. & Markesbery, W. R. 2007. Clinicopathologic correlations in a large Alzheimer disease center autopsy cohort: neuritic plaques and neurofibrillary tangles "do count" when staging disease severity. *J Neuropathol Exp Neurol*, 66, 1136-46.
- Newhouse, P., Kellar, K., Aisen, P., White, H., Wesnes, K., Coderre, E., Pfaff, A., Wilkins, H., Howard, D. & Levin, E. D. 2012. Nicotine treatment of mild cognitive impairment: a 6-month double-blind pilot clinical trial. *Neurology*, 78, 91-101.
- Ni, W. & Watts, S. W. 2006. 5-hydroxytryptamine in the cardiovascular system: focus on the serotonin transporter (SERT). *Clin Exp Pharmacol Physiol*, 33, 575-83.
- Nichols, D. E. & Nichols, C. D. 2008. Serotonin Receptors. *Chemical Reviews*, 108, 1614-1641.
- Nielsen, K., Brask, D., Knudsen, G. M. & Aznar, S. 2006. Immunodetection of the serotonin transporter protein is a more valid marker for serotonergic fibers than serotonin. *Synapse*, 59, 270-6.
- Nilsson, J., Halim, A., Grahn, A. & Larson, G. 2013. Targeting the glycoproteome. *Glycoconjugate journal*, 30, 119-136.
- Noristani, H. 2012. *Altered serotonergic neurotransmission as a main player in the pathophysiology of Alzheimer's disease: structural and ultrastructural studies in a triple transgenic mouse model of the disease*. PhD in Neuroscience University of Manchester
- Noristani, H. N., Olabarria, M., Verkhratsky, A. & Rodriguez, J. J. 2010. Serotonin fibre sprouting and increase in serotonin transporter immunoreactivity in the CA1 area of hippocampus in a triple transgenic mouse model of Alzheimer's disease. *Eur J Neurosci*, 32, 71-9.
- North, S. J., Huang, H. H., Sundaram, S., Jang-Lee, J., Etienne, A. T., Trollope, A., Chalabi, S., Dell, A., Stanley, P. & Haslam, S. M. 2010. Glycomics profiling of Chinese hamster ovary cell glycosylation mutants reveals N-glycans of a novel size and complexity. *J Biol Chem*, 285, 5759-75.



- Norum, J. H., Hart, K. & Levy, F. O. 2003. Ras-dependent ERK activation by the human G(s)-coupled serotonin receptors 5-HT<sub>4</sub>(b) and 5-HT<sub>7</sub>(a). *J Biol Chem*, 278, 3098-104.
- Nygaard, H. B. 2018. Targeting Fyn Kinase in Alzheimer's Disease. *Biol Psychiatry*, 83, 369-376.
- Oakley, H., Cole, S. L., Logan, S., Maus, E., Shao, P., Craft, J., Guillozet-Bongaarts, A., Ohno, M., Disterhoft, J., Van Eldik, L., Berry, R. & Vassar, R. 2006. Intraneuronal beta-amyloid aggregates, neurodegeneration, and neuron loss in transgenic mice with five familial Alzheimer's disease mutations: potential factors in amyloid plaque formation. *J Neurosci*, 26, 10129-40.
- Oddo, S. 2012. The role of mTOR signaling in Alzheimer disease. *Frontiers in bioscience (Scholar edition)*, 4, 941.
- Olsen, M. A., Nawoschik, S. P., Schurman, B. R., Schmitt, H. L., Burno, M., Smith, D. L. & Schechter, L. E. 1999. Identification of a human 5-HT<sub>6</sub> receptor variant produced by alternative splicing. *Brain Res Mol Brain Res*, 64, 255-63.
- Orlacchio, A., Kawarai, T., Paciotti, E., Stefani, A., Orlacchio, A., Sorbi, S., St George-Hyslop, P. H. & Bernardi, G. 2002. Association study of the 5-hydroxytryptamine<sub>6</sub> receptor gene in Alzheimer's disease. *Neuroscience Letters*, 325, 13-16.
- Ouchi, Y., Yoshikawa, E., Futatsubashi, M., Yagi, S., Ueki, T. & Nakamura, K. 2009. Altered brain serotonin transporter and associated glucose metabolism in Alzheimer disease. *J Nucl Med*, 50, 1260-6.
- Oulhaj, A., Refsum, H., Beaumont, H., Williams, J., King, E., Jacoby, R. & Smith, A. D. 2010. Homocysteine as a predictor of cognitive decline in Alzheimer's disease. *Int J Geriatr Psychiatry*, 25, 82-90.
- Pascual-Brazo, J., Castro, E., Diaz, A., Valdizan, E. M., Pilar-Cuellar, F., Vidal, R., Treceno, B. & Pazos, A. 2012. Modulation of neuroplasticity pathways and antidepressant-like behavioural responses following the short-term (3 and 7 days) administration of the 5-HT<sub>4</sub> receptor agonist RS67333. *Int J Neuropsychopharmacol*, 15, 631-43.
- Penas-Cazorla, R. & Vilaro, M. T. 2015. Serotonin 5-HT<sub>4</sub> receptors and forebrain cholinergic system: receptor expression in identified cell populations. *Brain Struct Funct*, 220, 3413-34.
- Peng, S., Zhang, Y., Zhang, J., Wang, H. & Ren, B. 2010. ERK in Learning and Memory: A Review of Recent Research. *International Journal of Molecular Sciences*, 11, 222-232.
- Penna, I., Vella, S., Gigoni, A., Russo, C., Cancedda, R. & Pagano, A. 2011. Selection of candidate housekeeping genes for normalization in human postmortem brain samples. *Int J Mol Sci*, 12, 5461-70.
- Perry, G., Cash, A. D. & Smith, M. A. 2002. Alzheimer Disease and Oxidative Stress. *Journal of Biomedicine and Biotechnology*, 2, 120-123.
- Pezawas, L., Meyer-Lindenberg, A., Drabant, E. M., Verchinski, B. A., Munoz, K. E., Kolachana, B. S., Egan, M. F., Mattay, V. S., Hariri, A. R. & Weinberger, D. R. 2005. 5-HTTLPR polymorphism impacts human cingulate-amygdala interactions: a genetic susceptibility mechanism for depression. *Nat Neurosci*, 8, 828-34.
- Pimenova, A. A., Thathiah, A., De Strooper, B. & Tesseur, I. 2014. Regulation of amyloid precursor protein processing by serotonin signaling. *PLoS One*, 9, e87014.
- Pirkmajer, S. & Chibalin, A. V. 2011. Serum starvation: caveat emptor. *Am J Physiol Cell Physiol*, 301, C272-9.
- Potter, P. E., Rauschkolb, P. K., Pandya, Y., Sue, L. I., Sabbagh, M. N., Walker, D. G. & Beach, T. G. 2011. Pre- and post-synaptic cortical cholinergic deficits are proportional to amyloid plaque presence and density at preclinical stages of Alzheimer's disease. *Acta Neuropathologica*, 122, 49-60.
- Puig, M. V. & Gener, T. 2015. Serotonin Modulation of Prefronto-Hippocampal Rhythms in Health and Disease. *ACS Chem Neurosci*, 6, 1017-25.

- Pytliak, M., Vargova, V., Mechirova, V. & Felsoci, M. 2011. Serotonin receptors - from molecular biology to clinical applications. *Physiol Res*, 60, 15-25.
- Qi, X. L., Xiu, J., Shan, K. R., Xiao, Y., Gu, R., Liu, R. Y. & Guan, Z. Z. 2005. Oxidative stress induced by beta-amyloid peptide(1-42) is involved in the altered composition of cellular membrane lipids and the decreased expression of nicotinic receptors in human SH-SY5Y neuroblastoma cells. *Neurochem Int*, 46, 613-21.
- Raghanti, M. A., Stimpson, C. D., Sherwood, C. C., Marcinkiewicz, J. L., Erwin, J. M. & Hof, P. R. 2007. Differences in Cortical Serotonergic Innervation among Humans, Chimpanzees, and Macaque Monkeys: A Comparative Study. *Cerebral Cortex*, 18, 584-597.
- Ramamoorthy, S., Bauman, A. L., Moore, K. R., Han, H., Yang-Feng, T., Chang, A. S., Ganapathy, V. & Blakely, R. D. 1993. Antidepressant- and cocaine-sensitive human serotonin transporter: molecular cloning, expression, and chromosomal localization. *Proc Natl Acad Sci U S A*, 90, 2542-6.
- Ramirez, M. J. 2013. 5-HT6 receptors and Alzheimer's disease. *Alzheimers Res Ther*, 5, 15.
- Ramos-Cejudo, J., Wisniewski, T., Marmar, C., Zetterberg, H., Blennow, K., De Leon, M. J. & Fossati, S. 2018. Traumatic Brain Injury and Alzheimer's Disease: The Cerebrovascular Link. *EBioMedicine*, 28, 21-30.
- Rebholz, H., Friedman, E. & Castello, J. 2018. Alterations of Expression of the Serotonin 5-HT4 Receptor in Brain Disorders. *Int J Mol Sci*, 19.
- Reeves, P. J., Callewaert, N., Contreras, R. & Khorana, H. G. 2002. Structure and function in rhodopsin: high-level expression of rhodopsin with restricted and homogeneous N-glycosylation by a tetracycline-inducible N-acetylglucosaminyltransferase I-negative HEK293S stable mammalian cell line. *Proceedings of the National Academy of Sciences of the United States of America*, 99, 13419-13424.
- Reiman, E. M., Chen, K., Alexander, G. E., Caselli, R. J., Bandy, D., Osborne, D., Saunders, A. M. & Hardy, J. 2004. Functional brain abnormalities in young adults at genetic risk for late-onset Alzheimer's dementia. *Proc Natl Acad Sci U S A*, 101, 284-9.
- Restivo, L., Roman, F., Dumuis, A., Bockaert, J., Marchetti, E. & Ammassari-Teule, M. 2008. The promnesic effect of G-protein-coupled 5-HT4 receptors activation is mediated by a potentiation of learning-induced spine growth in the mouse hippocampus. *Neuropsychopharmacology*, 33, 2427-2434.
- Revett, T., Baker, G., Jhamandas, J. & Kar, S. 2013. Glutamate system, amyloid  $\beta$  peptides and tau protein: functional interrelationships and relevance to Alzheimer disease pathology. *Journal of Psychiatry & Neuroscience*, 38, 6-23.
- Reynolds, G. P., Mason, S. L., Meldrum, A., De Keczer, S., Parnes, H., Eglen, R. M. & Wong, E. H. 1995. 5-Hydroxytryptamine (5-HT)4 receptors in post mortem human brain tissue: distribution, pharmacology and effects of neurodegenerative diseases. *Br J Pharmacol*, 114, 993-8.
- Riccioni, T., Bordini, F., Minetti, P., Spadoni, G., Yun, H. M., Im, B. H., Tarzia, G., Rhim, H. & Borsini, F. 2011. ST1936 stimulates cAMP, Ca<sup>2+</sup>, ERK1/2 and Fyn kinase through a full activation of cloned human 5-HT6 receptors. *Eur J Pharmacol*, 661, 8-14.
- Riedel, B. C., Thompson, P. M. & Brinton, R. D. 2016. Age, APOE and Sex: Triad of Risk of Alzheimer's Disease. *The Journal of steroid biochemistry and molecular biology*, 160, 134-147.
- Rius-Perez, S., Tormos, A. M., Perez, S. & Talens-Visconti, R. 2018. Vascular pathology: Cause or effect in Alzheimer disease? *Neurologia*, 33, 112-120.
- Roberson, E. D., Halabisky, B., Yoo, J. W., Yao, J., Chin, J., Yan, F., Wu, T., Hamto, P., Devidze, N., Yu, G. Q., Palop, J. J., Noebels, J. L. & Mucke, L. 2011. Amyloid-beta/Fyn-induced synaptic, network, and cognitive impairments depend on tau levels in multiple mouse models of Alzheimer's disease. *J Neurosci*, 31, 700-11.

- Robert, S., Maillet, M., Morel, E., Launay, J. M., Fischmeister, R., Mercken, L. & Lezoualc'h, F. 2005. Regulation of the amyloid precursor protein ectodomain shedding by the 5-HT<sub>4</sub> receptor and Epac. *FEBS Lett*, 579, 1136-42.
- Rockland, K. S. 2017. Chapter 1 - Anatomy of the Cerebral Cortex. In: Cechetto, D. F. and Weishaupt, N. (eds.) *The Cerebral Cortex in Neurodegenerative and Neuropsychiatric Disorders*. San Diego: Academic Press.
- Rodriguez, J. J., Noristani, H. N. & Verkhatsky, A. 2012. The serotonergic system in ageing and Alzheimer's disease. *Prog Neurobiol*, 99, 15-41.
- Rosethorne, E. M., Nahorski, S. R. & Challiss, R. a. J. 2008. Regulation of cyclic AMP response-element binding-protein (CREB) by G(q/11)-protein-coupled receptors in human SH-SY5Y neuroblastoma cells. *Biochemical Pharmacology*, 75, 942-955.
- Roth, B. L. 2006. *The Serotonin Receptors: From Molecular Pharmacology to Human Therapeutics*, Humana Press.
- Ruat, M., Traiffort, E., Arrang, J. M., Tardivel-Lacombe, J., Diaz, J., Leurs, R. & Schwartz, J. C. 1993. A novel rat serotonin (5-HT<sub>6</sub>) receptor: molecular cloning, localization and stimulation of cAMP accumulation. *Biochem Biophys Res Commun*, 193, 268-76.
- Sabri, O., Meyer, P. M., Gräf, S., Hesse, S., Wilke, S., Becker, G.-A., Rullmann, M., Patt, M., Luthardt, J., Wagenknecht, G., Hoepping, A., Smits, R., Franke, A., Sattler, B., Tiepolt, S., Fischer, S., Deuther-Conrad, W., Hegerl, U., Barthel, H., Schönknecht, P. & Brust, P. 2018. Cognitive correlates of  $\alpha 4\beta 2$  nicotinic acetylcholine receptors in mild Alzheimer's dementia. *Brain*, 141, 1840-1854.
- Sadeghi, H. M., Innamorati, G. & Birnbaumer, M. 1997. Maturation of receptor proteins in eukaryotic expression systems. *J Recept Signal Transduct Res*, 17, 433-45.
- Salom, D., Wang, B., Dong, Z., Sun, W., Padayatti, P., Jordan, S., Salon, J. A. & Palczewski, K. 2012. Post-translational modifications of the serotonin type 4 receptor heterologously expressed in mouse rod cells. *Biochemistry*, 51, 214-24.
- Salter, M. W. & Kalia, L. V. 2004. Src kinases: a hub for NMDA receptor regulation. *Nature Reviews Neuroscience*, 5, 317-328.
- Schildkraut, J. J. 1965. The catecholamine hypothesis of affective disorders: a review of supporting evidence. *Am J Psychiatry*, 122, 509-22.
- Schliebs, R. & Arendt, T. 2011. The cholinergic system in aging and neuronal degeneration. *Behav Brain Res*, 221, 555-63.
- Segovia, G., Porras, A., Del Arco, A. & Mora, F. 2001. Glutamatergic neurotransmission in aging: a critical perspective. *Mech Ageing Dev*, 122, 1-29.
- Selkoe, D. J. 2001. Alzheimer's disease: genes, proteins, and therapy. *Physiol Rev*, 81, 741-66.
- Selkoe, D. J. & Hardy, J. 2016. The amyloid hypothesis of Alzheimer's disease at 25 years. *EMBO Mol Med*, 8, 595-608.
- Seyedabadi, M., Fakhfouri, G., Ramezani, V., Mehr, S. E. & Rahimian, R. 2014. The role of serotonin in memory: interactions with neurotransmitters and downstream signaling. *Exp Brain Res*, 232, 723-38.
- Shakin-Eshleman, S., Remaley, A., Eshleman, J., Wunner, W. & Spitalnik, S. 1992. N-Linked Glycosylation of Rabies Virus Glycoprotein. *The Journal of Biological Chemistry*, 267, 10690-10698.
- Shankavaram, U. T., Reinhold, W. C., Nishizuka, S., Major, S., Morita, D., Chary, K. K., Reimers, M. A., Scherf, U., Kahn, A., Dolginow, D., Cossman, J., Kaldjian, E. P., Scudiero, D. A., Petricoin, E., Liotta, L., Lee, J. K. & Weinstein, J. N. 2007. Transcript and protein expression profiles of the NCI-60 cancer cell panel: an integrative microarray study. *Mol Cancer Ther*, 6, 820-32.
- Sharp, T. & Cowen, P. J. 2011. 5-HT and depression: is the glass half-full? *Curr Opin Pharmacol*, 11, 45-51.
- Small, G. W., Ercoli, L. M., Silverman, D. H., Huang, S. C., Komo, S., Bookheimer, S. Y., Lavretsky, H., Miller, K., Siddarth, P., Rasgon, N. L., Mazziotta, J. C., Saxena, S., Wu, H. M., Mega, M. S., Cummings, J. L., Saunders, A. M., Pericak-Vance, M. A., Roses,

- A. D., Barrio, J. R. & Phelps, M. E. 2000. Cerebral metabolic and cognitive decline in persons at genetic risk for Alzheimer's disease. *Proc Natl Acad Sci U S A*, 97, 6037-42.
- Smith, A. D. & Refsum, H. 2016. Homocysteine, B Vitamins, and Cognitive Impairment. *Annual Review of Nutrition*, 36, 211-239.
- Smith, G. S., Barrett, F. S., Joo, J. H., Nassery, N., Savonenko, A., Sodums, D. J., Marano, C. M., Munro, C. A., Brandt, J., Kraut, M. A., Zhou, Y., Wong, D. F. & Workman, C. I. 2017. Molecular imaging of serotonin degeneration in mild cognitive impairment. *Neurobiology of Disease*, 105, 33-41.
- Soiza-Reilly, M., Meye, F. J., Olusakin, J., Telley, L., Petit, E., Chen, X., Mameli, M., Jabaudon, D., Sze, J. Y. & Gaspar, P. 2018. SSRIs target prefrontal to raphe circuits during development modulating synaptic connectivity and emotional behavior. *Mol Psychiatry*.
- Sommer, C., Strahle, C., Köthe, U. & Hamprecht, F. A. Ilastik: Interactive learning and segmentation toolkit. 2011 IEEE International Symposium on Biomedical Imaging: From Nano to Macro, 30 March-2 April 2011. 230-233.
- Spilman, P., Podlutska, N., Hart, M. J., Debnath, J., Gorostiza, O., Bredesen, D., Richardson, A., Strong, R. & Galvan, V. 2010. Inhibition of mTOR by rapamycin abolishes cognitive deficits and reduces amyloid-beta levels in a mouse model of Alzheimer's disease. *PLoS One*, 5, e9979.
- Suzuki, A., Fukushima, H., Mukawa, T., Toyoda, H., Wu, L. J., Zhao, M. G., Xu, H., Shang, Y., Endoh, K., Iwamoto, T., Mamiya, N., Okano, E., Hasegawa, S., Mercaldo, V., Zhang, Y., Maeda, R., Ohta, M., Josselyn, S. A., Zhuo, M. & Kida, S. 2011. Upregulation of CREB-mediated transcription enhances both short- and long-term memory. *J Neurosci*, 31, 8786-802.
- Svob Strac, D., Pivac, N. & Muck-Seler, D. 2016. The serotonergic system and cognitive function. *Transl Neurosci*, 7, 35-49.
- Tam, J. H. K. & Pasternak, S. H. 2017. Chapter 4 - Alzheimer's Disease A2 - Cechetto, David F. In: Weishaupt, N. (ed.) *The Cerebral Cortex in Neurodegenerative and Neuropsychiatric Disorders*. San Diego: Academic Press.
- Tamagno, E., Robino, G., Obbili, A., Bardini, P., Aragno, M., Parola, M. & Danni, O. 2003. H<sub>2</sub>O<sub>2</sub> and 4-hydroxynonenal mediate amyloid beta-induced neuronal apoptosis by activating JNKs and p38MAPK. *Exp Neurol*, 180, 144-55.
- Tamir, H. & Gershon, M. D. 1990. Serotonin-storing secretory vesicles. *Ann N Y Acad Sci*, 600, 53-66; discussion 67.
- Teich, A. F., Nicholls, R. E., Puzzo, D., Fiorito, J., Purgatorio, R., Fa, M. & Arancio, O. 2015. Synaptic therapy in Alzheimer's disease: a CREB-centric approach. *Neurotherapeutics*, 12, 29-41.
- Terry, A. V., Jr., Buccafusco, J. J. & Wilson, C. 2008. Cognitive dysfunction in neuropsychiatric disorders: selected serotonin receptor subtypes as therapeutic targets. *Behav Brain Res*, 195, 30-8.
- Thomas, A. J., Hendriksen, M., Piggott, M., Ferrier, I. N., Perry, E., Ince, P. & O'Brien, J. T. 2006. A study of the serotonin transporter in the prefrontal cortex in late-life depression and Alzheimer's disease with and without depression. *Neuropathol Appl Neurobiol*, 32, 296-303.
- Thome, J., Retz, W., Baader, M., Pesold, B., Hu, M., Cowen, M., Durany, N., Adler, G., Henn, F. A. & Rösler, M. 2001. Association analysis of HTR6 and HTR2A polymorphisms in sporadic Alzheimer's disease. *J Neural Transm*, 108.
- Tork, I. 1990. Anatomy of the serotonergic system. *Ann N Y Acad Sci*, 600, 9-34; discussion 34-5.
- Tsai, S. J., Liu, H. C., Liu, T. Y., Wang, Y. C. & Hong, C. J. 1999. Association analysis of the 5-HT<sub>6</sub> receptor polymorphism C267T in Alzheimer's disease. *Neurosci Lett*, 276, 138-9.

- Tsang, S. W., Lai, M. K., Kirvell, S., Francis, P. T., Esiri, M. M., Hope, T., Chen, C. P. & Wong, P. T. 2006. Impaired coupling of muscarinic M1 receptors to G-proteins in the neocortex is associated with severity of dementia in Alzheimer's disease. *Neurobiol Aging*, 27, 1216-23.
- Tubio, M. R., Fernandez, N., Fitzsimons, C. P., Copsel, S., Santiago, S., Shayo, C., Davio, C. & Monczor, F. 2010. Expression of a G Protein-coupled Receptor (GPCR) Leads to Attenuation of Signaling by Other GPCRs: experimental evidence for a spontaneous GPCR constitutive inactive form. *The Journal of Biological Chemistry*, 285, 14990-14998.
- Ulas, J., Brunner, L. C., Geddes, J. W., Choe, W. & Cotman, C. W. 1992. N-methyl-D-aspartate receptor complex in the hippocampus of elderly, normal individuals and those with Alzheimer's disease. *Neuroscience*, 49, 45-61.
- Van Der Loos, C. M. 2008. Multiple immunoenzyme staining: methods and visualizations for the observation with spectral imaging. *The journal of histochemistry and cytochemistry : official journal of the Histochemistry Society*, 56, 313-328.
- Velasquez, J. C., Goeden, N. & Bonnin, A. 2013. Placental serotonin: implications for the developmental effects of SSRIs and maternal depression. *Frontiers in cellular neuroscience*, 7, 47-47.
- Verney, C., Lebrand, C. & Gaspar, P. 2002. Changing distribution of monoaminergic markers in the developing human cerebral cortex with special emphasis on the serotonin transporter. *Anat Rec*, 267, 87-93.
- Villemagne, V. L., Burnham, S., Bourgeat, P., Brown, B., Ellis, K. A., Salvado, O., Szoek, C., Macaulay, S. L., Martins, R., Maruff, P., Ames, D., Rowe, C. C. & Masters, C. L. 2013. Amyloid beta deposition, neurodegeneration, and cognitive decline in sporadic Alzheimer's disease: a prospective cohort study. *Lancet Neurol*, 12, 357-67.
- Vincent, I., Jicha, G., Rosado, M. & Dickson, D. W. 1997. Aberrant expression of mitotic cdc2/cyclin B1 kinase in degenerating neurons of Alzheimer's disease brain. *J Neurosci*, 17, 3588-98.
- Vitolo, O. V., Sant'angelo, A., Costanzo, V., Battaglia, F., Arancio, O. & Shelanski, M. 2002. Amyloid beta -peptide inhibition of the PKA/CREB pathway and long-term potentiation: reversibility by drugs that enhance cAMP signaling. *Proc Natl Acad Sci U S A*, 99, 13217-21.
- Vogel, C. & Marcotte, E. M. 2012. Insights into the regulation of protein abundance from proteomic and transcriptomic analyses. *Nature reviews. Genetics*, 13, 227-232.
- Voronkov, M., Braithwaite, S. P. & Stock, J. B. 2011. Phosphoprotein phosphatase 2A: a novel druggable target for Alzheimer's disease. *Future Medicinal Chemistry*, 3, 821-833.
- Walther, D. J., Peter, J. U., Bashammakh, S., Hortnagl, H., Voits, M., Fink, H. & Bader, M. 2003. Synthesis of serotonin by a second tryptophan hydroxylase isoform. *Science*, 299, 76.
- Wang, H. Y., Lee, D. H., D'andrea, M. R., Peterson, P. A., Shank, R. P. & Reitz, A. B. 2000a. beta-Amyloid(1-42) binds to alpha7 nicotinic acetylcholine receptor with high affinity. Implications for Alzheimer's disease pathology. *J Biol Chem*, 275, 5626-32.
- Wang, H. Y., Lee, D. H., Davis, C. B. & Shank, R. P. 2000b. Amyloid peptide Abeta(1-42) binds selectively and with picomolar affinity to alpha7 nicotinic acetylcholine receptors. *J Neurochem*, 75, 1155-61.
- Wang, Y., Ulland, T. K., Ulrich, J. D., Song, W., Tzaferis, J. A., Hole, J. T., Yuan, P., Mahan, T. E., Shi, Y., Gilfillan, S., Cella, M., Grutzendler, J., Demattos, R. B., Cirrito, J. R., Holtzman, D. M. & Colonna, M. 2016. TREM2-mediated early microglial response limits diffusion and toxicity of amyloid plaques. *J Exp Med*, 213, 667-75.
- Wheatley, M. & Hawtin, S. R. 1999. Glycosylation of G-protein-coupled receptors for hormones central to normal reproductive functioning: its occurrence and role. *Hum Reprod Update*, 5, 356-64.

- Whitaker-Azmitia, P. M. 1999. The Discovery of Serotonin and its Role in Neuroscience. *Neuropsychopharmacology*, 21, 2S-8S.
- Who. 2017. *Dementia* [Online]. Available: <http://www.who.int/mediacentre/factsheets/fs362/en/> [Accessed 10 November 2017].
- Wischik, C. M., Harrington, C. R. & Storey, J. M. 2014. Tau-aggregation inhibitor therapy for Alzheimer's disease. *Biochem Pharmacol*, 88, 529-39.
- Wishart, H. A., Saykin, A. J., Mcallister, T. W., Rabin, L. A., Mcdonald, B. C., Flashman, L. A., Roth, R. M., Mamourian, A. C., Tsongalis, G. J. & Rhodes, C. H. 2006. Regional brain atrophy in cognitively intact adults with a single APOE epsilon4 allele. *Neurology*, 67, 1221-4.
- Woods, S., Clarke, N. N., Layfield, R. & Fone, K. C. 2012. 5-HT(6) receptor agonists and antagonists enhance learning and memory in a conditioned emotion response paradigm by modulation of cholinergic and glutamatergic mechanisms. *Br J Pharmacol*, 167, 436-49.
- Woolley, M. L., Bentley, J. C., Sleight, A. J., Marsden, C. A. & Fone, K. C. F. 2001. A role for 5-HT6 receptors in retention of spatial learning in the Morris water maze. *Neuropharmacology*, 41, 210-219.
- Yahiaoui, S., Hamidouche, K., Ballandonne, C., Davis, A., De Oliveira Santos, J. S., Freret, T., Boulouard, M., Rochais, C. & Dallemagne, P. 2016. Design, synthesis, and pharmacological evaluation of multitarget-directed ligands with both serotonergic subtype 4 receptor (5-HT4R) partial agonist and 5-HT6R antagonist activities, as potential treatment of Alzheimer's disease. *Eur J Med Chem*, 121, 283-93.
- Yates, S. C., Zafar, A., Hubbard, P., Nagy, S., Durant, S., Bicknell, R., Wilcock, G., Christie, S., Esiri, M. M., Smith, A. D. & Nagy, Z. 2013. Dysfunction of the mTOR pathway is a risk factor for Alzheimer's disease. *Acta Neuropathol Commun*, 1, 3.
- Yun, H. M., Baik, J. H., Kang, I., Jin, C. & Rhim, H. 2010. Physical interaction of Jab1 with human serotonin 6 G-protein-coupled receptor and their possible roles in cell survival. *J Biol Chem*, 285, 10016-29.
- Yun, H. M., Kim, S., Kim, H. J., Kostenis, E., Kim, J. I., Seong, J. Y., Baik, J. H. & Rhim, H. 2007. The novel cellular mechanism of human 5-HT6 receptor through an interaction with Fyn. *J Biol Chem*, 282, 5496-505.
- Zenaro, E., Piacentino, G. & Constantin, G. 2017. The blood-brain barrier in Alzheimer's disease. *Neurobiol Dis*, 107, 41-56.
- Zhang, X., Beaulieu, J. M., Sotnikova, T. D., Gainetdinov, R. R. & Caron, M. G. 2004. Tryptophan hydroxylase-2 controls brain serotonin synthesis. *Science*, 305, 217.
- Zhao, J., O'connor, T. & Vassar, R. 2011. The contribution of activated astrocytes to Aβ production: implications for Alzheimer's disease pathogenesis. *J Neuroinflammation*, 8, 150.
- Zhou, M., Engel, K. & Wang, J. 2007. Evidence for Significant Contribution of a Newly Identified Monoamine Transporter (PMAT) to Serotonin Uptake in the Human Brain. *Biochemical pharmacology*, 73, 147-154.
- Zhu, X., Siedlak, S. L., Wang, Y., Perry, G., Castellani, R. J., Cohen, M. L. & Smith, M. A. 2008. Neuronal binucleation in Alzheimer disease hippocampus. *Neuropathol Appl Neurobiol*, 34, 457-65.
- Zhuo, J.-M., Wang, H. & Praticò, D. 2011. Is Hyperhomocysteinemia an Alzheimer's disease (AD) risk factor, an AD marker or neither? *Trends in pharmacological sciences*, 32, 562-571.
- Zhuo, J. M. & Pratico, D. 2010. Acceleration of brain amyloidosis in an Alzheimer's disease mouse model by a folate, vitamin B6 and B12-deficient diet. *Exp Gerontol*, 45, 195-201.

## **Chapter 9. Appendices**

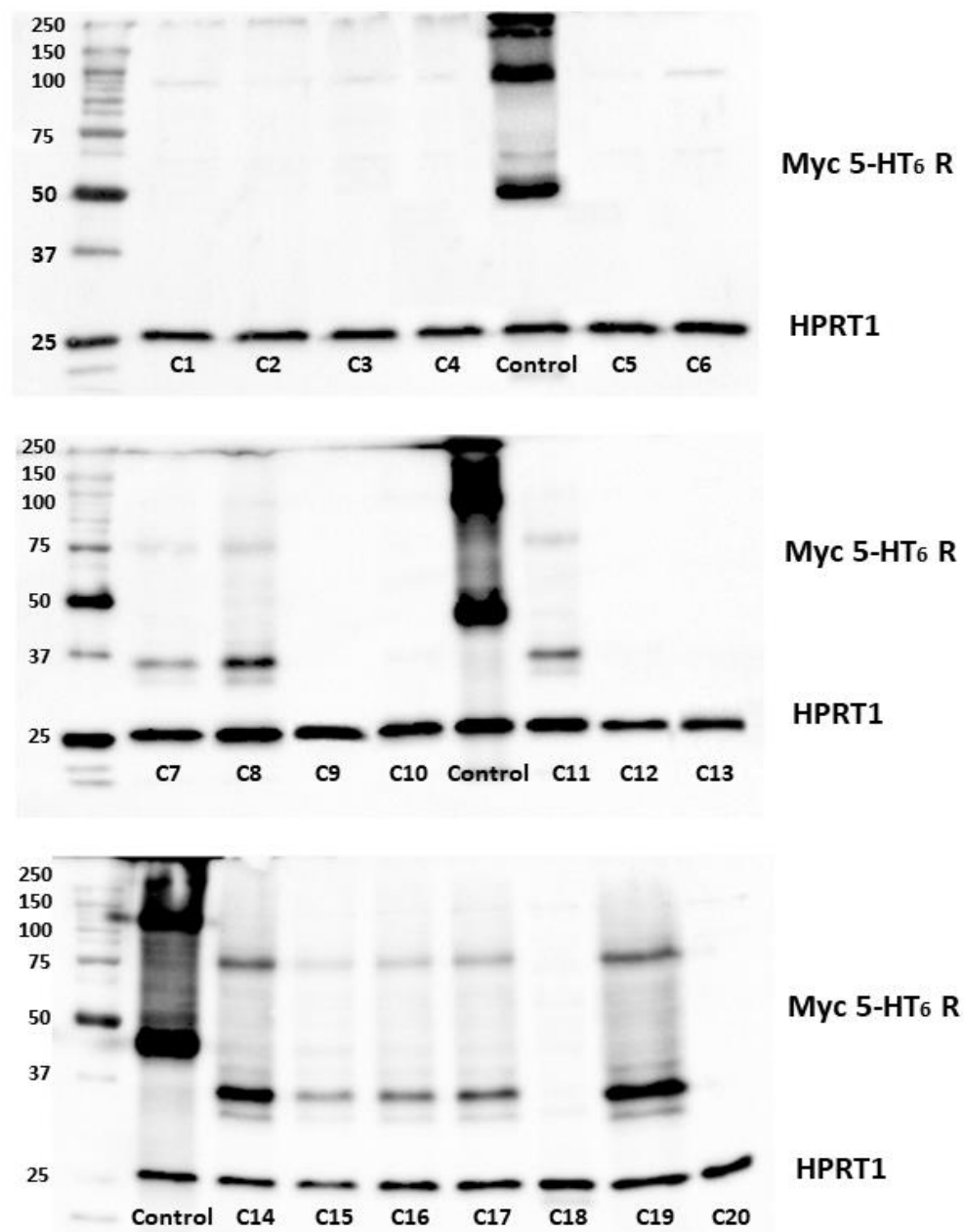
## 9. Appendices

### **9.1. Peer reviewed posters**

- Wedad Sarawi, Gillian Grafton, Zsuzsanna Nagy, Nicholas M. Barnes (2018).  
Investigating the expression of 5-HT<sub>4</sub> and 5-HT<sub>6</sub> receptors and SERT in mild and advanced stages of AD relative to healthy age-matched controls, Pharmacology 2018, Abstract Number, P205.
- Wedad Sarawi, Gillian Grafton, Zsuzsanna Nagy, Nicholas M. Barnes (2019).  
The presence and impact of *N*-linked glycosylation of the human 5-HT<sub>4</sub> receptor, Life Sciences 2019: Post-Translational Modifications and Cell Signalling, Abstract Number, P035.

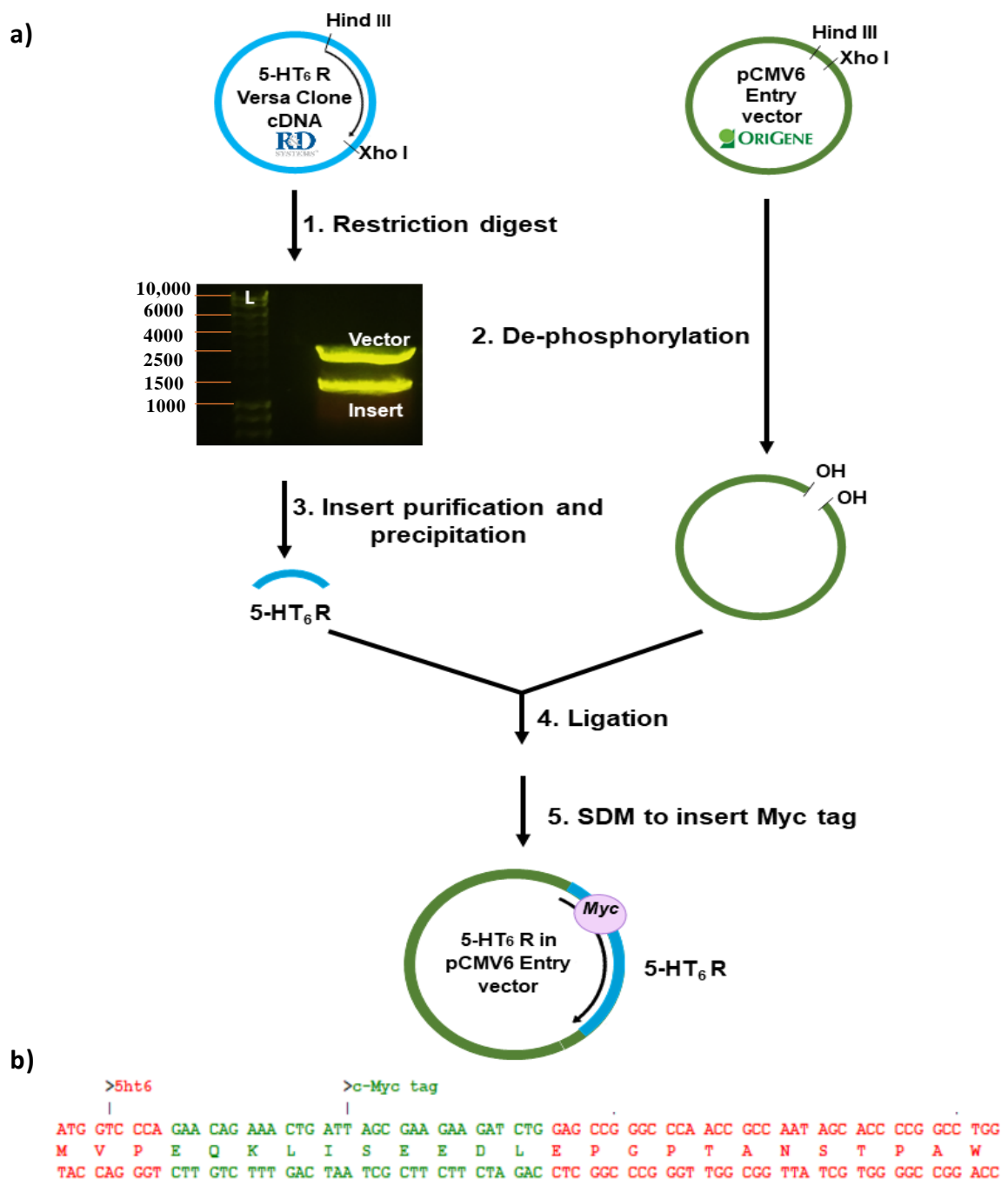


## 9.2. Supplementary figures



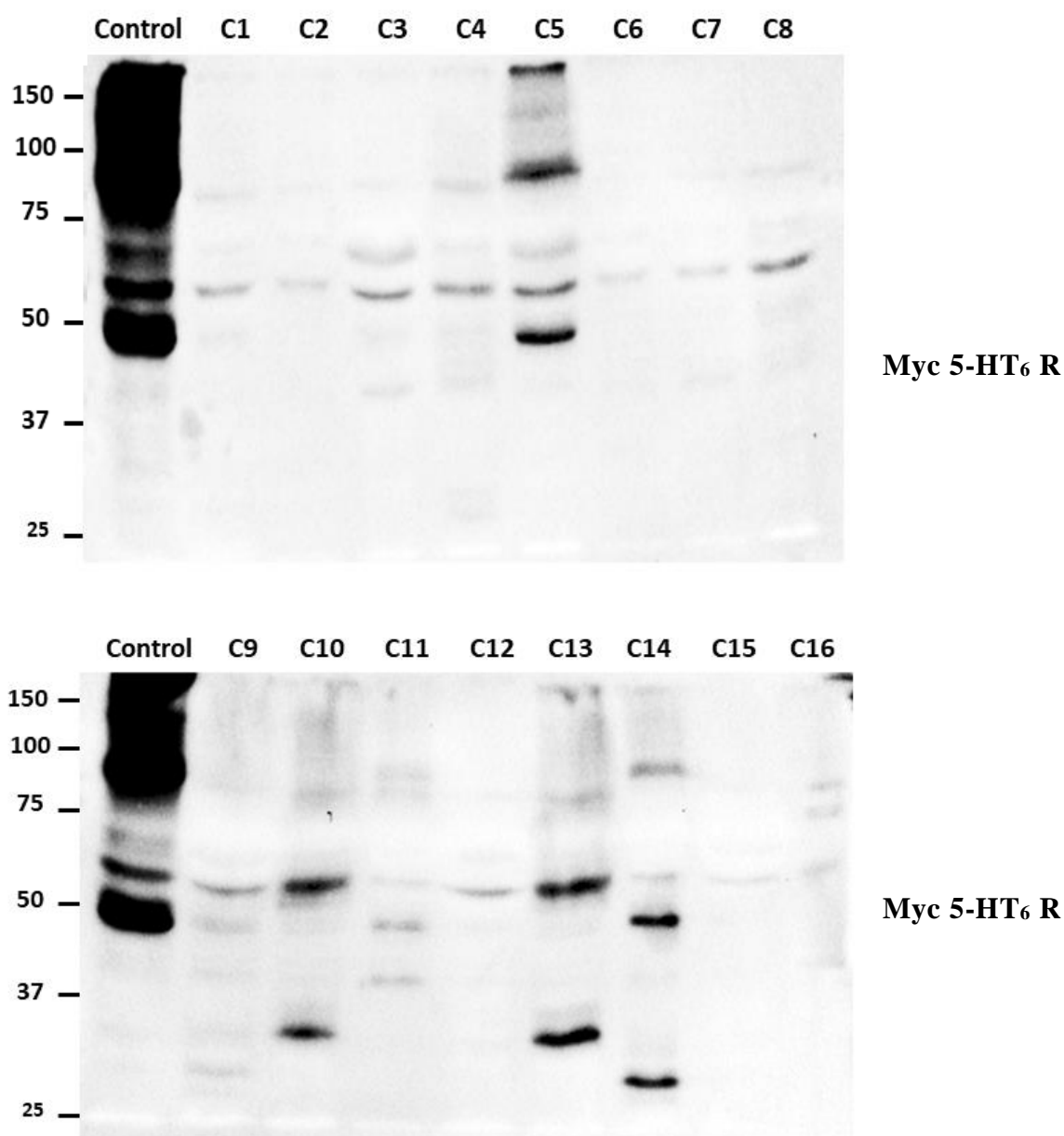
**Supplementary figure 1. Assessment of the stable expression 5-HT<sub>6</sub> receptor in individual clones**

*Three weeks after the transfection with Myc tagged 5-HT<sub>6</sub> construct, twenty clones were individually picked by cloning discs, and expanded for an additional two weeks in the presence of the selection antibiotic G418. None of these clones expressed 5-HT<sub>6</sub> receptors as most of them were negative while others showed the truncated form. The control was transiently transfected by the same construct.*



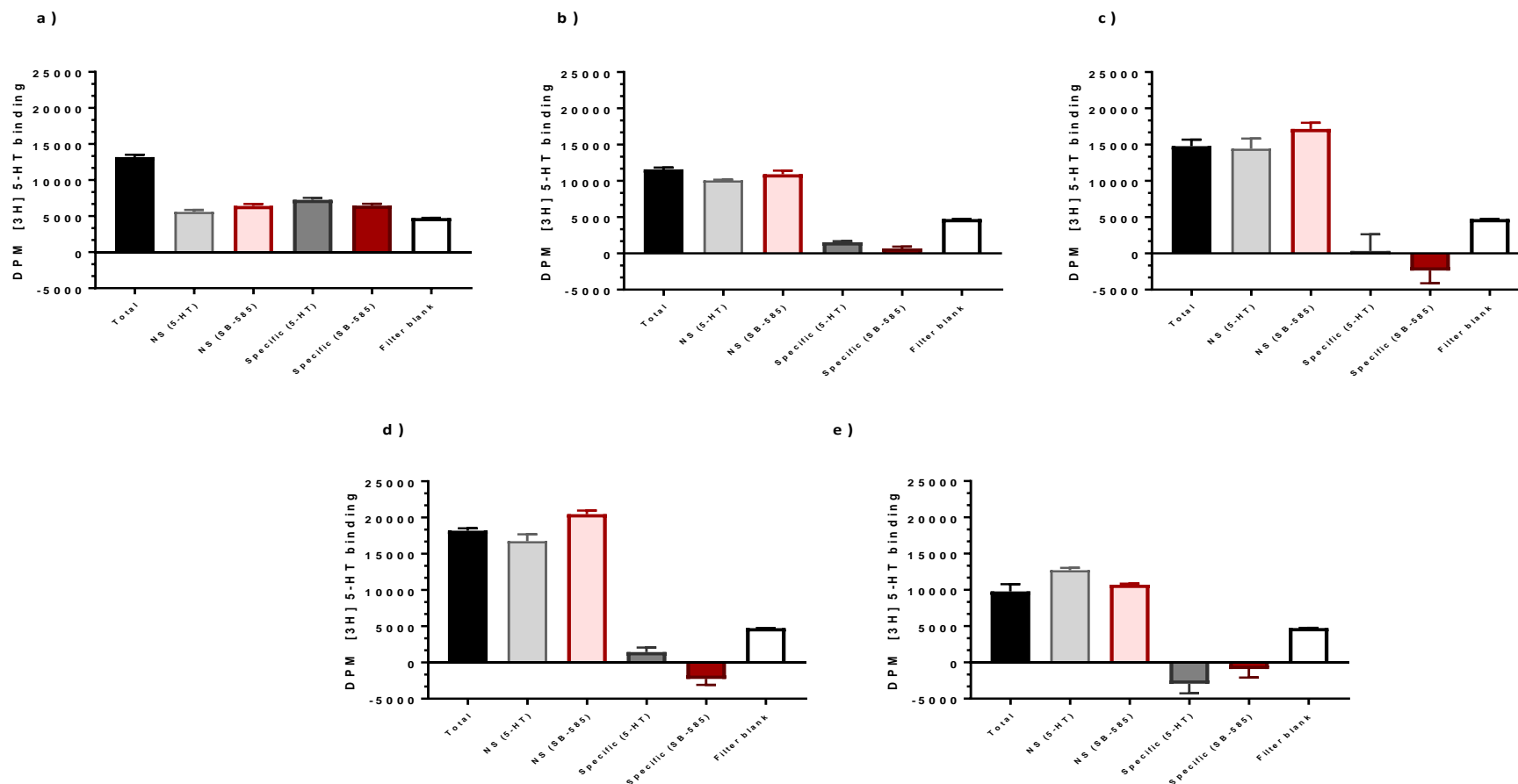
**Supplementary figure 2. The sub-cloning of second construct of 5-HT<sub>6</sub> receptor**

a) This clone was constructed in the hope of overcoming the formation of unwanted truncated receptor proteins with the first construct of 5-HT<sub>6</sub> receptor which was previously shown in **Figure 13** and assessed in **Supplementary figure 1**. b) Represents the position of the Myc tag within the first 15 amino acids of the 5-HT<sub>6</sub> receptor coding sequence.



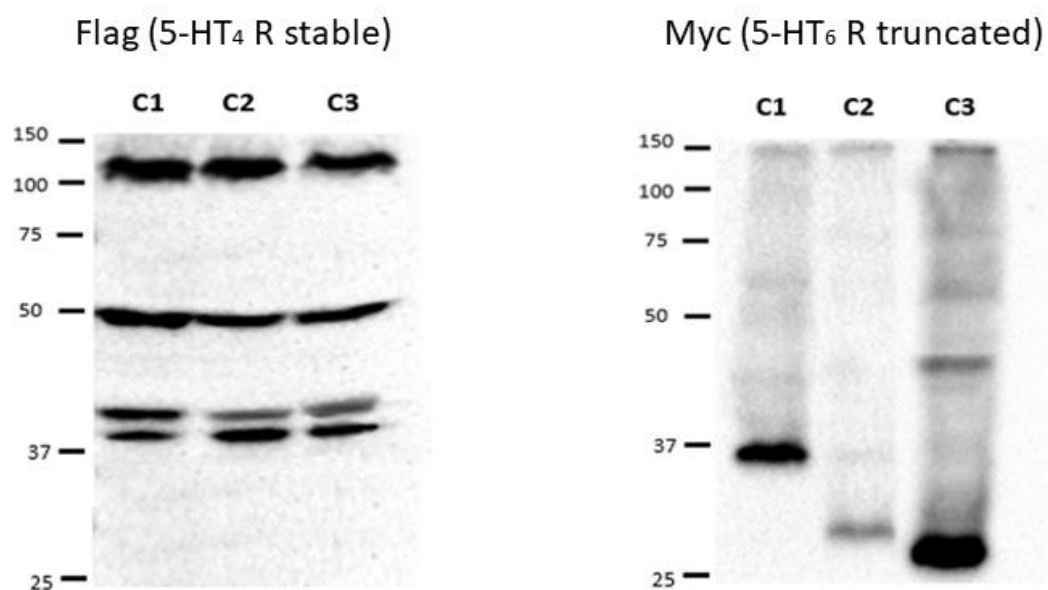
**Supplementary figure 3. Assessment of the stable expression of 5-HT<sub>6</sub> receptor in HEK293 cells transfected with the second 5-HT<sub>6</sub> receptor construct illustrated in the previous figure**

*Three weeks after transfection with the second Myc tagged 5-HT<sub>6</sub> receptor construct, 30 clones were individually picked by cloning discs, and expanded for an additional two weeks in the presence of the selection antibiotic G418. Western blots only showed 16 clones. Clone 5 expressed 5-HT<sub>6</sub> receptors at the correct band size. The control was transiently transfected by the same construct.*



**Supplementary figure 4. Radioligand binding of transiently and stably expressing 5-HT<sub>6</sub> receptor in HEK293 cells**

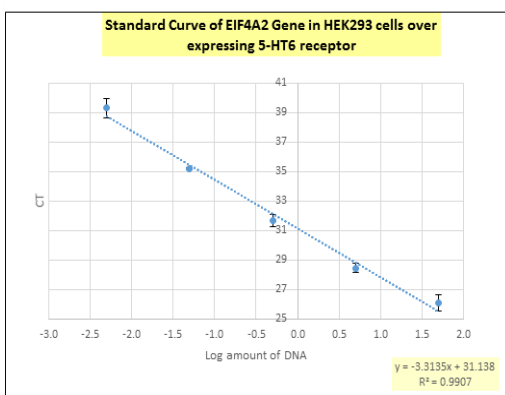
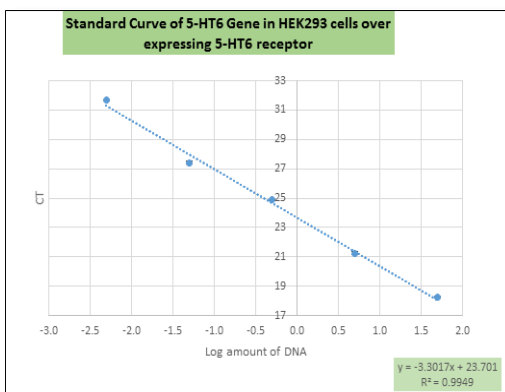
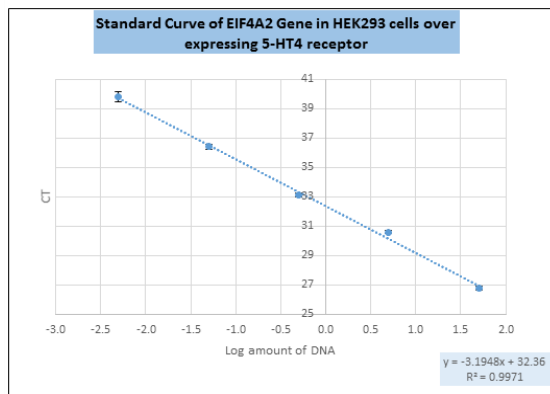
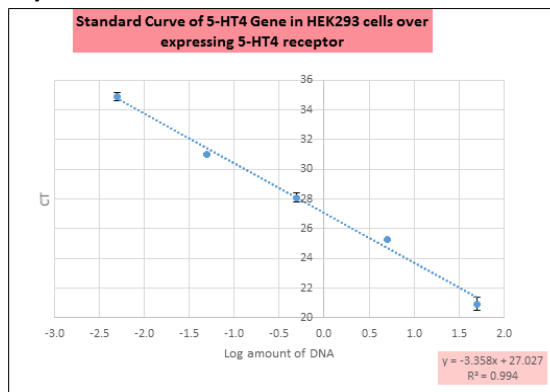
Single point radioligand binding of 10 nM of [<sup>3</sup>H]-5-HT to the membrane fraction of **a)** 0.2 mg/ml of transient 5-HT<sub>6</sub> receptor (positive control), **b)** 0.2 mg/ml, **c)** 0.4 mg/ml, **d)** 0.8 mg/ml of stable 5-HT<sub>6</sub> receptor (clone 5), and **e)** 0.2 mg/ml of HEK293 cells (negative control). The NS binding was assessed by 10 μM of either 5-HT or SB-2585. Data are represented as mean ± SD of three technical repeats. DPM of the radioligand were measured by a Tri-carb counter.



**Supplementary figure 5. The attempt to stabilise the 5-HT<sub>6</sub> receptor in the stable 5-HT<sub>4</sub> receptor cell line**

*The stable 5-HT<sub>4</sub> receptor cell line was transfected with the second 5-HT<sub>6</sub> receptor construct and the cells were then grown in the presence of G418 and hygromycin. This was followed by the picking and expansion of the clones. The blots showed three clones which are positive for the 5-HT<sub>4</sub> receptor but not the 5-HT<sub>6</sub> receptor.*

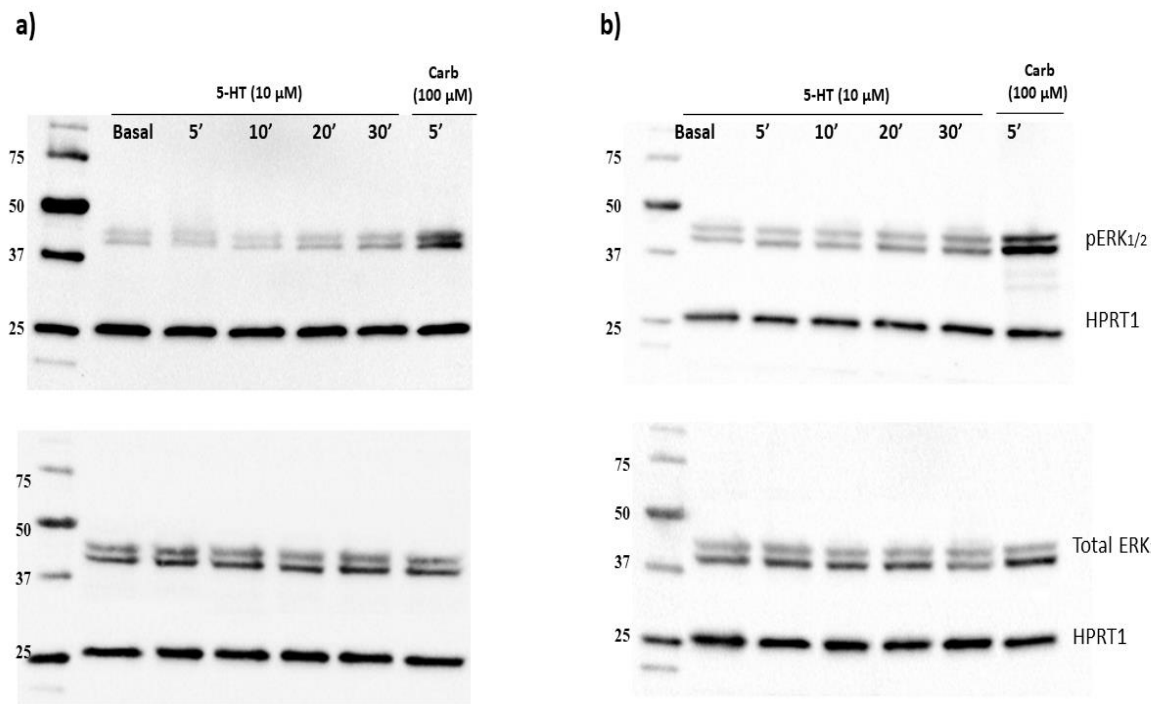
a) b)



Supplementary figure 6. An example

**of standard curves of PCR amplification of the transcript of 5-HT<sub>4</sub> and 5-HT<sub>6</sub> receptors and EIF4A2**

*Ten-fold dilution series from 50 ng to 5 pg of the cDNA were used with every PCR reaction to generate standard curves which were used for the interpolation of the unknown DNA amount from the curve by using the Ct values and to validate  $\Delta\Delta CT$  calculations. (a) The gene expression of the 5-HT<sub>4</sub> receptor and EIF4A2 in HEK293 cells transiently transfected with 5-HT<sub>4</sub> receptor plasmid. (b) The gene expression of the 5-HT<sub>6</sub> receptor and EIF4A2 in HEK293 cells transiently transfected with 5-HT<sub>6</sub> receptor plasmid. Each point of the standard curve repeated in triplicate and presented as mean  $\pm$  SD. CT; cycle threshold.*



**Supplementary figure 7. The effect of 5-HT and carbachol on ERK<sub>1/2</sub> phosphorylation**

*Following overnight serum-starvation, **a)** HEK293 cells and **b)** SH-SY5Y cells were treated with the 10  $\mu$ M of 5-HT and 100  $\mu$ M of carbachol for the indicated time points. Total ERK<sub>1/2</sub> and HPRT1 were used as loading controls. The blot shown is the representative of 3 repeats.*